OPTIMIZATION OF SHEAR WALL THICKNESS, CONFIGURATION, AND PLACEMENT FOR IRREGULARLY SHAPED RC BUILDINGS UNDER SEISMIC LOAD

FTIMA MOHAMED SHWIHDI

COLLEGE OF GRADUATE STUDIES
UNIVERSITI TENAGA NASIONAL

2025

OPTIMIZATION OF SHEAR WALL THICKNESS, CONFIGURATION, AND PLACEMENT FOR IRREGULARLY SHAPED RC BUILDINGS UNDER SEISMIC LOAD

FTIMA MOHAMED SHWIHDI

A Project Report Submitted to the College of Graduate Studies, Universiti Tenaga Nasional in Partial Fulfilment of the Requirements for the Degree of

Master of Structural Engineering

AUGUST 2025

DECLARATION

I hereby declare that the thesis is my original work except for quotations and citations which have been duly acknowledged. I also declare that it has not been previously, and is not concurrently submitted for any other degree at Universiti Tenaga Nasional or at any other institutions. This thesis may be made available within the university library and may be photocopied and loaned to other libraries for the purpose of consultation.

SIGN

FTIMA MOHAMED SHWIHDI

Date:30/8/2025

ABSTRACT

The rapid evolution of contemporary architecture has seen a marked increase in the construction of irregularly shaped buildings, such as L-shaped reinforced concrete (RC) structures, driven by a blend of aesthetic appeal and functional demands; however, these designs pose substantial challenges in seismic engineering due to their inherent geometrical asymmetry, which exacerbates vulnerabilities under seismic loads. L-shaped buildings, in particular, suffer from torsional irregularity stemming from uneven mass and stiffness distribution, leading to amplified lateral displacements, stress concentrations at re-entrant corners, and an overall reduction in structural stability during earthquakes—issues that are inadequately addressed by conventional seismic design methods. This challenge is especially pertinent in regions of low to moderate seismicity, such as Malaysia, where seismic considerations are often overshadowed by other design priorities, and where existing guidelines lack specificity for optimizing structural elements like shear walls in irregular configurations. This Master Project Thesis aims to bridge this gap by investigating the optimization of shear wall thickness, configuration, and placement in L-shaped RC buildings to enhance their seismic resilience, with a focus on mitigating torsional effects, reducing stress concentrations, and controlling lateral displacements. The research employs advanced computational tools, specifically Tekla Structural Designer(TSD), to model a 20-story L-shaped RC building and analyze its seismic performance using two robust methods: Response Spectrum Analysis (RSA), which captures dynamic structural responses across a range of frequencies, and Equivalent Lateral Force method(ELF), which simplifies seismic forces into equivalent static loads for comparative assessment. Through parametric studies, various shear wall layouts—differing in thickness, positioning (e.g., along exterior walls, core areas, or critical corners), and distribution—are simulated under seismic loading conditions representative of low to moderate seismic zones, allowing for a detailed evaluation of their effectiveness in improving structural integrity. The expected outcomes include a comprehensive comparative analysis of shear wall configurations, pinpointing optimal thickness parameters that balance material efficiency with seismic performance, alongside the development of a structured, replicable methodology that can guide future investigations into irregular building design. By addressing critical deficiencies in current seismic design practices, this study leverages computational optimization to deliver practical, evidence-based recommendations for structural engineers, enhancing the safety and durability of irregularly shaped RC buildings. Furthermore, the research contributes to the broader field of performance-based seismic design by offering insights that are adaptable to other irregular geometries and seismic contexts, thereby fostering safer urban environments in seismically active regions worldwide.

ACKNOWLEDGMENT

First and foremost, I praise Allah, the Almighty, for granting me the strength, wisdom, and perseverance to complete this research work despite the challenges encountered along this journey.

I would like to express my deepest gratitude and thanks to my supervisor, Dr. Agusril, whose guidance and expertise have been invaluable throughout this research. Beyond his academic mentorship, I am particularly grateful that he first introduced me to the Tekla Structural Designer program during my studies.

I also thank my university for providing the software licenses and facilities that enabled the analyses. I appreciate the support of departmental staff and my peers.

My heartfelt gratitude goes to my beloved mother, whose constant prayers and unwavering support have been my pillar of strength throughout this academic journey. Her love and encouragement have sustained me through every challenge.

I am deeply grateful to my children and my husband, Kamal, for his sacrifice and patience. His support has been instrumental in making this achievement possible.

DEDICATION

This work is dedicated to the blessed memory of my beloved father, whose soul departed to Allah's mercy while I was pursuing this academic journey far from home. Though I was denied the opportunity to bid him farewell or hold his hand one last time, his teachings, values, and the strength he instilled in me continue to guide every step I take. May Allah grant him Jannah and eternal peace.

To my father - your legacy lives on through the knowledge I seek and the dreams you encouraged me to pursue.

TABLE OF CONTENTS

LIST OF TABLES

LIST OF FIGURES

LIST OF SYMBOLS

H	Total building height
T1	Fundamental period
C_t	EC8 period coefficient
ag,R	Reference peak ground acceleration
a_g	Design ground acceleration
S	Soil factor (EC8)
η	Damping correction factor
T_B, T_C, T_D	Corner periods of EC8 spectrum
q	Behaviour (response reduction) factor
γ_I	Importance factor
α_u/α_y	Overstrength ratio
ψ_2	Combination factor for live load in seismic mass
$S_e(T)$, $S_d(T)$	Elastic / design spectral ordinate
F_b	Design base shear
F_i	Storey lateral force
m, m_i	Total / storey mass
z_i	Storey height above base
$\Delta_{max}/\Delta_{avg}$	Torsional irregularity (twist) ratio
U_X, U_Y	Translational mode components
R_z	Rotational mode component
E_c	Concrete elastic modulus
f_{ck}	Concrete characteristic strength
f_{yk}	Reinforcement yield strength

LIST OF ABBREVIATIONS

RC	Reinforced Concrete
EC2	Eurocode 2: Design of Concrete Structures
EC8	Eurocode 8: Design of Structures for Earthquake Resistance
TSD	Tekla Structural Designer
RSA	Response Spectrum Analysis
ELF	Equivalent Lateral Force method
SFRS	Seismic Force-Resisting System
PGA	Peak Ground Acceleration
SSI	Soil–Structure Interaction
FRP	Fibre-Reinforced Polymer
GA	Genetic Algorithm
RSM	Response Surface Method

LIST OF GLOSSARIES

Accidental eccentricity	Code-prescribed ±5% offset of the mass centre to model torsion.
Base shear	Resultant horizontal shear at the foundation from seismic action.
CQC	Method for combining modal responses in RSA.
Core wall	Central wall system (lifts/stairs) providing primary lateral resistance.
Inter-storey drift ratio	Relative floor displacement divided by storey height.
L-intersection wall	Shear wall(s) at the L-corner that stiffen the short wing.
Modal mass participation	Percentage of total mass mobilised by a vibration mode.
Perimeter wall	Shear wall along exterior bays to distribute plan stiffness.
Re-entrant corner	Internal corner in an L-plan.
Thickness taper	Stepwise reduction of wall thickness with height for efficiency.
Torsional irregularity	Twist ratio $\Delta_{max}/\Delta_{avg}$; EC8 limit ≤ 1.2.

CHAPTER 1

INTRODUCTION

1.1 Background of Study

The progression of modern architecture and urban development has increasingly favoured irregularly shaped reinforced-concrete (RC) buildings, owing to the need for optimised spatial use, aesthetic appeal and specific functional requirements. Buildings of this type, characterised by unconventional plan and elevation layouts, have challenged traditional seismic design methodologies. Irregular configurations, particularly prevalent in densely populated urban environments, are associated with significant structural-engineering challenges because complexities are introduced into the distribution of seismic forces, resulting in non-uniform structural responses during seismic events [1], [3]. Pronounced vulnerabilities— including amplified torsional movements and stress concentrations—have therefore been observed, and comprehensive analyses together with advanced optimisation techniques are required.

One specific typology that has become prevalent is the RC frame-shear-wall dual system, which is employed widely in commercial and residential high-rise structures. Architectural flexibility is combined with enhanced lateral stiffness and strength in this system, which are essential for resisting seismic loads. However, while conventional buildings with regular geometries have well-established design frameworks, irregular forms—such as the common L-shaped configuration—have been less thoroughly characterised seismically, particularly with respect to the optimal design and placement of shear walls. The significance of this gap has been evidenced by the distinct seismic responses observed in past earthquakes, where inadequate shear-wall configurations have contributed to disproportionate damage or even catastrophic structural failures [2], [4], [5].

Irregularities in structural geometry are generally classified into two primary categories: plan irregularities, where asymmetrical distributions of mass and stiffness induce significant torsional behaviour; and vertical irregularities, typically

characterised by abrupt changes in stiffness or strength along a building's height. Architectural designs that emphasise visual aesthetics—such as those influenced by deconstructivism—often incorporate irregular geometries without fully addressing the structural implications, leading to pronounced vulnerabilities during seismic events. Notably, such tendencies necessitate closer collaboration between architects and structural engineers at early design stages so that seismic risks can be mitigated effectively [1].

Plan irregularities, common in L-shaped buildings, result in amplified torsional effects due to eccentric distributions of mass and rigidity. This eccentricity significantly influences seismic performance, often producing uneven lateral displacements, excessive inter-storey drifts and critical stress accumulations at re-entrant corners. Targeted mitigation measures are therefore required, primarily involving the strategic placement and optimisation of shear walls to enhance torsional resistance and overall lateral stiffness [6], [7].

Numerous seismic design codes, including Eurocode 8, recognise the increased vulnerability of irregular structures and mandate stricter design criteria to counteract the adverse effects associated with geometric irregularities. However, existing guidelines often rely on generalised approaches, leading to overly conservative or insufficiently targeted design solutions. Recent studies have underlined that traditional empirical methods for determining fundamental periods and lateral force distributions can underestimate seismic demands in irregular buildings. Such discrepancies emphasise the necessity for more accurate modelling and analytical techniques that account for torsional irregularities and the complex dynamic behaviours typical of irregular configurations [10], [11].

Research specifically addressing L-shaped buildings has shown that these structures experience heightened lateral displacements, storey drifts and torsional rotations when compared with regular counterparts. Investigations employing detailed finite-element analysis and dynamic simulations have consistently revealed significant deviations from code-prescribed estimates of fundamental periods and seismic load distributions. For instance, empirical formulae in prevalent seismic codes have been found to

underestimate the fundamental period of L-shaped buildings by up to 150 %, reflecting the inadequacy of conventional methods in accurately predicting the dynamic characteristics of irregular structures [13], [14], [15].

Moreover, seismic studies of L-shaped buildings have revealed critical vulnerabilities at re-entrant corners, where stress concentrations due to torsional rotations frequently result in localised failures. These localised stresses necessitate specialised reinforcement detailing and optimised shear-wall configurations so that the adverse effects can be mitigated. When shear walls are configured appropriately—strategically positioned at corners or along key axes—torsional irregularities are reduced effectively, with seismic resilience and structural integrity improved significantly. Comparative analyses have clearly illustrated that optimally positioned shear walls in irregular buildings substantially reduce maximum displacements, storey drifts and torsional irregularities, underscoring the criticality of shear-wall configuration optimisation [16], [17], [18].

Additionally, contemporary software tools such as Tekla Structural Designer (TSD) offer substantial potential for optimising shear-wall designs through detailed structural modelling and advanced analytical capabilities. Despite these advantages, such tools have seen limited application to irregular RC buildings, indicating a gap in the utilisation of advanced modelling for seismic optimisation. Tekla's robust analysis features, when appropriately leveraged, can provide significant insights into structural behaviour under seismic loads, thereby enabling refined design solutions tailored to irregular configurations [19].

Recognising these challenges and opportunities, the primary aim of this research project is to investigate and optimise shear-wall thickness, configuration and placement for L-shaped RC buildings subjected to seismic loading. Rigorous finite-element modelling using Tekla Structural Designer (TSD) software will be employed, integrating both Response Spectrum Analysis and Equivalent Static Load Analysis to characterise seismic responses comprehensively and to develop optimised shear-wall arrangements. The ultimate objective is to enhance the seismic resilience of irregular RC buildings, with vulnerabilities inherent to their configurations reduced, and with

design recommendations grounded in thorough analytical evaluations and validated modelling techniques.

In the subsequent chapters of this thesis, existing knowledge gaps will be explored systematically, various shear-wall configurations will be analysed critically, numerical models will be validated through comparative analyses, and optimisation strategies—tailored to the unique seismic demands of L-shaped RC structures—will be proposed. By bridging the gap between theoretical insights and practical design methodologies, it is sought to contribute meaningfully to the safe and efficient seismic design of irregular RC buildings, aligning architectural aspirations with structural-safety imperatives.

To make your document look professionally produced, Word provides header, footer, cover page, and text box designs that complement each other. For example, you can add a matching cover page, header, and sidebar.

1.2 Problem Statement

Despite significant advancements in seismic design methodologies, reinforced concrete (RC) buildings with irregular shapes—particularly L-shaped configurations—continue to present considerable challenges for structural engineers. The increasing prevalence of these buildings is primarily driven by architectural and urban planning considerations that prioritise aesthetics and functionality, often at the expense of structural regularity and seismic resilience [1, 2, 3]. It has been clearly demonstrated in previous studies that irregular geometries, such as L-shaped buildings, suffer significantly from torsional irregularities due to asymmetric mass and stiffness distribution [6, 7]. This irregularity is associated with exacerbated stress concentrations, notably at re-entrant corners, leading to higher lateral displacement and amplified torsional responses under seismic loads [13, 14, 15].

Currently, simplified seismic design guidelines used in practice are mainly derived from regular building designs. These methods do not adequately capture the complex dynamic behaviours exhibited by irregular configurations, especially in terms of

torsion and non-uniform stress distribution [6, 10, 11]. Moreover, limited guidance is available on how shear wall configurations, thickness and placements specifically interact within L-shaped buildings to mitigate seismic vulnerabilities effectively. Additionally, while Tekla Structural Designer (TSD) software possesses advanced capabilities for modelling and structural analysis, its potential remains underutilised in the optimization of shear wall designs in irregular RC structures [20, 21]. Consequently, trial-and-error approaches are often adopted rather than systematic, analytical optimization frameworks, resulting in suboptimal seismic designs that may be either overly conservative or insufficiently resilient [19, 20].

Addressing these knowledge gaps, this research is intended to systematically investigate and optimize shear wall thickness, placement and configuration specifically tailored for L-shaped RC buildings, leveraging Tekla Structural Designer (TSD) software capabilities and adhering to Eurocode 8 (EC8) requirements for seismic design.

1.3 Research Objectives.

1.3.1 General Objective:

The general objective of this research is to develop an optimized shear wall design methodology for L-shaped reinforced concrete buildings, specifically targeting enhanced seismic performance by systematically exploring shear wall thickness, placement, and configuration using Tekla Structural Designer (TSD), in full compliance with Eurocode 8 (EC8).

1.3.2 Specific Objectives:

To achieve the general objective, this research outlines the following specific objectives:

- Evaluate seismic performance of multiple shear wall configurations within L-shaped RC buildings under seismic loading, analysing variations in structural responses such as lateral displacement, inter-storey drift, and base shear distribution [6, 14, 16].

- Investigate the impact of varying shear wall thicknesses on seismic parameters, including lateral stiffness, displacement control, and torsional response, identifying optimal thickness distributions across different building heights [17, 18].

- Compare the effectiveness of seismic analysis methods, specifically Response Spectrum Analysis (RSA) and Equivalent Lateral Force method(ELF), in accurately capturing the dynamic behaviour of irregular RC structures [10, 15].

- Determine optimal shear wall placement strategies that enhance structural stability and seismic resilience while ensuring efficient use of materials, emphasising the mitigation of stress concentrations, particularly at re-entrant corners [5, 9].

1.4 Significance of the Study

The significance of this research extends across several dimensions within structural engineering practice and seismic safety:

- Enhanced Seismic Safety: This research directly addresses the seismic vulnerability of irregular L-shaped buildings, significantly improving their earthquake resilience and occupant safety, particularly relevant in low to moderate seismic zones such as Malaysia, where specific guidelines are sparse [1, 10].

- Development of Analytical Frameworks: By employing advanced optimization techniques within Tekla Structural Designer (TSD) , this study contributes to filling the existing methodological gaps in the analytical optimization of shear walls for complex building geometries, introducing structured computational approaches to engineering practice [20, 21].

- Practical Engineering Guidelines: The findings from this study will provide clear, actionable recommendations for structural engineers and designers, enabling informed decision-making in the initial stages of architectural and structural design. This will

facilitate the integration of optimized shear wall solutions into irregular RC buildings efficiently [18, 19].

- Cost and Material Efficiency: By establishing optimized shear wall thickness distributions and placements, this research will aid in reducing unnecessary material usage and associated construction costs, promoting more economical yet structurally resilient buildings [17, 20].

1.5 Scope of Work.

The scope comprises detailed seismic analysis, configuration comparison, and structural optimisation of shear-wall systems within an irregular L-shaped reinforced-concrete (RC) high-rise. The influence of shear-wall thickness, location, and layout configuration on seismic performance is investigated using computational modelling and analytical methods in Tekla Structural Designer (TSD), in full compliance with Eurocode 8 (EC8).

1.5.1 Project Description

A 20-storey L-shaped RC building located in Malaysia (low-to-moderate seismicity) is developed, simulated, and evaluated. The selected geometry reflects common urban irregularities such as re-entrant corners and mass eccentricity. The study seeks to optimise the placement and thickness of shear walls to mitigate seismic vulnerabilities, including lateral drift, torsional irregularity, and excessive deformation.

1.5.2 Building Details and Modelling Framework

- Structure Type: Reinforced Concrete L-shaped high-rise building
- Total Height: 64.0 m (3.2 m per storey, 20 storeys)
- Plan Dimensions: 30 m × 20 m (long and short wings)
- Software: Tekla Structural Designer (TSD)
- Design Standards: Eurocode 2 (RC design) and Eurocode 8 (seismic analysis)
- Location: Malaysia (Eurocode-based seismic classification

The building is designed with realistic boundary conditions, including rigid diaphragms and fixed base supports. Structural irregularities typical of L-shaped plans are captured, including stress concentrations and torsional imbalances.

1.5.3 Shear Wall Configuration and Thickness Adjustment Strategy

Three seismic force-resisting systems (SFRS) are defined:

- Layout A: Core walls only
- Layout B: Core + Perimeter walls
- Layout C: Core + L-intersection (re-entrant corner) walls

Each configuration is analysed using an adaptive thickness strategy. Storeys initially adopt the minimum practical thickness; thickness is increased only when performance indicators (e.g., inter-storey drift, torsional irregularity, base shear) exceed EC8 limits. Table 1.1 summarises the Wall Thickness Variation Strategy by Storey.

Table 1.1 Wall Thickness Variation Strategy by Storey.

Building Height	Core Wall Thickness (mm)	Perimeter / L-Intersection Wall Thickness (mm)
Ground to 7th Floor	400, 350	400, 350, 300
8th to 13th Floor	350, 300	350, 300, 250
14th to 17th Floor	300, 250	300, 250, 200
18th to 20th Floor	250, 200	250, 200, 150

Figure 1.1 summarises the overall project workflow from model development through definition of shear-wall configurations and thickness variation to seismic analysis, comparison, and recommendations.

Figure 1.1 Project workflow from model development to final recommendations.

1.5.4 Seismic Analysis and Performance Metrics

Two analysis procedures are employed:

- Response Spectrum Analysis (RSA): to establish modal behaviour and peak seismic response.
- Equivalent Lateral Force method(ELF): to evaluate design base shear and lateral force distribution.

Each configuration–thickness case is evaluated against storey displacement, inter-storey drift ratio, base shear and its distribution; torsional irregularity coefficient

($\Delta_{max}/\Delta_{avg}$); diaphragm rotation and wall-line force concentration. Results are validated against EC8 performance limits.

1.5.5 Comparative Analysis and Final Deliverables

Performance across all cases is compared using structured data sheets and graphics. Final deliverables include:

- Identification of the optimal wall layout and thickness distribution.
- Evaluation of seismic stability and structural safety.
- Recommendations for shear wall design in irregular buildings.
- A replicable optimisation methodology for similar RC structures.

CHAPTER 2

LITERATURE REVIEW

2.1 Introduction

Seismic resilience in reinforced concrete (RC) buildings, particularly those with irregular geometries, has been a central focus in structural engineering research over the past two decades [24]. Historical seismic events provide compelling evidence that irregular buildings, characterised by torsional unbalances, suffer severe damage during earthquakes, highlighting the devastating impacts of torsional vibrations [25]. These incidents underscore the vulnerability posed by configuration irregularities, primarily due to asymmetric distributions of mass and stiffness within these structures [3].

Architectural and functional demands frequently necessitate the use of irregular building forms, significantly complicating structural responses under seismic loads. Recent studies have identified shear walls as vital components for enhancing lateral resistance in RC buildings [4], [5], [26]. However, to effectively control torsional irregularities, lateral drift, and seismic demands, the thickness, configuration, and optimal placement of shear walls require detailed investigation and careful optimisation [27].

This literature review synthesises existing knowledge on the seismic behaviour of irregular RC structures, specifically focusing on structural irregularities, their effects on seismic responses, and torsional irregularities in L-shaped buildings. The review integrates recent research findings and identifies critical gaps, guiding future investigations towards performance-based design approaches, efficient placement strategies, and advanced computational modelling techniques.

2.2 Seismic Behaviour of Irregular RC Buildings

2.2.1 Structural Irregularity and Effects on Seismic Response

Structural irregularities, including variations in plan geometry and vertical discontinuities, significantly impact the seismic performance of RC buildings. Irregularities generally induce uneven lateral displacement distributions, increased torsional effects, and stress concentrations, particularly at re-entrant corners [3], [13], [28]. According to comprehensive seismic simulations conducted by recent studies [29], irregular structures consistently demonstrate higher torsional forces due to asymmetric mass distribution compared to regular configurations.

For example, research analysing various irregular configurations revealed significant differences in fundamental dynamic characteristics such as natural periods and mode shapes, compared to regular structures [14]. Specifically, plan irregularities, notably L-shaped, T-shaped, and C-shaped configurations, lead to non-uniform stiffness distributions, which exacerbate torsional responses and stress concentrations [13], [28]. Vertical irregularities, including setbacks, introduce sudden stiffness reductions that escalate storey drift and displacement at irregularity locations, potentially jeopardising structural integrity [3].

2.2.2 Torsional Irregularities in L-shaped Structures

Among plan irregularities, L-shaped buildings are particularly vulnerable due to their high centre-of-mass eccentricity, amplifying torsional responses and resulting in elevated structural demands during seismic events [14], [23]. Several studies have observed significant increases in corner displacements and diaphragm rotations, particularly around re-entrant corners, compared to regular, symmetric buildings [18], [23].

Detailed modal analysis of L-shaped buildings indicates that the presence of re-entrant corners distinctly alters natural vibration modes, increasing the complexity and coupling of translational and torsional responses. Research findings suggest

substantial variations in natural periods (by 15–30 %) and mode shapes in irregular structures, in stark contrast to the predictable behaviour of regular buildings [14], [30].

Moreover, the torsional irregularity ratio, defined as the ratio of maximum to average lateral displacement, frequently exceeds code-prescribed thresholds in L-shaped buildings, indicating critical torsional imbalances requiring careful structural consideration [14], [29]. Empirical studies highlight significant diaphragm rotations, increasing stress concentrations at structural interfaces and potentially leading to localised damage or failure during seismic excitation [13], [23].

Overall, these findings underscore the necessity for rigorous analysis and optimisation strategies specifically tailored to mitigate torsional effects in irregularly shaped RC structures.

2.3 Shear Wall Systems in High-rise Buildings

2.3.1 Core Wall Systems

Core wall systems are widely recognised for their efficiency in enhancing structural performance, particularly in high-rise buildings subjected to seismic loads. Central core walls provide substantial lateral resistance and significantly reduce lateral displacements—up to 40 % reduction as highlighted by recent studies [17]. Additionally, symmetrically located core walls offer superior torsional resistance due to their concentrated stiffness at the centre of the building's mass [31]. Core wall systems integrate efficiently with critical architectural components such as lift shafts and stairwells, thereby optimising both structural and architectural considerations.

Despite their benefits, core wall systems exhibit certain limitations, especially when applied to irregular building configurations. Specifically, studies have indicated reduced effectiveness in L-shaped structures, primarily due to inherent asymmetries causing uneven stiffness distribution [6], [32], [33]. Moreover, core walls in irregular plans typically result in stress concentrations at re-entrant corners, complicating construction sequences and potentially escalating construction costs [33].

2.3.2 Distributed Wall Systems

Distributed shear wall systems are employed to mitigate the limitations associated with central core walls, particularly in irregular building configurations. Studies advocate distributed wall placements along building perimeters or strategic locations within the building's layout to enhance overall structural resilience [32], [34], [35]. Edge-placed shear walls have demonstrated significant advantages, including improved torsional control due to balanced stiffness distribution, effectively reducing stress concentrations at critical re-entrant corners [34]. Additionally, distributed shear wall systems increase redundancy and seismic resilience by spreading lateral load resistance across multiple elements, thus reducing vulnerability to local failures during seismic events [35].

Comparative analyses between core and distributed systems emphasise that the latter provides superior performance in irregular structures by minimising torsional irregularities and enhancing structural robustness under seismic excitations [32].

2.4 Shear Wall Thickness Optimisation

2.4.1 Uniform Thickness Approach

The uniform thickness approach involves using a consistent shear wall thickness throughout the height of the building. This approach simplifies structural design and construction processes significantly. However, research indicates that this strategy may lead to increased material usage and cost inefficiency, particularly in high-rise structures where lower floors typically require thicker walls than upper floors [17]. Although uniform thickness simplifies construction, it does not always yield optimal seismic performance due to a lack of stiffness gradation.

2.4.2 Variable Thickness Approach

Variable thickness strategies involve adjusting shear wall thickness at specific building levels, typically decreasing thickness progressively from lower to upper floors. This approach significantly enhances seismic performance by optimally distributing stiffness, thus effectively controlling displacement and storey drift.

A study of a 25-storey building in seismic zone IV demonstrated substantial reductions in lateral displacement and drift by adopting varying shear wall thicknesses, particularly when strategically positioned at mid-span locations [17]. However, this method introduces complexities in structural design and increases the construction intricacy due to the changing dimensions and detailing required at different floors.

2.4.3 Hybrid Approach

The hybrid approach integrates both uniform and variable thickness strategies, aiming to balance structural efficiency, seismic performance, and practicality in construction. By combining a consistent thickness across most of the structure with targeted variations at critical sections, this approach achieves optimal material usage and structural performance. Research has indicated that the hybrid method effectively manages construction complexity and delivers superior seismic response compared to purely uniform or purely variable thickness strategies [17]. It requires meticulous structural design considerations to balance construction feasibility with seismic optimisation.

In conclusion, selecting an appropriate shear wall thickness optimisation strategy depends heavily on specific project conditions, including seismic demand, cost constraints, and practical construction considerations. The hybrid method generally offers the most balanced approach, optimising both material efficiency and structural integrity while effectively controlling seismic-induced displacement and drift.

2.5 Computational Methods for Structural Optimisation

2.5.1 Genetic Algorithms

Genetic Algorithms (GA) have emerged as robust optimisation tools for structural engineering problems, particularly in optimising shear wall dimensions and placements in reinforced concrete (RC) buildings. Research [21] demonstrates that GA-based optimisation methods can achieve significant material efficiency improvements to 31 % material reduction by iteratively refining wall dimensions and configurations. Additionally, genetic algorithms have been effectively employed to

minimise torsional drift by optimising the sizing of structural elements such as column dimensions and shear wall thicknesses, particularly in irregularly shaped RC buildings [36]. GA achieves this by systematically adjusting structural member dimensions to minimise eccentricity between the centre of mass and the centre of rigidity, thereby enhancing the building's overall seismic performance. However, despite their effectiveness, genetic algorithms have limitations such as intensive computational demands and potential convergence on local optima rather than global solutions.

2.5.2 Response Surface Methods

Response Surface Methods (RSM) provide an alternative computational technique aimed at reducing the complexity and computational intensity inherent in traditional structural optimisation processes. Specifically, RSM approximates the objective and constraint functions derived from finite-element analyses, converting complex structural optimisation problems into simpler mathematical forms that are more easily solvable [20]. This method significantly improves computational efficiency, as evidenced by the reduction in required structural analyses by up to 87.5 % when integrated with optimisation frameworks such as Particle Swarm Optimisation (PSO). Nonetheless, despite their efficiency and accuracy benefits, RSM approaches are limited in handling highly complex, multi-variable optimisation scenarios. Their effectiveness diminishes when applied to intricate structural design challenges that involve numerous variables or heavily nonlinear relationships, posing challenges for their widespread adoption in structural engineering applications.

In summary, both Genetic Algorithms and Response Surface Methods offer powerful computational strategies for structural optimisation. While GA excels in optimising irregular and torsionally sensitive structures through iterative, population-based search mechanisms, RSM excels in efficiently approximating and simplifying complex optimisation problems. Selecting the appropriate computational method requires careful consideration of the specific structural context, computational resources available, and the complexity level of the optimisation objectives.

2.6 Current Knowledge and Research Gaps

Current research has provided valuable insights into shear wall optimisation and seismic performance enhancement for irregular RC buildings. Studies [25], [28], [39], [29], [40] have demonstrated substantial advancements in understanding the behaviour of structural systems under seismic loads. Notably, the effectiveness of various shear wall configurations, especially in controlling torsional irregularity and drift, has been extensively examined. Research has also highlighted innovative computational approaches, including Genetic Algorithms and Response Surface Methods, to optimise structural designs, significantly reducing computational time and enhancing performance.

Despite these advancements, several critical knowledge gaps and methodological limitations persist. Primarily, many studies still rely heavily on linear analysis methods, overlooking the complexities of nonlinear structural behaviour under severe seismic events. Moreover, the simplified loading conditions and the limited incorporation of realistic seismic excitations frequently undermine the generalisability of findings to real-world conditions [28], [39]. Soil–structure interaction, a crucial factor influencing seismic response, remains under-examined in most optimisation studies, potentially leading to incomplete assessments of structural safety.

Validation methodologies also exhibit notable shortcomings. Experimental validation, especially through large-scale or full-scale testing, remains scarce in literature. Most studies predominantly depend on numerical simulations and analytical models, which, although sophisticated, can contain significant uncertainties that are seldom quantified or thoroughly evaluated [39], [41]. These methodological deficiencies suggest a critical need for enhanced experimental frameworks and rigorous uncertainty quantification in computational modelling.

Research specifically targeting L-shaped buildings and other irregular configurations remains limited, despite their known vulnerabilities, particularly regarding re-entrant corner stresses and torsional effects [23], [33], [40]. Additionally, the integration of architectural constraints into shear wall optimisation has not been sufficiently

addressed, often leading to theoretically optimal but practically infeasible solutions. The long-term performance, durability, and economic viability of optimised shear wall systems also require comprehensive examination through detailed cost–benefit analyses and life-cycle assessments.

2.7 Summary

This literature review underscores the significant advancements and persistent challenges in optimising shear wall configurations for irregular RC buildings subjected to seismic loads. Studies affirm the efficacy of shear walls in improving seismic resilience, particularly in controlling lateral displacement, drift, and torsional responses. Computational techniques like Genetic Algorithms and Response Surface Methods have revolutionised structural optimisation, achieving substantial reductions in material usage and computational costs.

However, critical gaps remain, including inadequate nonlinear behaviour representation, limited soil–structure interaction analyses, and insufficient experimental validations. Future research must address these gaps by incorporating comprehensive experimental frameworks, rigorous uncertainty assessments, and multi-objective optimisation considering practical architectural constraints. Addressing these issues is vital for developing robust, efficient, and economically viable shear wall configurations, ultimately contributing to safer and more resilient urban infrastructure.

CHAPTER 3

METHODOLOGY

3.1 Introduction

The purpose of this research is to investigate and optimise shear wall configurations in an irregular L-shaped reinforced-concrete (RC) building subject to seismic loading. A quantitative, computer-based approach has been adopted to evaluate how the thickness, layout and placement of shear walls affect seismic performance. Tekla Structural Designer (TSD) has been used to model and analyse a series of wall configurations using both response spectrum analysis (RSA) and Equivalent Lateral Force method (ELF), in accordance with Eurocode 8. The methodology is structured to ensure that all models are developed consistently, analysed under identical loading conditions and assessed against the same performance criteria, thus allowing direct comparison between different design options.

3.2 Project Setup

3.2.1 Building description and geometry

The case study building is a 20-storey L-shaped RC structure representing a typical high-rise office or residential block in urban Malaysia. The principal dimensions are 30 m along the long wing and 20 m along the short wing, producing a plan irregularity with a re-entrant corner of 15 m × 10 m. Each storey is 3.2 m high, giving an overall height of 64 m. Floor systems are 250 mm thick RC slabs without beams, and columns step down in size with height: 500 mm × 500 mm from the base to the seventh floor, 400 mm × 400 mm from the seventh to the thirteenth floor, and 350 mm × 350 mm from the thirteenth to the roof. The four columns around the core follow the same thicknesses as the core walls (Figure 3.1).

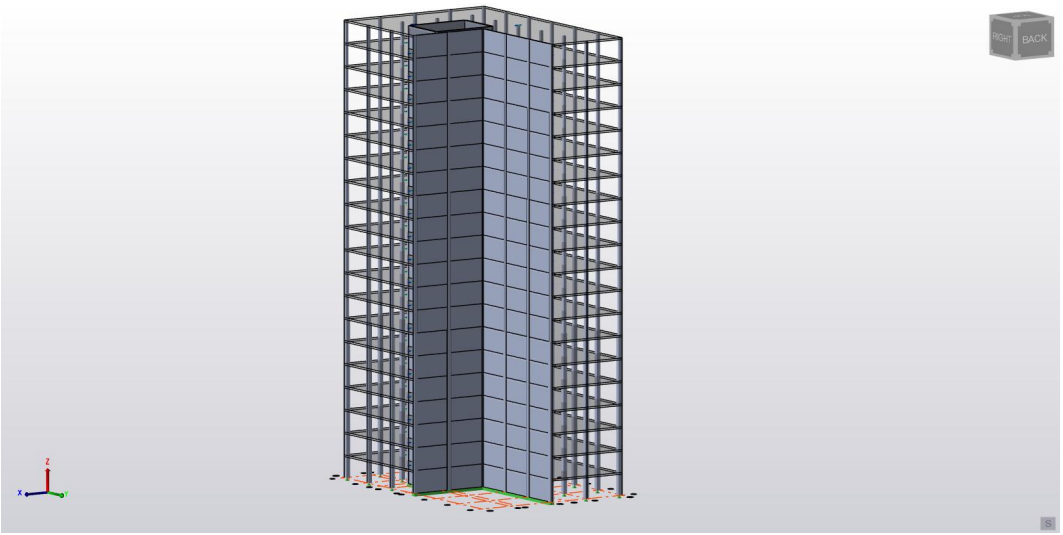

Figure 3.1 Elevation view of the 20-storey building

A 6 m × 8 m central core accommodates lifts and services; its wall thickness varies by storey according to the model type. The building is assumed to have a fixed base for analysis purposes. The location is Peninsular Malaysia, which is classed as a low-to-moderate seismic region (Figure 3.2).

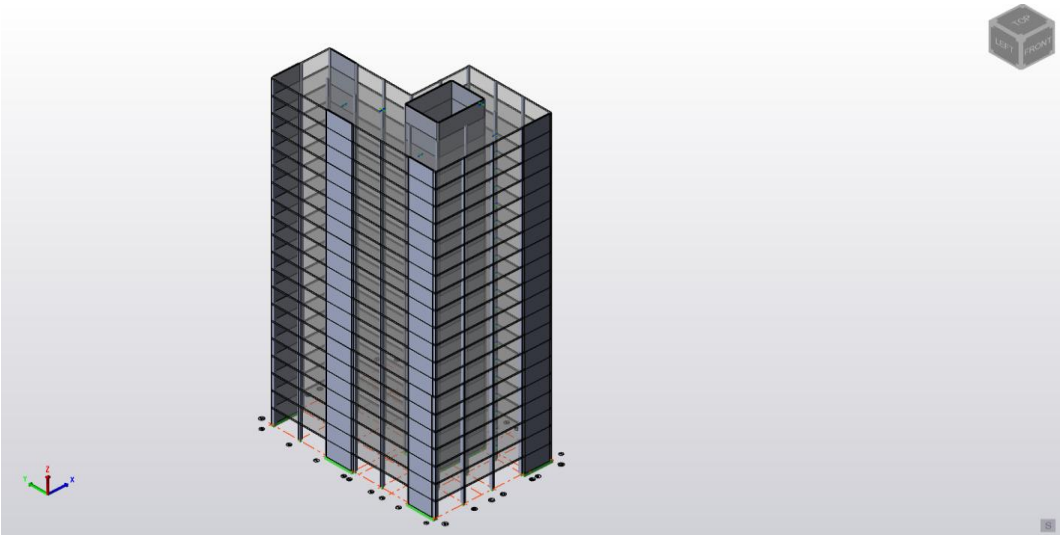

Figure 3.2 L-shaped building plan view

3.2.2 Material and structural properties

Concrete of grade C30/37 is used for all structural elements (walls, columns, slabs). The reinforcement has a yield strength of 500 MPa. The concrete elastic modulus is 35,000 MPa, Poisson's ratio is 0.20, and a damping ratio of 5 % is assumed for dynamic analysis.

Permanent loads include the self-weight of structural elements and an allowance of 2 KN/m² for finishes and partitions. The live load is 2.5 KN/m². Load cases defined in TSD comprise (Figure 3.3):

- self-weight (excluding slabs).
- slab self-weight.
- dead load (superimposed dead load and façade load);
- live load.
- seismic loads in Dir 1 and Dir 2 (X and Y directions);
- seismic torsion load cases (100 % Dir 1 + 30 % Dir 2 and 30 % Dir 1 + 100 % Dir 2).

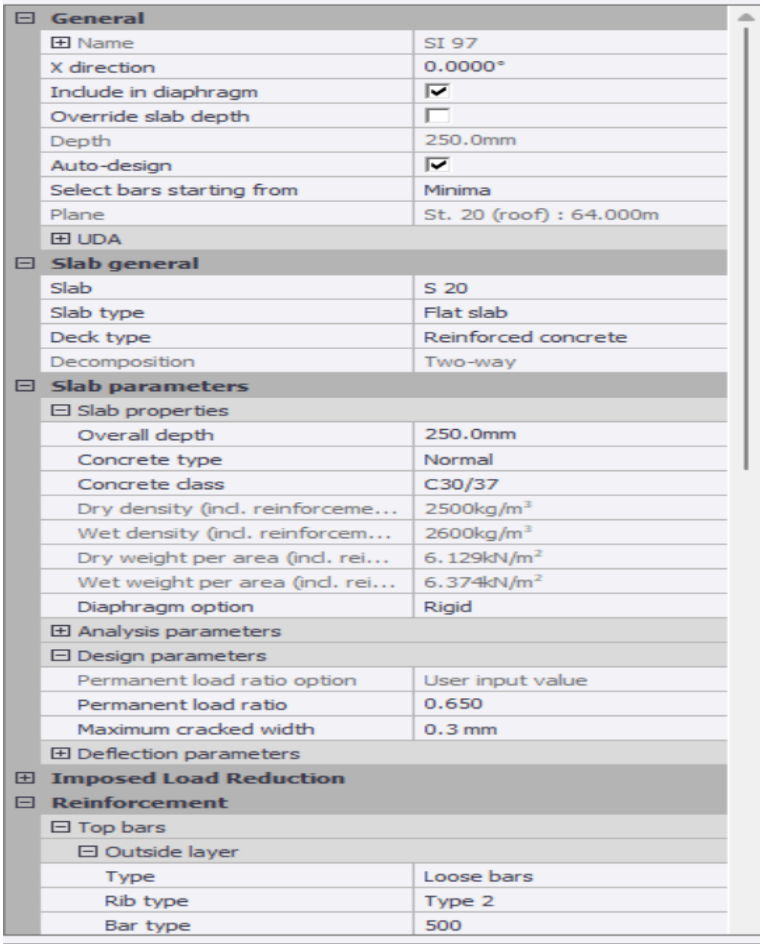

Figure 3.3 Material properties defined in TSD

3.2.3 Seismic loading criteria (Eurocode 8)

Seismic input was defined using the Tekla Seismic Wizard in line with Eurocode 8. The building height was set as 64 m and 20 storeys, with the base storey ignored in seismic calculations. Importance class II (importance factor $\gamma_i = 1.0$) and ground type C were selected. The reference peak ground acceleration is 0.06 g and the design ground acceleration is 0.588 m/s². The structural ductility class was taken as Low and the elastic spectrum type 1 was used. A behaviour factor q = 1.5 and $\alpha_u/\alpha_y = 1.2$ were specified in both directions. Live loads were included in the seismic mass at 30 % ($\psi_2 = 0.3$). Accidental torsion was accounted for by adding an eccentricity equal to ±5 % of the plan dimension perpendicular to each seismic direction (Figure 3.4).

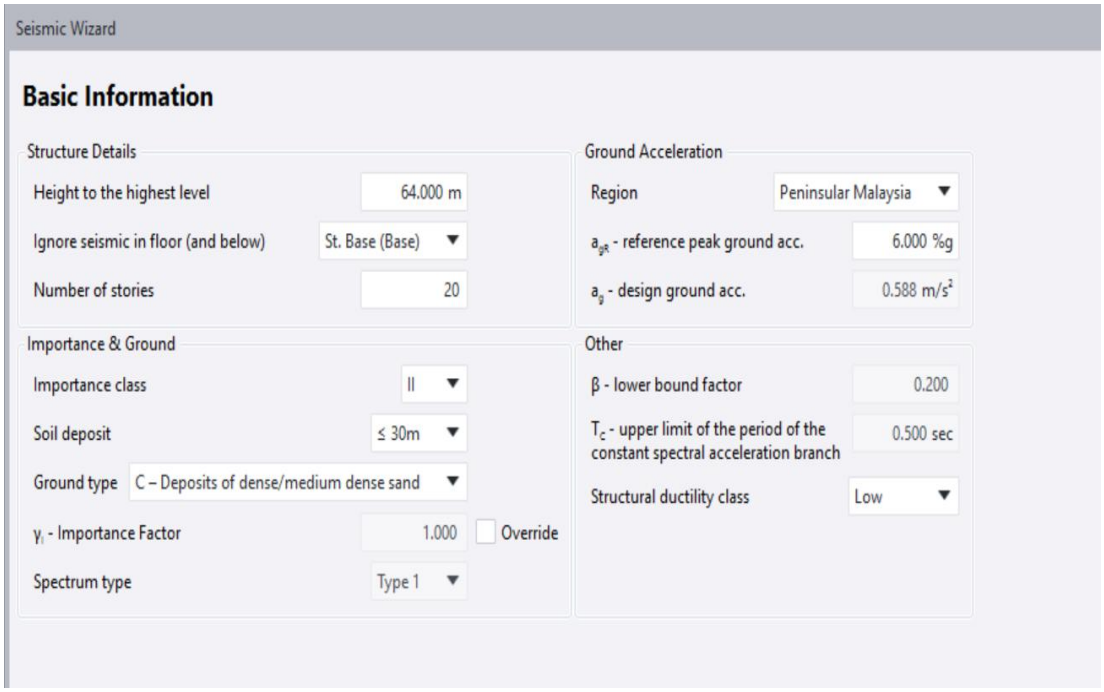

Figure 3.4 Seismic Wizard basic settings

3.2.4 Load combinations

Tekla generated a series of load combinations incorporating gravity loads and seismic actions (Figure 3.5). These include:

- seismic inertia (C1), defining the mass matrix.

• ultimate gravity combination (C2):

$$1.35\,G\ +\ 1.50\,Q\ +\ 1.50\,RQ \qquad (3.1)$$

• seismic combinations with live load (SEIS₁,) (C3–C6) applied in Dir 1 and Dir 2 with ± signs:

$$G\ +\ \psi_2\,Q\ +\ \psi_2\,RQ\ \pm\ A_{Ed}\ \pm\ EHF \qquad (3.2)$$

• seismic combinations without live load (SEIS₃,) (C7–C10) representing minimum live load conditions:

$$G\ \pm\ A_{Ed}\ \pm\ EHF \qquad (3.3)$$

These combinations were used consistently across all models in both RSA and ELF.

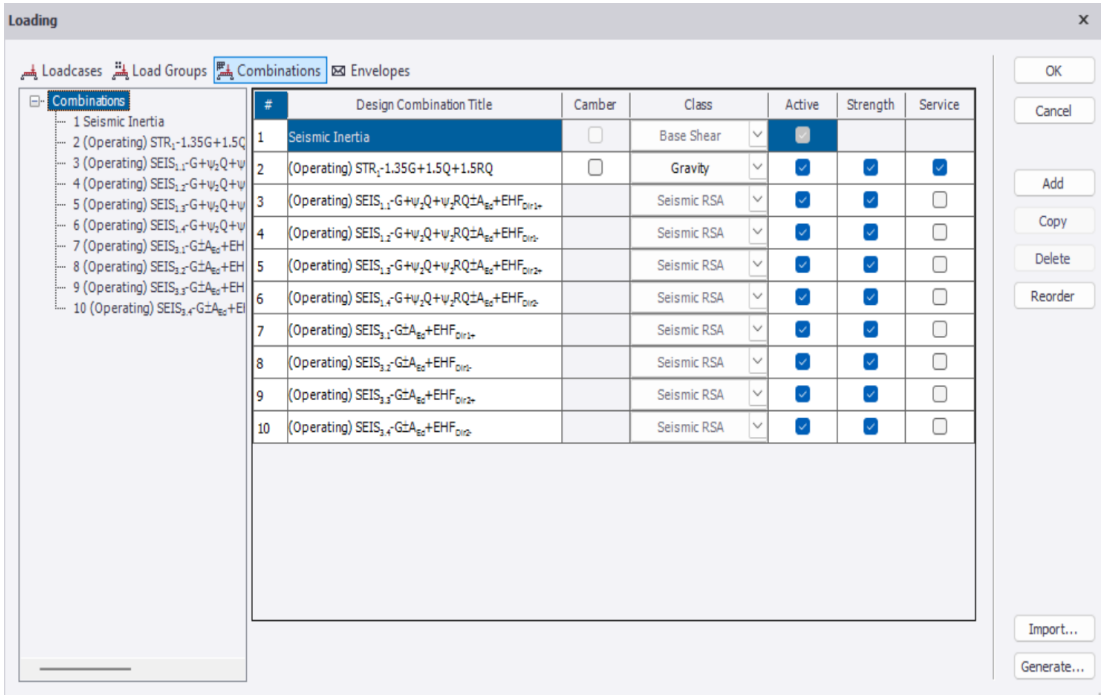

Figure 3.5 load combinations

3.2.5 Methodology flow chart

The overall methodological process is summarised in the flow chart provided (Figure 3.6). It starts with building model creation, followed by defining wall layouts (core only, core + perimeter, core + L-intersection), performing RSA and ELF, checking code compliance (drift, torsion, base shear), documenting results or adjusting thicknesses as necessary, and finally comparing all configurations to derive optimal recommendations.

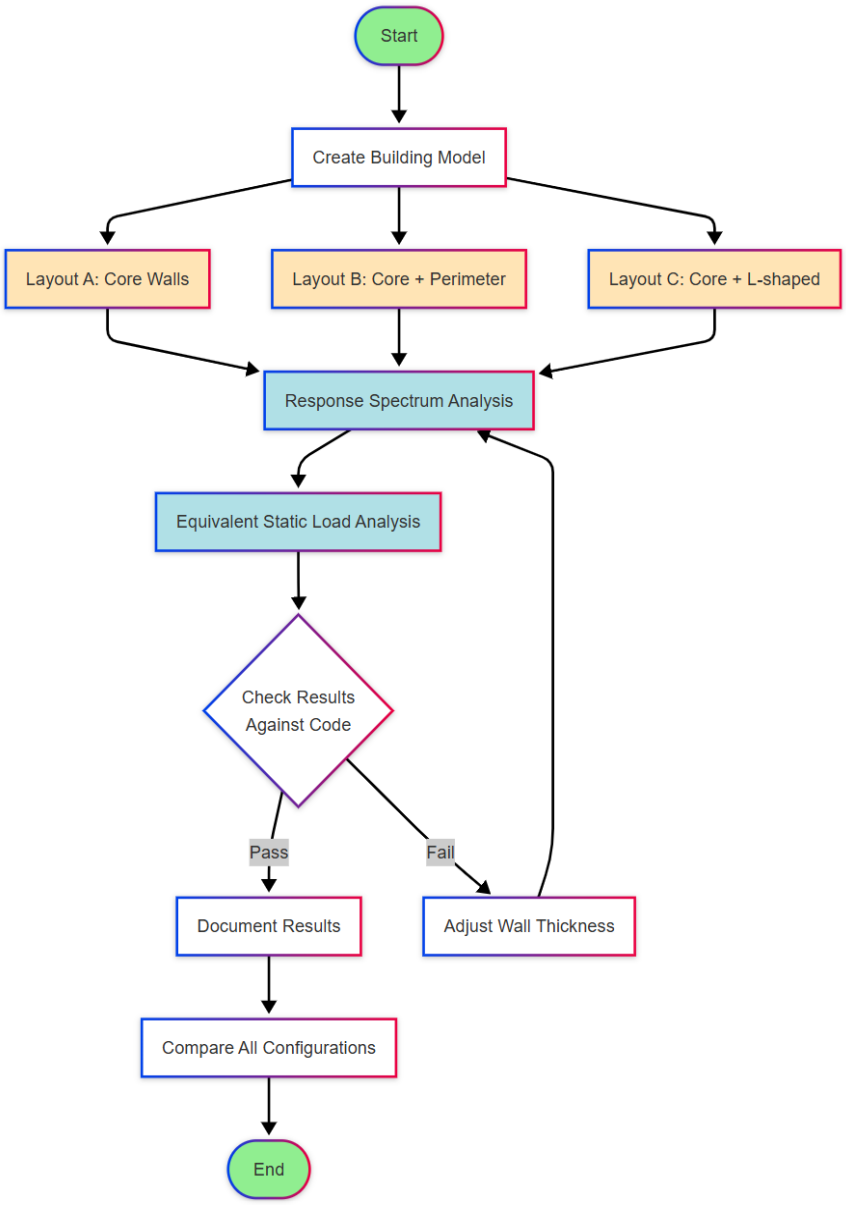

Figure 3.6 Flowchart of the Research Methodology

3.3 Shear wall configurations, thickness variations, and data collection

3.3.1 Shear wall configurations and thickness variations

Fourteen models were developed to explore three wall layout strategies:

• Core only (Models 1–2): lateral resistance provided solely by the core walls (Figure 3.7).

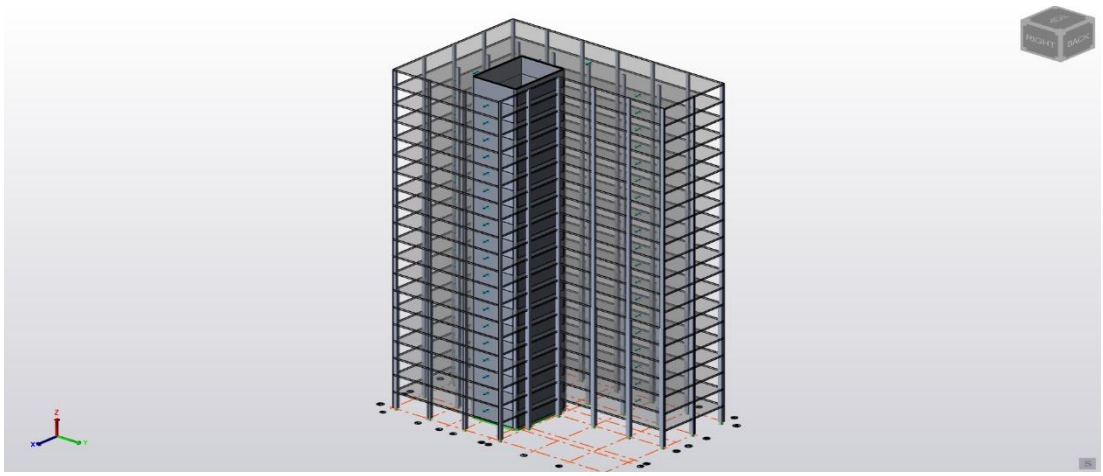

Figure 3.7 Core Only.

• Core + perimeter walls (Models 3–8): the core walls supplemented by perimeter walls of various thicknesses placed along the external bays (Figure 3.8).

Figure 3.8 Core + perimeter walls

- Core + L-intersection walls (Models 9–14): core walls with additional walls positioned at the re-entrant corner to address torsional effects (Figure 3.9).

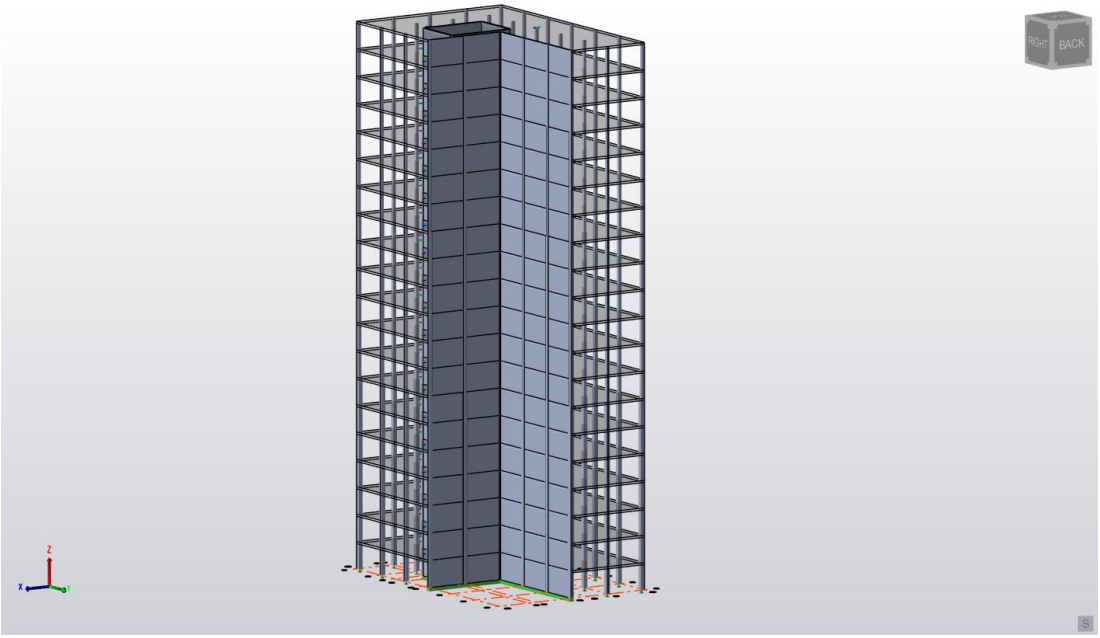

Figure 3.9 Core + L-intersection walls

Each model uses a stepped thickness profile that decreases with height to optimise material use while maintaining adequate stiffness. Table 3.1 summarises the core and added wall thicknesses assigned to each model. For each layout type, it lists the storey range and the corresponding thicknesses of the core walls and the perimeter or L-intersection walls.

Table 3.1Wall thickness by storey and layout (Models 1–14).

Model	**Layout Type**	**Floor**	**Core Thickness(mm)**	**Added Wall Type**	**Added Wall Thickness(mm)**
1	Core Only	1^{st}-7^{th}	350	/	/
		8^{th}-13^{th}	300		
		14^{th}-17^{th}	250		
		18^{th}-20^{th}	200		
2	Core Only	1^{st}-7^{th}	400	/	/
		8^{th}-13^{th}	350		
		14^{th}-17^{th}	300		
		18^{th}-20^{th}	250		

Model	Layout Type	Floor	Core Thickness(mm)	Added Wall Type	Added Wall Thickness(mm)
3	Core + Perimeter	1^{st}-7^{th}	350	Perimeter	300
		8^{th}-13^{th}	300		250
		14^{th}-17^{th}	250		200
		18^{th}-20^{th}	200		150
4	Core + Perimeter	1^{st}-7^{th}	350	Perimeter	350
		8^{th}-13^{th}	300		300
		14^{th}-17^{th}	250		250
		18^{th}-20^{th}	200		200
5	Core + Perimeter	1^{st}-7^{th}	350	Perimeter	400
		8^{th}-13^{th}	300		350
		14^{th}-17^{th}	250		300
		18^{th}-20^{th}	200		250
6	Core + Perimeter	1^{st}-7^{th}	400	Perimeter	300
		8^{th}-13^{th}	350		250
		14^{th}-17^{th}	300		200
		18^{th}-20^{th}	250		150
7	Core + Perimeter	1^{st}-7^{th}	400	Perimeter	350
		8^{th}-13^{th}	350		300
		14^{th}-17^{th}	300		250
		18^{th}-20^{th}	250		200
8	Core + Perimeter	1^{st}-7^{th}	400	Perimeter	400
		8^{th}-13^{th}	350		350
		14^{th}-17^{th}	300		300
		18^{th}-20^{th}	250		250
9	Core + L-Intersection	1^{st}-7^{th}	350	L-Intersection	300
		8^{th}-13^{th}	300		250
		14^{th}-17^{th}	250		200
		18^{th}-20^{th}	200		150
10	Core + L-Intersection	1^{st}-7^{th}	350	L-Intersection	350
		8^{th}-13^{th}	300		300
		14^{th}-17^{th}	250		250
		18^{th}-20^{th}	200		200
11	Core + L-Intersection	1^{st}-7^{th}	350	L-Intersection	400
		8^{th}-13^{th}	300		350
		14^{th}-17^{th}	250		300
		18^{th}-20^{th}	200		250
12	Core + L-Intersection	1^{st}-7^{th}	400	L-Intersection	300
		8^{th}-13^{th}	350		250
		14^{th}-17^{th}	300		200
		18^{th}-20^{th}	250		150
13	Core + L-Intersection	1^{st}-7^{th}	400	L-Intersection	350
		8^{th}-13^{th}	350		300
		14^{th}-17^{th}	300		250
		18^{th}-20^{th}	250		200
14	Core + L-Intersection	1^{st}-7^{th}	400	L-Intersection	400
		8^{th}-13^{th}	350		350
		14^{th}-17^{th}	300		300
		18^{th}-20^{th}	250		250

Specific thickness combinations are assigned to each model according to the project specification. For example, Model 1 uses core walls of 350/300/250/200 mm from base to roof and has no perimeter walls, while Model 8 uses core walls of 400/350/300/250 mm together with perimeter walls of 400/350/300/250 mm (Figure 3.10).

Figure 3.10 Wall Thickness Variation

3.3.2 Data Collection and Processing

For each analysis case and wall configuration, the following data were extracted from TSD:

• Fundamental periods and modal mass participation in Dir 1 and Dir 2 Figure (3.11)
• Base shear and storey shear distributions.
• Storey displacements and inter-storey drift ratios in both directions.
•Torsional irregularity coefficient, defined as the ratio of maximum to average lateral displacement at each floor.

• all forces (axial, shear and bending moment) along the core, perimeter and L-intersection walls.

Modal Frequencies

Mode Number	Period [sec]	Frequency [Hz]	Error [%]	Mass Participation Dir 1 [%]	Mass Participation Dir 2 [%]	Mass ParticipationZ [%]	Modal Mass [kN]
1	2.292	0.44	0.00	0.01	60.85	0.00	24798.3
2	1.979	0.51	0.00	61.14	0.01	0.00	23635.2
3	0.995	1.00	0.00	0.03	0.02	0.00	12378.2
4	0.445	2.25	0.00	0.08	20.43	0.00	21710.4
5	0.390	2.56	0.00	20.21	0.18	0.00	16359.2
6	0.319	3.14	0.00	0.94	0.35	0.00	8763.3
7	0.189	5.29	0.00	0.28	5.74	0.00	12480.8
8	0.172	5.80	0.00	3.12	1.63	0.00	10905.4
9	0.157	6.36	0.00	4.25	0.24	0.00	10711.0
10	0.112	8.90	0.00	0.26	1.89	0.00	10078.6

Figure 3.11 Modal Frequencies

These data were exported to spreadsheets for comparison. Drift profiles were plotted against storey height, and shear distributions were charted to assess how loads are shared among the walls. Modes with cumulative mass participation below 90 % were excluded to ensure completeness (Figure 3.12).

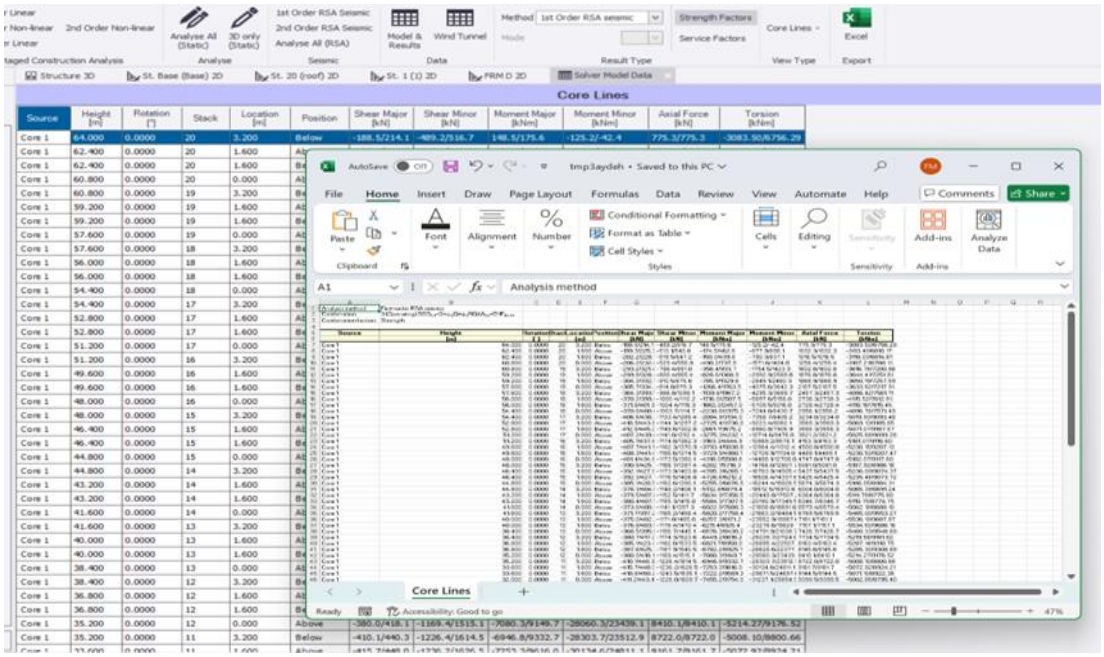

Figure 3.12 Data Collection and Processing

3.4 Analysis Methods

3.4.1 Response spectrum analysis (RSA)

A modal analysis was first performed to extract natural periods, mode shapes and modal participation factors. The EC8 Type 1 response spectrum was then applied in the X and Y directions. Modal results were combined using the Complete Quadratic Combination (CQC) method and the 100 % + 30 % directional rule. Accidental torsion was included by shifting the mass centre by ±5 %. Outputs include base shears, storey shears, inter-storey drifts, torsional irregularity indices and integrated wall forces (Figure 3.13).

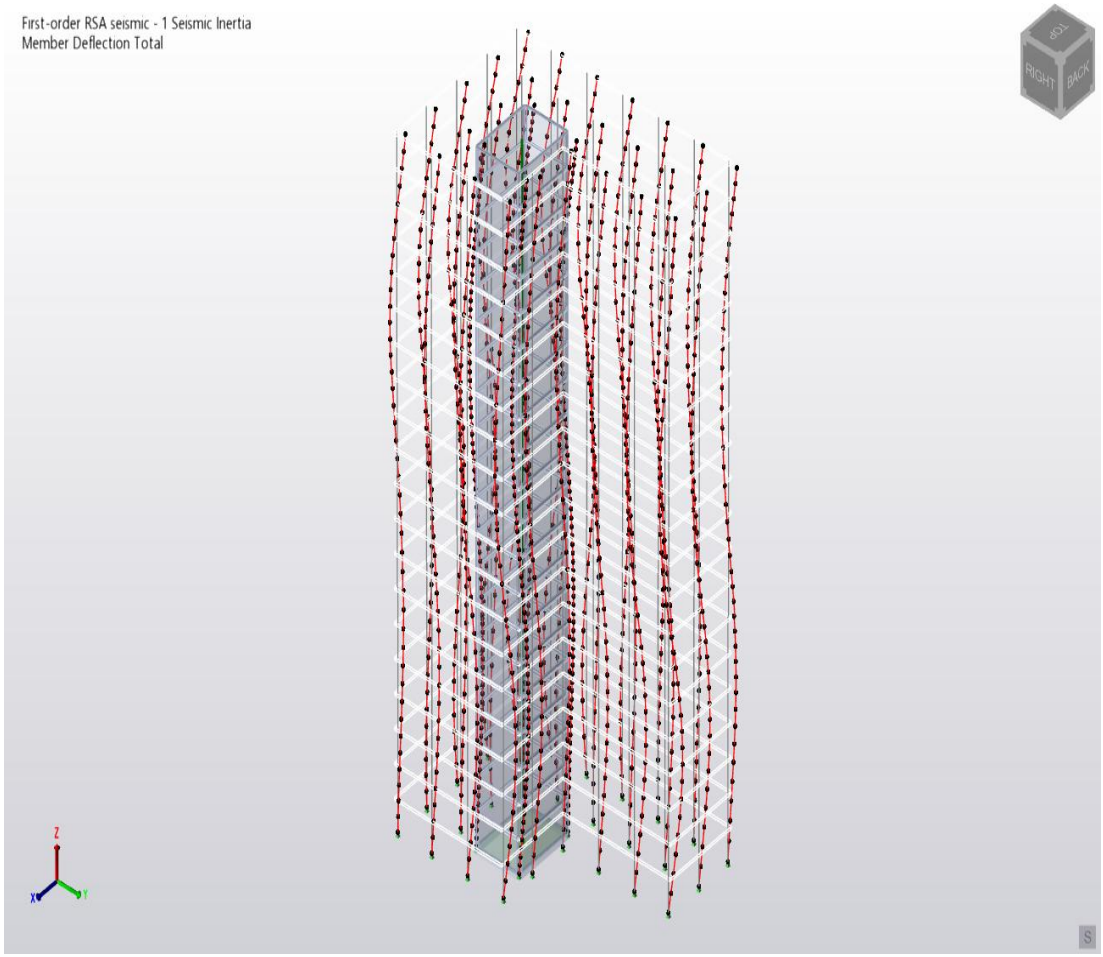

Figure 3.13 Response Spectrum Analysis (RSA)

3.4.2 Equivalent Lateral Force method (ELF)

A simplified method was used for comparison. The fundamental period was estimated using the EC8 formula

$$T_1 = C_t \cdot H^{3/4} \tag{3.4}$$

and the design base shear was computed accordingly. Lateral forces were distributed along the height proportional to the product of storey mass and height. Results from ELF provide shear distribution, lateral displacements and drifts, serving as a benchmark to validate the RSA outputs.

3.5 Performance evaluation and validation

3.5.1 Performance evaluation metrics

Performance was assessed against Eurocode 8 criteria. The maximum inter-storey drift ratio was required to be below 0.5 % for the damage limitation state. The torsional irregularity ratio ($\Delta_{max}/\Delta_{avg}$) was required to be less than 1.2 to avoid torsional irregularity. Base shear from RSA was compared with the minimum design base shear to ensure adequacy; differences between RSA and ELF were checked to be within 20 %. Modal mass participation in each principal direction needed to exceed 90 %.

3.5.2 Validation of analysis results

Where wall thickness was excessive relative to drift requirements, iterative reductions were considered; where drift or torsional limits were exceeded, thicknesses were increased. The final comparison ranked models by stiffness, drift control, torsional performance and material efficiency. Cross-checks between RSA and ELF results were performed to verify that base shears and displacements were consistent; analytical periods were compared with empirical estimates, and mass participation ratios were verified. Any model failing to meet the validation criteria was refined until compliance was achieved.

CHAPTER 4

RESULT AND DISCUSSION

4.1 Introduction

This chapter presents the analytical results obtained from the fourteen structural models introduced in Chapter 3. The discussion focuses on the dynamic and seismic response of the buildings when subjected to earthquake loading, evaluated using both the Equivalent Static Load Analysis (ELF) and Response Spectrum Analysis (RSA) procedures in accordance with Eurocode 8. Emphasis is placed on the influence of wall configuration and thickness on the fundamental periods, modal mass participation ratios, lateral displacements, and torsional behaviour. The findings are interpreted in the context of structural design implications for irregular reinforced-concrete buildings.

4.2 Model Summary

A total of fourteen analytical models were prepared in Tekla Structural Designer (TSD). The models were categorised into three distinct groups based on the adopted seismic force-resisting system (SFRS):

- Models 1–2: Core-only systems, where the central reinforced-concrete core walls provide the sole lateral resistance.
- Models 3–8: Core plus perimeter wall systems, in which additional shear walls were distributed along the external bays to provide stiffness around the building footprint.
- Models 9–14: Core plus L-intersection wall systems, in which shear walls were introduced at the re-entrant corner of the L-shaped plan to enhance torsional restraint.

Each group was further sub-categorised by varying wall thickness profiles, reducing in steps with building height. This was undertaken to reflect practical construction

practice while allowing the influence of both layout and thickness to be assessed. A schematic of the three configurations is shown in Figure 4.1

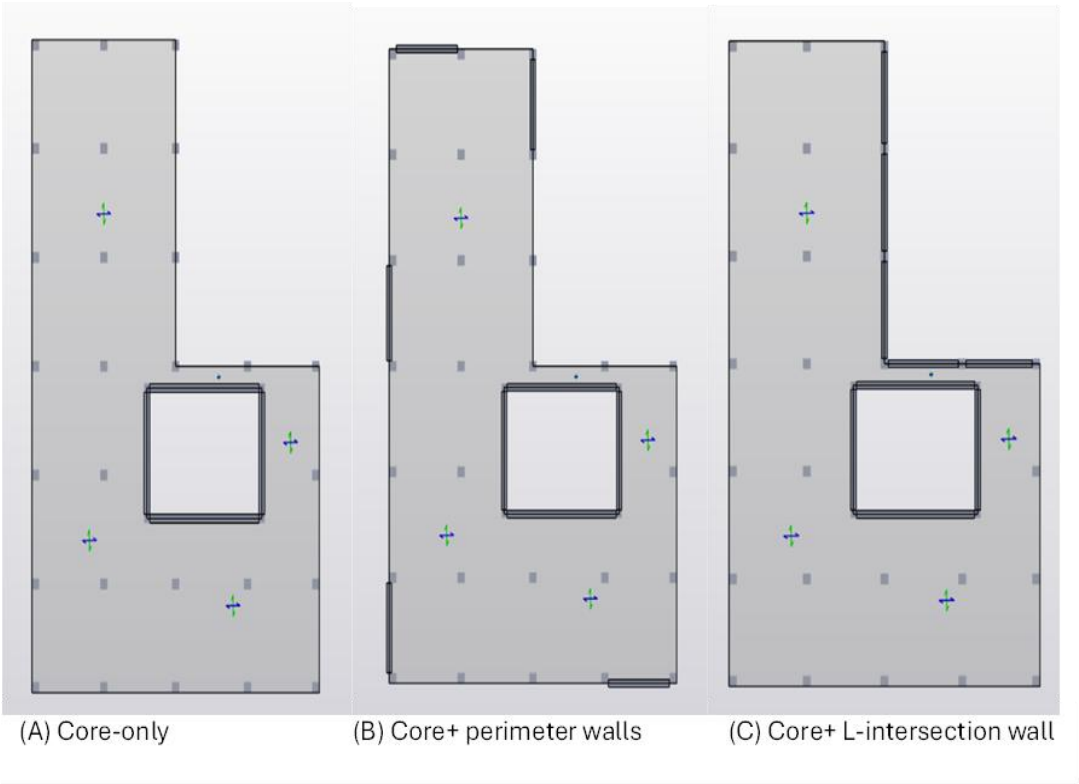

Figure 4.1 Plan view of the L-shaped building with core, perimeter, and L-wall positions.

4.3 Dynamic Characteristics

The dynamic properties of the models were evaluated through modal analysis. Of particular significance are the fundamental periods in each principal direction and the distribution of modal mass participation among the translational and torsional modes. These parameters govern the effective seismic response of the structure and provide a basis for assessing stiffness, regularity, and torsional sensitivity.

4.3.1 Fundamental Periods and Mass Participation

The fundamental period of a structure is inversely proportional to its lateral stiffness; hence, stiffer systems exhibit shorter periods. The modal analysis results (Table 4.1, Figure 4.2, and Figure 4.3) confirm this principle and reveal three consistent behavioural themes.

Table 4.1 Modal analysis results-fundamental periods and mass participation (Dir1/ Dir2)

Model ID	Layout Type	Fundamental period Dir 1 (s)	Mass participation Dir 1 (%)	Fundamental period Dir 2 (s)	Mass participation Dir 2 (%)
1	Core Only	2.187	61.56	2.753	61.64
2		2.044	61.71	2.576	61.78
3	Core+ Perimeter	2.097	60.98	2.401	60.69
4		2.105	60.99	2.400	60.72
5		2.113	61.01	2.399	60.75
6		1.979	61.14	2.292	60.85
7		1.988	61.16	2.292	60.87
8		1.996	61.17	2.293	60.89
9	Core + L-Intersection	1.869	44.51	1.331	33.76
10		1.845	45.20	1.297	29.31
11		1.824	45.73	1.272	24.08
12		1.798	43.81	1.297	38.34
13		1.778	44.65	1.258	36.24
14		1.760	45.29	1.227	33

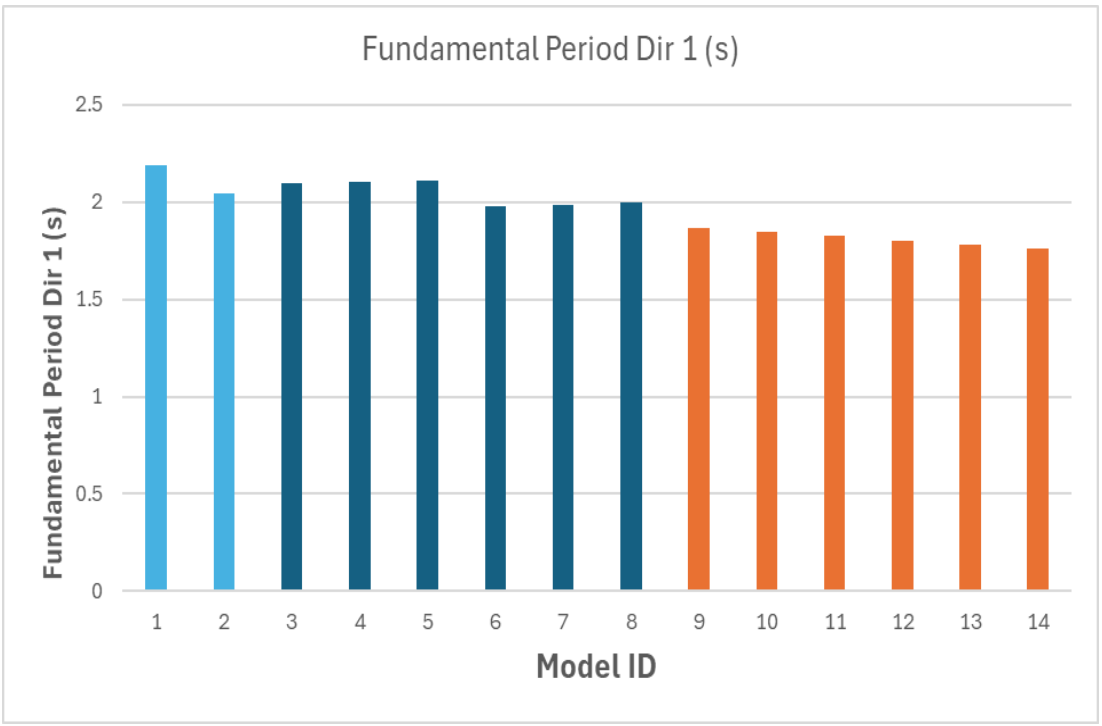

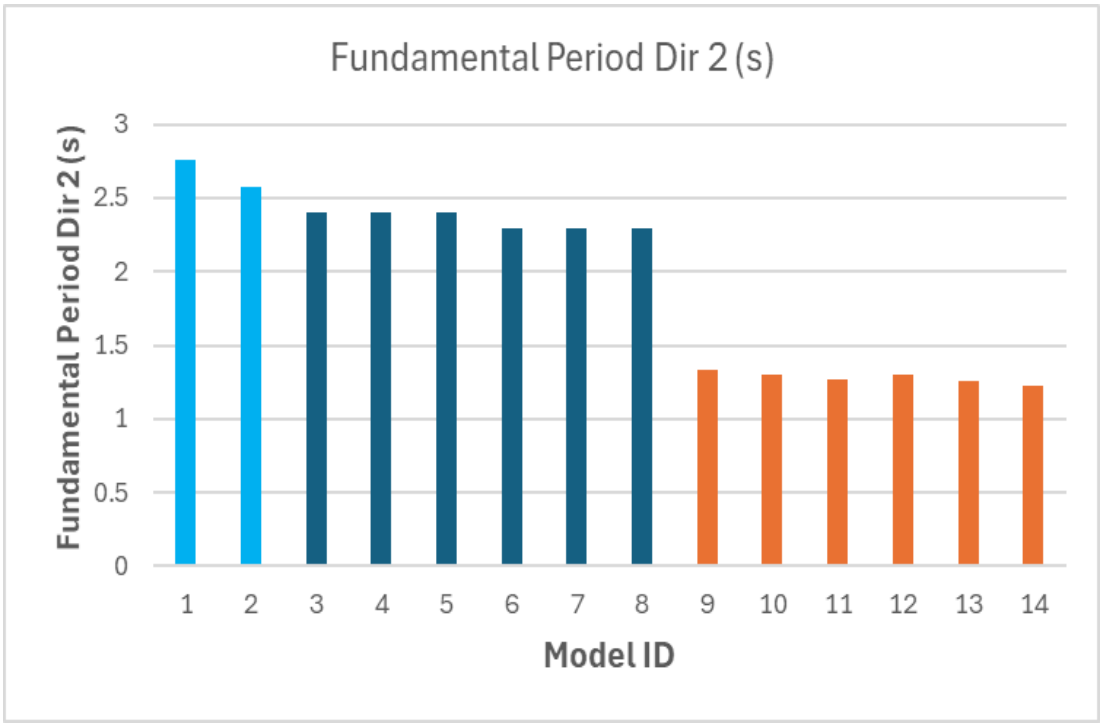

Figure 4.2 Comparison of fundamental period in Dir 1 and Dir 2 (s), Models 1–14.

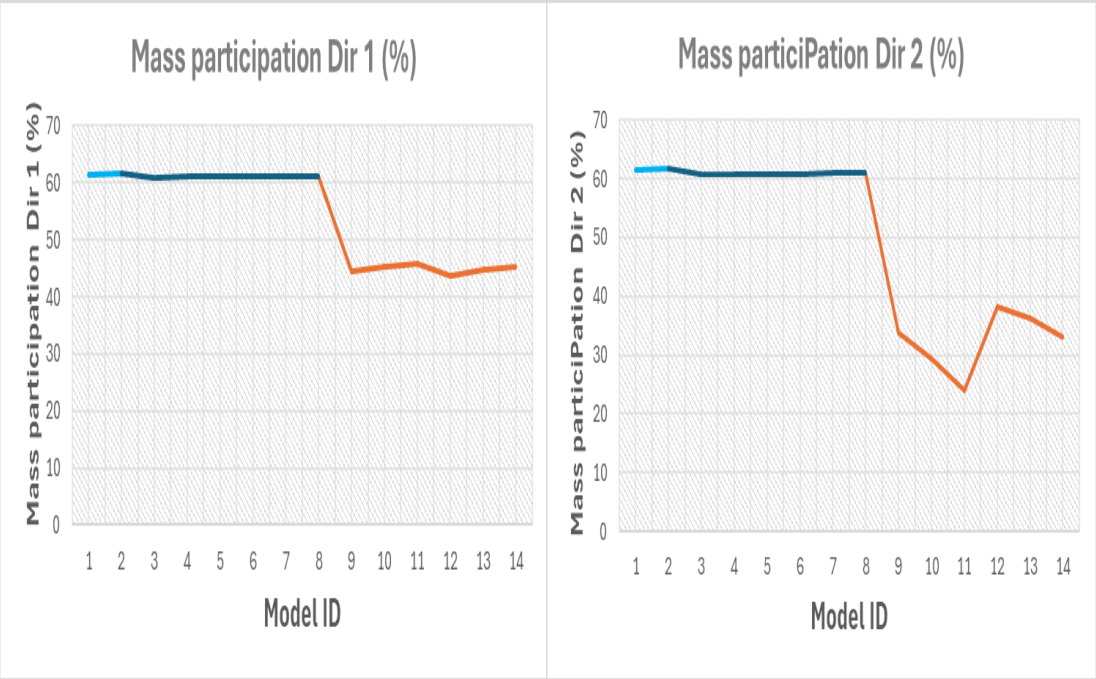

Figure 4.3 Comparison of Mass Participation in Dir 1 and Dir 2 (%), Models 1–14

Stiffness Trends

• Core-only models (1-2): These exhibited the longest periods, approximately 2.1 s in Dir 1 and 2.4-2.8 s in Dir 2. The lateral stiffness was provided solely by the core, resulting in flexible behaviour.

• Core + Perimeter walls (3-8): The introduction of perimeter walls reduced the periods modestly to around 2.0-2.1 s in Dir 1 and 2.3-2.4 s in Dir 2. For instance, Model 6 (300/250/200/150 mm walls) achieved 1.979 s in Dir 1 and 2.292 s in Dir 2, demonstrating the benefit of distributed stiffness.

• Core + L-intersection walls (9-14): These produced the most dramatic reduction, with Dir 1 periods of 1.76-1.87 s and Dir 2 periods of 1.23-1.33 s. In the short-wing direction, the period was nearly halved relative to the core-only case, reflecting a step change in rigidity.

Torsional Behaviour

- In core-only and perimeter-wall models, the first translational mode mobilised around 60 % of the seismic mass in each direction, indicating dominance of a single sway mode. RSA interpretation is thereby simplified, although susceptibility to torsional irregularity is increased.
- In L-intersection models, the first translational mode in Dir 2 no longer appeared as the fundamental mode. Instead, it shifted to Mode 2 with participation as low as 24-38 %. For example, Model 9 (core: 350-300-250-200 mm; L-walls: 300-250-200-150 mm) achieved periods of 1.869 s (Dir 1) and 1.331 s (Dir 2), with mass participation of 44.5 % and 33.8 % respectively. Strong torsional coupling is evidenced, and additional modes are required in RSA to capture 90 % cumulative participation.

Material Efficiency

It is indicated by the results that increasing wall thickness beyond 350 mm yields diminishing returns in stiffness, particularly for core-only and perimeter systems. In perimeter models, 350 mm represents an effective threshold. In L-intersection systems, even 200-250 mm thick walls provide substantial torsional restraint, making them more efficient in terms of material use.

Discussion of results

The influence of wall configuration on the building's dynamic characteristics is highlighted by the comparative evaluation of fundamental periods and mass participation ratios across the 14 models. Core-only systems exhibit the longest periods and lowest mass participation, reflecting their reduced stiffness and limited control of higher-mode effects. Introducing perimeter walls significantly shortens the periods and enhances participation ratios, indicating a more efficient and dynamically balanced system. In contrast, the addition of L-intersection walls provides even greater stiffness and period reduction, but this comes at the expense of increased torsional sensitivity and uneven mass participation between the two principal directions. Overall, it is suggested by the results that while perimeter walls achieve a favourable balance between stiffness and dynamic efficiency, L-intersection walls, despite their apparent stiffness advantage, may introduce irregularities that could compromise seismic performance.

4.3.2 Mode shapes

To complement the modal periods and mass participation results, mode-shape profiles were examined for representative models from each shear-wall layout. In each case, the first two modes were plotted as translation in the global X and Y directions and rotation about the vertical axis against storey level. These plots reveal how the building deforms in its fundamental and second vibration modes and whether any soft-storey or torsional behaviour is present. Models 1, 4 and 9 were selected as representatives of the Core-only, Core + Perimeter, and Core + L-intersection layouts, respectively, and their mode shapes were reviewed in detail. The remaining models exhibited mode-shape patterns like those of the most appropriate representative.

Core-only layout (Model 1). In the fundamental mode [Figure 4.4], the red curve (Y-translation) dominates the response, decreasing smoothly from base to roof, while both the blue (X-translation) and green (torsional rotation) curves lie close to the horizontal axis. This indicates that the first vibration mode is almost a pure sway along the long wing of the building; there is no significant twisting or movement in the short wing. In the second mode [Figure 4.5], the situation is reversed: the blue curve (X-translation) dominates, falling linearly from the base to the roof, and the Y-translation and torsional components are negligible. Thus, the building's second vibration mode is a pure sway along the short wing. Taken together, these results show that, despite the L-shaped plan, the first two modes of the core-only model are translational and uncoupled; torsional participation is confined to higher modes.

Figure 4.4 Model 1 (core-only), Mode 1 — UX, UY, Rz versus Level.

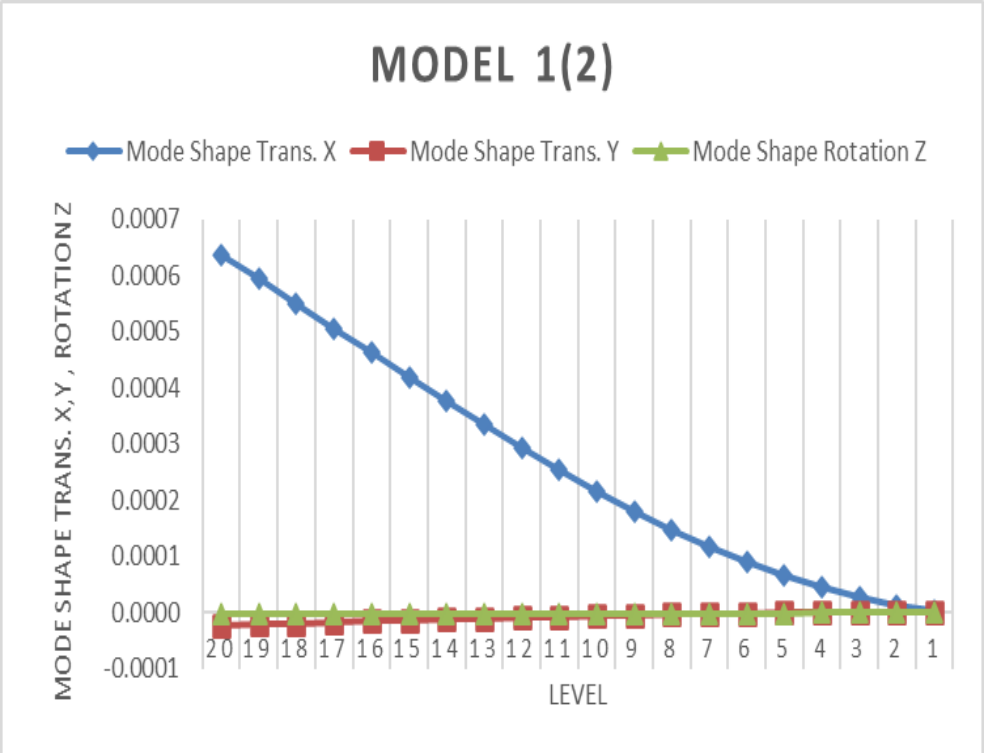

Figure 4.5 Model 1 (core-only), Mode 2 -UX, UY, Rz versus Level.

Core only with increased thickness (Model 2) and Core + Perimeter layouts (Models 3-7). Increasing the Core wall thickness alone (Model 2) [Figure 4.6 and Figure 4.7] or adding perimeter walls (Models 3-7) yields almost identical mode shapes. The first mode is an essentially pure translation in the Y-direction; both the X-translation and torsional rotation are negligible, confirming that the building sways in a single plane without twisting. The second mode is dominated by X-translation, with the Y and torsional components effectively zero. Hence, adding perimeter walls or thickening the core does not change the direction of the dominant sway; it suppresses the torsional response that was present in the core-only model. In the most heavily walled perimeter configuration (Model 8), the second mode [Figure 4.8] exhibits a pure X-translation with the Y and rotational curves lying on the horizontal axis. The negative slope in the X-curve simply denotes a reversal of motion direction relative to the first mode; it does not affect the interpretation.

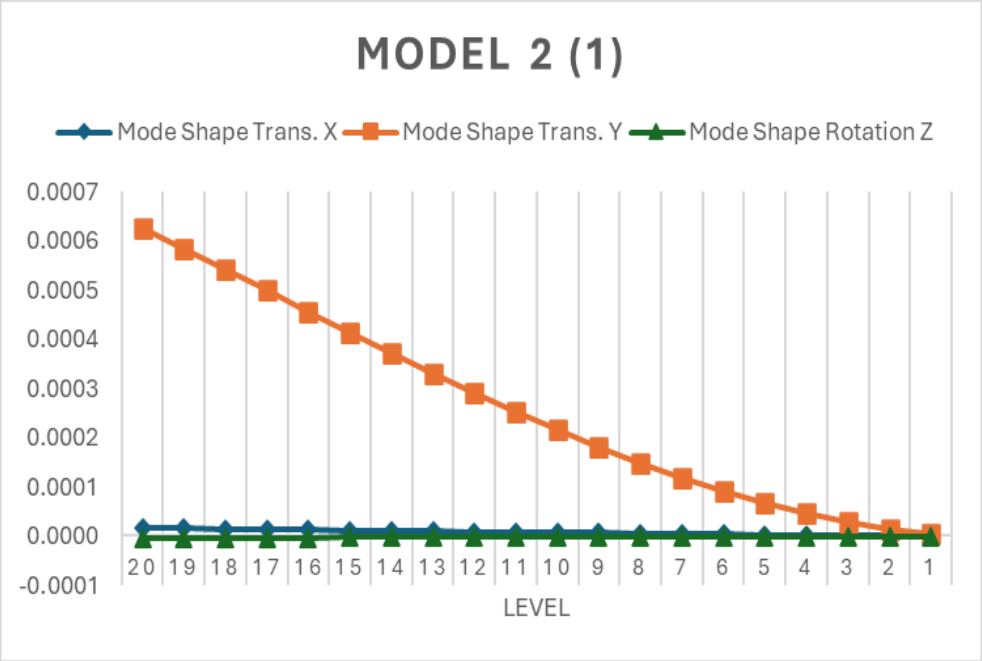

Figure 4.6 Model 2 (core-only), Mode 1- UX, UY, Rz versus Level.

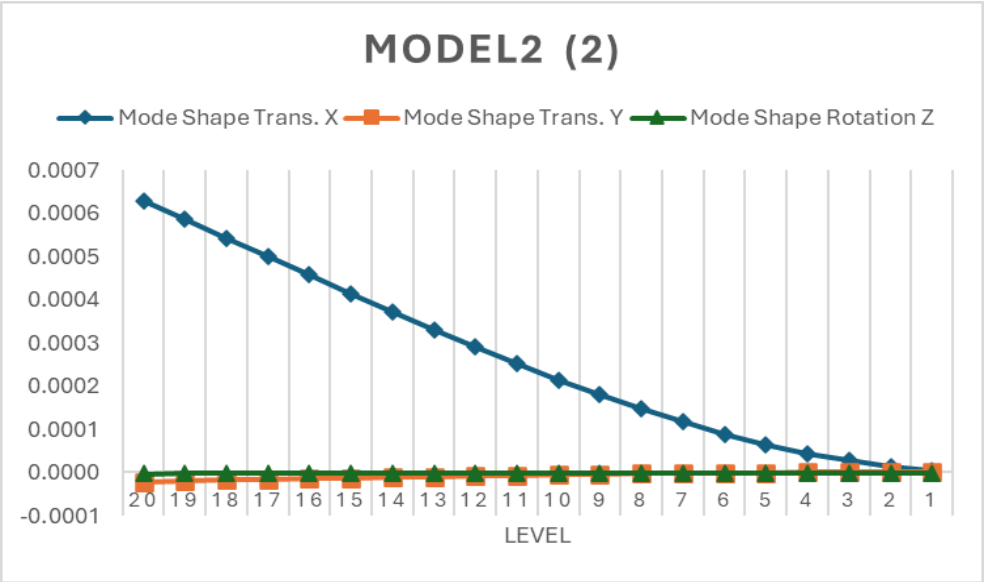

Figure 4.7 Model 2 (core-only), Mode 2- UX, UY, Rz versus Level

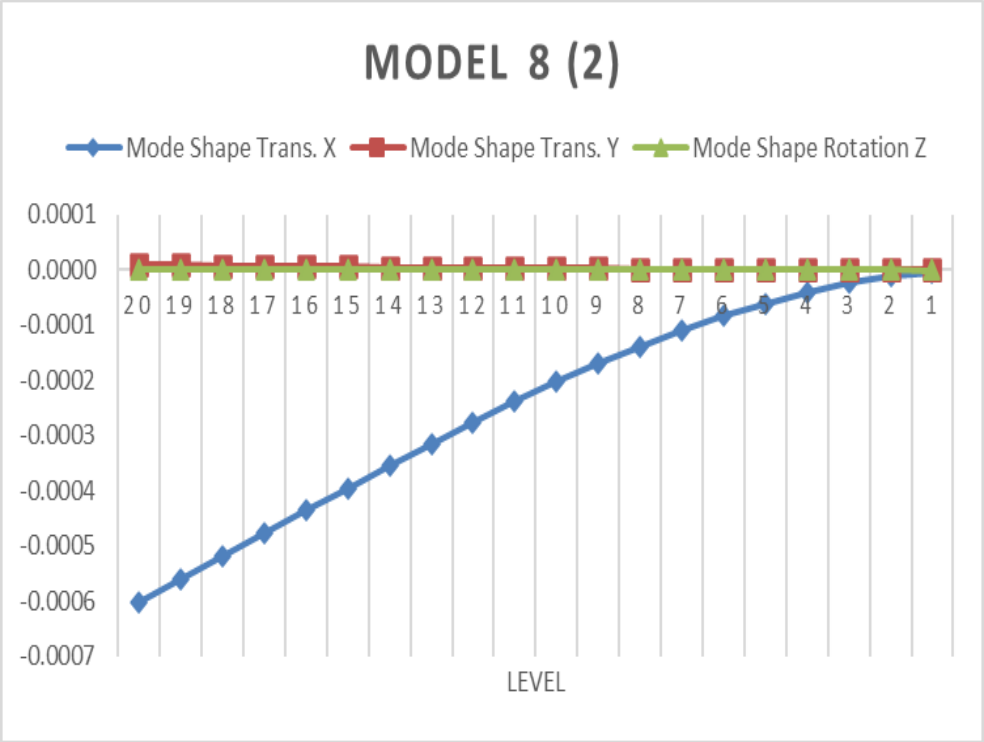

Figure 4.8 Model 8 (core + perimeter layout), Mode 2 -UX, UY, Rz versus Level

Core +Perimeter layout (Model 4). Model 4, representing the Core + Perimeter layout, is shown in Figures 4.9 (Mode 1) and 4.10 (Mode 2). The first mode shows almost pure Y-translation; the rotation curve lies on the axis, indicating that torsion has been suppressed completely. The second mode is a pure X-translation. The linearity of the

mode-shape profiles from roof to base confirms that the stepped wall thickness has not produced any soft-storey effects.

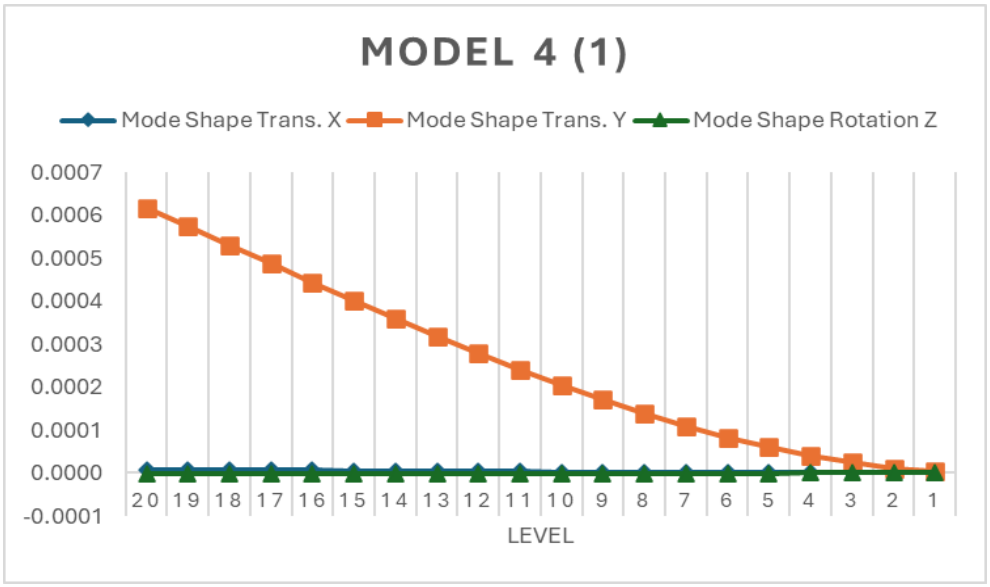

Figure 4.9 Model 4 (core + perimeter layout), Mode 1- UX, UY, Rz versus Level

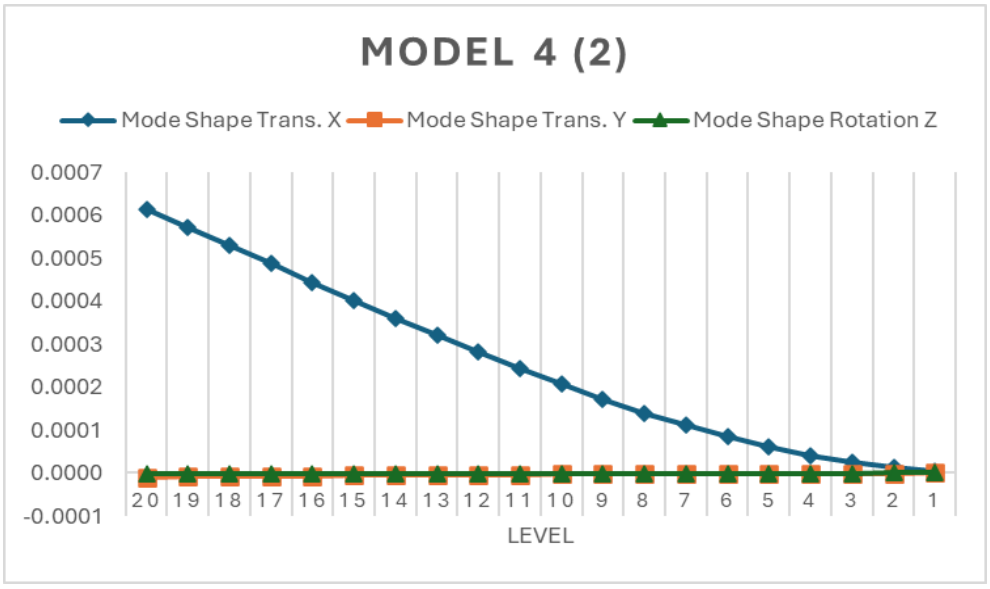

Figure 4.10 Model 4 (core + perimeter layout), Mode 2 -UX, UY, Rz versus Level

Core + L-intersection layout (Models 9–14). Locating walls at the re-entrant corner changes the modal hierarchy. In Model 9 [Figure 4.11], the first mode is dominated by X-translation, while the second mode [Figure 4.12] is dominated by Y-translation; torsional rotation remains negligible in both. This reversal of modal order occurs because the L-intersection walls stiffen the short wing more than the long wing.

All other L-intersection models (10–14) exhibit the same pattern: the first two modes are pure translations in orthogonal directions, with no significant torsional component. This confirms that the corner walls effectively control twist and rearrange the relative stiffness between the two wings.

Figure 4.11 Model 9 (core + L-intersection layout), Mode 1 -UX, UY, Rz versus Level

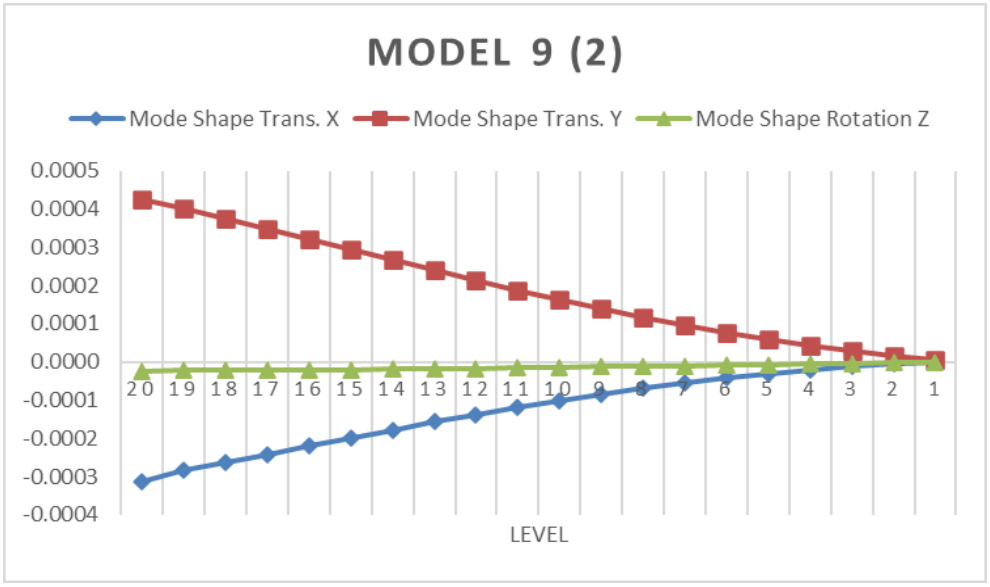

Figure 4.12 Model 9 (core + L-intersection layout), Mode 2 -UX, UY, Rz versus Level

Across all models, the mode-shape profiles are smooth and monotonic, with no abrupt changes in slope. This demonstrates that the tapered wall thickness does not induce

soft-storey behaviour. Torsional components appear only in higher modes of the core-only model; the inclusion of perimeter or L-intersection walls eliminates torsional participation in the first two modes. The mode-shape analysis, therefore, reinforces the importance of wall placement: distributed walls along the perimeter or at the re-entrant corner not only increase stiffness and shorten periods but also decouple torsional motion, leading to a more regular seismic response.

4.4 Comparison of Shear-Wall Configurations

4.4.1 Base Shear and Storey Shear Distribution

Base Shear Comparison

The base shear for each model was extracted in both principal directions from the pure seismic load-cases (Seismic Dir 1 and Seismic Dir 2) and from the RSA Combined (CQC) load-cases. These values are summarised in Table 4.2. For the ELF method, the base shear reflects the lateral forces derived directly from the code-prescribed formula; for RSA, it represents the combined effect of the modal responses. A consistent increase in base shear is observed as wall stiffness and area are increased. Core-only models (1-2) display the lowest base shear because lateral resistance is provided solely by the central core. Introducing perimeter walls (Models 3-8) raises the base shear in both directions; the increase is more pronounced in the long-wing direction because the additional walls distribute stiffness around the plan. L-intersection models (9-14) exhibit the highest base shears, particularly in Direction 2, because the corner walls substantially stiffen the short wing and attract more load. In most cases, the RSA base shear slightly exceeds the ELF base shear. In several L-intersection models, the RSA base shear in Direction 2 falls below 85 % of the ELF base shear; Eurocode 8 would require those RSA results to be scaled up for design, but no scaling has been applied in this study. The data, therefore, highlight where the dynamic analysis underestimates the ELF demand.

Table 4.2 Base Shear Comparison (ELF and RSA)

Model ID	ELF base shear Dir 1 (KN)	ELF base shear Dir2(KN)	RSA base shearDir1(KN)	RSA base shear Dir2(KN)	Observation
1	1803.2	1069.1	2068.3	1624.6	Core only; RSA > ELF; system flexible in Dir 2
2	1990.8	1263.0	2176.7	1816.6	Thicker core; moderate increase in both directions
3	2231.5	1756.8	2547.0	2396.9	Perimeter walls; pronounced rise in Dir 2
4	2271.9	1793.1	2598.2	2435.1	Slight increase over Model 3
5	2311.6	1828.4	2646.8	2498.4	Heaviest perimeter walls; diminishing returns
6	2410.2	1963.2	2637.4	2470.0	Heavier core with light perimeter; balanced
7	2451.2	2000.2	2684.6	2523.0	Balanced core and perimeter; the highest of the perimeter set
8	2491.4	2036.0	2731.4	2575.6	Marginal gain; approaching stiffness saturation
9	2441.1	3442.2	2191.3	2195.3	L-intersection stiffens short wing; RSA < 0.85 ELF in Dir 2
10	2519.3	3602.1	2237.4	2291.2	Like Model 9; moderate Dir 1 increase
11	2596.2	3741.4	2282.4	2407.0	Heaviest L-intersection; very high Dir 2 base shear
12	2593.1	3604.4	2255.7	2295.2	Heavy core with lighter L-walls; balanced
13	2670.6	3787.3	2297.3	2377.3	Intermediate case; RSA < 0.85 ELF in Dir 2
14	2746.7	3955.2	2343.5	2458.4	Maximum stiffness; RSA < 0.85 ELF in Dir 2

Models 1–8 show a progressive increase in base shear as wall thickness and perimeter stiffness are increased. Models 9–14 exhibit much higher base shears in Dir 2 because the L-intersection walls greatly stiffen the short wing. While the RSA base shear generally exceeds the ELF base shear, the opposite occurs in Dir 2 for the L-intersection models: the RSA values are below 85 % of the ELF values. Eurocode 8 requires scaling of RSA results in such cases to avoid underestimating seismic demand; in this study, the differences are acknowledged, but no scaling has been applied.

- **Storey Shear Distribution**

Figures 4.13-4.18 plot the storey shear distribution for Models 1, 3 and 11 under both ELF and RSA. Each graph shows the sum of shear in Dir 1 and Dir 2 against storey level.

Model 1-ELF (Figure 4.13). The ELF curves rise almost linearly from the roof to the base. Dir 1 shears are higher than Dir 2 shears at every floor because the long wing has greater inertia. A slight plateau appears in the uppermost levels of Dir 1, reflecting the reduced core thickness at the top; Dir 2 follows a smoother gradient.

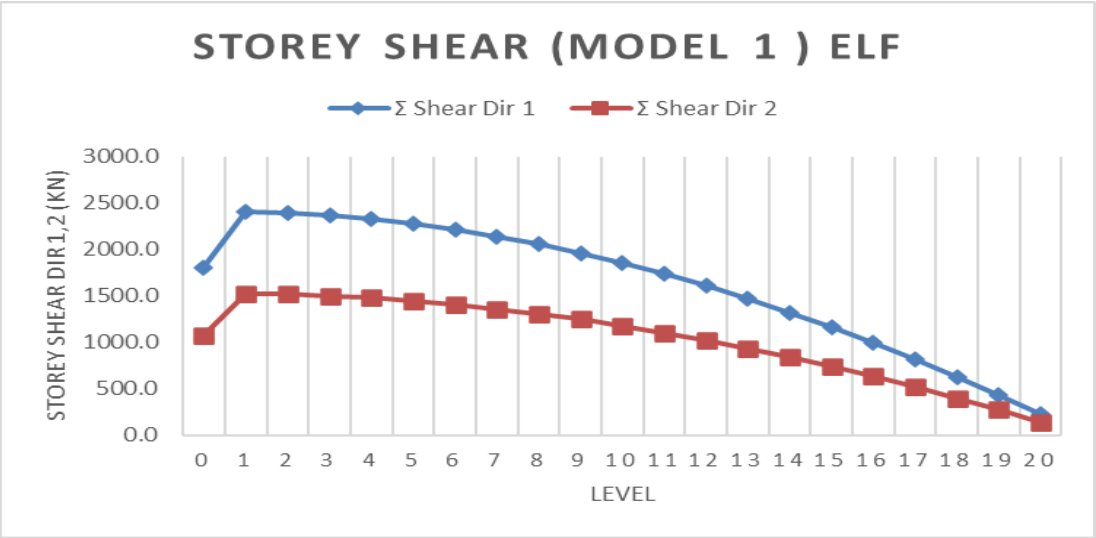

Figure 4.13 Storey shear distribution for Model 1 (ELF)

Model 1 - RSA (Figure 4.14). The RSA curves peak at mid-height: shear increases sharply from the roof to the third floor and then decreases towards the base. The bell-shaped profile indicates that higher modes contribute significantly to the total response in this flexible core-only structure. The Dir 1 curve remains above the Dir 2 curve, mirroring the stiffness difference.

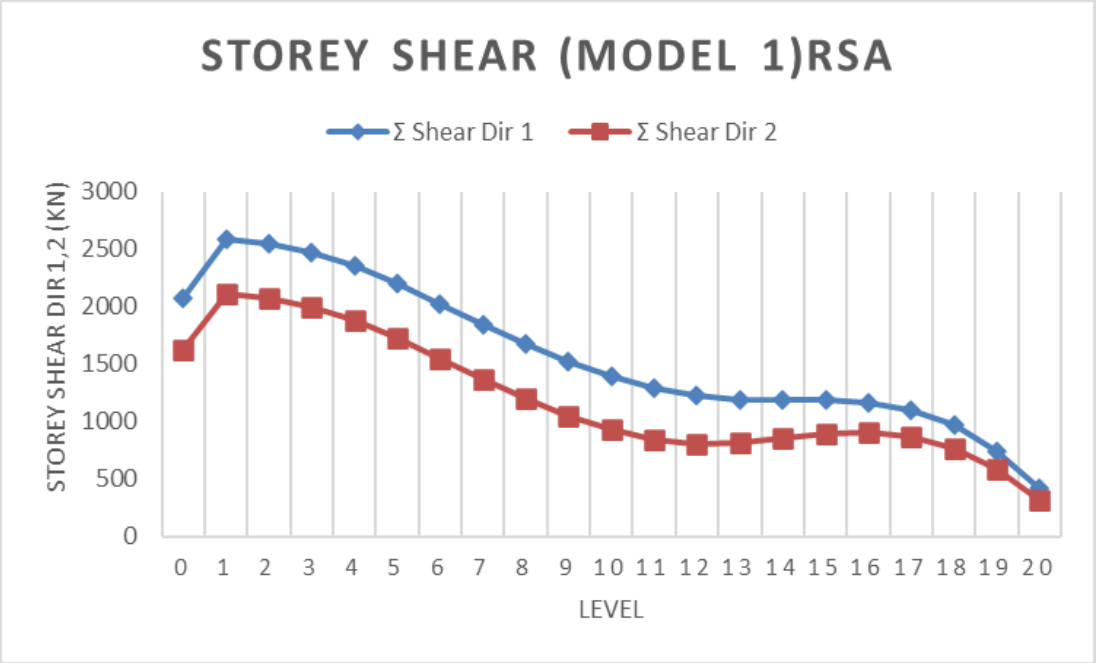

Figure 4.14 Storey shear distribution for Model 1 (RSA)

Model 3 - ELF (Figure 4.15). Adding perimeter walls increases shears in both directions and reduces the difference between Dir 1 and Dir 2. The ELF curves remain smooth and steep from the roof to mid-height, with a less pronounced plateau near the top, as perimeter walls reduce the effect of core tapering.

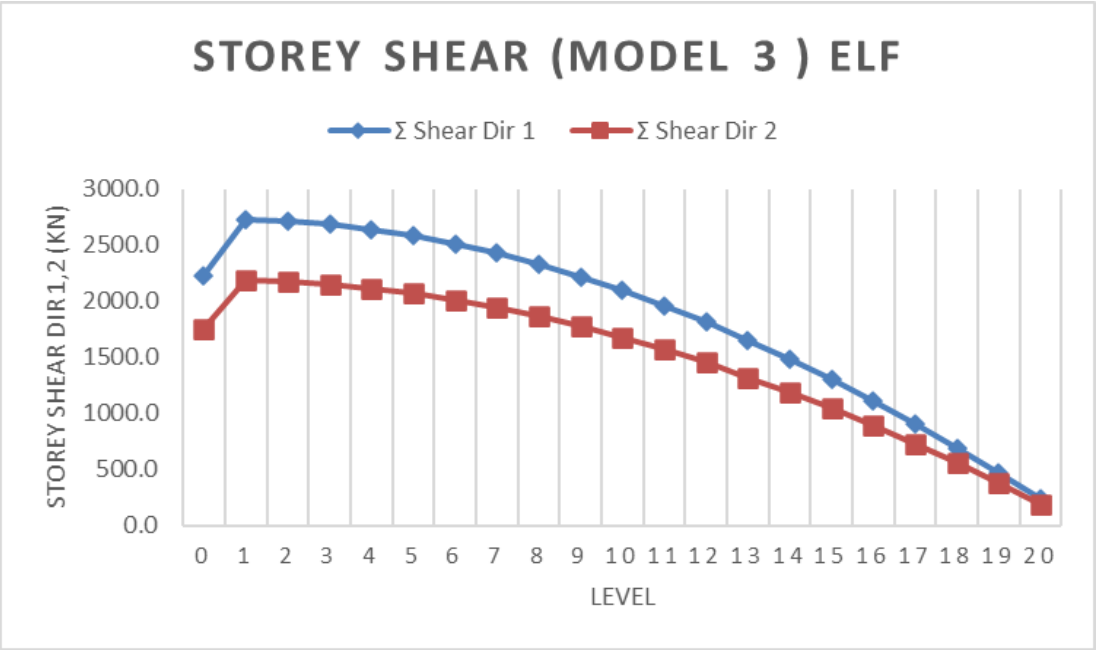

Figure 4.15 Storey shear distribution for Model 3 (ELF)

Model 3 - RSA (Figure 4.16). The RSA curves for Dir 1 and Dir 2 almost coincide below the fifth floor, demonstrating that perimeter walls balance the stiffness around the plan. Peak shear values are higher than in Model 1 because the additional walls attract more force.

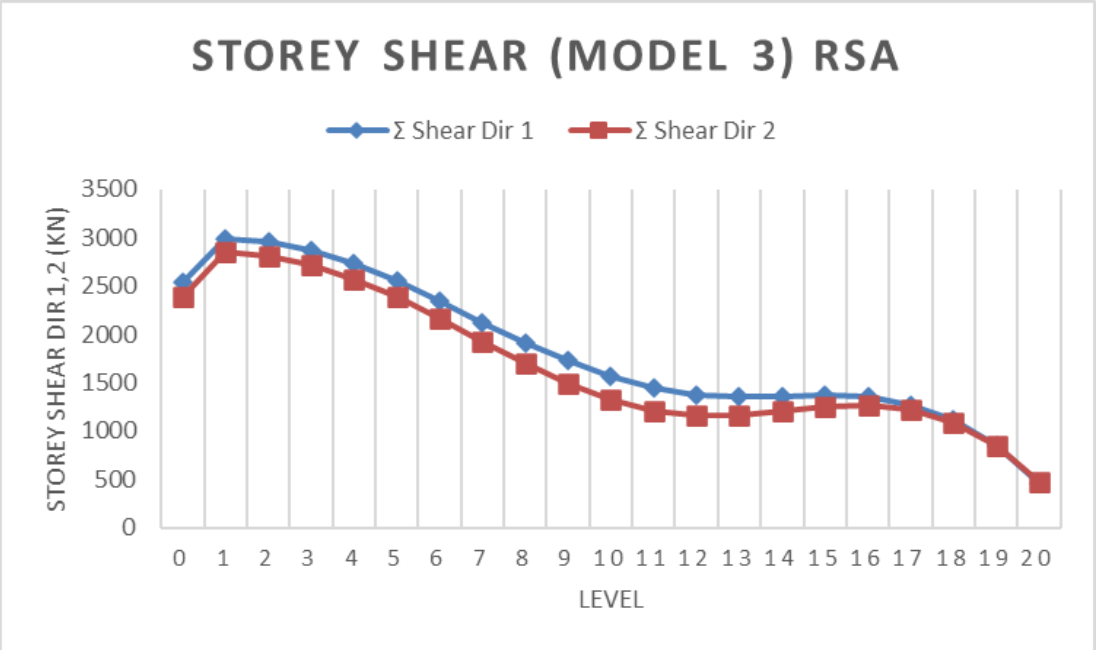

Figure 4.16 Storey shear distribution for Model 3 (RSA)

Model 11 - ELF (Figure 4.17). Introducing L-intersection walls produces much larger shears in Dir 2 than in Dir 1 at every level. The short wing has become the stiffer direction, and the Dir 2 curve exhibits a steeper gradient near the roof, signifying that the corner walls carry more of the lateral load.

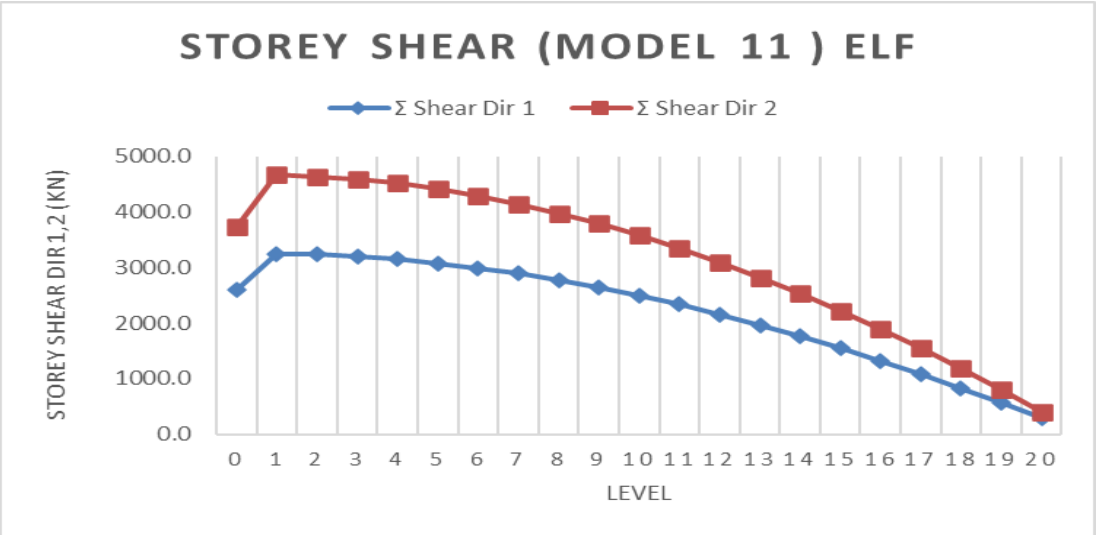

Figure 4.17 Storey shear distribution for Model 11 (ELF)

Model 11 -RSA (Figure 4.18). The RSA curves maintain the dominance of Dir 2 shears. Both directions show smoother gradients than the core-only case, indicating that higher-mode effects are less pronounced when stiffness is distributed to the corner.

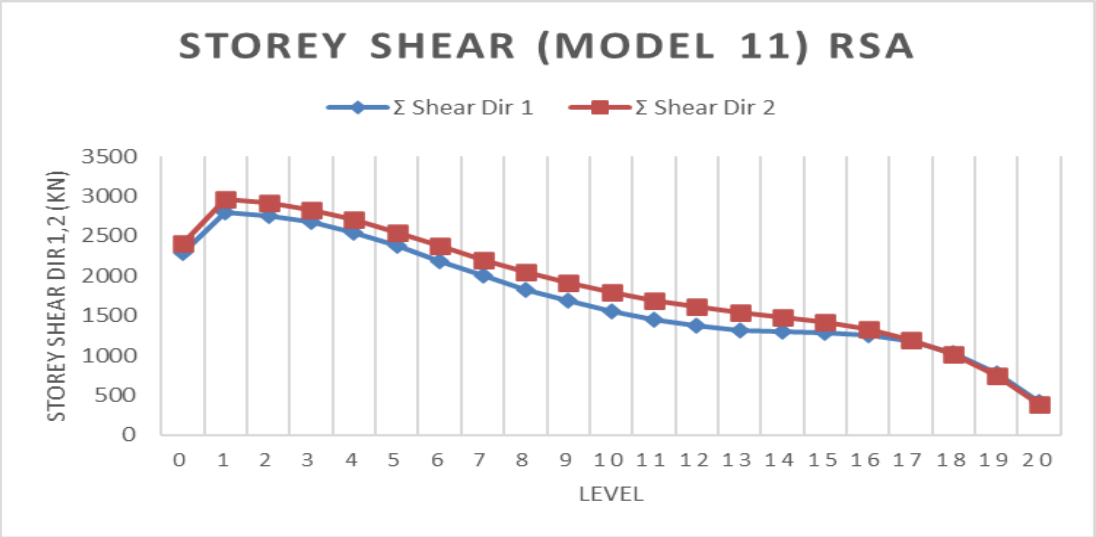

Figure 4.18 Storey shear distribution for Model 11 (RSA)

These plots confirm that ELF forces concentrate towards the base, whereas RSA forces peak nearer mid-height due to mode coupling. Perimeter and L-intersection walls redistribute the shear more evenly and reduce directional imbalance.

Storey Force Distribution

Storey forces – the net shear carried by all vertical elements at each level – were also examined for Models 1, 3 and 11 using RSA results. In Model 1 [Figure 4.19], the forces are highly variable, with a sharp peak at the base, a sudden dip at the second storey and a secondary peak at mid-height. This oscillation reflects the shifting share of load between the core and the frame as different modes dominate. In Model 3 [Figure 4.20], the forces are nearly uniform from the second storey to the fourteenth storey, rising again near the roof; Dir 1 and Dir 2 curves overlap, confirming that the perimeter walls share the load evenly. Model 11 [Figure 4.21] displays a similar pattern but with higher magnitudes because the L-walls attract more shear. These results underline the efficiency of distributed walls in smoothing force distribution and reducing local concentrations.

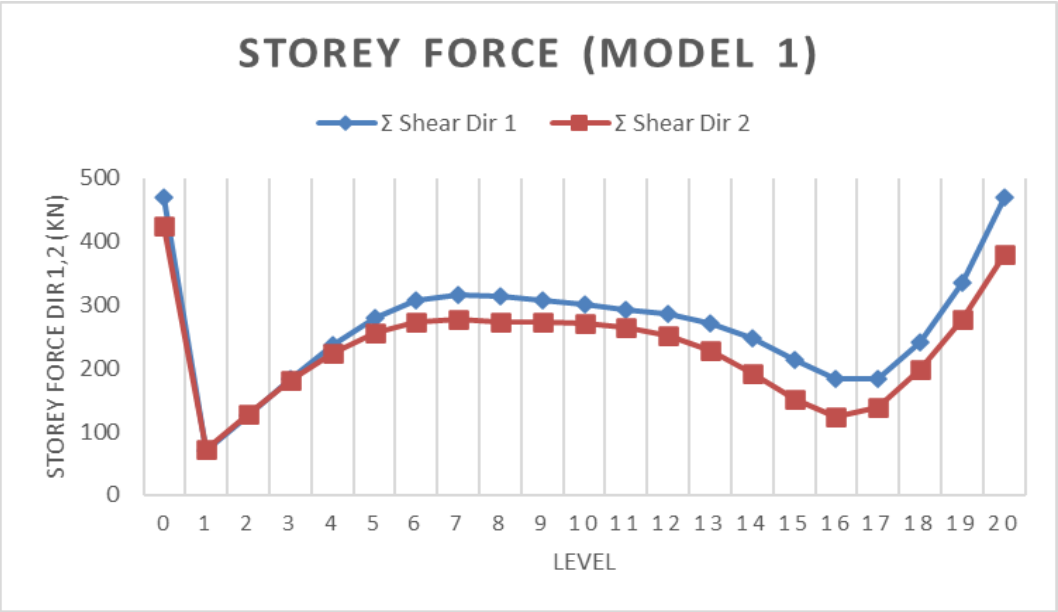

Figure 4.19 Storey Force distribution for Model 1

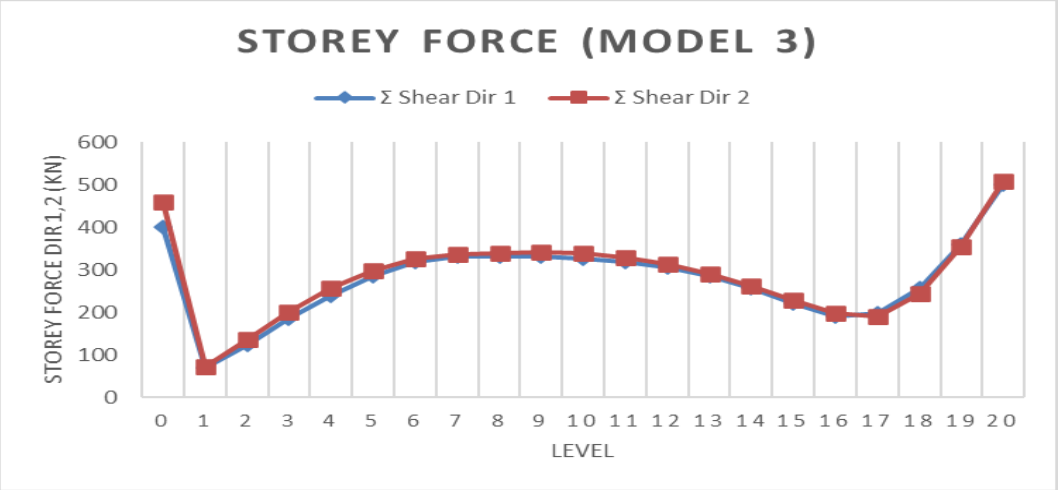

Figure 4.20 Storey Force distribution for Model 3

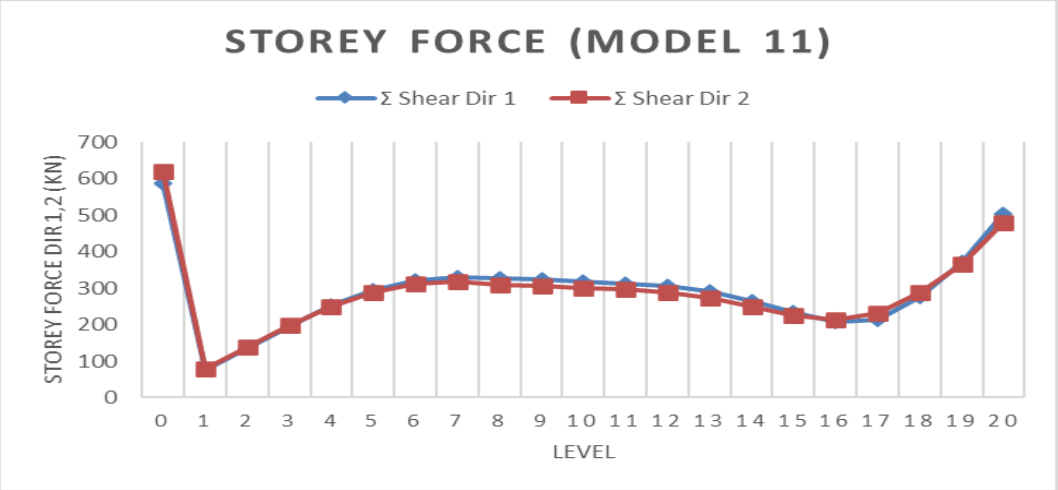

Figure 4.21 Storey Force distribution for Model 11

DISCUSSION

The base shear comparison shows that increasing wall thickness and adding perimeter or L-intersection walls raise the overall seismic demand. However, the gain in base shear diminishes beyond a certain wall thickness, suggesting that very thick walls yield little additional benefit. L-intersection walls produce the highest base shear, particularly in the stiffened direction, and in this study, the RSA base shears in that direction were lower than 85 % of the ELF values, implying that the dynamic analysis underestimates the demand; Eurocode 8 would require scaling of these RSA results for design, although no scaling has been applied in this comparative assessment. The storey shear profiles reveal that the ELF forces are concentrated towards the base, while the RSA forces peak nearer mid-height due to higher-mode effects. Perimeter and L-intersection walls smooth the RSA shear distribution and balance the shear between directions, illustrating the benefit of distributed stiffness. The storey force plots show that core-only systems experience larger variability in force distribution, whereas distributed walls promote uniformity. Overall, the results confirm that wall placement and thickness have a significant influence on seismic load distribution, and that perimeter walls offer a balanced improvement in both directions, while L-intersection walls further stiffen the short wing but at the cost of higher base shear.

4.4.2 Lateral Displacement and Inter-Storey Drift

Maximum lateral displacements were first extracted from Tekla Structural Designer for each model at the roof level (Level 20), Table 4.3. Displacements in the global X and Y directions (Dx and Dy) indicate the overall flexibility of each configuration. Core-only models exhibit the largest roof displacements (up to 79.3 mm in X and 95.3 mm in Y for Model 1), while the introduction of perimeter walls reduces roof drift in both directions. The L-intersection configurations (Models 9–14) yield the smallest displacements: roof drifts are less than 60 mm in X and 42 mm in Y for all L-wall models. These values illustrate the progressive stiffening effect of added wall area and improved plan symmetry.

Table 4.3 Maximum lateral displacements (Dir1/ Dir2)

Model ID	Level Ref	Max Displacement D_x(mm)	Level Ref	Max Displacement D_y(mm)
1	20	79.3	20	95.3
2	20	72.3	20	88.9
3	20	78.2	20	79.2
4	20	78.6	20	79.2
5	20	79	20	79.3
6	20	72.1	20	75.6
7	20	72.5	20	75.7
8	20	72.9	20	75.8
9	20	59.8	20	41.4
10	20	60.6	20	39.1
11	20	61.1	20	36.4
12	20	54.7	20	40.6
13	20	55.6	20	39.4
14	20	56.3	20	38

To assess compliance with Eurocode 8 damage-limitation criteria, inter-storey drift ratios were obtained from the *Seismic Drift* check in Tekla. For each model, the storey where the maximum drift ratio occurs and its magnitude were recorded for both principal directions. Table 4.4 and Table 4.5 summarise these results. The EC8 limit for damage limitation is 0.5 % (i.e. drift ratio < 0.005); all models are well within this limit, with maximum drift ratios ranging from 0.14 % to 0.194 % in Direction 1 and from 0.105 % to 0.174 % in Direction 2. Nevertheless, clear differences exist between configurations. Core-only models (1 and 2) have the highest drift ratios in both directions, with a maximum Dir 1 drift ratio of 0.194 % at Level 18 (Model 1) and a maximum Dir 2 ratio of 0.174 % at Level 18. Adding perimeter walls (Models 3–8) reduces the peak drift ratio by about 10–15 % in each direction. L-intersection models (9–14) achieve the greatest reduction, bringing the maximum drift ratio down to between 0.105 % and 0.127 % in Direction 2.

Table 4.4 Maximum inter-storey drift ratios, Dir1 from RSA drift check

Model ID	Level Ref`	Max drift ratio Dir 1 (%)	Meets EC8 Limit
1	18	0.194	Yes
2	15	0.178	Yes
3	18	0.171	Yes
4	19	0.159	Yes
5	20	0.172	Yes
6	20	0.161	Yes
7	18	0.161	Yes
8	19	0.151	Yes
9	15	0.164	Yes
10	18	0.158	Yes
11	15	0.171	Yes
12	18	0.140	Yes
13	17	0.135	Yes
14	19	0.143	Yes

Table 4.5 Maximum inter-storey drift ratios, Dir2 from RSA drift check

Model ID	Level Ref`	Max drift ratio Dir 2 (%)	Meets EC8 Limit
1	18	0.174	Yes
2	18	0.171	Yes
3	18	0.171	Yes
4	19	0.171	Yes
5	19	0.170	Yes
6	18	0.169	Yes
7	18	0.169	Yes
8	18	0.169	Yes
9	15	0.118	Yes
10	18	0.122	Yes
11	20	0.105	Yes
12	18	0.127	Yes
13	17	0.121	Yes
14	19	0.121	Yes

While the overall drift limit of 0.5 % is satisfied by every model, the table shows that wall configuration strongly influences drift performance. Models 1 and 2 exceed 0.17 % in both directions; Models 3–8 are around 0.15-0.17 % in Dir 1 and 0.16-0.17 % in Dir 2; Models 9-14 reduce the Dir 2 drift to between 0.105 % and 0.127 %. The storey at which the maximum drift occurs also shifts for core-only and perimeter models; the peak drift generally occurs between Levels 18 and 20, whereas for L-intersection models, the peak in Direction 2 moves lower (around Level 15-17), indicating that the corner walls redistribute stiffness along the height.

Drift ratio versus height

Figures 4.22-4.24 plot the drift ratio (inter-storey drift expressed in millimetres) against storey level for three representative models: Model 1 (Core only), Model 4 (Core + Perimeter) and Model 11 (Core + L-intersection). The blue bars represent Direction 1, and the red bars represent Direction 2.

Model 1 (core only) – Figure 4.22**.** Drifts increase steadily from the base towards the roof in both directions. Direction 1 drifts remain slightly larger than Direction 2 throughout most of the height. There is no abrupt change in slope, indicating that the tapered core thickness does not create a soft storey. However, the maximum drifts occur close to the roof, reaching approximately 6.5 mm in Dir 1 and 6.0 mm in Dir 2, corresponding to the drift ratios reported in Table 4.4.

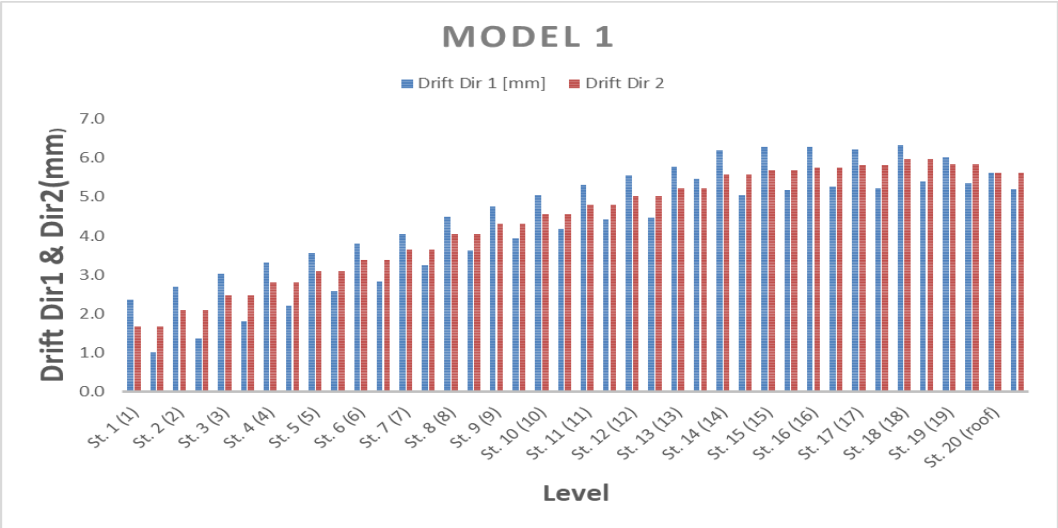

Figure 4.22 Drift ratio versus height for Model 1 (core only)

Model 4 (core + perimeter) – Figure 4.23. The addition of perimeter walls reduces the drift magnitudes throughout the height. Both directions have very similar drift values, with Dir 2 being marginally larger. The maximum drifts are approximately 6.0 mm in Dir 2 and 5.5 mm in Dir 1 at Levels 18–20. Overall, the drifts are lower than in the core-only model, demonstrating the effectiveness of perimeter walls in controlling lateral displacement.

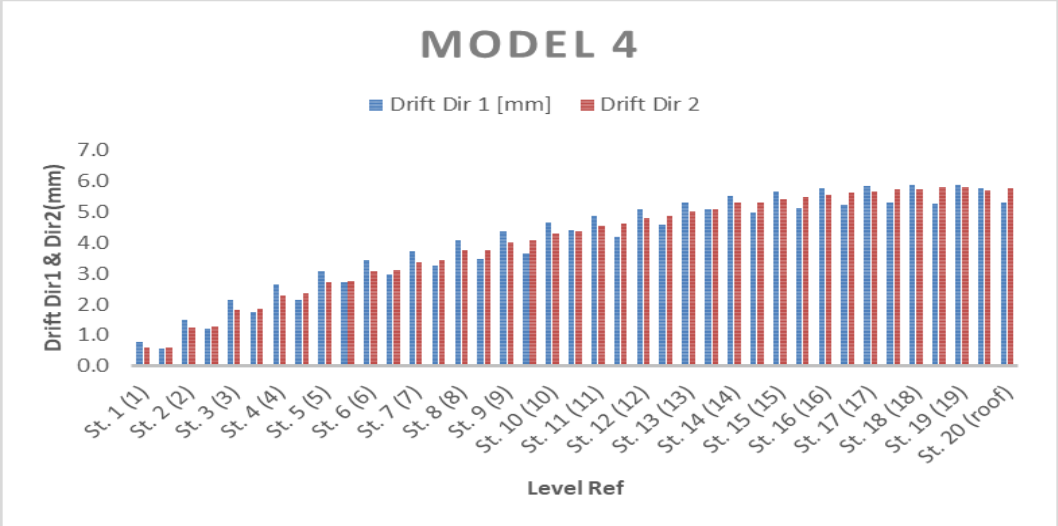

Figure 4.23 Drift ratio versus height for Model 4 (core + perimeter)

Model 11 (core + L-intersection)– Figure 4.24. L-intersection walls produce a more pronounced difference between directions: drifts in Dir 1 are noticeably higher than in Dir 2. The peak Dir 1 drift is about 5.5 mm at Level 15, while the peak Dir 2 drift is around 3.2 mm at the same level. The drifts then decrease towards the roof. This behaviour reflects the increased stiffness in the short wing (Dir 2) provided by the corner walls.

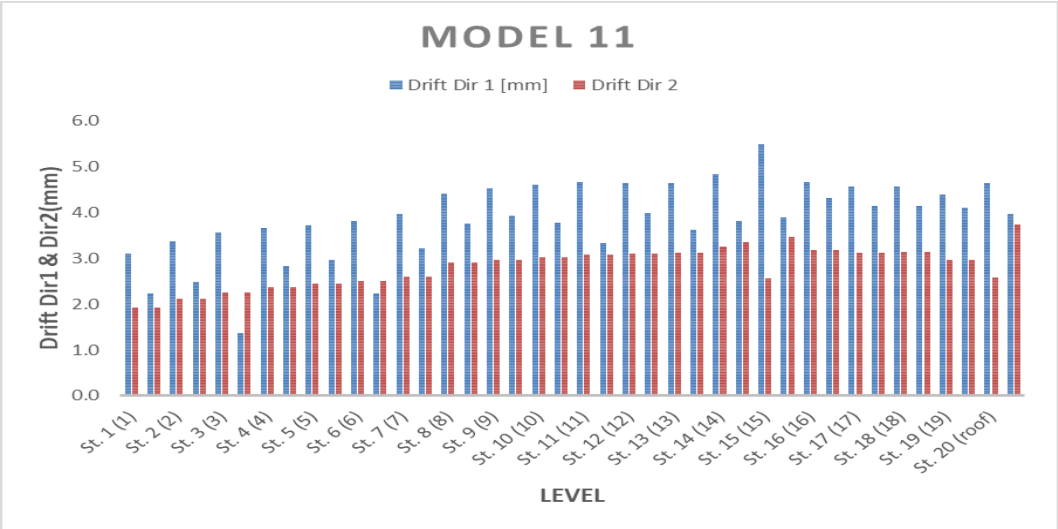

Figure 4.24 Drift ratio versus height for Model 11 (core + L-intersection)

These drift profiles confirm that adding perimeter and L-intersection walls not only reduces the magnitude of inter-storey drifts but also influences the distribution of drifts along the height. Perimeter walls provide balanced stiffness in both directions, whereas L-intersection walls preferentially stiffen the short wing, leading to lower drift ratios in Dir 2 and a shift of the peak Dir 2 drift to lower storeys. All models meet the EC8 drift limits, but the L-intersection configurations offer the best performance, reducing peak drift ratios by up to 40 % relative to the core-only case.

4.4.3 Torsional irregularity

In addition to the translational drifts, Tekla's *Critical Sway* results were used to assess torsional behaviour. The twist ratio ($\Delta_{max}/\Delta_{avg}$) was extracted for each model, and the storey where this peak occurred was identified. Table 4.6 presents the maximum twist ratios, together with an indication of whether the EC8 torsional irregularity limit of 1.2 is satisfied.

Table 4.6 Maximum twist ratios and EC8 compliance

Model ID	Storey	Max Twist Ratio	EC8 Torsion Limit (≤ 1.2)
1	1	1.619	No
2	1	1.610	No
3	1	1.001	Yes
4	1	1.001	Yes
5	1	1.002	Yes
6	1	1.001	Yes
7	2	1.001	Yes
8	2	1.001	Yes
9	1	4.064	No
10	1	4.299	No
11	1	4.509	No
12	1	3.241	No
13	1	3.347	No
14	1	3.433	No

Models 1 and 2 (core only) exhibit maximum twist ratios around 1.61-1.62 at the ground storey, exceeding the Eurocode threshold. The Perimeter-Wall models (3-8) have twist ratios very close to unity (approximately 1.001-1.002) at the first or second storey, comfortably within the limit. By contrast, the L-intersection models (9-14) show severe torsional irregularity: maximum twist ratios range from 3.24 to 4.51, all occurring at the base storey. These values greatly exceed the EC8 limit, indicating that, although L-walls increase overall stiffness, they concentrate torsional demands at the ground floor. In practice, such torsional irregularity would require additional measures (e.g. more distributed walls or diaphragmatic stiffening) to mitigate the rotation.

Figures 4.25-4.27 plot the twist ratio versus storey height for representative models. For the core-only model (Fig. 4.25), the twist ratio peaks at approximately 1.25 at the first two storeys, then drops to unity for the remainder of the height. The perimeter-wall configuration (Fig. 4.26) exhibits a very slight peak of 1.002 at the first storey and essentially unity, thereafter, demonstrating excellent torsional control. In contrast, the L-intersection model (Fig. 4.27) shows a dramatic peak of about 4.7 at the ground storey and a subsequent reduction to 1.3 at the second storey before

approaching unity above. The stiff L-walls at the re-entrant corner attract large torsional forces at the base, leading to excessive rotation. Thus, while perimeter walls effectively suppress torsional irregularity, L-intersection walls on their own are inadequate for torsion control; they increase stiffness in one direction but introduce significant twisting.

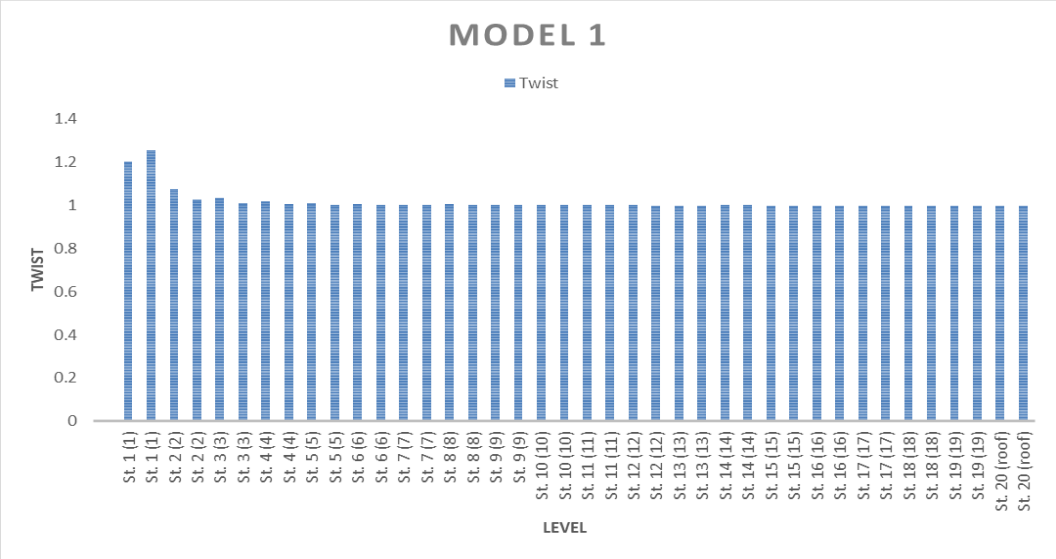

Figure 4.25 Twist ratio versus height for Model 1 (core only)

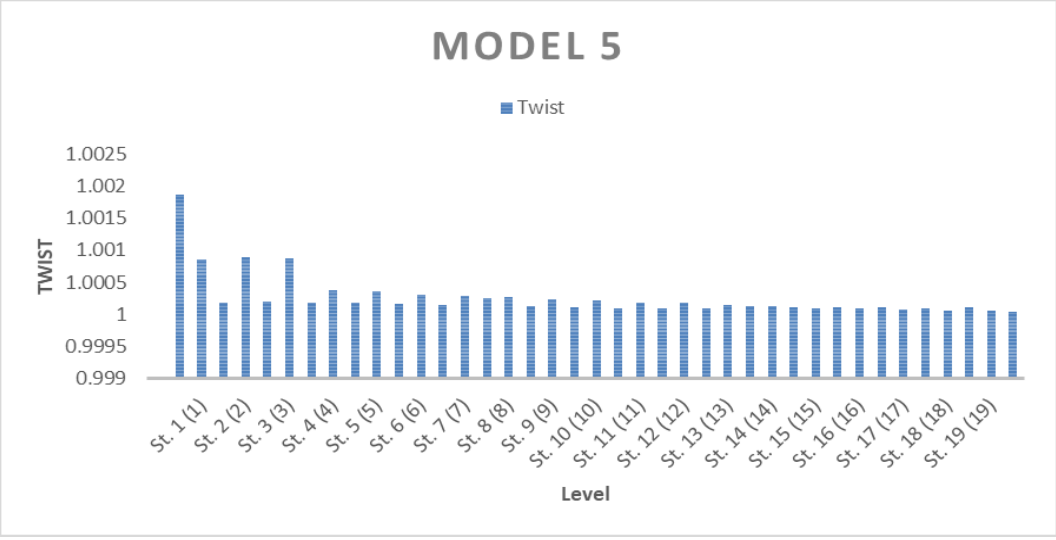

Figure 4.26 Twist ratio versus height for Model 5 (core + perimeter)

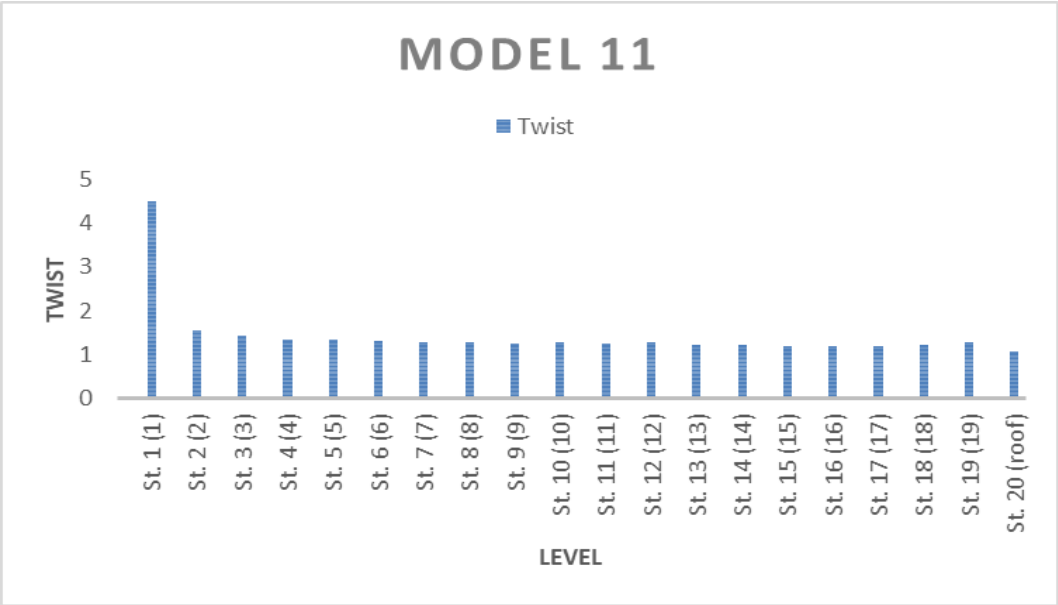

Figure 4.27 Twist ratio versus height for Model 11 (core + L-intersection)

4.4.4 Wall Force and Stress Distribution

The distribution of shear, bending moment and torsion among the different wall types was examined by extracting the peak values from Tekla's *Wall Lines* and *2D Integrated Results*. Table 4.7, Table 4.8, and Table 4.9 summarise the maximum shear, maximum bending moment and maximum torsion recorded in the core walls, perimeter walls and L-intersection walls for all fourteen models, respectively. The storey at which each maximum occurs is also reported

Table 4.7 Maximum Shear for Core, Perimeter and L-walls

Model ID	Wall Type	Max Shear (KN)	Storey
1	Core only	3257.1	1
2	Core only	3408.3	1
3	Core	1886.4	4
	Perimeter	548.2	1
4	Core	1891.8	4
	Perimeter	263.5	1
5	Core	1888.1	4
	Perimeter	258.3	1
6	Core	2039.9	4
	Perimeter	247.9	1
7	Core	2042.4	4
	perimeter	792.8	1
8	Core	2045.3	4
	perimeter	849.7	1
9	Core	2516.8	1
	L-intersection	950.9	1
10	Core	2552.3	1
	L-intersection	1076.6	1
11	Core	2553.6	1
	L-intersection	1198.7	1
12	Core	2572.1	1
	L-intersection	893.7	1
13	Core	2634.0	1
	L-intersection	976.5	1
14	Core	2686.8	1
	L-intersection	1130.7	1

Table 4.8 Maximum Moment for Core, Perimeter and L-walls

Model ID	Wall type	Max Moment (KN.m)	Storey
1	Core only	76695.5	1
2	Core only	80614.4	1
3	Core	11344.6	1
	perimeter	4209.9	1
4	Core	11355	1
	perimeter	4909.6	1
5	Core	11368.8	1
	perimeter	5586.8	1
6	Core	12120.9	1
	perimeter	4032.8	1
7	Core	12142.5	1
	perimeter	3389.3	1
8	Core	12167.2	1
	perimeter	3887.7	1
9	Core	10001.4	1
	L-intersection	1576.6	1
10	Core	9869.6	1
	L-intersection	1765.5	1
11	Core	9724	1
	L-intersection	1720.6	1
12	Core	10800.5	1
	L-intersection	1588.0	1
13	Core	10717.6	1
	L-intersection	1790.4	1
14	Core	10617.6	1
	L-intersection	1976.1	1

Table 4.9 Maximum Torsion for Core, Perimeter and L-walls

Model ID	Wall type	Max Torsion (KN.m)	Storey
1	Core only	15787.82	1
2	Core only	16819.22	1
3	Core	147.73	2
	perimeter	19.08	1
4	Core	147.78	2
	perimeter	26.23	1
5	Core	147.72	2
	perimeter	33.39	1
6	Core	185.83	2
	perimeter	18.62	1
7	Core	185.79	2
	perimeter	25.54	1
8	Core	185.87	2
	perimeter	32.59	1
9	Core	164.05	1
	L-intersection	30.48	2
10	Core	163.66	1
	L-intersection	45.14	2
11	Core	161.63	1
	L-intersection	62.46	2
12	Core	201.16	1
	L-intersection	29.35	2
13	Core	202.76	1
	L-intersection	43.49	2
14	Core	203.41	1
	L-intersection	60.23	2

The results highlight the influence of wall layout on force distribution. In the core-only models (1 and 2), the maximum shear demands on the core wall are very high (around 3,300-3,400 KN at the ground storey), and bending moments exceed 76,000 KN · m. Torsion in the core of these models is extraordinarily large (15,800-16,800 KN · m), reflecting the absence of distributed torsional resistance. When perimeter walls are added (Models 3-8), the maximum shear on the core drops dramatically to around 1,860-2,045 KN and occurs at the fourth storey; additional perimeter walls carry between 250 KN and 850 KN at the first storey. Bending moments on the core are reduced by about 85 % to between 11,300-12,170 KN.m, while perimeter walls carry moments of 3,400-5,600 KN · m. Torsion demands decrease by two orders of magnitude, to approximately 147-186 KN.m on the core (storey 2) and 19-33 KN.m on the perimeter walls (storey 1).

For the L-intersection configurations (Models 9-14), the maximum core shear increases compared with perimeter walls, ranging from 2,517 to 2,687 KN at the ground storey; the L-walls carry between 950 and 1,200 KN. Core bending moments are in the range of 9,700-12,175 KN.m, and L-walls carry moments between 1,580 and 1,975KN.m. Torsion on the core is around 162-203 KN · m at the ground floor, while torsion on the L-walls is 30-60 K.Nm at the second floor. Although torsion demands are vastly reduced relative to the core-only models, they are somewhat higher than those in the perimeter-wall models, indicating that L-walls provide partial but not complete torsional restraint.

Assuming typical shear, moment and torsion capacities for C30/37 reinforced concrete walls of thickness 200-400 mm (which are in the order of several thousand kilonewtons and tens of thousands of kilonewton-metres), all of the recorded demands in the perimeter and L-wall models are likely to fall within the design capacities prescribed by Eurocode 2, provided adequate reinforcement is detailed. However, the very high shear, moment and torsion values in the core-only models would require significant wall thickness or reinforcement and might not be acceptable without additional lateral elements.

A representative diagram of how shear and bending moment vary along the height of the core wall is presented in Figure 4.28 (a), (b). In this example (Model 2, RSA), shear demands are highest at the base and decrease nearly linearly with height, while bending moments increase towards the base, reflecting cantilever behaviour typical of shear walls. Similar patterns were observed in other models, with the presence of perimeter or L-walls reducing the peak shear on the core and modifying the distribution profile.

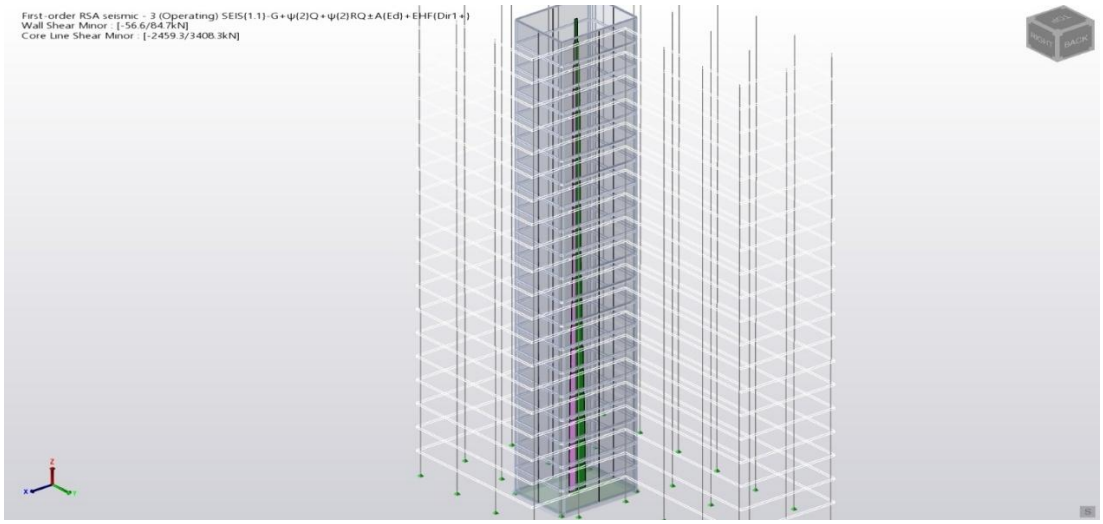

(a)

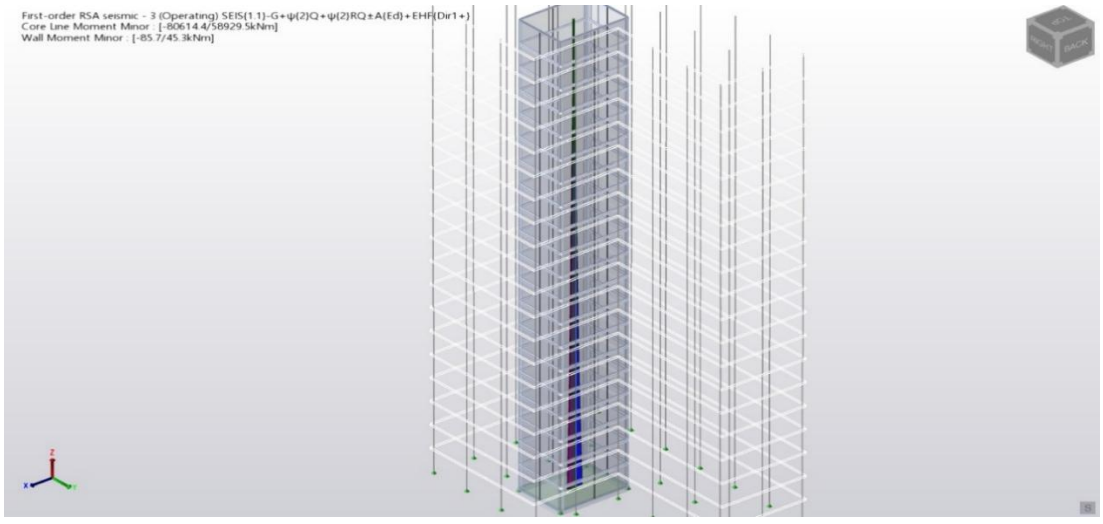

(b)

Figure 4.28 (a)&(b) Shear and bending moment distribution along core wall height for Model 2 (RSA)

These results demonstrate that the introduction of perimeter and L-intersection walls not only reduces overall displacements but also redistributes internal forces among walls. Perimeter walls alleviate shear, moment and torsional demands on the core by sharing lateral loads, while L-walls attract additional forces near the base. Core-only models exhibit dangerously high torsion and bending demands, underscoring the need for distributed wall systems in irregular L-shaped buildings.

4.5 Optimisation of Wall Thickness

4.5.1 Influence of Thickness Variation

To understand whether thicker walls alone could enhance performance, sets of models with the same plan layout but different wall thicknesses were compared. The average thicknesses were calculated by taking the mean of the thickness bands used for each height range (e.g., Model 1: 350 mm, 300 mm, 250 mm, and 200 mm give an average core thickness of 275 mm). Table 4.10 summarises the results. The average perimeter or L-wall thickness was calculated only for models where such walls were present. Base shear values are the larger of the two directions (RSA), and the maximum drift ratio is the peak value from Tables 4.4 and 4.5.

Table 4.10 Comparison of thickness groups

Layout	**Model IDs**	**Average Core Thickness (mm)**	**Average Perimeter/L Wall thickness (mm)**	**RSA base shear (KN)**	**Max drift ratio (%)**	**Observation**
Core-only	1	275	-	2068	0.194	Baseline: highest drift ratios and low base shear due to slender core.
	2	325	-	2177	0.178	Increasing all core thickness bands by 50 mm raises base shear by ~5 % and reduces drift ratio by ~8 %.
Core + perimeter	3-5	275	225-325	2547-2647	0.151-0.171	Perimeter walls supplement the core; increasing perimeter wall thickness from 225 mm (Model 3) to 325 mm (Model 5) raises base shear by only ~ 4 % and reduces drift ratio by ~12 %.
	6-8	325	225-325	2637-2731	0.151-0.161	Increasing core thickness while maintaining perimeter walls yields only marginal additional benefits – base shear rises ~3 % and drift ratio decreases by ~7 %.

Layout	Model IDs	Average Core Thickness (mm)	Average Perimeter/L Wall thickness (mm)	RSA base shear (KN)	Max drift ratio (%)	Observation
Core + L-intersection	9-11	275	225-325	2637-2731	0.118-0.171	These models stiffen the short wing; Dir 2 base shear increases dramatically (to 2,195-2,407 KN), and Dir 1 base shear is lower than in perimeter-wall models. Drift ratio in Dir 2 drops to 0.105-0.171 %.
	12-14	325	225-325	2255-2344	0.105-0.143	Using thicker cores with L-intersection walls raises base shear by 3-4 % and further reduces the maximum drift ratio to 0.105-0.143 %.

The data show that, within each layout, wall thickness has a secondary effect compared with wall arrangement. For core-only walls, increasing thickness from an average of 275 mm to 325 mm decreases the maximum drift ratio by about 0.02 % and increases base shear by roughly 5 %. For perimeter walls, the improvement from thicker walls is less pronounced: Models 3-5 and 6-8 show that base shear increases by less than 4 % and the drift ratio reduces by only about 0.01-0.02 % when the thickness bands are increased. The L-intersection layouts display a similar trend - thicker cores reduce drift by roughly 10 % but also raise the base shear slightly. These diminishing returns indicate that judicious placement of walls is more effective than simply increasing wall thickness.

the maximum drift ratio and RSA base shear against the average core thickness for all models. The trend lines illustrate that while drift ratios decrease steadily as core thickness increases, the reduction becomes marginal beyond an average core thickness of about 300 mm; similarly, base shear increases gradually but plateaus once the walls are moderately thick. In perimeter and L-wall systems, the effect of perimeter or corner wall thickness is even smaller, with scatter showing that other factors (such as wall placement and torsional restraint) govern the response.

4.5.2 Proposed Optimal Thickness Strategy

Considering the diminishing returns observed above and the practicalities of construction, a three-step taper is proposed as the optimal thickness profile for the 20-storey L-shaped building:

Lower floors (ground to 7th floor) walls 350 mm thick for both the core and the perimeter/L-walls. This provides sufficient stiffness where storey shears and overturning moments are highest.

Middle floors (8th to 13th floor) walls reduced to 300 mm. Analytical results show that decreasing the thickness from 350 mm to 300 mm on these levels has little effect on drift or torsion but offers material savings.

Upper floors (14th to roof) walls reduced to 250 mm. Lateral forces and moments are smaller in the upper levels, so thinner walls are adequate without causing a soft-storey response.

This three-step taper is simpler to construct than the four-step taper used in the initial models (400-350-300-250 mm) and provides similar performance. For the perimeter or L-intersection walls, a taper of 300-250-200 mm is recommended. The proposed scheme represents a balanced solution: it maintains adequate stiffness in the lower half of the building to control drift and torsion while reducing material usage in the upper storeys.

4.6 Validation Against Eurocode 8 Criteria

Several Eurocode 8 criteria were used to check the acceptability of each model:

Inter-storey drift ratio

EC8 limits the drift ratio to 0.5 % (1/200) for the damage limitation state. Table 4.4 and Table 4.5 show that all models have maximum drift ratios below 0.2 %, well within the limit. Perimeter and L-intersection walls reduce the drift ratios by 10-40 % compared with core-only systems, giving a wide margin of safety.

Torsional irregularity

EC8 defines torsional irregularity when the ratio of maximum to average storey displacement ($\Delta_{max}/\Delta_{avg}$) exceeds 1.2. As reported in Table 4.6, core-only models (1-2) and all L-intersection models (9-14) exceeded this limit, with twist ratios between 1.61 and 4.51 at the base storey. Perimeter-wall models (3-8) achieved twist ratios near unity and complied with the EC8 limit. The data imply that L-intersection walls stiffen the short wing but concentrate torsional demand at the base; additional perimeter walls or diaphragm stiffening would be required to meet the code.

Base Shear Scaling

EC8 requires that RSA design base shear values should not fall below 85 % of the ELF base shear. Base shear comparisons in Table 4.2 reveal that RSA base shears exceed ELF values for most models, but in Dir 2 for L-intersection models (9-14) the RSA results are only about 70-80 % of the ELF values. In practice, these RSA base shears would need to be scaled up to 85 % of the ELF values for design. This confirms that L-intersection layouts demand careful attention to dynamic effects.

Wall Stresses and Capacities

The maximum shear forces, moments, and torsions recorded in Section 4.4.4 were compared to the design capacities of C30/37 walls of thickness 200-400 mm. For perimeter and L-intersection models, the demands are well within the capacity envelopes specified by Eurocode 2. However, the core-only models exhibit extremely high shear (3,300 KN), moment (76000 KN·m), and torsion (16,000 KN.m) at the base, which would require thick walls and heavy reinforcement beyond practical limits. This demonstrates that a core-only system is not feasible for the given building without supplementary walls.

In summary, all models satisfy the drift requirement, but only those with perimeter walls meet the torsional irregularity criterion without scaling. RSA base shears for L-intersection layouts need adjustment to meet EC8 provisions. These observations confirm that wall placement, not thickness, controls compliance with seismic design criteria.

4.7 Discussion of Findings

The systematic evaluation of fourteen models provides several clear insights into the seismic behaviour of L-shaped RC buildings:

Wall layout Dominates Performance

The change from a core-only system to one with perimeter walls reduces inter-storey drift by roughly 15-20 % and virtually eliminates torsional irregularity. Adding L-intersection walls further stiffens the structure and shortens periods, but does not address torsional coupling; indeed, twist ratios increase dramatically at the ground floor. This confirms that distributing walls around the perimeter provides a more balanced and effective lateral-force-resisting system than relying on corner walls alone.

Thickness has diminishing returns

Within each layout, increasing wall thickness results in modest reductions in drift ratio and only slight increases in base shear. For example, thickening the core from an average of 275 mm to 325 mm reduces the maximum drift ratio by about 8 % and raises base shear by approximately 5 %. Thickening perimeter or L-intersection walls beyond 300 mm yields minimal additional benefit. This indicates that once an adequate wall thickness is chosen to resist shear and moment demands, further increases in thickness are inefficient.

Perimeter vs. L-intersection walls

Perimeter walls provide the most consistent improvement across all performance metrics. They reduce drifts, control torsion, share shear forces evenly between directions, and limit demands on the core. L-intersection walls are highly effective at stiffening the short wing and lowering drift ratios in that direction, but without perimeter walls, they create a torsional irregular system. They are therefore best used in conjunction with perimeter walls or other distributed elements.

ELF vs. RSA results

Response spectrum analysis tends to produce slightly higher base shears and highlights torsional coupling that the ELF method does not capture. The RSA storey shear curves

often show mid-height peaks, reflecting higher mode contributions, whereas ELF curves concentrate shear near the base. For design, RSA should be used to evaluate dynamic behaviour and scaled if necessary to satisfy the ELF-based base shear minimum.

Design implications

Several core-only models violate torsional limits and impose impractically high stresses on the core walls. The addition of perimeter walls resolves these issues and allows wall thickness to be reduced above mid-height. L-intersection walls must be supplemented by perimeter walls or other torsion-resisting elements if used in practice. The proposed three-step thickness taper provides a practical solution that balances performance and material economy.

4.8 Summary

This chapter analysed fourteen shear-wall configurations for a 20-storey L-shaped RC building, focusing on the effects of wall layout and thickness on seismic performance. The key conclusions are as follows:

- **Layout dominates behaviour**.

Perimeter walls reduce inter-storey drift by approximately 15-20 % and virtually eliminate torsional irregularity compared with core-only walls. L-intersection walls stiffen the short wing but induce large twist ratios unless complemented by perimeter walls.

- **Thickness has a secondary influence**.

Increasing wall thickness beyond about 300 mm yields diminishing returns. A three-step taper (350 mm at lower floors, 300 mm in mid-levels, and 250 mm at the top) produces performance comparable to a four-step taper while using less material. For perimeter and L-walls, a taper of 300-250-200 mm is sufficient.

• **Compliance with Eurocode 8**.

All configurations satisfy the drift limit of 0.5 %, but only the perimeter models meet the torsional irregularity criterion without scaling. RSA base shears for L-intersection walls fall below 85 % of ELF values and require scaling. Core-only systems attract excessive shear, moment and torsion demands on the core, making them impractical.

• **Recommended configuration**.

The optimal solution for the studied building is a core plus perimeter wall system with a three-step thickness taper. This arrangement delivers a well-balanced distribution of stiffness, keeps drifts and torsion within code limits and minimises material usage. L-intersection walls can be used to supplement the core but should not replace perimeter walls.

These findings provide a clear framework for engineers designing irregular high-rise buildings in low to moderate seismic zones. By emphasising wall placement and adopting moderate, tapered wall thicknesses, designers can achieve seismic resilience without unnecessary material expenditure.

CHAPTER 5

CONCLUSION AND RECOMMENDATIONS FOR FUTURE WORK

5.1 Conclusion

The analytical investigation undertaken in this project has provided a detailed appraisal of how shear-wall configuration and thickness influence the seismic performance of a 20-storey L-shaped reinforced-concrete building modelled in Tekla Structural Designer (TSD). The study compared three fundamental shear-wall layouts: core only, core with perimeter walls, and core with L-intersection walls, under both Equivalent Static Load Analysis (ELF) and Response Spectrum Analysis (RSA) procedures. Fourteen models with varying wall thicknesses were analysed systematically.

Several key observations have emerged:

- **Seismic performance of shear wall configurations:** The study found that fundamental periods decreased as wall stiffness increased. Core-only systems had the longest periods (≈2.1 s in Direction 1 and 2.4–2.8 s in Direction 2); adding perimeter or L-walls reduced these periods to 1.76 s and 1.23 s, respectively. Roof displacements were greatest in core-only models (up to 79 mm in Direction 1 and 95 mm in Direction 2) and progressively decreased with perimeter or L-walls. All models met Eurocode drift limits, with maximum inter-storey drift ratios between 0.105 % and 0.194 %. Core-only arrangements exhibited the largest drift ratios, while L-intersection walls reduced drift by up to 40 % in the stiffened direction. Core-only models showed significant torsional response with twist ratios around 1.6; perimeter walls brought the twist ratio close to unity, whereas L-intersection layouts concentrated torsional demand at the base (twist ratios exceeded 3.0). Introducing perimeter walls also redistributed shear and moment from the core to outer walls, reducing peak shear on the core by roughly 40 % and bending moments by 80 %.

• **Impact of wall thickness on seismic parameters:** Increasing wall thickness beyond 350 mm yielded diminishing reductions in drift and only modest increases in base shear. A three-step taper (for example, 350-300-250 mm) delivered nearly the same performance as a four-step taper while saving material. Perimeter wall thickness had a smaller effect than wall placement, and L-wall stiffness influenced torsion more than drift. Overall, wall layout had a greater impact on seismic response than thickness alone.

• **Effectiveness of seismic analysis methods (RSA vs. ELF):** Response Spectrum Analysis generally produced higher base shears than Equivalent Static Load Analysis; differences ranged from roughly 10 % to 20 % in core-only and perimeter configurations. In L-intersection cases, RSA base shear in Direction 2 fell below 85 % of the ELF value, suggesting that simplified static analysis overestimated demand in that direction. As wall stiffness increased, base shear grew but in a diminishing manner across both analysis methods.

• **Optimal shear wall placement strategies and material efficiency:** Perimeter walls offered the most balanced improvements, reducing drift, controlling torsion and alleviating force concentrations while using material efficiently. L-intersection walls increased stiffness but introduced significant torsional irregularities at lower levels. Core-only configurations were inadequate for L-shaped buildings due to excessive drift and torsional response. The study underscores that distributed perimeter walls or combinations of core and perimeter walls provide better seismic resilience than core-only or isolated corner walls, and tapered wall thicknesses enhance material efficiency without compromising performance.

In summary, the study demonstrated that the seismic performance of L-shaped reinforced-concrete buildings is governed more by the layout of shear walls than by their thickness. Adding perimeter walls significantly reduced natural periods, lateral displacements, and drift while suppressing torsional effects; core-only configurations exhibited the longest periods, the largest drifts, and pronounced torsional irregularity, making them unsuitable. L-intersection walls provided notable stiffness and drift reduction but introduced considerable torsional demand at the base. Increasing wall

thickness beyond about 350 mm gave diminishing improvements, and a tapered thickness strategy achieved nearly equivalent performance while conserving material.

The comparison of analysis methods showed that Response Spectrum Analysis generally produced higher base shears than the Equivalent Static approach, highlighting the importance of dynamic analysis for irregular structures. Overall, distributed perimeter walls or balanced combinations of core and perimeter walls, coupled with judicious use of wall thickness, offer the most effective and efficient means of enhancing seismic resilience and material economy in L-shaped reinforced-concrete buildings.

5.2 Recommendations for Practice

The following recommendations can be drawn for practising engineers involved in the seismic design of irregular reinforced-concrete buildings:

- Adopt distributed shear walls: Perimeter walls should be provided along both wings of an L-shaped plan to balance stiffness, share shear demand, and reduce torsional irregularity. Relying on a central core alone is not advised, as this configuration was shown to violate torsional limits.

- Use L-intersection walls judiciously: Walls placed at the re-entrant corner are effective in stiffening the short wing, but they should not be the sole additional walls. Combining L-intersection walls with perimeter walls or stiff diaphragms will provide better torsional control.

- Select appropriate wall thicknesses: A tapered wall strategy is recommended. Walls in the lower third of the building should be at least 350 mm thick, tapering to 300 mm in the middle and 250 mm or 200 mm in the upper storeys. Increasing thickness beyond 350 mm at the base yields little benefit relative to the extra material cost. In low-to-moderate seismic zones, perimeter walls should not exceed 250 mm above mid-height.

• Check torsional irregularity: The twist ratio ($\Delta_{max}/\Delta_{avg}$) should be calculated for all designs. If the ratio exceeds 1.2, additional perimeter or corner walls should be introduced, or the floor diaphragm should be stiffened to redistribute torsional demand.

• Validate RSA results against ELF demands: Where RSA base shear is less than 85 % of the ELF base shear, scale the RSA results up to ensure compliance with Eurocode 8. Designs should not be based solely on unscaled RSA forces when they underestimate ELF demands. For buildings with plan irregularity, RSA (or time-history where appropriate) should be preferred over simplified ELF; when ELF is used, cross-check and scale in accordance with Eurocode 8 if RSA < 85 % of the static value.

• Detail walls for shear, moment, and torsion: Even when walls provide adequate stiffness, the reinforcement must be designed to resist the peak shear, bending moment, and torsion values. The core-only models exhibited very high torsional demands; additional confinement and boundary reinforcement would be required in such cases. At Perimeter walls, detailing should account for bi-axial bending and shear interaction. For L-intersection walls, increase reinforcement around the corner and at wall-to-slab interfaces to accommodate concentrated torsional stresses.

• Verify inter-storey drift: Even when global drift limits are satisfied, localised drifts at the re-entrant corner may be critical for non-structural components. Check relative displacements between orthogonal wings and provide flexible joints or movement allowances in finishes and services.

• Quality control and construction tolerance: Accurate alignment of shear walls and columns is vital in irregular buildings to avoid inadvertent eccentricities. Rigorous construction supervision and peer review of design models are advised. Sensitivity checks can be undertaken to assess the impact of minor dimensional deviations on dynamic response.

5.3 Recommendations for Future Research

Whilst this study offers a detailed analytical assessment, several areas merit further investigation to refine and extend the findings:

Experimental validation: Physical testing of scaled L-shaped RC buildings under shake-table excitation would provide valuable data on the actual stress distribution, cracking patterns and torsional responses. Such experiments could confirm the analytical trends observed and calibrate numerical models.

Material enhancements: Investigating high-performance materials—such as fibre-reinforced polymer wraps at re-entrant corners, high-strength concrete in critical columns or supplemental damping devices—could improve seismic resilience without extensive thickening of walls. Studies should quantify the benefits of these techniques in reducing stress concentrations and drift.

Nonlinear analysis: The present work used linear RSA and ELF methods. Pushover and time-history analyses should be conducted to assess behaviour beyond the elastic range, capture stiffness degradation, and identify potential soft-storey mechanisms. This would provide a more realistic understanding of failure modes and reserve strength.

Soil–structure interaction and foundation design: The models assumed a fixed base. Future studies should consider soil flexibility, especially in soft soil regions, and explore foundation systems such as piles or mats that could mitigate torsional rotations.

Extension to other irregular plans: Further research should examine T-shaped, C-shaped, and more complex plan irregularities. The influence of openings, setbacks, and vertical irregularities could be studied to provide comprehensive guidelines for a wider range of building forms.

Cost optimisation and sustainability: Assess both initial and life-cycle costs for different wall layouts/thicknesses, and evaluate environmental impacts to encourage optimisation of material quantities without compromising safety.

Codification: Use findings to inform code provisions on torsional-irregularity limits, dynamic-analysis requirements, and recommended detailing at re-entrant corners; develop simplified yet accurate procedures suitable for irregular buildings

By addressing these topics, future research can contribute to more robust design recommendations, enabling safer and more economical irregular buildings in seismically active regions.

REFERENCES

.

[1] V. Alecci and M. De Stefano, “Building irregularity issues and architectural design in seismic areas,” Frattura ed Integrita Strutturale, vol. 13, no. 47, pp. 161–168, Jan. 2019, doi: 10.3221/IGF-ESIS.47.13.

[2] H. Jiang, Y. Huang, L. He, T. Huang, and S. Zhang, “Seismic performance of RC frame-shear wall structures with vertical setback,” Structures, vol. 33, pp. 4203–4217, Oct. 2021, doi: 10.1016/J.ISTRUC.2021.07.018.

[3] P. Singh and M. Z. Aryan, “Effect of (Vertical & Horizontal) Geometric Irregularities on the Seismic Response of RC Structures,” 2020.

[4] M. Akhavan Salmassi, A. Kheyroddin, and A. Hemmati, “Seismic behavior of end walls in RC tall buildings with torsional irregularity,” Magazine of Civil Engineering, vol. 97, no. 5, Sep. 2020, doi: 10.18720/MCE.97.7.

[5] W. Xu, Y. Zhao, W. Yang, J. Zhang, and D. Chen, “Seismic performance of RC frame-shear wall dual structural systems,” Structures, vol. 58, p. 105610, Dec. 2023, doi: 10.1016/J.ISTRUC.2023.105610.

[6] M. M. M. Ahmed, S. E. Abdel Raheem, M. M. Ahmed, and A. G. A. Abdel Shafy, “IRREGULARITY EFFECTS ON THE SEISMIC PERFORMANCE OF L-SHAPED MULTI-STORY BUILDINGS,” JES. Journal of Engineering Sciences, vol. 44, no. No 5, pp. 513–536, Sep. 2016, doi: 10.21608/JESAUN.2016.111440.

[7] S. E. A. Raheem, M. M. Ahmed, M. M. Ahmed, and A. G. A. Abdel-Shafy, “Seismic performance of L-shaped multi-storey buildings with moment-resisting frames,” https://doi.org/10.1680/jstbu.16.00122, vol. 171, no. 5, pp. 395–408, Apr. 2018, doi: 10.1680/JSTBU.16.00122.

[8] M. Haque, S. Ray, A. Chakraborty, M. Elias, and I. Alam, “Seismic Performance Analysis of RCC Multi-Storied Buildings with Plan Irregularity,” American Journal of Civil Engineering, vol. 4, no. 3, pp. 68–73, 2016, doi: 10.11648/j.ajce.20160403.11.

[9] A. Koçak, B. Zengin, and F. Kadioğlu, “Performance assessment of irregular RC buildings with shear walls after Earthquake,” Eng Fail Anal, vol. 55, pp. 157–168, Sep. 2015, doi: 10.1016/J.ENGFAILANAL.2015.05.016.

[10] S. Tomer and M. Bhandari, “Evaluation of Seismic Response of Irregular Buildings: A Review,” IOP Conf Ser Earth Environ Sci, vol. 1110, no. 1, p. 012012, Feb. 2023, doi: 10.1088/1755-1315/1110/1/012012.

[11] R. C M, B. Narayan K S, S. B V, and V. Reddy D, “Effect of Irregular Configurations on Seismic Vulnerability of RC Buildings,” Architecture Research, vol. 2, no. 3, pp. 20–26, Aug. 2012, doi: 10.5923/J.ARCH.20120203.01.

[12] M. De Stefano and B. Pintucchi, “A review of research on seismic behaviour of irregular building structures since 2002,” Bulletin of Earthquake Engineering, vol. 6, no. 2, pp. 285–308, May 2008, doi: 10.1007/s10518-007-9052-3.

[13] B. Khanal and H. Chaulagain, “Seismic elastic performance of L-shaped building frames through plan irregularities,” Structures, vol. 27, pp. 22–36, Oct. 2020, doi: 10.1016/J.ISTRUC.2020.05.017.

[14] S. E. Abdel Raheem, M. M. M. Ahmed, M. M. Ahmed, and A. G. A. Abdel-shafy, “Evaluation of plan configuration irregularity effects on seismic response demands of L-shaped MRF buildings,” Bulletin of Earthquake Engineering, vol. 16, no. 9, pp. 3845–3869, Sep. 2018, doi: 10.1007/s10518-018-0319-7.

[15] B. Khanal and H. Chaulagain, “Study of Seismic Response Demands of Different L-shaped Buildings,” Himalayan Journal of Applied Science and Engineering, vol. 1, no. 1, pp. 23–29, Dec. 2020, doi: 10.3126/HIJASE.V1I1.33537.

[16] P. P. Chandurkar and P. S. Pajgade, “Seismic Analysis of RCC Building with and Without Shear Wall,” International Journal of Modern Engineering Research (IJMER) www.ijmer.com, vol. 3, no. 3, pp. 1805–1810, Accessed: Feb. 18, 2025. [Online]. Available: www.ijmer.com

[17] G. S. Hiremath1 and S. Hussain2, “Effect of Change in Shear Wall Location with Uniform and Varying Thickness in High Rise Building,” International Journal of Science and Research (IJSR) ISSN, vol. 3, 2012, Accessed: Feb. 18, 2025. [Online]. Available: www.ijsr.net

[18] M. Rathore and S. S. Bhadauria, “Comparative Study of RC Shear Walls of Various Configurations in L Shape Building,” 2017.

[19] J. Pejovic, N. Serdar, R. Pejovic, and S. Jankovic, “Shear force magnification in reinforced concrete walls of high-rise buildings designed according to Eurocode 8,” Eng Struct, vol. 200, p. 109668, Dec. 2019, doi: 10.1016/J.ENGSTRUCT.2019.109668.

[20] H. Lou et al., “Size optimization design of members for shear wall high-rise buildings,” Journal of Building Engineering, vol. 61, p. 105292, Dec. 2022, doi: 10.1016/J.JOBE.2022.105292.

[21] X. Zhou, L. Wang, J. Liu, G. Cheng, D. Chen, and P. Yu, “Automated structural design of shear wall structures based on modified genetic algorithm and prior knowledge,” Autom Constr, vol. 139, p. 104318, Jul. 2022, doi: 10.1016/J.AUTCON.2022.104318.

[22] M. Sharma, G. Sharma, A. Tanta, M. T. Scholar, and O. D. 123, “COMPARATIVE STUDY AND SEISMIC ANALYSIS OF MULTI-STOREY BUILDING WITH AND WITHOUT SHEAR WALLS USING STAAD. Pro,” International Journal of Research and Analytical Reviews, vol. 5, no. 3, 2018, Accessed: Feb. 18, 2025. [Online]. Available: www.ijrar.org

[23] J. Suthar and S. Purohit, “Seismic behaviour of re-entrant dominant RC frame buildings,” Research on Engineering Structures and Materials, vol. 9, no. 3, pp. 901–920, Jan. 2023, doi: 10.17515/resm2022.629me1230.

[24] Y. Zhang and C. Mueller, “Shear wall layout optimization for conceptual design of tall buildings,” Eng Struct, vol. 140, pp. 225–240, Jun. 2017, doi: 10.1016/J.ENGSTRUCT.2017.02.059.

[25] K. M. Alaa, K. F. El-Kashif, and H. M. Salem, “New definition for torsional irregularity based on floors rotations of reinforced concrete buildings,” Journal of Engineering and Applied Science, vol. 69, no. 1, p. 12, Dec. 2022, doi: 10.1186/s44147-021-00061-5.

[26] J. Ahmed and S. A. Raza, “Seismic Vulnerability of Rc Buildings by Considering Plan Irregularities Using Pushover Analysis,” Glob J Res Anal, 2014.

[27] “(PDF) Significance of Shear Wall in Highrise Irregular Buildings 1.” Accessed: Feb. 18, 2025. [Online]. Available: https://www.researchgate.net/publication/268819430_Significance_of_Shear_Wall_in_High rise_Irregular_Buildings_1

[28] A. Khosravi Larijani and P. Tehrani, “Investigating the effect of earthquake incident angle on seismic response and fragility analysis of irregular RC buildings with nonparallel systems,” Structures, vol. 68, p. 107135, Oct. 2024, doi: 10.1016/J.ISTRUC.2024.107135.

[29] S. Neelavathi, K. G. Shwetha, and C. L. Mahesh Kumar, “Torsional behavior of irregular rc building under static and dynamic loading,” Materials Science Forum, vol. 969, pp. 247–252, Jan. 2019, doi: 10.4028/www.scientific.net/MSF.969.247.

[30] H. Arabzadeh and K. Galal, “Seismic-Response Analysis of RC C-Shaped Core Walls Subjected to Combined Flexure, Shear, and Torsion,” Journal of Structural Engineering (United States), vol. 144, no. 10, p. 04018165, Oct. 2018, doi: 10.1061/(ASCE)ST.1943-541X.0002181.

[31] A. Shrestha, B. Kandel, M. Shrestha, B. Adhikari, and A. Poudel, “Impact of Shear Wall Location on the Response of RC Framed Building,” OCEM Journal of Management, Technology & Social Sciences, vol. 2, no. 2, pp. 115–125, Apr. 2023, doi: 10.3126/OCEMJMTSS.V2I2.54248.

[32] S. Akhil Ahamad and K. V. Pratap, “Dynamic analysis of G+20 multi storied building by using shear walls in various locations for different seismic zones by using Etabs,” Mater Today Proc, vol. 43, pp. 1043–1048, Jan. 2020, doi: 10.1016/j.matpr.2020.08.014.

[33] S. Adhikari, T. B. Katuwal, D. Thapa, S. Lamichhane, and D. Adhikari, “Analysis of L-Shape Building with Lift Core at Different Locations And Its Torsional Effect,” Technical Journal, vol. 2, no. 1, pp. 1–10, Nov. 2020, doi: 10.3126/TJ.V2I1.32822.

[34] V. N. K. Varma and U. P. Kumar, “Seismic response on multi-storied building having shear walls with and without openings,” Mater Today Proc, vol. 37, no. Part 2, pp. 801–805, Jan. 2021, doi: 10.1016/J.MATPR.2020.05.827.

[35] N. K. Meshram and G. M. Munde, “Seismic Analysis of Shear Wall at Different Location on Multi-storey RCC Building,” International Journal of Interdisciplinary Innovative Research & Development, Accessed: Feb. 22, 2025. [Online]. Available: www.ijiird.com

[36] Z. Sadat and A. Arslan, “Automatic Minimization of the Drift Performance of RC 3D Irregular Buildings Using Genetic Algorithm,” Advances in Civil Engineering, vol. 2023, 2023, doi: 10.1155/2023/8275138.

[37] A. R. Simon, F. K. Hridoy, M. Fahim Siddique, and S. A. Safat, “Orientation and location of shear walls in RC buildings to control deflection and drifts,” Procedia Structural Integrity, vol. 46, pp. 162–168, Jan. 2023, doi: 10.1016/j.prostr.2023.06.028.

[38] A. Alavi and P. Srinivasa Rao, “Pages: 1-6 To Cite This Article: Amin Alavi, P. Srinivasa Rao., Effect of Plan Irregular RC Buildings In High Seismic Zone,” Aust J Basic Appl Sci, vol. 7, no. 13, pp. 1–6, 2013, Accessed: Feb. 22, 2025. [Online]. Available: www.ajbasweb.com

[39] K. M. Alaa, K. F. El-Kashif, and H. M. Salem, “New definition for torsional irregularity based on floors rotations of reinforced concrete buildings,” Journal of Engineering and Applied Science, vol. 69, no. 1, p. 12, Dec. 2022, doi: 10.1186/s44147-021-00061-5.

[40] M. Barser, B. Rc, and A. I. Shirkol, “Performance analysis of asymmetrical RC structures using different configurations of shear wall,” Mater Today Proc, vol. 88, pp. 52–65, Jan. 2023, doi: 10.1016/J.MATPR.2023.04.493.

[41] H. Singh Rathore, A. Mathur, and S. Hussain, “Seismic analysis of irregular buildings with Re-Entrant corners and Autoclaved Aerated concrete blocks,” Mater Today Proc, vol. 62, pp. 1643–1650, Jan. 2022, doi: 10.1016/J.MATPR.2022.04.372.

[42] M. Mouhine, M. Derife, S. Aboumdian, and E. Hilali, “Improving Seismic Vulnerability of Irregular Reinforced Concrete Moment-Resisting Frames using Shear Walls,” International Journal of Engineering, Transactions A: Basics, vol. 37, no. 2, pp. 425–438, Feb. 2024, doi: 10.5829/ije.2024.37.02b.17.

APPENDIX A
MODELLING INPUTS

Model Geometries:

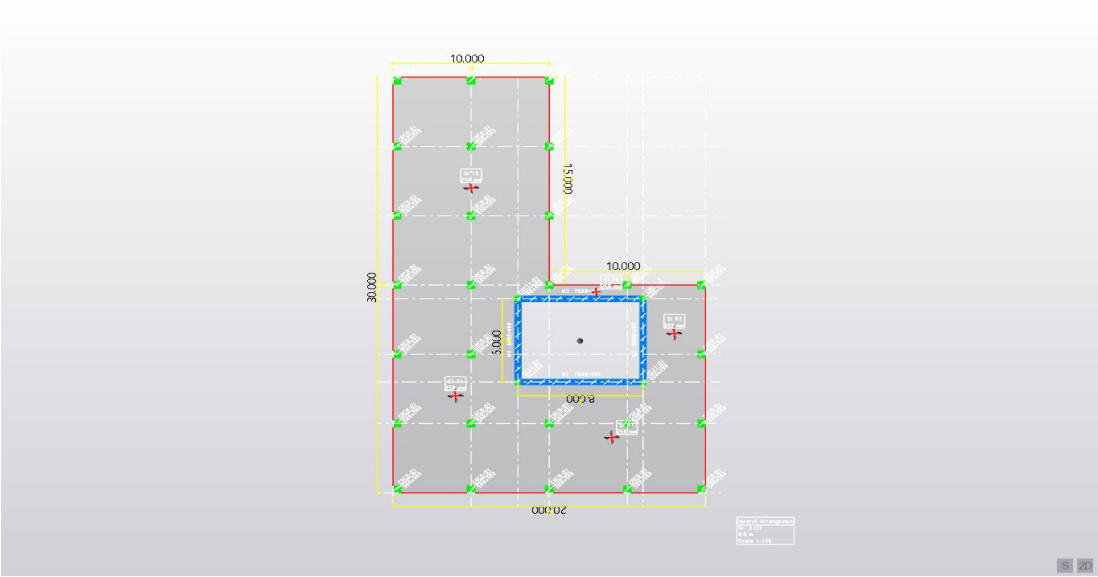

Figure A.1 Model 1 (Core-only) - Plan view with dimensions

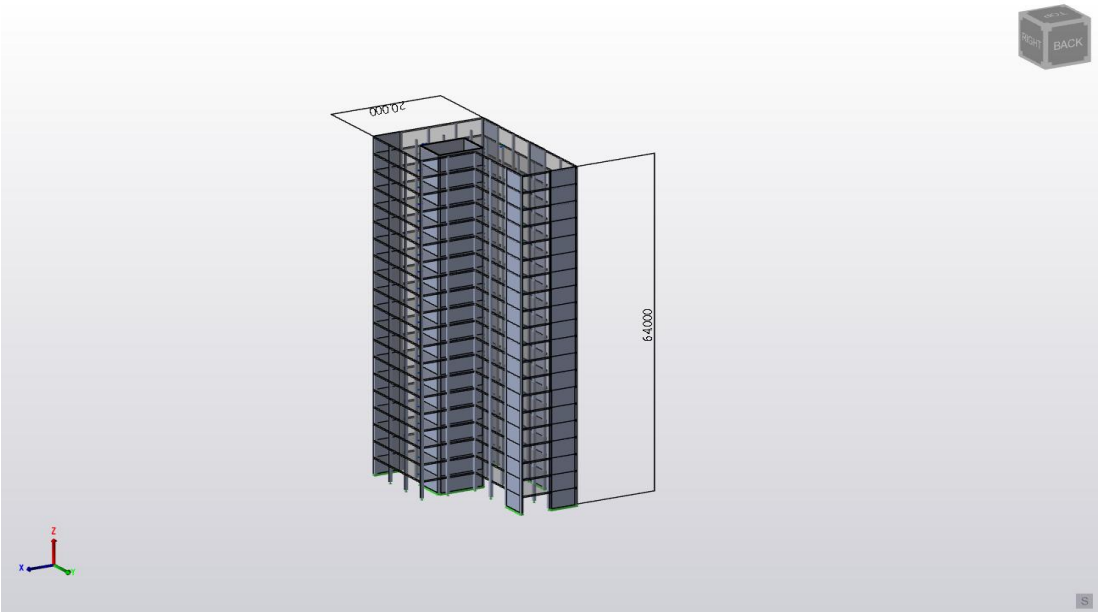

Figure A.2 Model 4 (Core + Perimeter) - Plan view with wall locations

EC8 Spectrum & Damping Settings:

FigureA.3 TSD Seismic Wizard panel with drift 0.005, accidental torsion ±5 %, base shear preview.

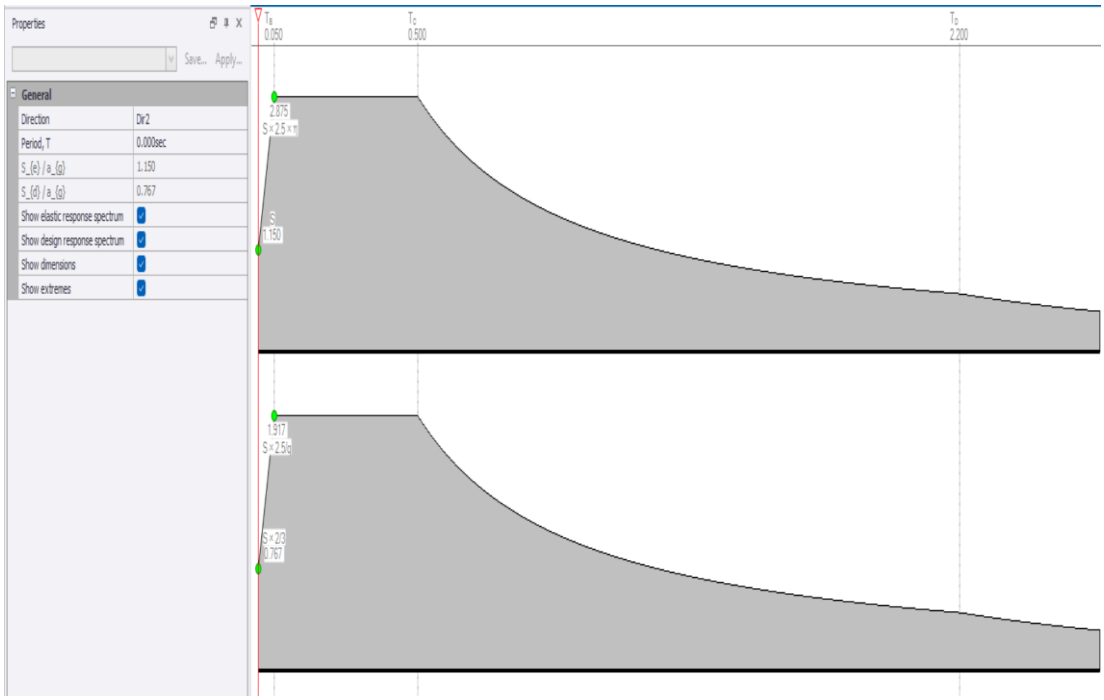

Figure A.4 EC8 Type 1 horizontal spectra showing plateau then decay; elastic vs design.

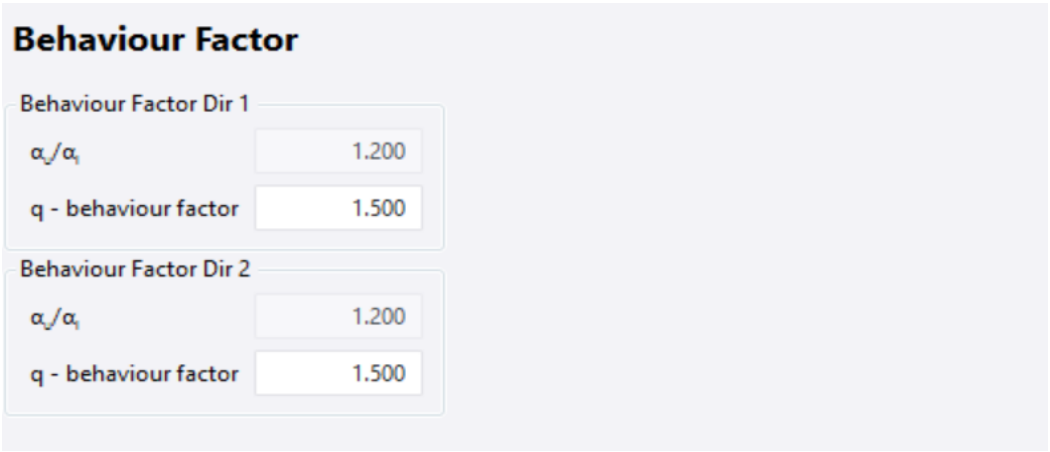

Figure A.5 Behaviour/overstrength factors for both directions

Table A.1 Load Combinations (as generated by TSD)

#	Design Combination Title	Camber	Class	Active	Strength	Service
1	Seismic Inertia	☐	Base Shear	☑		
2	(Operating) STR_1-1.35G+1.5Q+1.5RQ	☐	Gravity	☑	☑	☑
3	(Operating) $SEIS_{1.1}$-G+ψ_2Q+ψ_2RQ±A_{Ed}+EHF_{Dir1+}		Seismic RSA	☑	☑	☐
4	(Operating) $SEIS_{1.2}$-G+ψ_2Q+ψ_2RQ±A_{Ed}+EHF_{Dir1-}		Seismic RSA	☑	☑	☐
5	(Operating) $SEIS_{1.3}$-G+ψ_2Q+ψ_2RQ±A_{Ed}+EHF_{Dir2+}		Seismic RSA	☑	☑	☐
6	(Operating) $SEIS_{1.4}$-G+ψ_2Q+ψ_2RQ±A_{Ed}+EHF_{Dir2-}		Seismic RSA	☑	☑	☐
7	(Operating) $SEIS_{3.1}$-G±A_{Ed}+EHF_{Dir1+}		Seismic RSA	☑	☑	☐
8	(Operating) $SEIS_{3.2}$-G±A_{Ed}+EHF_{Dir1-}		Seismic RSA	☑	☑	☐
9	(Operating) $SEIS_{3.3}$-G±A_{Ed}+EHF_{Dir2+}		Seismic RSA	☑	☑	☐
10	(Operating) $SEIS_{3.4}$-G±A_{Ed}+EHF_{Dir2-}		Seismic RSA	☑	☑	☐

APPENDIX B EXTENDED RESULTS

CRITICAL ANALYSIS OUTPUTS

Table B.1 All 14 models - periods and mass participation (condensed format)

MODEL1

Mode Number	Period [sec]	Frequency [Hz]	Error [%]	Mass Participation Dir 1 [%]	Mass Participation Dir 2 [%]	Mass ParticipationZ [%]	Modal Mass [kN]
1	2.753	0.36	0.00	0.06	61.64	0.00	21821.1
2	2.187	0.46	0.00	61.56	0.06	0.00	21050.1
3	1.156	0.86	0.00	0.05	0.00	0.00	12123.8
4	0.567	1.76	0.00	0.33	18.70	0.00	13178.7
5	0.441	2.27	0.00	17.23	1.16	0.00	13280.0
6	0.385	2.60	0.00	3.57	0.66	0.00	10303.9
7	0.289	3.45	0.00	0.50	4.08	0.00	8981.6
8	0.211	4.74	0.00	0.55	0.74	0.00	13746.6
9	0.198	5.05	0.00	1.13	3.78	0.00	8691.3
10	0.178	5.61	0.00	5.82	0.72	0.00	13079.6

MODEL2

Mode Number	Period [sec]	Frequency [Hz]	Error [%]	Mass Participation Dir 1 [%]	Mass Participation Dir 2 [%]	Mass ParticipationZ [%]	Modal Mass [kN]
1	2.576	0.39	0.00	0.05	61.78	0.00	22457.6
2	2.044	0.49	0.00	61.71	0.05	0.00	21684.9
3	1.077	0.93	0.00	0.04	0.00	0.00	12553.2
4	0.525	1.91	0.00	0.31	18.93	0.00	13866.8
5	0.410	2.44	0.00	17.53	1.05	0.00	13840.0
6	0.357	2.80	0.00	3.37	0.63	0.00	10703.4
7	0.266	3.76	0.00	0.48	4.07	0.00	9322.7
8	0.195	5.13	0.00	0.60	1.01	0.00	14035.3
9	0.183	5.48	0.00	1.11	3.43	0.00	8734.1
10	0.165	6.04	0.00	5.75	0.76	0.00	13438.1

MODEL3

Mode Number	Period [sec]	Frequency [Hz]	Error [%]	Mass Participation Dir 1 [%]	Mass Participation Dir 2 [%]	Mass ParticipationZ [%]	Modal Mass [kN]
1	2.401	0.42	0.00	0.01	60.69	0.00	24246.2
2	2.097	0.48	0.00	60.98	0.01	0.00	23054.3
3	1.059	0.94	0.00	0.04	0.02	0.00	11845.0
4	0.468	2.14	0.00	0.07	20.47	0.00	22020.9
5	0.415	2.41	0.00	20.22	0.15	0.00	16067.2
6	0.339	2.95	0.00	0.87	0.29	0.00	8464.2
7	0.197	5.08	0.00	0.23	6.26	0.00	14272.7
8	0.182	5.49	0.00	3.63	1.18	0.00	10295.0
9	0.167	5.99	0.00	3.81	0.20	0.00	9876.8
10	0.116	8.65	0.00	0.26	2.37	0.00	11754.8

MODEL4

Mode Number	Period [sec]	Frequency [Hz]	Error [%]	Mass Participation Dir 1 [%]	Mass Participation Dir 2 [%]	Mass ParticipationZ [%]	Modal Mass [kN]
1	2.400	0.42	0.00	0.01	60.72	0.00	24706.3
2	2.105	0.48	0.00	60.99	0.01	0.00	23414.0
3	1.069	0.94	0.00	0.04	0.02	0.00	12170.4
4	0.465	2.15	0.00	0.07	20.47	0.00	22925.5
5	0.415	2.41	0.00	20.17	0.14	0.00	16319.5
6	0.339	2.95	0.00	0.88	0.25	0.00	8636.4
7	0.194	5.16	0.00	0.21	6.51	0.00	16107.4
8	0.181	5.51	0.00	3.88	0.94	0.00	10210.3
9	0.166	6.01	0.00	3.56	0.16	0.00	9821.7
10	0.113	8.86	0.00	0.23	2.85	0.00	14750.4

MODEL5

Mode Number	Period [sec]	Frequency [Hz]	Error [%]	Mass Participation Dir 1 [%]	Mass Participation Dir 2 [%]	Mass ParticipationZ [%]	Modal Mass [kN]
1	2.399	0.42	0.00	0.01	60.75	0.00	25167.7
2	2.113	0.47	0.00	61.01	0.01	0.00	23775.0
3	1.079	0.93	0.00	0.04	0.02	0.00	12506.5
4	0.462	2.16	0.00	0.07	20.46	0.00	23825.1
5	0.416	2.40	0.00	20.12	0.13	0.00	16574.7
6	0.340	2.94	0.00	0.88	0.22	0.00	8819.1
7	0.192	5.22	0.00	0.18	6.75	0.00	18273.7
8	0.181	5.53	0.00	4.13	0.71	0.00	10166.4
9	0.166	6.03	0.00	3.31	0.12	0.00	9827.4
10	0.111	9.02	0.00	0.11	3.45	0.00	22293.0
11	0.109	9.20	0.00	1.41	0.38	0.00	10189.4

MODEL6

Mode Number	Period [sec]	Frequency [Hz]	Error [%]	Mass Participation Dir 1 [%]	Mass Participation Dir 2 [%]	Mass ParticipationZ [%]	Modal Mass [kN]
1	2.292	0.44	0.00	0.01	60.85	0.00	24798.3
2	1.979	0.51	0.00	61.14	0.01	0.00	23635.2
3	0.995	1.00	0.00	0.03	0.02	0.00	12378.2
4	0.445	2.25	0.00	0.08	20.43	0.00	21710.4
5	0.390	2.56	0.00	20.21	0.18	0.00	16359.2
6	0.319	3.14	0.00	0.94	0.35	0.00	8763.3
7	0.189	5.29	0.00	0.28	5.74	0.00	12480.8
8	0.172	5.80	0.00	3.12	1.63	0.00	10905.4
9	0.157	6.36	0.00	4.25	0.24	0.00	10711.0
10	0.112	8.90	0.00	0.26	1.89	0.00	10078.6

MODEL7

Mode Number	Period [sec]	Frequency [Hz]	Error [%]	Mass Participation Dir 1 [%]	Mass Participation Dir 2 [%]	Mass ParticipationZ [%]	Modal Mass [kN]
1	2.292	0.44	0.00	0.01	60.87	0.00	25249.8
2	1.988	0.50	0.00	61.16	0.01	0.00	23991.4
3	1.005	1.00	0.00	0.04	0.02	0.00	12719.6
4	0.443	2.26	0.00	0.08	20.42	0.00	22496.9
5	0.391	2.56	0.00	20.15	0.17	0.00	16572.8
6	0.319	3.13	0.00	0.96	0.32	0.00	8912.3
7	0.186	5.36	0.00	0.27	5.92	0.00	13542.2
8	0.172	5.81	0.00	3.28	1.45	0.00	10954.0
9	0.157	6.37	0.00	4.06	0.21	0.00	10627.5
10	0.110	9.11	0.00	0.28	2.06	0.00	10889.8

MODEL8

Mode Number	Period [sec]	Frequency [Hz]	Error [%]	Mass Participation Dir 1 [%]	Mass Participation Dir 2 [%]	Mass ParticipationZ [%]	Modal Mass [kN]
1	2.293	0.44	0.00	0.01	60.89	0.00	25702.5
2	1.996	0.50	0.00	61.17	0.01	0.00	24348.6
3	1.014	0.99	0.00	0.04	0.03	0.00	13012.1
4	0.441	2.27	0.00	0.08	20.40	0.00	23279.1
5	0.392	2.55	0.00	20.09	0.17	0.00	16789.8
6	0.320	3.12	0.00	0.97	0.29	0.00	9072.3
7	0.184	5.42	0.00	0.26	6.10	0.00	14723.2
8	0.172	5.83	0.00	3.44	1.27	0.00	11001.1
9	0.157	6.38	0.00	3.89	0.18	0.00	10595.8
10	0.108	9.29	0.00	0.30	2.28	0.00	12028.4

MODEL9

Mode Number	Period [sec]	Frequency [Hz]	Error [%]	Mass Participation Dir 1 [%]	Mass Participation Dir 2 [%]	Mass ParticipationZ [%]	Modal Mass [kN]
1	1.869	0.53	0.00	44.51	16.26	0.00	19503.7
2	1.331	0.75	0.00	14.68	33.76	0.00	13111.5
3	1.105	0.91	0.00	2.33	12.22	0.00	13061.2
4	0.443	2.26	0.00	1.69	4.68	0.00	8342.1
5	0.357	2.80	0.00	15.79	1.38	0.00	15323.8
6	0.289	3.46	0.00	4.12	13.63	0.00	22833.9
7	0.257	3.89	0.00	0.02	2.85	0.00	9433.0
8	0.181	5.52	0.00	0.00	0.03	0.00	9219.3
9	0.156	6.41	0.00	6.41	1.02	0.00	18515.7
10	0.139	7.18	0.00	0.00	0.38	0.00	12413.2
11	0.136	7.37	0.00	1.12	5.31	0.00	16257.6

MODEL10

Mode Number	Period [sec]	Frequency [Hz]	Error [%]	Mass Participation Dir 1 [%]	Mass Participation Dir 2 [%]	Mass ParticipationZ [%]	Modal Mass [kN]
1	1.845	0.54	0.00	45.20	15.58	0.00	19768.8
2	1.297	0.77	0.00	12.85	29.31	0.00	12347.3
3	1.096	0.91	0.00	3.55	17.49	0.00	13349.0
4	0.440	2.27	0.00	1.47	3.95	0.00	8507.0
5	0.352	2.84	0.00	16.02	1.67	0.00	16093.8
6	0.277	3.61	0.00	4.11	13.07	0.00	26835.6
7	0.256	3.91	0.00	0.00	3.78	0.00	9751.0
8	0.180	5.56	0.00	0.00	0.04	0.00	9453.0
9	0.153	6.53	0.00	6.41	1.01	0.00	19729.8
10	0.138	7.24	0.00	0.02	0.20	0.00	12458.8
11	0.130	7.72	0.00	1.07	5.49	0.00	18429.1

MODEL11

Mode Number	Period [sec]	Frequency [Hz]	Error [%]	Mass Participation Dir 1 [%]	Mass Participation Dir 2 [%]	Mass ParticipationZ [%]	Modal Mass [kN]
1	1.824	0.55	0.00	45.73	15.06	0.00	20008.7
2	1.272	0.79	0.00	10.97	24.08	0.00	11856.9
3	1.084	0.92	0.00	4.98	23.35	0.00	13893.2
4	0.439	2.28	0.00	1.29	3.38	0.00	8693.9
5	0.348	2.88	0.00	16.23	1.90	0.00	16884.0
6	0.268	3.73	0.00	3.91	10.94	0.00	22582.5
7	0.254	3.94	0.00	0.17	6.19	0.00	10523.6
8	0.179	5.59	0.00	0.01	0.05	0.00	9686.3
9	0.150	6.65	0.00	6.41	1.00	0.00	20699.0
10	0.137	7.29	0.00	0.03	0.17	0.00	12752.0
11	0.125	8.03	0.00	1.03	5.51	0.00	19746.6

MODEL12

Mode Number	Period [sec]	Frequency [Hz]	Error [%]	Mass Participation Dir 1 [%]	Mass Participation Dir 2 [%]	Mass ParticipationZ [%]	Modal Mass [kN]
1	1.798	0.56	0.00	43.81	17.13	0.00	20144.2
2	1.297	0.77	0.00	16.70	38.34	0.00	15146.6
3	1.049	0.95	0.00	1.10	6.79	0.00	13087.7
4	0.414	2.41	0.00	2.37	5.51	0.00	8574.6
5	0.338	2.96	0.00	15.05	0.97	0.00	14832.2
6	0.283	3.53	0.00	4.18	13.91	0.00	20960.7
7	0.239	4.18	0.00	0.12	2.21	0.00	9678.7
8	0.169	5.93	0.00	0.00	0.01	0.00	9381.8
9	0.148	6.75	0.00	6.26	1.07	0.00	17416.5
10	0.133	7.54	0.00	1.10	5.60	0.00	22492.5

MODEL13

Mode Number	Period [sec]	Frequency [Hz]	Error [%]	Mass Participation Dir 1 [%]	Mass Participation Dir 2 [%]	Mass ParticipationZ [%]	Modal Mass [kN]
1	1.778	0.56	0.00	44.65	16.30	0.00	20431.6
2	1.258	0.79	0.00	15.30	36.24	0.00	14222.9
3	1.047	0.96	0.00	1.73	9.85	0.00	13424.0
4	0.412	2.43	0.00	2.16	4.67	0.00	8684.6
5	0.335	2.99	0.00	15.23	1.29	0.00	15404.5
6	0.272	3.67	0.00	4.23	14.19	0.00	23218.7
7	0.238	4.20	0.00	0.07	2.37	0.00	9892.1
8	0.167	5.97	0.00	0.00	0.02	0.00	9547.4
9	0.146	6.86	0.00	6.30	1.05	0.00	18599.8
10	0.129	7.75	0.00	0.01	0.72	0.00	13190.7
11	0.127	7.88	0.00	1.14	4.91	0.00	15570.5

MODEL14

Mode Number	Period [sec]	Frequency [Hz]	Error [%]	Mass Participation Dir 1 [%]	Mass Participation Dir 2 [%]	Mass ParticipationZ [%]	Modal Mass [kN]
1	1.760	0.57	0.00	45.29	15.67	0.00	20696.9
2	1.227	0.82	0.00	13.86	33.00	0.00	13384.0
3	1.042	0.96	0.00	2.60	13.84	0.00	13935.3
4	0.410	2.44	0.00	1.96	4.01	0.00	8830.9
5	0.331	3.02	0.00	15.44	1.55	0.00	16052.0
6	0.263	3.80	0.00	4.25	14.13	0.00	25885.4
7	0.237	4.21	0.00	0.02	2.76	0.00	10137.7
8	0.167	6.00	0.00	0.00	0.03	0.00	9740.5
9	0.144	6.96	0.00	6.32	1.03	0.00	19659.0
10	0.128	7.81	0.00	0.01	0.25	0.00	12625.6
11	0.122	8.17	0.00	1.10	5.39	0.00	18765.2

RSA & ELF Storey Shear (Models 1–14, Dir1)

Table B.2 Storey shear Dir1 (RSA), Model (1-14)

MODEL1

Level [m]	Reference	Σ Shear Dir 1 [kN]	Σ Shear Dir 2 [kN]
64.000	St. 20 (roof)	-469.1/425.6	-223.8/223.8
60.800	St. 19 (19)	-844.9/758.8	-391.2/391.2
57.600	St. 18 (18)	-1104.7/976.0	-492.7/492.7
54.400	St. 17 (17)	-1261.4/1089.5	-535.3/535.3
51.200	St. 16 (16)	-1343.2/1127.5	-530.6/530.6
48.000	St. 15 (15)	-1376.3/1116.9	-491.3/491.3
44.800	St. 14 (14)	-1393.7/1090.6	-436.9/436.9
41.600	St. 13 (13)	-1422.8/1074.9	-393.1/393.1
38.400	St. 12 (12)	-1481.6/1088.2	-387.5/387.5
35.200	St. 11 (11)	-1573.7/1134.6	-427.1/427.1
32.000	St. 10 (10)	-1697.3/1212.6	-493.7/493.7
28.800	St. 9 (9)	-1850.6/1320.2	-571.8/571.8
25.600	St. 8 (8)	-2031.3/1455.3	-653.9/653.9
22.400	St. 7 (7)	-2236.3/1613.2	-739.8/739.8
19.200	St. 6 (6)	-2463.4/1791.7	-835.3/835.3
16.000	St. 5 (5)	-2684.9/1964.5	-931.9/931.9
12.800	St. 4 (4)	-2882.5/2113.5	-1021.6/1021.6
9.600	St. 3 (3)	-3041.5/2223.9	-1094.7/1094.7
6.400	St. 2 (2)	-3153.5/2287.3	-1143.5/1143.5
3.200	St. 1 (1)	-3218.6/2303.7	-1166.0/1166.0
0.000	St. Base (Base)	-2563.5/1865.1	-896.1/923.1

MODEL2

Level [m]	Reference	Σ Shear Dir 1 [kN]	Σ Shear Dir 2 [kN]
64.000	St. 20 (roof)	-475.1/431.1	-226.6/226.6
60.800	St. 19 (19)	-868.7/780.9	-402.9/402.9
57.600	St. 18 (18)	-1145.9/1014.3	-512.6/512.6
54.400	St. 17 (17)	-1319.1/1143.2	-562.6/562.6
51.200	St. 16 (16)	-1415.5/1194.7	-563.9/563.9
48.000	St. 15 (15)	-1461.0/1195.3	-528.5/528.5
44.800	St. 14 (14)	-1488.8/1178.3	-474.6/474.6
41.600	St. 13 (13)	-1527.0/1170.7	-426.2/426.2
38.400	St. 12 (12)	-1594.2/1191.0	-413.4/413.4
35.200	St. 11 (11)	-1693.2/1243.3	-450.7/450.7
32.000	St. 10 (10)	-1822.2/1325.5	-521.4/521.4
28.800	St. 9 (9)	-1979.2/1435.8	-607.3/607.3
25.600	St. 8 (8)	-2162.3/1572.1	-698.1/698.1
22.400	St. 7 (7)	-2369.4/1730.9	-790.9/790.9
19.200	St. 6 (6)	-2598.8/1910.5	-890.1/890.1
16.000	St. 5 (5)	-2823.4/2085.3	-987.6/987.6
12.800	St. 4 (4)	-3024.6/2236.8	-1076.8/1076.8
9.600	St. 3 (3)	-3187.2/2349.6	-1149.2/1149.2
6.400	St. 2 (2)	-3302.3/2414.9	-1197.6/1197.6
3.200	St. 1 (1)	-3369.4/2432.3	-1220.1/1220.1
0.000	St. Base (Base)	-2681.9/1964.6	-938.2/963.9

MODEL3

Level [m]	Reference	Σ Shear Dir 1 [kN]	Σ Shear Dir 2 [kN]
64.000	St. 20 (roof)	-499.9/455.1	-200.4/200.4
60.800	St. 19 (19)	-923.4/833.3	-354.5/354.5
57.600	St. 18 (18)	-1216.4/1081.0	-442.5/442.5
54.400	St. 17 (17)	-1394.6/1212.9	-477.8/477.8
51.200	St. 16 (16)	-1489.6/1260.7	-481.8/481.8
48.000	St. 15 (15)	-1528.6/1252.4	-471.9/471.9
44.800	St. 14 (14)	-1546.0/1222.5	-459.2/459.2
41.600	St. 13 (13)	-1569.5/1197.4	-448.1/448.1
38.400	St. 12 (12)	-1624.3/1202.2	-447.5/447.5
35.200	St. 11 (11)	-1722.4/1250.3	-466.7/466.7
32.000	St. 10 (10)	-1865.2/1343.2	-508.8/508.8
28.800	St. 9 (9)	-2047.2/1475.1	-568.6/568.6
25.600	St. 8 (8)	-2258.4/1636.3	-637.6/637.6
22.400	St. 7 (7)	-2490.8/1817.0	-712.0/712.0
19.200	St. 6 (6)	-2744.6/2017.1	-797.7/797.7
16.000	St. 5 (5)	-2989.9/2208.7	-888.8/888.8
12.800	St. 4 (4)	-3207.1/2372.2	-977.0/977.0
9.600	St. 3 (3)	-3379.9/2491.3	-1050.8/1050.8
6.400	St. 2 (2)	-3499.6/2557.3	-1100.9/1100.9
3.200	St. 1 (1)	-3568.1/2572.1	-1124.3/1124.3
0.000	St. Base (Base)	-3023.1/2205.3	-874.7/997.1

MODEL4

Level [m]	Reference	Σ Shear Dir 1 [kN]	Σ Shear Dir 2 [kN]
64.000	St. 20 (roof)	-499.3/454.1	-195.7/195.7
60.800	St. 19 (19)	-930.1/838.7	-348.6/348.6
57.600	St. 18 (18)	-1229.0/1091.4	-436.3/436.3
54.400	St. 17 (17)	-1412.2/1227.5	-473.1/473.1
51.200	St. 16 (16)	-1511.5/1278.6	-480.8/480.8
48.000	St. 15 (15)	-1552.9/1271.9	-475.5/475.5
44.800	St. 14 (14)	-1569.2/1239.9	-464.3/464.3
41.600	St. 13 (13)	-1589.5/1210.7	-449.6/449.6
38.400	St. 12 (12)	-1641.1/1211.5	-441.7/441.7
35.200	St. 11 (11)	-1738.1/1257.6	-455.5/455.5
32.000	St. 10 (10)	-1883.4/1352.1	-498.7/498.7
28.800	St. 9 (9)	-2071.0/1488.8	-564.6/564.6
25.600	St. 8 (8)	-2289.3/1656.3	-640.1/640.1
22.400	St. 7 (7)	-2528.5/1842.8	-717.7/717.7
19.200	St. 6 (6)	-2786.7/2046.5	-801.9/801.9
16.000	St. 5 (5)	-3034.0/2239.2	-888.6/888.6
12.800	St. 4 (4)	-3252.1/2402.8	-972.5/972.5
9.600	St. 3 (3)	-3425.5/2521.6	-1043.6/1043.6
6.400	St. 2 (2)	-3545.5/2587.1	-1092.2/1092.2
3.200	St. 1 (1)	-3614.0/2601.2	-1114.9/1114.9
0.000	St. Base (Base)	-3076.4/2240.3	-864.7/1003.1

MODEL5

Level [m]	Reference	Σ Shear Dir 1 [kN]	Σ Shear Dir 2 [kN]
64.000	St. 20 (roof)	-500.3/454.7	-204.7/204.7
60.800	St. 19 (19)	-938.7/846.0	-365.7/365.7
57.600	St. 18 (18)	-1242.7/1102.9	-456.4/456.4
54.400	St. 17 (17)	-1430.0/1242.1	-491.1/491.1
51.200	St. 16 (16)	-1532.3/1295.4	-493.3/493.3
48.000	St. 15 (15)	-1575.3/1289.4	-483.8/483.8
44.800	St. 14 (14)	-1591.8/1256.8	-475.4/475.4
41.600	St. 13 (13)	-1611.2/1225.8	-469.0/469.0
38.400	St. 12 (12)	-1661.3/1224.2	-470.4/470.4
35.200	St. 11 (11)	-1758.4/1269.5	-488.5/488.5
32.000	St. 10 (10)	-1906.3/1365.8	-529.1/529.1
28.800	St. 9 (9)	-2098.2/1505.9	-588.4/588.4
25.600	St. 8 (8)	-2320.8/1676.8	-657.4/657.4
22.400	St. 7 (7)	-2563.7/1866.1	-731.7/731.7
19.200	St. 6 (6)	-2824.7/2071.7	-817.3/817.3
16.000	St. 5 (5)	-3074.2/2265.9	-909.4/909.4
12.800	St. 4 (4)	-3294.4/2430.8	-1000.5/1000.5
9.600	St. 3 (3)	-3469.9/2550.9	-1078.5/1078.5
6.400	St. 2 (2)	-3591.8/2617.4	-1132.5/1132.5
3.200	St. 1 (1)	-3661.6/2631.8	-1158.1/1158.1
0.000	St. Base (Base)	-3130.3/2276.1	-890.0/1044.4

MODEL6

Level [m]	Reference	Σ Shear Dir 1 [kN]	Σ Shear Dir 2 [kN]
64.000	St. 20 (roof)	-503.6/458.3	-205.4/205.4
60.800	St. 19 (19)	-943.8/852.1	-370.3/370.3
57.600	St. 18 (18)	-1253.7/1115.5	-468.1/468.1
54.400	St. 17 (17)	-1448.0/1262.4	-509.7/509.7
51.200	St. 16 (16)	-1557.0/1322.9	-515.0/515.0
48.000	St. 15 (15)	-1607.3/1324.9	-502.7/502.7
44.800	St. 14 (14)	-1636.5/1305.6	-490.6/490.6
41.600	St. 13 (13)	-1672.5/1291.9	-487.0/487.0
38.400	St. 12 (12)	-1738.7/1306.9	-497.8/497.8
35.200	St. 11 (11)	-1844.6/1361.7	-525.2/525.2
32.000	St. 10 (10)	-1991.4/1457.4	-568.3/568.3
28.800	St. 9 (9)	-2173.9/1588.8	-623.4/623.4
25.600	St. 8 (8)	-2383.9/1747.7	-686.8/686.8
22.400	St. 7 (7)	-2615.7/1926.4	-759.2/759.2
19.200	St. 6 (6)	-2871.3/2127.2	-848.3/848.3
16.000	St. 5 (5)	-3121.1/2322.2	-945.7/945.7
12.800	St. 4 (4)	-3343.8/2490.0	-1040.0/1040.0
9.600	St. 3 (3)	-3521.5/2612.9	-1118.1/1118.1
6.400	St. 2 (2)	-3645.1/2681.7	-1170.6/1170.6
3.200	St. 1 (1)	-3716.0/2697.8	-1195.0/1195.0
0.000	St. Base (Base)	-3129.3/2297.6	-927.2/1048.9

MODEL7

Level [m]	Reference	Σ Shear Dir 1 [kN]	Σ Shear Dir 2 [kN]
64.000	St. 20 (roof)	-504.6/458.9	-205.0/205.0
60.800	St. 19 (19)	-953.0/859.9	-371.8/371.8
57.600	St. 18 (18)	-1268.7/1128.3	-470.3/470.3
54.400	St. 17 (17)	-1467.0/1278.3	-512.9/512.9
51.200	St. 16 (16)	-1578.6/1340.6	-520.2/520.2
48.000	St. 15 (15)	-1631.0/1343.6	-511.1/511.1
44.800	St. 14 (14)	-1660.4/1323.7	-500.4/500.4
41.600	St. 13 (13)	-1695.3/1308.1	-494.4/494.4
38.400	St. 12 (12)	-1760.4/1321.1	-500.5/500.5
35.200	St. 11 (11)	-1866.3/1375.1	-524.7/524.7
32.000	St. 10 (10)	-2015.0/1471.8	-568.3/568.3
28.800	St. 9 (9)	-2201.2/1605.9	-627.3/627.3
25.600	St. 8 (8)	-2416.0/1768.8	-695.5/695.5
22.400	St. 7 (7)	-2652.7/1951.6	-770.9/770.9
19.200	St. 6 (6)	-2911.9/2155.1	-859.9/859.9
16.000	St. 5 (5)	-3164.0/2351.5	-955.9/955.9
12.800	St. 4 (4)	-3388.5/2520.4	-1049.1/1049.1
9.600	St. 3 (3)	-3567.8/2644.0	-1127.0/1127.0
6.400	St. 2 (2)	-3692.4/2712.9	-1179.7/1179.7
3.200	St. 1 (1)	-3763.8/2728.7	-1204.3/1204.3
0.000	St. Base (Base)	-3183.6/2333.8	-930.2/1067.9

MODEL8

Level [m]	Reference	Σ Shear Dir 1 [kN]	Σ Shear Dir 2 [kN]
64.000	St. 20 (roof)	-505.6/459.4	-204.9/204.9
60.800	St. 19 (19)	-962.2/867.8	-373.4/373.4
57.600	St. 18 (18)	-1283.7/1141.1	-472.6/472.6
54.400	St. 17 (17)	-1485.9/1294.1	-515.9/515.9
51.200	St. 16 (16)	-1600.3/1358.3	-525.4/525.4
48.000	St. 15 (15)	-1654.5/1362.4	-519.6/519.6
44.800	St. 14 (14)	-1684.3/1341.9	-510.5/510.5
41.600	St. 13 (13)	-1718.2/1324.3	-502.2/502.2
38.400	St. 12 (12)	-1782.0/1335.2	-503.3/503.3
35.200	St. 11 (11)	-1887.9/1388.2	-523.6/523.6
32.000	St. 10 (10)	-2038.4/1485.9	-567.7/567.7
28.800	St. 9 (9)	-2228.3/1623.0	-631.1/631.1
25.600	St. 8 (8)	-2448.1/1789.9	-704.3/704.3
22.400	St. 7 (7)	-2689.7/1976.8	-782.8/782.8
19.200	St. 6 (6)	-2952.4/2182.9	-871.7/871.7
16.000	St. 5 (5)	-3206.8/2380.8	-966.0/966.0
12.800	St. 4 (4)	-3433.2/2550.7	-1058.1/1058.1
9.600	St. 3 (3)	-3614.0/2675.0	-1135.9/1135.9
6.400	St. 2 (2)	-3739.7/2744.2	-1189.0/1189.0
3.200	St. 1 (1)	-3811.8/2759.7	-1213.8/1213.8
0.000	St. Base (Base)	-3237.2/2369.6	-933.0/1086.6

MODEL9

Level [m]	Reference	Σ Shear Dir 1 [kN]	Σ Shear Dir 2 [kN]
64.000	St. 20 (roof)	-453.9/498.7	-346.8/346.8
60.800	St. 19 (19)	-836.6/926.7	-655.5/655.5
57.600	St. 18 (18)	-1096.8/1232.3	-887.1/887.1
54.400	St. 17 (17)	-1248.0/1429.8	-1049.6/1049.6
51.200	St. 16 (16)	-1321.9/1551.1	-1162.8/1162.8
48.000	St. 15 (15)	-1343.3/1619.7	-1238.1/1238.1
44.800	St. 14 (14)	-1345.1/1668.9	-1295.6/1295.6
41.600	St. 13 (13)	-1354.0/1726.6	-1353.5/1353.5
38.400	St. 12 (12)	-1390.6/1813.2	-1426.4/1426.4
35.200	St. 11 (11)	-1457.9/1930.6	-1514.8/1514.8
32.000	St. 10 (10)	-1553.1/2075.8	-1616.1/1616.1
28.800	St. 9 (9)	-1672.6/2245.3	-1726.5/1726.5
25.600	St. 8 (8)	-1813.4/2436.2	-1842.6/1842.6
22.400	St. 7 (7)	-1972.4/2647.2	-1963.0/1963.0
19.200	St. 6 (6)	-2152.4/2881.0	-2091.2/2091.2
16.000	St. 5 (5)	-2328.3/3110.7	-2212.7/2212.7
12.800	St. 4 (4)	-2482.0/3318.2	-2318.5/2318.5
9.600	St. 3 (3)	-2597.7/3487.6	-2400.8/2400.8
6.400	St. 2 (2)	-2665.1/3608.9	-2454.9/2454.9
3.200	St. 1 (1)	-2683.1/3680.6	-2480.6/2480.6
0.000	St. Base (Base)	-2154.0/3042.3	-1936.3/2031.8

MODEL10

Level [m]	Reference	Σ Shear Dir 1 [kN]	Σ Shear Dir 2 [kN]
64.000	St. 20 (roof)	-455.6/500.8	-353.8/353.8
60.800	St. 19 (19)	-847.4/938.8	-674.1/674.1
57.600	St. 18 (18)	-1115.6/1253.3	-913.7/913.7
54.400	St. 17 (17)	-1273.3/1458.3	-1081.2/1081.2
51.200	St. 16 (16)	-1351.8/1585.0	-1197.1/1197.1
48.000	St. 15 (15)	-1375.5/1656.9	-1273.5/1273.5
44.800	St. 14 (14)	-1378.3/1707.9	-1331.7/1331.7
41.600	St. 13 (13)	-1387.6/1766.8	-1390.1/1390.1
38.400	St. 12 (12)	-1424.7/1854.9	-1463.8/1463.8
35.200	St. 11 (11)	-1493.2/1974.3	-1553.4/1553.4
32.000	St. 10 (10)	-1590.3/2122.4	-1656.6/1656.6
28.800	St. 9 (9)	-1712.6/2295.6	-1769.3/1769.3
25.600	St. 8 (8)	-1856.7/2490.7	-1888.1/1888.1
22.400	St. 7 (7)	-2019.7/2706.5	-2011.8/2011.8
19.200	St. 6 (6)	-2203.7/2945.2	-2143.8/2143.8
16.000	St. 5 (5)	-2383.3/3179.4	-2269.4/2269.4
12.800	St. 4 (4)	-2539.9/3390.7	-2379.6/2379.6
9.600	St. 3 (3)	-2657.5/3563.0	-2465.9/2465.9
6.400	St. 2 (2)	-2726.0/3686.1	-2523.0/2523.0
3.200	St. 1 (1)	-2744.1/3758.9	-2550.4/2550.4
0.000	St. Base (Base)	-2198.4/3114.8	-1987.9/2099.0

MODEL11

Level [m]	Reference	Σ Shear Dir 1 [kN]	Σ Shear Dir 2 [kN]
64.000	St. 20 (roof)	-457.2/502.9	-355.6/355.6
60.800	St. 19 (19)	-858.0/950.8	-683.9/683.9
57.600	St. 18 (18)	-1133.8/1273.8	-930.6/930.6
54.400	St. 17 (17)	-1297.8/1485.9	-1104.2/1104.2
51.200	St. 16 (16)	-1380.8/1618.0	-1225.7/1225.7
48.000	St. 15 (15)	-1407.4/1693.8	-1307.7/1307.7
44.800	St. 14 (14)	-1411.9/1747.4	-1371.6/1371.6
41.600	St. 13 (13)	-1422.6/1808.6	-1435.9/1435.9
38.400	St. 12 (12)	-1461.2/1899.0	-1515.2/1515.2
35.200	St. 11 (11)	-1531.4/2021.0	-1609.0/1609.0
32.000	St. 10 (10)	-1630.7/2172.2	-1714.6/1714.6
28.800	St. 9 (9)	-1755.6/2348.9	-1827.9/1827.9
25.600	St. 8 (8)	-1902.7/2547.8	-1945.9/1945.9
22.400	St. 7 (7)	-2068.9/2767.8	-2068.0/2068.0
19.200	St. 6 (6)	-2256.2/3010.6	-2197.9/2197.9
16.000	St. 5 (5)	-2438.8/3248.7	-2321.8/2321.8
12.800	St. 4 (4)	-2597.9/3463.3	-2430.7/2430.7
9.600	St. 3 (3)	-2717.3/3638.2	-2516.3/2516.3
6.400	St. 2 (2)	-2786.6/3763.1	-2573.1/2573.1
3.200	St. 1 (1)	-2804.9/3836.9	-2600.4/2600.4
0.000	St. Base (Base)	-2242.5/3187.2	-2021.3/2148.4

MODEL12

Level [m]	Reference	Σ Shear Dir 1 [kN]	Σ Shear Dir 2 [kN]
64.000	St. 20 (roof)	-452.6/497.9	-350.8/350.8
60.800	St. 19 (19)	-846.7/938.5	-671.9/671.9
57.600	St. 18 (18)	-1120.2/1258.5	-916.0/916.0
54.400	St. 17 (17)	-1286.2/1472.0	-1092.8/1092.8
51.200	St. 16 (16)	-1375.3/1609.5	-1223.4/1223.4
48.000	St. 15 (15)	-1411.0/1693.8	-1318.3/1318.3
44.800	St. 14 (14)	-1426.5/1757.7	-1394.9/1394.9
41.600	St. 13 (13)	-1448.2/1829.2	-1468.5/1468.5
38.400	St. 12 (12)	-1496.2/1928.4	-1552.9/1552.9
35.200	St. 11 (11)	-1571.8/2055.2	-1649.0/1649.0
32.000	St. 10 (10)	-1671.0/2205.6	-1755.9/1755.9
28.800	St. 9 (9)	-1790.1/2375.9	-1870.5/1870.5
25.600	St. 8 (8)	-1927.2/2564.3	-1989.0/1989.0
22.400	St. 7 (7)	-2081.3/2771.4	-2109.6/2109.6
19.200	St. 6 (6)	-2256.6/3001.7	-2236.0/2236.0
16.000	St. 5 (5)	-2429.4/3229.4	-2355.4/2355.4
12.800	St. 4 (4)	-2581.7/3436.7	-2460.7/2460.7
9.600	St. 3 (3)	-2697.0/3606.9	-2544.2/2544.2
6.400	St. 2 (2)	-2764.4/3729.3	-2600.4/2600.4
3.200	St. 1 (1)	-2782.3/3802.1	-2627.8/2627.8
0.000	St. Base (Base)	-2230.0/3135.7	-2049.4/2144.7

MODEL13

Level [m]	Reference	Σ Shear Dir 1 [kN]	Σ Shear Dir 2 [kN]
64.000	St. 20 (roof)	-457.2/503.0	-355.5/355.5
60.800	St. 19 (19)	-862.1/955.2	-689.4/689.4
57.600	St. 18 (18)	-1143.3/1283.8	-945.8/945.8
54.400	St. 17 (17)	-1314.5/1503.4	-1132.1/1132.1
51.200	St. 16 (16)	-1407.1/1645.4	-1266.9/1266.9
48.000	St. 15 (15)	-1445.5/1733.1	-1360.5/1360.5
44.800	St. 14 (14)	-1462.8/1799.8	-1433.4/1433.4
41.600	St. 13 (13)	-1485.5/1873.2	-1504.4/1504.4
38.400	St. 12 (12)	-1533.8/1973.6	-1589.1/1589.1
35.200	St. 11 (11)	-1609.9/2101.8	-1687.8/1687.8
32.000	St. 10 (10)	-1710.9/2254.9	-1797.9/1797.9
28.800	St. 9 (9)	-1833.2/2429.4	-1915.8/1915.8
25.600	St. 8 (8)	-1974.6/2622.8	-2038.4/2038.4
22.400	St. 7 (7)	-2133.0/2835.2	-2165.3/2165.3
19.200	St. 6 (6)	-2312.1/3070.1	-2299.9/2299.9
16.000	St. 5 (5)	-2488.1/3301.9	-2427.6/2427.6
12.800	St. 4 (4)	-2643.2/3512.8	-2538.9/2538.9
9.600	St. 3 (3)	-2760.9/3686.3	-2625.6/2625.6
6.400	St. 2 (2)	-2830.1/3811.4	-2682.6/2682.6
3.200	St. 1 (1)	-2848.8/3885.8	-2709.8/2709.8
0.000	St. Base (Base)	-2279.0/3212.7	-2112.0/2223.0

MODEL 14

Level [m]	Reference	Σ Shear Dir 1 [kN]	Σ Shear Dir 2 [kN]
64.000	St. 20 (roof)	-458.1/504.4	-363.2/363.2
60.800	St. 19 (19)	-871.8/966.3	-709.0/709.0
57.600	St. 18 (18)	-1161.1/1303.9	-973.0/973.0
54.400	St. 17 (17)	-1339.1/1531.2	-1163.5/1163.5
51.200	St. 16 (16)	-1436.5/1678.8	-1300.2/1300.2
48.000	St. 15 (15)	-1477.5/1770.1	-1394.6/1394.6
44.800	St. 14 (14)	-1495.9/1838.8	-1467.8/1467.8
41.600	St. 13 (13)	-1519.2/1913.7	-1538.8/1538.8
38.400	St. 12 (12)	-1568.2/2015.7	-1623.4/1623.4
35.200	St. 11 (11)	-1645.7/2146.2	-1722.7/1722.7
32.000	St. 10 (10)	-1748.8/2302.2	-1834.7/1834.7
28.800	St. 9 (9)	-1873.9/2480.3	-1955.6/1955.6
25.600	St. 8 (8)	-2018.5/2677.9	-2082.2/2082.2
22.400	St. 7 (7)	-2180.6/2894.8	-2213.2/2213.2
19.200	St. 6 (6)	-2363.2/3134.1	-2352.1/2352.1
16.000	St. 5 (5)	-2542.4/3369.9	-2484.1/2484.1
12.800	St. 4 (4)	-2699.8/3584.1	-2599.9/2599.9
9.600	St. 3 (3)	-2818.8/3759.8	-2690.8/2690.8
6.400	St. 2 (2)	-2888.6/3886.2	-2751.2/2751.2
3.200	St. 1 (1)	-2907.2/3961.5	-2780.3/2780.3
0.000	St. Base (Base)	-2321.2/3283.1	-2164.5/2291.4

Table B.3 Storey shear Dir1 (ELF), Model (1-14)

MODEL1

Level [m]	Reference	Σ Shear Dir 1 [kN]	Σ Shear Dir 2 [kN]
64.000	St. 20 (roof)	244.9	42.5
60.800	St. 19 (19)	474.5	82.1
57.600	St. 18 (18)	693.0	119.7
54.400	St. 17 (17)	903.3	155.6
51.200	St. 16 (16)	1105.0	189.8
48.000	St. 15 (15)	1295.5	221.9
44.800	St. 14 (14)	1474.7	251.9
41.600	St. 13 (13)	1646.3	280.3
38.400	St. 12 (12)	1809.8	307.1
35.200	St. 11 (11)	1961.5	331.6
32.000	St. 10 (10)	2101.6	354.0
28.800	St. 9 (9)	2229.9	374.0
25.600	St. 8 (8)	2346.5	391.9
22.400	St. 7 (7)	2454.8	408.0
19.200	St. 6 (6)	2554.1	422.3
16.000	St. 5 (5)	2640.8	434.2
12.800	St. 4 (4)	2715.1	443.7
9.600	St. 3 (3)	2776.9	450.8
6.400	St. 2 (2)	2826.2	455.6
3.200	St. 1 (1)	2863.0	458.0
0.000	St. Base (Base)	2147.2	334.3

MODEL2

Level [m]	Reference	Σ Shear Dir 1 [kN]	Σ Shear Dir 2 [kN]
64.000	St. 20 (roof)	263.8	49.2
60.800	St. 19 (19)	514.3	95.7
57.600	St. 18 (18)	752.8	139.7
54.400	St. 17 (17)	982.1	181.9
51.200	St. 16 (16)	1201.9	222.0
48.000	St. 15 (15)	1409.3	259.6
44.800	St. 14 (14)	1604.4	294.7
41.600	St. 13 (13)	1791.0	328.0
38.400	St. 12 (12)	1968.7	359.4
35.200	St. 11 (11)	2133.5	388.2
32.000	St. 10 (10)	2285.4	414.3
28.800	St. 9 (9)	2424.5	437.9
25.600	St. 8 (8)	2550.7	458.8
22.400	St. 7 (7)	2667.7	477.7
19.200	St. 6 (6)	2774.6	494.4
16.000	St. 5 (5)	2867.9	508.3
12.800	St. 4 (4)	2947.5	519.4
9.600	St. 3 (3)	3013.5	527.7
6.400	St. 2 (2)	3065.7	533.3
3.200	St. 1 (1)	3104.3	536.1
0.000	St. Base (Base)	2345.2	391.8

MODEL3

Level [m]	Reference	Σ Shear Dir 1 [kN]	Σ Shear Dir 2 [kN]
64.000	St. 20 (roof)	264.3	58.1
60.800	St. 19 (19)	519.6	113.9
57.600	St. 18 (18)	762.6	166.8
54.400	St. 17 (17)	998.4	217.8
51.200	St. 16 (16)	1226.5	266.9
48.000	St. 15 (15)	1441.8	312.9
44.800	St. 14 (14)	1644.3	355.8
41.600	St. 13 (13)	1839.4	396.8
38.400	St. 12 (12)	2026.5	435.7
35.200	St. 11 (11)	2200.0	471.3
32.000	St. 10 (10)	2360.1	503.7
28.800	St. 9 (9)	2506.6	532.9
25.600	St. 8 (8)	2639.7	558.8
22.400	St. 7 (7)	2763.7	582.4
19.200	St. 6 (6)	2877.5	603.3
16.000	St. 5 (5)	2976.9	620.7
12.800	St. 4 (4)	3061.8	634.6
9.600	St. 3 (3)	3132.1	645.0
6.400	St. 2 (2)	3188.0	652.0
3.200	St. 1 (1)	3229.3	655.5
0.000	St. Base (Base)	2633.6	576.7

MODEL4

Level [m]	Reference	Σ Shear Dir 1 [kN]	Σ Shear Dir 2 [kN]
64.000	St. 20 (roof)	265.8	58.7
60.800	St. 19 (19)	525.1	115.6
57.600	St. 18 (18)	771.9	169.6
54.400	St. 17 (17)	1011.2	221.6
51.200	St. 16 (16)	1242.7	271.6
48.000	St. 15 (15)	1461.1	318.5
44.800	St. 14 (14)	1666.6	362.2
41.600	St. 13 (13)	1864.5	404.0
38.400	St. 12 (12)	2054.2	443.6
35.200	St. 11 (11)	2230.1	479.9
32.000	St. 10 (10)	2392.3	512.9
28.800	St. 9 (9)	2540.9	542.6
25.600	St. 8 (8)	2675.8	569.0
22.400	St. 7 (7)	2801.3	592.9
19.200	St. 6 (6)	2916.6	614.2
16.000	St. 5 (5)	3017.2	631.8
12.800	St. 4 (4)	3103.2	646.0
9.600	St. 3 (3)	3174.5	656.6
6.400	St. 2 (2)	3231.1	663.7
3.200	St. 1 (1)	3273.0	667.2
0.000	St. Base (Base)	2683.1	594.9

MODEL5

Level [m]	Reference	Σ Shear Dir 1 [kN]	Σ Shear Dir 2 [kN]
64.000	St. 20 (roof)	267.4	59.3
60.800	St. 19 (19)	530.6	117.3
57.600	St. 18 (18)	781.1	172.3
54.400	St. 17 (17)	1024.0	225.4
51.200	St. 16 (16)	1258.8	276.3
48.000	St. 15 (15)	1480.5	324.1
44.800	St. 14 (14)	1688.9	368.7
41.600	St. 13 (13)	1889.6	411.2
38.400	St. 12 (12)	2081.8	451.5
35.200	St. 11 (11)	2260.1	488.4
32.000	St. 10 (10)	2424.5	522.0
28.800	St. 9 (9)	2575.1	552.2
25.600	St. 8 (8)	2711.8	579.1
22.400	St. 7 (7)	2839.0	603.4
19.200	St. 6 (6)	2955.7	625.0
16.000	St. 5 (5)	3057.5	642.9
12.800	St. 4 (4)	3144.5	657.3
9.600	St. 3 (3)	3216.7	668.1
6.400	St. 2 (2)	3274.1	675.3
3.200	St. 1 (1)	3316.6	678.9
0.000	St. Base (Base)	2743.3	651.8

MODEL6

Level [m]	Reference	Σ Shear Dir 1 [kN]	Σ Shear Dir 2 [kN]
64.000	St. 20 (roof)	282.2	64.5
60.800	St. 19 (19)	558.0	127.3
57.600	St. 18 (18)	820.5	186.9
54.400	St. 17 (17)	1075.0	244.3
51.200	St. 16 (16)	1321.0	299.4
48.000	St. 15 (15)	1553.1	351.1
44.800	St. 14 (14)	1771.4	399.4
41.600	St. 13 (13)	1981.5	445.4
38.400	St. 12 (12)	2182.7	489.1
35.200	St. 11 (11)	2369.3	529.1
32.000	St. 10 (10)	2541.2	565.5
28.800	St. 9 (9)	2698.5	598.3
25.600	St. 8 (8)	2841.2	627.4
22.400	St. 7 (7)	2973.9	653.8
19.200	St. 6 (6)	3095.5	677.2
16.000	St. 5 (5)	3201.4	696.8
12.800	St. 4 (4)	3291.6	712.4
9.600	St. 3 (3)	3366.1	724.1
6.400	St. 2 (2)	3424.9	731.9
3.200	St. 1 (1)	3468.0	735.8
0.000	St. Base (Base)	2831.7	679.8

MODEL7

Level [m]	Reference	Σ Shear Dir 1 [kN]	Σ Shear Dir 2 [kN]
64.000	St. 20 (roof)	283.7	65.1
60.800	St. 19 (19)	563.5	129.0
57.600	St. 18 (18)	829.9	189.6
54.400	St. 17 (17)	1088.0	248.0
51.200	St. 16 (16)	1337.4	304.1
48.000	St. 15 (15)	1572.8	356.7
44.800	St. 14 (14)	1794.1	405.8
41.600	St. 13 (13)	2007.1	452.7
38.400	St. 12 (12)	2210.8	497.0
35.200	St. 11 (11)	2399.8	537.7
32.000	St. 10 (10)	2574.0	574.7
28.800	St. 9 (9)	2733.3	608.0
25.600	St. 8 (8)	2877.8	637.6
22.400	St. 7 (7)	3012.1	664.4
19.200	St. 6 (6)	3135.1	688.1
16.000	St. 5 (5)	3242.3	707.9
12.800	St. 4 (4)	3333.6	723.8
9.600	St. 3 (3)	3409.0	735.7
6.400	St. 2 (2)	3468.6	743.6
3.200	St. 1 (1)	3512.3	747.5
0.000	St. Base (Base)	2881.8	698.5

MODEL8

Level [m]	Reference	Σ Shear Dir 1 [kN]	Σ Shear Dir 2 [kN]
64.000	St. 20 (roof)	285.2	65.7
60.800	St. 19 (19)	569.1	130.7
57.600	St. 18 (18)	839.2	192.4
54.400	St. 17 (17)	1101.0	251.8
51.200	St. 16 (16)	1353.8	308.9
48.000	St. 15 (15)	1592.4	362.3
44.800	St. 14 (14)	1816.8	412.3
41.600	St. 13 (13)	2032.5	459.8
38.400	St. 12 (12)	2238.9	504.9
35.200	St. 11 (11)	2430.2	546.2
32.000	St. 10 (10)	2606.6	583.8
28.800	St. 9 (9)	2768.0	617.6
25.600	St. 8 (8)	2914.4	647.7
22.400	St. 7 (7)	3050.3	674.9
19.200	St. 6 (6)	3174.7	699.0
16.000	St. 5 (5)	3283.2	719.0
12.800	St. 4 (4)	3375.5	735.1
9.600	St. 3 (3)	3451.9	747.1
6.400	St. 2 (2)	3512.2	755.2
3.200	St. 1 (1)	3556.5	759.2
0.000	St. Base (Base)	2931.0	716.8

MODEL9

Level [m]	Reference	Σ Shear Dir 1 [kN]	Σ Shear Dir 2 [kN]
64.000	St. 20 (roof)	293.9	114.4
60.800	St. 19 (19)	577.8	224.4
57.600	St. 18 (18)	848.0	328.6
54.400	St. 17 (17)	1110.0	429.2
51.200	St. 16 (16)	1363.3	526.0
48.000	St. 15 (15)	1602.2	616.6
44.800	St. 14 (14)	1826.8	701.2
41.600	St. 13 (13)	2043.1	782.1
38.400	St. 12 (12)	2250.3	858.8
35.200	St. 11 (11)	2442.3	929.1
32.000	St. 10 (10)	2619.1	993.1
28.800	St. 9 (9)	2780.7	1050.6
25.600	St. 8 (8)	2927.1	1101.7
22.400	St. 7 (7)	3063.3	1148.1
19.200	St. 6 (6)	3188.1	1189.4
16.000	St. 5 (5)	3296.6	1223.7
12.800	St. 4 (4)	3388.7	1251.2
9.600	St. 3 (3)	3464.5	1271.8
6.400	St. 2 (2)	3524.1	1285.6
3.200	St. 1 (1)	3567.3	1292.4
0.000	St. Base (Base)	2847.8	1022.2

MODEL 10

Level [m]	Reference	Σ Shear Dir 1 [kN]	Σ Shear Dir 2 [kN]
64.000	St. 20 (roof)	300.3	118.5
60.800	St. 19 (19)	593.2	233.7
57.600	St. 18 (18)	871.9	342.8
54.400	St. 17 (17)	1142.0	448.0
51.200	St. 16 (16)	1403.1	549.1
48.000	St. 15 (15)	1649.3	643.9
44.800	St. 14 (14)	1880.7	732.4
41.600	St. 13 (13)	2103.4	816.9
38.400	St. 12 (12)	2316.6	897.0
35.200	St. 11 (11)	2514.1	970.5
32.000	St. 10 (10)	2696.0	1037.2
28.800	St. 9 (9)	2862.2	1097.3
25.600	St. 8 (8)	3012.8	1150.7
22.400	St. 7 (7)	3152.7	1199.2
19.200	St. 6 (6)	3280.7	1242.1
16.000	St. 5 (5)	3391.9	1278.0
12.800	St. 4 (4)	3486.4	1306.6
9.600	St. 3 (3)	3564.1	1328.1
6.400	St. 2 (2)	3625.0	1342.4
3.200	St. 1 (1)	3669.1	1349.6
0.000	St. Base (Base)	2940.3	1070.7

MODEL 11

Level [m]	Reference	Σ Shear Dir 1 [kN]	Σ Shear Dir 2 [kN]
64.000	St. 20 (roof)	306.5	122.0
60.800	St. 19 (19)	608.3	241.7
57.600	St. 18 (18)	895.4	355.0
54.400	St. 17 (17)	1173.5	464.3
51.200	St. 16 (16)	1442.2	569.3
48.000	St. 15 (15)	1695.6	667.8
44.800	St. 14 (14)	1933.8	759.6
41.600	St. 13 (13)	2162.8	847.3
38.400	St. 12 (12)	2381.9	930.4
35.200	St. 11 (11)	2584.9	1006.5
32.000	St. 10 (10)	2771.8	1075.7
28.800	St. 9 (9)	2942.5	1138.1
25.600	St. 8 (8)	3097.2	1193.4
22.400	St. 7 (7)	3240.7	1243.6
19.200	St. 6 (6)	3372.0	1288.1
16.000	St. 5 (5)	3485.9	1325.2
12.800	St. 4 (4)	3582.7	1354.9
9.600	St. 3 (3)	3662.2	1377.1
6.400	St. 2 (2)	3724.4	1392.0
3.200	St. 1 (1)	3769.4	1399.4
0.000	St. Base (Base)	3028.7	1115.2

MODEL 12

Level [m]	Reference	Σ Shear Dir 1 [kN]	Σ Shear Dir 2 [kN]
64.000	St. 20 (roof)	308.5	118.9
60.800	St. 19 (19)	610.1	234.6
57.600	St. 18 (18)	897.0	344.3
54.400	St. 17 (17)	1175.1	450.1
51.200	St. 16 (16)	1443.8	551.7
48.000	St. 15 (15)	1697.1	647.0
44.800	St. 14 (14)	1935.3	736.0
41.600	St. 13 (13)	2164.4	820.9
38.400	St. 12 (12)	2383.7	901.4
35.200	St. 11 (11)	2586.8	975.3
32.000	St. 10 (10)	2773.8	1042.4
28.800	St. 9 (9)	2944.6	1102.8
25.600	St. 8 (8)	3099.3	1156.5
22.400	St. 7 (7)	3243.0	1205.2
19.200	St. 6 (6)	3374.4	1248.4
16.000	St. 5 (5)	3488.5	1284.4
12.800	St. 4 (4)	3585.2	1313.2
9.600	St. 3 (3)	3664.6	1334.8
6.400	St. 2 (2)	3726.8	1349.2
3.200	St. 1 (1)	3771.6	1356.4
0.000	St. Base (Base)	3011.1	1068.6

MODEL13

Level [m]	Reference	Σ Shear Dir 1 [kN]	Σ Shear Dir 2 [kN]
64.000	St. 20 (roof)	314.7	123.7
60.800	St. 19 (19)	625.2	245.3
57.600	St. 18 (18)	920.6	360.5
54.400	St. 17 (17)	1206.8	471.6
51.200	St. 16 (16)	1483.2	578.3
48.000	St. 15 (15)	1743.8	678.4
44.800	St. 14 (14)	1988.7	771.8
41.600	St. 13 (13)	2224.2	860.9
38.400	St. 12 (12)	2449.5	945.3
35.200	St. 11 (11)	2658.1	1022.7
32.000	St. 10 (10)	2850.1	1093.1
28.800	St. 9 (9)	3025.5	1156.4
25.600	St. 8 (8)	3184.3	1212.7
22.400	St. 7 (7)	3331.7	1263.7
19.200	St. 6 (6)	3466.3	1309.0
16.000	St. 5 (5)	3583.1	1346.7
12.800	St. 4 (4)	3682.2	1376.9
9.600	St. 3 (3)	3763.4	1399.5
6.400	St. 2 (2)	3826.9	1414.6
3.200	St. 1 (1)	3872.6	1422.1
0.000	St. Base (Base)	3094.6	1126.8

MODEL14

Level [m]	Reference	Σ Shear Dir 1 [kN]	Σ Shear Dir 2 [kN]
64.000	St. 20 (roof)	320.8	128.1
60.800	St. 19 (19)	640.1	255.1
57.600	St. 18 (18)	943.8	375.4
54.400	St. 17 (17)	1238.0	491.4
51.200	St. 16 (16)	1522.0	602.8
48.000	St. 15 (15)	1789.8	707.2
44.800	St. 14 (14)	2041.4	804.7
41.600	St. 13 (13)	2283.2	897.6
38.400	St. 12 (12)	2514.3	985.6
35.200	St. 11 (11)	2728.3	1066.3
32.000	St. 10 (10)	2925.3	1139.7
28.800	St. 9 (9)	3105.2	1205.7
25.600	St. 8 (8)	3268.1	1264.4
22.400	St. 7 (7)	3419.0	1317.5
19.200	St. 6 (6)	3556.8	1364.6
16.000	St. 5 (5)	3676.3	1403.9
12.800	St. 4 (4)	3777.6	1435.3
9.600	St. 3 (3)	3860.7	1458.8
6.400	St. 2 (2)	3925.5	1474.5
3.200	St. 1 (1)	3972.1	1482.4
0.000	St. Base (Base)	3186.4	1178.8

Table B.4 Seismic drift check by storey (RSA)

MODEL1

Seismic Drift										
Level ▲	Ref.	Stack	Combination Dir 1	Drift Dir 1 [mm]	θ_{Dir1}	Combination Dir 2	Drift Dir 2 [mm]	θ_{Dir2}	Status	Details
St. 2 (2)	C1	2	3 (Operating) $SEIS_{1.1}$-G+ψ_2Q+ψ_2RQ±A_{Ed}+EHF_{Dir1+}	1.4	0.014	5 (Operating) $SEIS_{1.3}$-G+ψ_2Q+ψ_2RQ±A_{Ed}+EHF_{Dir2+}	2.1	0.027	✔ Pass	Details...
St. 3 (3)	C23	3	3 (Operating) $SEIS_{1.1}$-G+ψ_2Q+ψ_2RQ±A_{Ed}+EHF_{Dir1+}	3.0	0.030	5 (Operating) $SEIS_{1.3}$-G+ψ_2Q+ψ_2RQ±A_{Ed}+EHF_{Dir2+}	2.5	0.030	✔ Pass	Details...
St. 3 (3)	C1	3	3 (Operating) $SEIS_{1.1}$-G+ψ_2Q+ψ_2RQ±A_{Ed}+EHF_{Dir1+}	1.8	0.018	5 (Operating) $SEIS_{1.3}$-G+ψ_2Q+ψ_2RQ±A_{Ed}+EHF_{Dir2+}	2.5	0.030	✔ Pass	Details...
St. 4 (4)	C23	4	3 (Operating) $SEIS_{1.1}$-G+ψ_2Q+ψ_2RQ±A_{Ed}+EHF_{Dir1+}	3.3	0.032	5 (Operating) $SEIS_{1.3}$-G+ψ_2Q+ψ_2RQ±A_{Ed}+EHF_{Dir2+}	2.8	0.033	✔ Pass	Details...
St. 4 (4)	C1	4	3 (Operating) $SEIS_{1.1}$-G+ψ_2Q+ψ_2RQ±A_{Ed}+EHF_{Dir1+}	2.2	0.021	5 (Operating) $SEIS_{1.3}$-G+ψ_2Q+ψ_2RQ±A_{Ed}+EHF_{Dir2+}	2.8	0.033	✔ Pass	Details...
St. 5 (5)	C23	5	3 (Operating) $SEIS_{1.1}$-G+ψ_2Q+ψ_2RQ±A_{Ed}+EHF_{Dir1+}	3.6	0.033	5 (Operating) $SEIS_{1.3}$-G+ψ_2Q+ψ_2RQ±A_{Ed}+EHF_{Dir2+}	3.1	0.035	✔ Pass	Details...
St. 5 (5)	C1	5	3 (Operating) $SEIS_{1.1}$-G+ψ_2Q+ψ_2RQ±A_{Ed}+EHF_{Dir1+}	2.6	0.024	5 (Operating) $SEIS_{1.3}$-G+ψ_2Q+ψ_2RQ±A_{Ed}+EHF_{Dir2+}	3.1	0.035	✔ Pass	Details...
St. 6 (6)	C23	6	3 (Operating) $SEIS_{1.1}$-G+ψ_2Q+ψ_2RQ±A_{Ed}+EHF_{Dir1+}	3.8	0.033	5 (Operating) $SEIS_{1.3}$-G+ψ_2Q+ψ_2RQ±A_{Ed}+EHF_{Dir2+}	3.4	0.036	✔ Pass	Details...
St. 6 (6)	C11	6	3 (Operating) $SEIS_{1.1}$-G+ψ_2Q+ψ_2RQ±A_{Ed}+EHF_{Dir1+}	2.8	0.025	5 (Operating) $SEIS_{1.3}$-G+ψ_2Q+ψ_2RQ±A_{Ed}+EHF_{Dir2+}	3.4	0.036	✔ Pass	Details...
St. 7 (7)	C23	7	3 (Operating) $SEIS_{1.1}$-G+ψ_2Q+ψ_2RQ±A_{Ed}+EHF_{Dir1+}	4.0	0.034	5 (Operating) $SEIS_{1.3}$-G+ψ_2Q+ψ_2RQ±A_{Ed}+EHF_{Dir2+}	3.7	0.038	✔ Pass	Details...
St. 7 (7)	C1	7	3 (Operating) $SEIS_{1.1}$-G+ψ_2Q+ψ_2RQ±A_{Ed}+EHF_{Dir1+}	3.3	0.027	5 (Operating) $SEIS_{1.3}$-G+ψ_2Q+ψ_2RQ±A_{Ed}+EHF_{Dir2+}	3.7	0.038	✔ Pass	Details...
St. 8 (8)	C48	1	3 (Operating) $SEIS_{1.1}$-G+ψ_2Q+ψ_2RQ±A_{Ed}+EHF_{Dir1+}	4.5	0.036	5 (Operating) $SEIS_{1.3}$-G+ψ_2Q+ψ_2RQ±A_{Ed}+EHF_{Dir2+}	4.0	0.040	✔ Pass	Details...
St. 8 (8)	C26	1	3 (Operating) $SEIS_{1.1}$-G+ψ_2Q+ψ_2RQ±A_{Ed}+EHF_{Dir1+}	3.6	0.029	5 (Operating) $SEIS_{1.3}$-G+ψ_2Q+ψ_2RQ±A_{Ed}+EHF_{Dir2+}	4.0	0.040	✔ Pass	Details...
St. 9 (9)	C48	2	3 (Operating) $SEIS_{1.1}$-G+ψ_2Q+ψ_2RQ±A_{Ed}+EHF_{Dir1+}	4.8	0.037	5 (Operating) $SEIS_{1.3}$-G+ψ_2Q+ψ_2RQ±A_{Ed}+EHF_{Dir2+}	4.3	0.041	✔ Pass	Details...
St. 9 (9)	C26	2	3 (Operating) $SEIS_{1.1}$-G+ψ_2Q+ψ_2RQ±A_{Ed}+EHF_{Dir1+}	3.9	0.031	5 (Operating) $SEIS_{1.3}$-G+ψ_2Q+ψ_2RQ±A_{Ed}+EHF_{Dir2+}	4.3	0.041	✔ Pass	Details...
St. 10 (10)	C48	3	3 (Operating) $SEIS_{1.1}$-G+ψ_2Q+ψ_2RQ±A_{Ed}+EHF_{Dir1+}	5.0	0.038	5 (Operating) $SEIS_{1.3}$-G+ψ_2Q+ψ_2RQ±A_{Ed}+EHF_{Dir2+}	4.6	0.042	✔ Pass	Details...
St. 10 (10)	C26	3	3 (Operating) $SEIS_{1.1}$-G+ψ_2Q+ψ_2RQ±A_{Ed}+EHF_{Dir1+}	4.2	0.032	5 (Operating) $SEIS_{1.3}$-G+ψ_2Q+ψ_2RQ±A_{Ed}+EHF_{Dir2+}	4.6	0.042	✔ Pass	Details...
St. 11 (11)	C48	4	3 (Operating) $SEIS_{1.1}$-G+ψ_2Q+ψ_2RQ±A_{Ed}+EHF_{Dir1+}	5.3	0.039	5 (Operating) $SEIS_{1.3}$-G+ψ_2Q+ψ_2RQ±A_{Ed}+EHF_{Dir2+}	4.8	0.043	✔ Pass	Details...
St. 11 (11)	C26	4	3 (Operating) $SEIS_{1.1}$-G+ψ_2Q+ψ_2RQ±A_{Ed}+EHF_{Dir1+}	4.4	0.032	5 (Operating) $SEIS_{1.3}$-G+ψ_2Q+ψ_2RQ±A_{Ed}+EHF_{Dir2+}	4.8	0.043	✔ Pass	Details...
St. 12 (12)	C48	5	3 (Operating) $SEIS_{1.1}$-G+ψ_2Q+ψ_2RQ±A_{Ed}+EHF_{Dir1+}	5.6	0.039	5 (Operating) $SEIS_{1.3}$-G+ψ_2Q+ψ_2RQ±A_{Ed}+EHF_{Dir2+}	5.0	0.043	✔ Pass	Details...
St. 12 (12)	C36	5	3 (Operating) $SEIS_{1.1}$-G+ψ_2Q+ψ_2RQ±A_{Ed}+EHF_{Dir1+}	4.5	0.032	5 (Operating) $SEIS_{1.3}$-G+ψ_2Q+ψ_2RQ±A_{Ed}+EHF_{Dir2+}	5.0	0.043	✔ Pass	Details...
St. 13 (13)	C48	6	3 (Operating) $SEIS_{1.1}$-G+ψ_2Q+ψ_2RQ±A_{Ed}+EHF_{Dir1+}	5.8	0.039	5 (Operating) $SEIS_{1.3}$-G+ψ_2Q+ψ_2RQ±A_{Ed}+EHF_{Dir2+}	5.2	0.044	✔ Pass	Details...
St. 13 (13)	C45	6	3 (Operating) $SEIS_{1.1}$-G+ψ_2Q+ψ_2RQ±A_{Ed}+EHF_{Dir1+}	5.5	0.037	5 (Operating) $SEIS_{1.3}$-G+ψ_2Q+ψ_2RQ±A_{Ed}+EHF_{Dir2+}	5.2	0.044	✔ Pass	Details...
St. 14 (14)	C77	1	3 (Operating) $SEIS_{1.1}$-G+ψ_2Q+ψ_2RQ±A_{Ed}+EHF_{Dir1+}	6.2	0.041	5 (Operating) $SEIS_{1.3}$-G+ψ_2Q+ψ_2RQ±A_{Ed}+EHF_{Dir2+}	5.6	0.045	✔ Pass	Details...
St. 14 (14)	C53	1	3 (Operating) $SEIS_{1.1}$-G+ψ_2Q+ψ_2RQ±A_{Ed}+EHF_{Dir1+}	5.0	0.033	5 (Operating) $SEIS_{1.3}$-G+ψ_2Q+ψ_2RQ±A_{Ed}+EHF_{Dir2+}	5.6	0.045	✔ Pass	Details...
St. 15 (15)	C77	2	3 (Operating) $SEIS_{1.1}$-G+ψ_2Q+ψ_2RQ±A_{Ed}+EHF_{Dir1+}	6.3	0.041	5 (Operating) $SEIS_{1.3}$-G+ψ_2Q+ψ_2RQ±A_{Ed}+EHF_{Dir2+}	5.7	0.045	✔ Pass	Details...
St. 15 (15)	C53	2	3 (Operating) $SEIS_{1.1}$-G+ψ_2Q+ψ_2RQ±A_{Ed}+EHF_{Dir1+}	5.2	0.033	5 (Operating) $SEIS_{1.3}$-G+ψ_2Q+ψ_2RQ±A_{Ed}+EHF_{Dir2+}	5.7	0.045	✔ Pass	Details...
St. 16 (16)	C77	3	3 (Operating) $SEIS_{1.1}$-G+ψ_2Q+ψ_2RQ±A_{Ed}+EHF_{Dir1+}	6.3	0.039	5 (Operating) $SEIS_{1.3}$-G+ψ_2Q+ψ_2RQ±A_{Ed}+EHF_{Dir2+}	5.8	0.044	✔ Pass	Details...
St. 16 (16)	C53	3	3 (Operating) $SEIS_{1.1}$-G+ψ_2Q+ψ_2RQ±A_{Ed}+EHF_{Dir1+}	5.3	0.033	5 (Operating) $SEIS_{1.3}$-G+ψ_2Q+ψ_2RQ±A_{Ed}+EHF_{Dir2+}	5.8	0.044	✔ Pass	Details...
St. 17 (17)	C77	4	3 (Operating) $SEIS_{1.1}$-G+ψ_2Q+ψ_2RQ±A_{Ed}+EHF_{Dir1+}	6.2	0.038	5 (Operating) $SEIS_{1.3}$-G+ψ_2Q+ψ_2RQ±A_{Ed}+EHF_{Dir2+}	5.8	0.043	✔ Pass	Details...
St. 17 (17)	C58	4	3 (Operating) $SEIS_{1.1}$-G+ψ_2Q+ψ_2RQ±A_{Ed}+EHF_{Dir1+}	5.2	0.032	5 (Operating) $SEIS_{1.3}$-G+ψ_2Q+ψ_2RQ±A_{Ed}+EHF_{Dir2+}	5.8	0.043	✔ Pass	Details...
St. 18 (18)	C77	5	3 (Operating) $SEIS_{1.1}$-G+ψ_2Q+ψ_2RQ±A_{Ed}+EHF_{Dir1+}	6.3	0.038	5 (Operating) $SEIS_{1.3}$-G+ψ_2Q+ψ_2RQ±A_{Ed}+EHF_{Dir2+}	6.0	0.043	✔ Pass	Details...
St. 18 (18)	C53	5	3 (Operating) $SEIS_{1.1}$-G+ψ_2Q+ψ_2RQ±A_{Ed}+EHF_{Dir1+}	5.4	0.032	5 (Operating) $SEIS_{1.3}$-G+ψ_2Q+ψ_2RQ±A_{Ed}+EHF_{Dir2+}	6.0	0.043	✔ Pass	Details...
St. 19 (19)	C77	6	3 (Operating) $SEIS_{1.1}$-G+ψ_2Q+ψ_2RQ±A_{Ed}+EHF_{Dir1+}	6.0	0.035	5 (Operating) $SEIS_{1.3}$-G+ψ_2Q+ψ_2RQ±A_{Ed}+EHF_{Dir2+}	5.8	0.041	✔ Pass	Details...
St. 19 (19)	C53	6	3 (Operating) $SEIS_{1.1}$-G+ψ_2Q+ψ_2RQ±A_{Ed}+EHF_{Dir1+}	5.3	0.031	5 (Operating) $SEIS_{1.3}$-G+ψ_2Q+ψ_2RQ±A_{Ed}+EHF_{Dir2+}	5.8	0.041	✔ Pass	Details...
St. 20 (roof)	C77	7	3 (Operating) $SEIS_{1.1}$-G+ψ_2Q+ψ_2RQ±A_{Ed}+EHF_{Dir1+}	5.6	0.032	5 (Operating) $SEIS_{1.3}$-G+ψ_2Q+ψ_2RQ±A_{Ed}+EHF_{Dir2+}	5.6	0.039	✔ Pass	Details...
St. 20 (roof)	C58	7	3 (Operating) $SEIS_{1.1}$-G+ψ_2Q+ψ_2RQ±A_{Ed}+EHF_{Dir1+}	5.2	0.029	5 (Operating) $SEIS_{1.3}$-G+ψ_2Q+ψ_2RQ±A_{Ed}+EHF_{Dir2+}	5.6	0.039	✔ Pass	Details...

MODEL2

Seismic Drift										
Level ▲	Ref.	Stack	Combination Dir 1	Drift Dir 1 [mm]	$\theta_{Dir\,1}$	Combination Dir 2	Drift Dir 2 [mm]	$\theta_{Dir\,2}$	Status	Details
St. 1 (1)	C23	1	3 (Operating) $SEIS_{1.1}$·G+ψ_2Q+ψ_2RQ±A_{Ed}+EHF_{Dir1+}	2.1	0.023	5 (Operating) $SEIS_{1.1}$·G+ψ_2Q+ψ_2RQ±A_{Ed}+EHF_{Dir2+}	1.6	0.020	Pass	Details...
St. 1 (1)	C1	1	3 (Operating) $SEIS_{1.1}$·G+ψ_2Q+ψ_2RQ±A_{Ed}+EHF_{Dir1+}	0.9	0.010	5 (Operating) $SEIS_{1.1}$·G+ψ_2Q+ψ_2RQ±A_{Ed}+EHF_{Dir2+}	1.6	0.020	Pass	Details...
St. 2 (2)	C23	2	3 (Operating) $SEIS_{1.1}$·G+ψ_2Q+ψ_2RQ±A_{Ed}+EHF_{Dir1+}	2.5	0.025	5 (Operating) $SEIS_{1.1}$·G+ψ_2Q+ψ_2RQ±A_{Ed}+EHF_{Dir2+}	2.0	0.024	Pass	Details...
St. 2 (2)	C1	2	3 (Operating) $SEIS_{1.1}$·G+ψ_2Q+ψ_2RQ±A_{Ed}+EHF_{Dir1+}	1.3	0.013	5 (Operating) $SEIS_{1.1}$·G+ψ_2Q+ψ_2RQ±A_{Ed}+EHF_{Dir2+}	2.0	0.024	Pass	Details...
St. 3 (3)	C23	3	3 (Operating) $SEIS_{1.1}$·G+ψ_2Q+ψ_2RQ±A_{Ed}+EHF_{Dir1+}	2.8	0.027	5 (Operating) $SEIS_{1.1}$·G+ψ_2Q+ψ_2RQ±A_{Ed}+EHF_{Dir2+}	2.4	0.027	Pass	Details...
St. 3 (3)	C20	3	3 (Operating) $SEIS_{1.1}$·G+ψ_2Q+ψ_2RQ±A_{Ed}+EHF_{Dir1+}	2.5	0.024	5 (Operating) $SEIS_{1.1}$·G+ψ_2Q+ψ_2RQ±A_{Ed}+EHF_{Dir2+}	2.4	0.027	Pass	Details...
St. 4 (4)	C23	4	3 (Operating) $SEIS_{1.1}$·G+ψ_2Q+ψ_2RQ±A_{Ed}+EHF_{Dir1+}	3.1	0.029	5 (Operating) $SEIS_{1.1}$·G+ψ_2Q+ψ_2RQ±A_{Ed}+EHF_{Dir2+}	2.8	0.030	Pass	Details...
St. 4 (4)	C11	4	3 (Operating) $SEIS_{1.1}$·G+ψ_2Q+ψ_2RQ±A_{Ed}+EHF_{Dir1+}	2.0	0.018	5 (Operating) $SEIS_{1.1}$·G+ψ_2Q+ψ_2RQ±A_{Ed}+EHF_{Dir2+}	2.8	0.030	Pass	Details...
St. 5 (5)	C23	5	3 (Operating) $SEIS_{1.1}$·G+ψ_2Q+ψ_2RQ±A_{Ed}+EHF_{Dir1+}	3.3	0.030	5 (Operating) $SEIS_{1.1}$·G+ψ_2Q+ψ_2RQ±A_{Ed}+EHF_{Dir2+}	3.1	0.032	Pass	Details...
St. 5 (5)	C1	5	3 (Operating) $SEIS_{1.1}$·G+ψ_2Q+ψ_2RQ±A_{Ed}+EHF_{Dir1+}	2.4	0.022	5 (Operating) $SEIS_{1.1}$·G+ψ_2Q+ψ_2RQ±A_{Ed}+EHF_{Dir2+}	3.1	0.032	Pass	Details...
St. 6 (6)	C23	6	3 (Operating) $SEIS_{1.1}$·G+ψ_2Q+ψ_2RQ±A_{Ed}+EHF_{Dir1+}	3.6	0.030	5 (Operating) $SEIS_{1.1}$·G+ψ_2Q+ψ_2RQ±A_{Ed}+EHF_{Dir2+}	3.4	0.033	Pass	Details...
St. 6 (6)	C1	6	3 (Operating) $SEIS_{1.1}$·G+ψ_2Q+ψ_2RQ±A_{Ed}+EHF_{Dir1+}	2.8	0.024	5 (Operating) $SEIS_{1.1}$·G+ψ_2Q+ψ_2RQ±A_{Ed}+EHF_{Dir2+}	3.4	0.033	Pass	Details...
St. 7 (7)	C23	7	3 (Operating) $SEIS_{1.1}$·G+ψ_2Q+ψ_2RQ±A_{Ed}+EHF_{Dir1+}	3.8	0.031	5 (Operating) $SEIS_{1.1}$·G+ψ_2Q+ψ_2RQ±A_{Ed}+EHF_{Dir2+}	3.6	0.034	Pass	Details...
St. 7 (7)	C1	7	3 (Operating) $SEIS_{1.1}$·G+ψ_2Q+ψ_2RQ±A_{Ed}+EHF_{Dir1+}	3.1	0.025	5 (Operating) $SEIS_{1.1}$·G+ψ_2Q+ψ_2RQ±A_{Ed}+EHF_{Dir2+}	3.6	0.034	Pass	Details...
St. 8 (8)	C48	1	3 (Operating) $SEIS_{1.1}$·G+ψ_2Q+ψ_2RQ±A_{Ed}+EHF_{Dir1+}	4.2	0.033	5 (Operating) $SEIS_{1.1}$·G+ψ_2Q+ψ_2RQ±A_{Ed}+EHF_{Dir2+}	4.0	0.037	Pass	Details...
St. 8 (8)	C26	1	3 (Operating) $SEIS_{1.1}$·G+ψ_2Q+ψ_2RQ±A_{Ed}+EHF_{Dir1+}	3.4	0.027	5 (Operating) $SEIS_{1.1}$·G+ψ_2Q+ψ_2RQ±A_{Ed}+EHF_{Dir2+}	4.0	0.037	Pass	Details...
St. 9 (9)	C48	2	3 (Operating) $SEIS_{1.1}$·G+ψ_2Q+ψ_2RQ±A_{Ed}+EHF_{Dir1+}	4.4	0.034	5 (Operating) $SEIS_{1.1}$·G+ψ_2Q+ψ_2RQ±A_{Ed}+EHF_{Dir2+}	4.3	0.037	Pass	Details...
St. 9 (9)	C45	2	3 (Operating) $SEIS_{1.1}$·G+ψ_2Q+ψ_2RQ±A_{Ed}+EHF_{Dir1+}	4.2	0.032	5 (Operating) $SEIS_{1.1}$·G+ψ_2Q+ψ_2RQ±A_{Ed}+EHF_{Dir2+}	4.3	0.037	Pass	Details...
St. 10 (10)	C48	3	3 (Operating) $SEIS_{1.1}$·G+ψ_2Q+ψ_2RQ±A_{Ed}+EHF_{Dir1+}	4.7	0.035	5 (Operating) $SEIS_{1.1}$·G+ψ_2Q+ψ_2RQ±A_{Ed}+EHF_{Dir2+}	4.5	0.038	Pass	Details...
St. 10 (10)	C26	3	3 (Operating) $SEIS_{1.1}$·G+ψ_2Q+ψ_2RQ±A_{Ed}+EHF_{Dir1+}	3.9	0.029	5 (Operating) $SEIS_{1.1}$·G+ψ_2Q+ψ_2RQ±A_{Ed}+EHF_{Dir2+}	4.5	0.038	Pass	Details...
St. 11 (11)	C48	4	3 (Operating) $SEIS_{1.1}$·G+ψ_2Q+ψ_2RQ±A_{Ed}+EHF_{Dir1+}	5.0	0.035	5 (Operating) $SEIS_{1.1}$·G+ψ_2Q+ψ_2RQ±A_{Ed}+EHF_{Dir2+}	4.8	0.039	Pass	Details...
St. 11 (11)	C26	4	3 (Operating) $SEIS_{1.1}$·G+ψ_2Q+ψ_2RQ±A_{Ed}+EHF_{Dir1+}	4.1	0.029	5 (Operating) $SEIS_{1.1}$·G+ψ_2Q+ψ_2RQ±A_{Ed}+EHF_{Dir2+}	4.8	0.039	Pass	Details...
St. 12 (12)	C48	5	3 (Operating) $SEIS_{1.1}$·G+ψ_2Q+ψ_2RQ±A_{Ed}+EHF_{Dir1+}	5.2	0.036	5 (Operating) $SEIS_{1.1}$·G+ψ_2Q+ψ_2RQ±A_{Ed}+EHF_{Dir2+}	5.0	0.040	Pass	Details...
St. 12 (12)	C26	5	3 (Operating) $SEIS_{1.1}$·G+ψ_2Q+ψ_2RQ±A_{Ed}+EHF_{Dir1+}	4.3	0.030	5 (Operating) $SEIS_{1.1}$·G+ψ_2Q+ψ_2RQ±A_{Ed}+EHF_{Dir2+}	5.0	0.040	Pass	Details...
St. 13 (13)	C48	6	3 (Operating) $SEIS_{1.1}$·G+ψ_2Q+ψ_2RQ±A_{Ed}+EHF_{Dir1+}	5.4	0.036	5 (Operating) $SEIS_{1.1}$·G+ψ_2Q+ψ_2RQ±A_{Ed}+EHF_{Dir2+}	5.2	0.040	Pass	Details...
St. 13 (13)	C26	6	3 (Operating) $SEIS_{1.1}$·G+ψ_2Q+ψ_2RQ±A_{Ed}+EHF_{Dir1+}	4.5	0.030	5 (Operating) $SEIS_{1.1}$·G+ψ_2Q+ψ_2RQ±A_{Ed}+EHF_{Dir2+}	5.2	0.040	Pass	Details...
St. 14 (14)	C77	1	3 (Operating) $SEIS_{1.1}$·G+ψ_2Q+ψ_2RQ±A_{Ed}+EHF_{Dir1+}	5.7	0.037	5 (Operating) $SEIS_{1.1}$·G+ψ_2Q+ψ_2RQ±A_{Ed}+EHF_{Dir2+}	5.5	0.041	Pass	Details...
St. 14 (14)	C53	1	3 (Operating) $SEIS_{1.1}$·G+ψ_2Q+ψ_2RQ±A_{Ed}+EHF_{Dir1+}	4.7	0.030	5 (Operating) $SEIS_{1.1}$·G+ψ_2Q+ψ_2RQ±A_{Ed}+EHF_{Dir2+}	5.5	0.041	Pass	Details...
St. 15 (15)	C77	2	3 (Operating) $SEIS_{1.1}$·G+ψ_2Q+ψ_2RQ±A_{Ed}+EHF_{Dir1+}	5.8	0.036	5 (Operating) $SEIS_{1.1}$·G+ψ_2Q+ψ_2RQ±A_{Ed}+EHF_{Dir2+}	5.6	0.040	Pass	Details...
St. 15 (15)	C53	2	3 (Operating) $SEIS_{1.1}$·G+ψ_2Q+ψ_2RQ±A_{Ed}+EHF_{Dir1+}	4.8	0.030	5 (Operating) $SEIS_{1.1}$·G+ψ_2Q+ψ_2RQ±A_{Ed}+EHF_{Dir2+}	5.6	0.040	Pass	Details...
St. 16 (16)	C77	3	3 (Operating) $SEIS_{1.1}$·G+ψ_2Q+ψ_2RQ±A_{Ed}+EHF_{Dir1+}	5.8	0.035	5 (Operating) $SEIS_{1.1}$·G+ψ_2Q+ψ_2RQ±A_{Ed}+EHF_{Dir2+}	5.6	0.040	Pass	Details...
St. 16 (16)	C53	3	3 (Operating) $SEIS_{1.1}$·G+ψ_2Q+ψ_2RQ±A_{Ed}+EHF_{Dir1+}	4.9	0.030	5 (Operating) $SEIS_{1.1}$·G+ψ_2Q+ψ_2RQ±A_{Ed}+EHF_{Dir2+}	5.6	0.040	Pass	Details...
St. 17 (17)	C77	4	3 (Operating) $SEIS_{1.1}$·G+ψ_2Q+ψ_2RQ±A_{Ed}+EHF_{Dir1+}	5.7	0.034	5 (Operating) $SEIS_{1.1}$·G+ψ_2Q+ψ_2RQ±A_{Ed}+EHF_{Dir2+}	5.7	0.039	Pass	Details...
St. 17 (17)	C53	4	3 (Operating) $SEIS_{1.1}$·G+ψ_2Q+ψ_2RQ±A_{Ed}+EHF_{Dir1+}	4.9	0.029	5 (Operating) $SEIS_{1.1}$·G+ψ_2Q+ψ_2RQ±A_{Ed}+EHF_{Dir2+}	5.7	0.039	Pass	Details...
St. 18 (18)	C77	5	3 (Operating) $SEIS_{1.1}$·G+ψ_2Q+ψ_2RQ±A_{Ed}+EHF_{Dir1+}	5.7	0.033	5 (Operating) $SEIS_{1.1}$·G+ψ_2Q+ψ_2RQ±A_{Ed}+EHF_{Dir2+}	5.8	0.038	Pass	Details...
St. 18 (18)	C71	5	3 (Operating) $SEIS_{1.1}$·G+ψ_2Q+ψ_2RQ±A_{Ed}+EHF_{Dir1+}	5.2	0.030	5 (Operating) $SEIS_{1.1}$·G+ψ_2Q+ψ_2RQ±A_{Ed}+EHF_{Dir2+}	5.8	0.038	Pass	Details...
St. 19 (19)	C77	6	3 (Operating) $SEIS_{1.1}$·G+ψ_2Q+ψ_2RQ±A_{Ed}+EHF_{Dir1+}	5.5	0.031	5 (Operating) $SEIS_{1.1}$·G+ψ_2Q+ψ_2RQ±A_{Ed}+EHF_{Dir2+}	5.7	0.037	Pass	Details...
St. 19 (19)	C53	6	3 (Operating) $SEIS_{1.1}$·G+ψ_2Q+ψ_2RQ±A_{Ed}+EHF_{Dir1+}	4.9	0.028	5 (Operating) $SEIS_{1.1}$·G+ψ_2Q+ψ_2RQ±A_{Ed}+EHF_{Dir2+}	5.7	0.037	Pass	Details...

MODEL3

Level ▲	Ref.	Stack	Combination Dir 1	Drift Dir 1 [mm]	θ_{Dir1}	Combination Dir 2	Drift Dir 2 [mm]	θ_{Dir2}	Status	Details
St. 1 (1)	W5	1	3 (Operating) $SEIS_{1.1}$-G+ψ_2Q+ψ_2RQ±A_{Ed}+EHF_{Dir1+}	0.8	0.008	5 (Operating) $SEIS_{1.3}$-G+ψ_2Q+ψ_2RQ±A_{Ed}+EHF_{Dir2+}	0.6	0.007	✔ Pass	Details...
St. 1 (1)	W6	1	3 (Operating) $SEIS_{1.1}$-G+ψ_2Q+ψ_2RQ±A_{Ed}+EHF_{Dir1+}	0.6	0.007	5 (Operating) $SEIS_{1.3}$-G+ψ_2Q+ψ_2RQ±A_{Ed}+EHF_{Dir2+}	0.6	0.007	✔ Pass	Details...
St. 2 (2)	W5	2	3 (Operating) $SEIS_{1.1}$-G+ψ_2Q+ψ_2RQ±A_{Ed}+EHF_{Dir1+}	1.5	0.015	5 (Operating) $SEIS_{1.3}$-G+ψ_2Q+ψ_2RQ±A_{Ed}+EHF_{Dir2+}	1.3	0.013	✔ Pass	Details...
St. 2 (2)	W6	2	3 (Operating) $SEIS_{1.1}$-G+ψ_2Q+ψ_2RQ±A_{Ed}+EHF_{Dir1+}	1.2	0.012	5 (Operating) $SEIS_{1.3}$-G+ψ_2Q+ψ_2RQ±A_{Ed}+EHF_{Dir2+}	1.3	0.013	✔ Pass	Details...
St. 3 (3)	W5	3	3 (Operating) $SEIS_{1.1}$-G+ψ_2Q+ψ_2RQ±A_{Ed}+EHF_{Dir1+}	2.1	0.020	5 (Operating) $SEIS_{1.3}$-G+ψ_2Q+ψ_2RQ±A_{Ed}+EHF_{Dir2+}	1.8	0.018	✔ Pass	Details...
St. 3 (3)	W6	3	3 (Operating) $SEIS_{1.1}$-G+ψ_2Q+ψ_2RQ±A_{Ed}+EHF_{Dir1+}	1.8	0.017	5 (Operating) $SEIS_{1.3}$-G+ψ_2Q+ψ_2RQ±A_{Ed}+EHF_{Dir2+}	1.9	0.018	✔ Pass	Details...
St. 4 (4)	W5	4	3 (Operating) $SEIS_{1.1}$-G+ψ_2Q+ψ_2RQ±A_{Ed}+EHF_{Dir1+}	2.6	0.024	5 (Operating) $SEIS_{1.3}$-G+ψ_2Q+ψ_2RQ±A_{Ed}+EHF_{Dir2+}	2.3	0.022	✔ Pass	Details...
St. 4 (4)	W6	4	3 (Operating) $SEIS_{1.1}$-G+ψ_2Q+ψ_2RQ±A_{Ed}+EHF_{Dir1+}	2.1	0.019	5 (Operating) $SEIS_{1.3}$-G+ψ_2Q+ψ_2RQ±A_{Ed}+EHF_{Dir2+}	2.4	0.022	✔ Pass	Details...
St. 5 (5)	W5	5	3 (Operating) $SEIS_{1.1}$-G+ψ_2Q+ψ_2RQ±A_{Ed}+EHF_{Dir1+}	3.1	0.026	5 (Operating) $SEIS_{1.3}$-G+ψ_2Q+ψ_2RQ±A_{Ed}+EHF_{Dir2+}	2.7	0.024	✔ Pass	Details...
St. 5 (5)	W6	5	3 (Operating) $SEIS_{1.1}$-G+ψ_2Q+ψ_2RQ±A_{Ed}+EHF_{Dir1+}	2.7	0.023	5 (Operating) $SEIS_{1.3}$-G+ψ_2Q+ψ_2RQ±A_{Ed}+EHF_{Dir2+}	2.8	0.025	✔ Pass	Details...
St. 6 (6)	W5	6	3 (Operating) $SEIS_{1.1}$-G+ψ_2Q+ψ_2RQ±A_{Ed}+EHF_{Dir1+}	3.4	0.028	5 (Operating) $SEIS_{1.3}$-G+ψ_2Q+ψ_2RQ±A_{Ed}+EHF_{Dir2+}	3.0	0.026	✔ Pass	Details...
St. 6 (6)	W6	6	3 (Operating) $SEIS_{1.1}$-G+ψ_2Q+ψ_2RQ±A_{Ed}+EHF_{Dir1+}	2.9	0.024	5 (Operating) $SEIS_{1.3}$-G+ψ_2Q+ψ_2RQ±A_{Ed}+EHF_{Dir2+}	3.1	0.027	✔ Pass	Details...
St. 7 (7)	W5	7	3 (Operating) $SEIS_{1.1}$-G+ψ_2Q+ψ_2RQ±A_{Ed}+EHF_{Dir1+}	3.7	0.029	5 (Operating) $SEIS_{1.3}$-G+ψ_2Q+ψ_2RQ±A_{Ed}+EHF_{Dir2+}	3.4	0.028	✔ Pass	Details...
St. 7 (7)	W6	7	3 (Operating) $SEIS_{1.1}$-G+ψ_2Q+ψ_2RQ±A_{Ed}+EHF_{Dir1+}	3.2	0.026	5 (Operating) $SEIS_{1.3}$-G+ψ_2Q+ψ_2RQ±A_{Ed}+EHF_{Dir2+}	3.4	0.028	✔ Pass	Details...
St. 8 (8)	C48	1	3 (Operating) $SEIS_{1.1}$-G+ψ_2Q+ψ_2RQ±A_{Ed}+EHF_{Dir1+}	4.1	0.031	5 (Operating) $SEIS_{1.3}$-G+ψ_2Q+ψ_2RQ±A_{Ed}+EHF_{Dir2+}	3.8	0.030	✔ Pass	Details...
St. 8 (8)	C26	1	3 (Operating) $SEIS_{1.1}$-G+ψ_2Q+ψ_2RQ±A_{Ed}+EHF_{Dir1+}	3.5	0.026	5 (Operating) $SEIS_{1.3}$-G+ψ_2Q+ψ_2RQ±A_{Ed}+EHF_{Dir2+}	3.8	0.030	✔ Pass	Details...
St. 9 (9)	W5	9	3 (Operating) $SEIS_{1.1}$-G+ψ_2Q+ψ_2RQ±A_{Ed}+EHF_{Dir1+}	4.4	0.032	5 (Operating) $SEIS_{1.3}$-G+ψ_2Q+ψ_2RQ±A_{Ed}+EHF_{Dir2+}	4.0	0.031	✔ Pass	Details...
St. 9 (9)	W6	9	3 (Operating) $SEIS_{1.1}$-G+ψ_2Q+ψ_2RQ±A_{Ed}+EHF_{Dir1+}	3.7	0.027	5 (Operating) $SEIS_{1.3}$-G+ψ_2Q+ψ_2RQ±A_{Ed}+EHF_{Dir2+}	4.1	0.031	✔ Pass	Details...
St. 10 (10)	W5	10	3 (Operating) $SEIS_{1.1}$-G+ψ_2Q+ψ_2RQ±A_{Ed}+EHF_{Dir1+}	4.6	0.033	5 (Operating) $SEIS_{1.3}$-G+ψ_2Q+ψ_2RQ±A_{Ed}+EHF_{Dir2+}	4.3	0.032	✔ Pass	Details...
St. 10 (10)	W6	10	3 (Operating) $SEIS_{1.1}$-G+ψ_2Q+ψ_2RQ±A_{Ed}+EHF_{Dir1+}	4.4	0.031	5 (Operating) $SEIS_{1.3}$-G+ψ_2Q+ψ_2RQ±A_{Ed}+EHF_{Dir2+}	4.4	0.032	✔ Pass	Details...
St. 11 (11)	W5	11	3 (Operating) $SEIS_{1.1}$-G+ψ_2Q+ψ_2RQ±A_{Ed}+EHF_{Dir1+}	4.9	0.033	5 (Operating) $SEIS_{1.3}$-G+ψ_2Q+ψ_2RQ±A_{Ed}+EHF_{Dir2+}	4.5	0.033	✔ Pass	Details...
St. 11 (11)	W6	11	3 (Operating) $SEIS_{1.1}$-G+ψ_2Q+ψ_2RQ±A_{Ed}+EHF_{Dir1+}	4.2	0.029	5 (Operating) $SEIS_{1.3}$-G+ψ_2Q+ψ_2RQ±A_{Ed}+EHF_{Dir2+}	4.6	0.033	✔ Pass	Details...
St. 12 (12)	W5	12	3 (Operating) $SEIS_{1.1}$-G+ψ_2Q+ψ_2RQ±A_{Ed}+EHF_{Dir1+}	5.1	0.034	5 (Operating) $SEIS_{1.3}$-G+ψ_2Q+ψ_2RQ±A_{Ed}+EHF_{Dir2+}	4.8	0.033	✔ Pass	Details...
St. 12 (12)	W6	12	3 (Operating) $SEIS_{1.1}$-G+ψ_2Q+ψ_2RQ±A_{Ed}+EHF_{Dir1+}	4.5	0.030	5 (Operating) $SEIS_{1.3}$-G+ψ_2Q+ψ_2RQ±A_{Ed}+EHF_{Dir2+}	4.9	0.034	✔ Pass	Details...
St. 13 (13)	W5	13	3 (Operating) $SEIS_{1.1}$-G+ψ_2Q+ψ_2RQ±A_{Ed}+EHF_{Dir1+}	5.3	0.034	5 (Operating) $SEIS_{1.3}$-G+ψ_2Q+ψ_2RQ±A_{Ed}+EHF_{Dir2+}	5.0	0.034	✔ Pass	Details...
St. 13 (13)	W6	13	3 (Operating) $SEIS_{1.1}$-G+ψ_2Q+ψ_2RQ±A_{Ed}+EHF_{Dir1+}	5.1	0.032	5 (Operating) $SEIS_{1.3}$-G+ψ_2Q+ψ_2RQ±A_{Ed}+EHF_{Dir2+}	5.1	0.034	✔ Pass	Details...
St. 14 (14)	C77	1	3 (Operating) $SEIS_{1.1}$-G+ψ_2Q+ψ_2RQ±A_{Ed}+EHF_{Dir1+}	5.5	0.034	5 (Operating) $SEIS_{1.3}$-G+ψ_2Q+ψ_2RQ±A_{Ed}+EHF_{Dir2+}	5.3	0.035	✔ Pass	Details...
St. 14 (14)	W6	14	3 (Operating) $SEIS_{1.1}$-G+ψ_2Q+ψ_2RQ±A_{Ed}+EHF_{Dir1+}	5.0	0.031	5 (Operating) $SEIS_{1.3}$-G+ψ_2Q+ψ_2RQ±A_{Ed}+EHF_{Dir2+}	5.3	0.035	✔ Pass	Details...
St. 15 (15)	W5	15	3 (Operating) $SEIS_{1.1}$-G+ψ_2Q+ψ_2RQ±A_{Ed}+EHF_{Dir1+}	5.6	0.034	5 (Operating) $SEIS_{1.3}$-G+ψ_2Q+ψ_2RQ±A_{Ed}+EHF_{Dir2+}	5.4	0.034	✔ Pass	Details...
St. 15 (15)	W6	15	3 (Operating) $SEIS_{1.1}$-G+ψ_2Q+ψ_2RQ±A_{Ed}+EHF_{Dir1+}	5.1	0.031	5 (Operating) $SEIS_{1.3}$-G+ψ_2Q+ψ_2RQ±A_{Ed}+EHF_{Dir2+}	5.5	0.035	✔ Pass	Details...
St. 16 (16)	W5	16	3 (Operating) $SEIS_{1.1}$-G+ψ_2Q+ψ_2RQ±A_{Ed}+EHF_{Dir1+}	5.7	0.034	5 (Operating) $SEIS_{1.3}$-G+ψ_2Q+ψ_2RQ±A_{Ed}+EHF_{Dir2+}	5.5	0.034	✔ Pass	Details...
St. 16 (16)	W6	16	3 (Operating) $SEIS_{1.1}$-G+ψ_2Q+ψ_2RQ±A_{Ed}+EHF_{Dir1+}	5.2	0.031	5 (Operating) $SEIS_{1.3}$-G+ψ_2Q+ψ_2RQ±A_{Ed}+EHF_{Dir2+}	5.6	0.035	✔ Pass	Details...
St. 17 (17)	W5	17	3 (Operating) $SEIS_{1.1}$-G+ψ_2Q+ψ_2RQ±A_{Ed}+EHF_{Dir1+}	5.8	0.033	5 (Operating) $SEIS_{1.3}$-G+ψ_2Q+ψ_2RQ±A_{Ed}+EHF_{Dir2+}	5.6	0.034	✔ Pass	Details...
St. 17 (17)	W6	17	3 (Operating) $SEIS_{1.1}$-G+ψ_2Q+ψ_2RQ±A_{Ed}+EHF_{Dir1+}	5.3	0.030	5 (Operating) $SEIS_{1.3}$-G+ψ_2Q+ψ_2RQ±A_{Ed}+EHF_{Dir2+}	5.7	0.034	✔ Pass	Details...
St. 18 (18)	W5	18	3 (Operating) $SEIS_{1.1}$-G+ψ_2Q+ψ_2RQ±A_{Ed}+EHF_{Dir1+}	5.9	0.033	5 (Operating) $SEIS_{1.3}$-G+ψ_2Q+ψ_2RQ±A_{Ed}+EHF_{Dir2+}	5.7	0.033	✔ Pass	Details...
St. 18 (18)	W6	18	3 (Operating) $SEIS_{1.1}$-G+ψ_2Q+ψ_2RQ±A_{Ed}+EHF_{Dir1+}	5.2	0.029	5 (Operating) $SEIS_{1.3}$-G+ψ_2Q+ψ_2RQ±A_{Ed}+EHF_{Dir2+}	5.8	0.034	✔ Pass	Details...
St. 19 (19)	W6	19	3 (Operating) $SEIS_{1.1}$-G+ψ_2Q+ψ_2RQ±A_{Ed}+EHF_{Dir1+}	5.9	0.032	5 (Operating) $SEIS_{1.3}$-G+ψ_2Q+ψ_2RQ±A_{Ed}+EHF_{Dir2+}	5.8	0.033	✔ Pass	Details...
St. 20 (roof)	W5	20	3 (Operating) $SEIS_{1.1}$-G+ψ_2Q+ψ_2RQ±A_{Ed}+EHF_{Dir1+}	5.7	0.030	5 (Operating) $SEIS_{1.3}$-G+ψ_2Q+ψ_2RQ±A_{Ed}+EHF_{Dir2+}	5.7	0.031	✔ Pass	Details...

MOREL4

Level ▲	Ref.	Stack	Combination Dir 1	Drift Dir 1 [mm]	θ_{Dir1}	Combination Dir 2	Drift Dir 2 [mm]	θ_{Dir2}	Status	Details
St. 1 (1)	W5	1	3 (Operating) $SEIS_{1.1}$-G+ψ_2Q+ψ_2RQ±A_{Ed}+EHF_{Dir1+}	0.8	0.008	5 (Operating) $SEIS_{1.1}$-G+ψ_2Q+ψ_2RQ±A_{Ed}+EHF_{Dir2+}	0.6	0.007	✔ Pass	Details...
St. 1 (1)	C5	1	3 (Operating) $SEIS_{1.1}$-G+ψ_2Q+ψ_2RQ±A_{Ed}+EHF_{Dir1+}	0.6	0.006	5 (Operating) $SEIS_{1.1}$-G+ψ_2Q+ψ_2RQ±A_{Ed}+EHF_{Dir2+}	0.6	0.007	✔ Pass	Details...
St. 2 (2)	W5	2	3 (Operating) $SEIS_{1.1}$-G+ψ_2Q+ψ_2RQ±A_{Ed}+EHF_{Dir1+}	1.5	0.015	5 (Operating) $SEIS_{1.1}$-G+ψ_2Q+ψ_2RQ±A_{Ed}+EHF_{Dir2+}	1.2	0.013	✔ Pass	Details...
St. 2 (2)	W7	2	3 (Operating) $SEIS_{1.1}$-G+ψ_2Q+ψ_2RQ±A_{Ed}+EHF_{Dir1+}	1.2	0.012	5 (Operating) $SEIS_{1.1}$-G+ψ_2Q+ψ_2RQ±A_{Ed}+EHF_{Dir2+}	1.3	0.013	✔ Pass	Details...
St. 3 (3)	W5	3	3 (Operating) $SEIS_{1.1}$-G+ψ_2Q+ψ_2RQ±A_{Ed}+EHF_{Dir1+}	2.1	0.020	5 (Operating) $SEIS_{1.1}$-G+ψ_2Q+ψ_2RQ±A_{Ed}+EHF_{Dir2+}	1.8	0.018	✔ Pass	Details...
St. 3 (3)	W7	3	3 (Operating) $SEIS_{1.1}$-G+ψ_2Q+ψ_2RQ±A_{Ed}+EHF_{Dir1+}	1.8	0.017	5 (Operating) $SEIS_{1.1}$-G+ψ_2Q+ψ_2RQ±A_{Ed}+EHF_{Dir2+}	1.9	0.019	✔ Pass	Details...
St. 4 (4)	W5	4	3 (Operating) $SEIS_{1.1}$-G+ψ_2Q+ψ_2RQ±A_{Ed}+EHF_{Dir1+}	2.6	0.024	5 (Operating) $SEIS_{1.1}$-G+ψ_2Q+ψ_2RQ±A_{Ed}+EHF_{Dir2+}	2.3	0.022	✔ Pass	Details...
St. 4 (4)	W7	4	3 (Operating) $SEIS_{1.1}$-G+ψ_2Q+ψ_2RQ±A_{Ed}+EHF_{Dir1+}	2.1	0.019	5 (Operating) $SEIS_{1.1}$-G+ψ_2Q+ψ_2RQ±A_{Ed}+EHF_{Dir2+}	2.4	0.022	✔ Pass	Details...
St. 5 (5)	W5	5	3 (Operating) $SEIS_{1.1}$-G+ψ_2Q+ψ_2RQ±A_{Ed}+EHF_{Dir1+}	3.1	0.026	5 (Operating) $SEIS_{1.1}$-G+ψ_2Q+ψ_2RQ±A_{Ed}+EHF_{Dir2+}	2.7	0.025	✔ Pass	Details...
St. 5 (5)	W7	5	3 (Operating) $SEIS_{1.1}$-G+ψ_2Q+ψ_2RQ±A_{Ed}+EHF_{Dir1+}	2.7	0.023	5 (Operating) $SEIS_{1.1}$-G+ψ_2Q+ψ_2RQ±A_{Ed}+EHF_{Dir2+}	2.8	0.025	✔ Pass	Details...
St. 6 (6)	W5	6	3 (Operating) $SEIS_{1.1}$-G+ψ_2Q+ψ_2RQ±A_{Ed}+EHF_{Dir1+}	3.4	0.028	5 (Operating) $SEIS_{1.1}$-G+ψ_2Q+ψ_2RQ±A_{Ed}+EHF_{Dir2+}	3.1	0.027	✔ Pass	Details...
St. 6 (6)	W7	6	3 (Operating) $SEIS_{1.1}$-G+ψ_2Q+ψ_2RQ±A_{Ed}+EHF_{Dir1+}	3.0	0.024	5 (Operating) $SEIS_{1.1}$-G+ψ_2Q+ψ_2RQ±A_{Ed}+EHF_{Dir2+}	3.1	0.027	✔ Pass	Details...
St. 7 (7)	W5	7	3 (Operating) $SEIS_{1.1}$-G+ψ_2Q+ψ_2RQ±A_{Ed}+EHF_{Dir1+}	3.7	0.030	5 (Operating) $SEIS_{1.1}$-G+ψ_2Q+ψ_2RQ±A_{Ed}+EHF_{Dir2+}	3.4	0.028	✔ Pass	Details...
St. 7 (7)	W7	7	3 (Operating) $SEIS_{1.1}$-G+ψ_2Q+ψ_2RQ±A_{Ed}+EHF_{Dir1+}	3.3	0.026	5 (Operating) $SEIS_{1.1}$-G+ψ_2Q+ψ_2RQ±A_{Ed}+EHF_{Dir2+}	3.4	0.029	✔ Pass	Details...
St. 8 (8)	C48	1	3 (Operating) $SEIS_{1.1}$-G+ψ_2Q+ψ_2RQ±A_{Ed}+EHF_{Dir1+}	4.1	0.031	5 (Operating) $SEIS_{1.1}$-G+ψ_2Q+ψ_2RQ±A_{Ed}+EHF_{Dir2+}	3.8	0.030	✔ Pass	Details...
St. 8 (8)	C26	1	3 (Operating) $SEIS_{1.1}$-G+ψ_2Q+ψ_2RQ±A_{Ed}+EHF_{Dir1+}	3.5	0.026	5 (Operating) $SEIS_{1.1}$-G+ψ_2Q+ψ_2RQ±A_{Ed}+EHF_{Dir2+}	3.8	0.030	✔ Pass	Details...
St. 9 (9)	W5	9	3 (Operating) $SEIS_{1.1}$-G+ψ_2Q+ψ_2RQ±A_{Ed}+EHF_{Dir1+}	4.4	0.032	5 (Operating) $SEIS_{1.1}$-G+ψ_2Q+ψ_2RQ±A_{Ed}+EHF_{Dir2+}	4.0	0.031	✔ Pass	Details...
St. 9 (9)	W7	9	3 (Operating) $SEIS_{1.1}$-G+ψ_2Q+ψ_2RQ±A_{Ed}+EHF_{Dir1+}	3.7	0.027	5 (Operating) $SEIS_{1.1}$-G+ψ_2Q+ψ_2RQ±A_{Ed}+EHF_{Dir2+}	4.1	0.031	✔ Pass	Details...
St. 10 (10)	W5	10	3 (Operating) $SEIS_{1.1}$-G+ψ_2Q+ψ_2RQ±A_{Ed}+EHF_{Dir1+}	4.6	0.033	5 (Operating) $SEIS_{1.1}$-G+ψ_2Q+ψ_2RQ±A_{Ed}+EHF_{Dir2+}	4.3	0.032	✔ Pass	Details...
St. 10 (10)	W7	10	3 (Operating) $SEIS_{1.1}$-G+ψ_2Q+ψ_2RQ±A_{Ed}+EHF_{Dir1+}	4.4	0.031	5 (Operating) $SEIS_{1.1}$-G+ψ_2Q+ψ_2RQ±A_{Ed}+EHF_{Dir2+}	4.4	0.033	✔ Pass	Details...
St. 11 (11)	W5	11	3 (Operating) $SEIS_{1.1}$-G+ψ_2Q+ψ_2RQ±A_{Ed}+EHF_{Dir1+}	4.9	0.033	5 (Operating) $SEIS_{1.1}$-G+ψ_2Q+ψ_2RQ±A_{Ed}+EHF_{Dir2+}	4.5	0.033	✔ Pass	Details...
St. 11 (11)	W7	11	3 (Operating) $SEIS_{1.1}$-G+ψ_2Q+ψ_2RQ±A_{Ed}+EHF_{Dir1+}	4.2	0.029	5 (Operating) $SEIS_{1.1}$-G+ψ_2Q+ψ_2RQ±A_{Ed}+EHF_{Dir2+}	4.6	0.033	✔ Pass	Details...
St. 12 (12)	W5	12	3 (Operating) $SEIS_{1.1}$-G+ψ_2Q+ψ_2RQ±A_{Ed}+EHF_{Dir1+}	5.1	0.034	5 (Operating) $SEIS_{1.1}$-G+ψ_2Q+ψ_2RQ±A_{Ed}+EHF_{Dir2+}	4.8	0.033	✔ Pass	Details...
St. 12 (12)	W7	12	3 (Operating) $SEIS_{1.1}$-G+ψ_2Q+ψ_2RQ±A_{Ed}+EHF_{Dir1+}	4.6	0.030	5 (Operating) $SEIS_{1.1}$-G+ψ_2Q+ψ_2RQ±A_{Ed}+EHF_{Dir2+}	4.9	0.034	✔ Pass	Details...
St. 13 (13)	W5	13	3 (Operating) $SEIS_{1.1}$-G+ψ_2Q+ψ_2RQ±A_{Ed}+EHF_{Dir1+}	5.3	0.034	5 (Operating) $SEIS_{1.1}$-G+ψ_2Q+ψ_2RQ±A_{Ed}+EHF_{Dir2+}	5.0	0.034	✔ Pass	Details...
St. 13 (13)	W7	13	3 (Operating) $SEIS_{1.1}$-G+ψ_2Q+ψ_2RQ±A_{Ed}+EHF_{Dir1+}	5.1	0.033	5 (Operating) $SEIS_{1.1}$-G+ψ_2Q+ψ_2RQ±A_{Ed}+EHF_{Dir2+}	5.1	0.034	✔ Pass	Details...
St. 14 (14)	C77	1	3 (Operating) $SEIS_{1.1}$-G+ψ_2Q+ψ_2RQ±A_{Ed}+EHF_{Dir1+}	5.5	0.034	5 (Operating) $SEIS_{1.1}$-G+ψ_2Q+ψ_2RQ±A_{Ed}+EHF_{Dir2+}	5.3	0.035	✔ Pass	Details...
St. 14 (14)	W7	14	3 (Operating) $SEIS_{1.1}$-G+ψ_2Q+ψ_2RQ±A_{Ed}+EHF_{Dir1+}	5.0	0.031	5 (Operating) $SEIS_{1.1}$-G+ψ_2Q+ψ_2RQ±A_{Ed}+EHF_{Dir2+}	5.3	0.035	✔ Pass	Details...
St. 15 (15)	W5	15	3 (Operating) $SEIS_{1.1}$-G+ψ_2Q+ψ_2RQ±A_{Ed}+EHF_{Dir1+}	5.6	0.034	5 (Operating) $SEIS_{1.1}$-G+ψ_2Q+ψ_2RQ±A_{Ed}+EHF_{Dir2+}	5.4	0.034	✔ Pass	Details...
St. 15 (15)	W7	15	3 (Operating) $SEIS_{1.1}$-G+ψ_2Q+ψ_2RQ±A_{Ed}+EHF_{Dir1+}	5.1	0.031	5 (Operating) $SEIS_{1.1}$-G+ψ_2Q+ψ_2RQ±A_{Ed}+EHF_{Dir2+}	5.5	0.035	✔ Pass	Details...
St. 16 (16)	W5	16	3 (Operating) $SEIS_{1.1}$-G+ψ_2Q+ψ_2RQ±A_{Ed}+EHF_{Dir1+}	5.8	0.034	5 (Operating) $SEIS_{1.1}$-G+ψ_2Q+ψ_2RQ±A_{Ed}+EHF_{Dir2+}	5.5	0.034	✔ Pass	Details...
St. 16 (16)	W7	16	3 (Operating) $SEIS_{1.1}$-G+ψ_2Q+ψ_2RQ±A_{Ed}+EHF_{Dir1+}	5.2	0.031	5 (Operating) $SEIS_{1.1}$-G+ψ_2Q+ψ_2RQ±A_{Ed}+EHF_{Dir2+}	5.6	0.035	✔ Pass	Details...
St. 17 (17)	W5	17	3 (Operating) $SEIS_{1.1}$-G+ψ_2Q+ψ_2RQ±A_{Ed}+EHF_{Dir1+}	5.8	0.033	5 (Operating) $SEIS_{1.1}$-G+ψ_2Q+ψ_2RQ±A_{Ed}+EHF_{Dir2+}	5.6	0.034	✔ Pass	Details...
St. 17 (17)	W7	17	3 (Operating) $SEIS_{1.1}$-G+ψ_2Q+ψ_2RQ±A_{Ed}+EHF_{Dir1+}	5.3	0.030	5 (Operating) $SEIS_{1.1}$-G+ψ_2Q+ψ_2RQ±A_{Ed}+EHF_{Dir2+}	5.7	0.034	✔ Pass	Details...
St. 18 (18)	W5	18	3 (Operating) $SEIS_{1.1}$-G+ψ_2Q+ψ_2RQ±A_{Ed}+EHF_{Dir1+}	5.9	0.033	5 (Operating) $SEIS_{1.1}$-G+ψ_2Q+ψ_2RQ±A_{Ed}+EHF_{Dir2+}	5.7	0.033	✔ Pass	Details...
St. 18 (18)	W7	18	3 (Operating) $SEIS_{1.1}$-G+ψ_2Q+ψ_2RQ±A_{Ed}+EHF_{Dir1+}	5.2	0.029	5 (Operating) $SEIS_{1.1}$-G+ψ_2Q+ψ_2RQ±A_{Ed}+EHF_{Dir2+}	5.8	0.034	✔ Pass	Details...
St. 19 (19)	W7	19	3 (Operating) $SEIS_{1.1}$-G+ψ_2Q+ψ_2RQ±A_{Ed}+EHF_{Dir1+}	5.9	0.032	5 (Operating) $SEIS_{1.1}$-G+ψ_2Q+ψ_2RQ±A_{Ed}+EHF_{Dir2+}	5.8	0.033	✔ Pass	Details...
St. 20 (roof)	W5	20	3 (Operating) $SEIS_{1.1}$-G+ψ_2Q+ψ_2RQ±A_{Ed}+EHF_{Dir1+}	5.8	0.030	5 (Operating) $SEIS_{1.1}$-G+ψ_2Q+ψ_2RQ±A_{Ed}+EHF_{Dir2+}	5.7	0.032	✔ Pass	Details...

MODEL5

Level ▲	Ref.	Stack	Combination Dir 1	Drift Dir 1 [mm]	$\theta_{Dir\,1}$	Combination Dir 2	Drift Dir 2 [mm]	$\theta_{Dir\,2}$	Status	Details
St. 1 (1)	W5	1	3 (Operating) $SEIS_{1.1}$-G+ψ_2Q+ψ_2RQ±A_{Ed}+EHF_{Dir1}	0.8	0.008	5 (Operating) $SEIS_{1.1}$-G+ψ_2Q+ψ_2RQ±A_{Ed}+EHF_{Dir2}	0.6	0.006	✔ Pass	Details...
St. 1 (1)	C5	1	3 (Operating) $SEIS_{1.1}$-G+ψ_2Q+ψ_2RQ±A_{Ed}+EHF_{Dir1}	0.5	0.006	5 (Operating) $SEIS_{1.1}$-G+ψ_2Q+ψ_2RQ±A_{Ed}+EHF_{Dir2}	0.6	0.007	✔ Pass	Details...
St. 2 (2)	W5	2	3 (Operating) $SEIS_{1.1}$-G+ψ_2Q+ψ_2RQ±A_{Ed}+EHF_{Dir1}	1.5	0.015	5 (Operating) $SEIS_{1.1}$-G+ψ_2Q+ψ_2RQ±A_{Ed}+EHF_{Dir2}	1.2	0.013	✔ Pass	Details...
St. 2 (2)	W6	2	3 (Operating) $SEIS_{1.1}$-G+ψ_2Q+ψ_2RQ±A_{Ed}+EHF_{Dir1}	1.2	0.012	5 (Operating) $SEIS_{1.1}$-G+ψ_2Q+ψ_2RQ±A_{Ed}+EHF_{Dir2}	1.3	0.013	✔ Pass	Details...
St. 3 (3)	W5	3	3 (Operating) $SEIS_{1.1}$-G+ψ_2Q+ψ_2RQ±A_{Ed}+EHF_{Dir1}	2.1	0.020	5 (Operating) $SEIS_{1.1}$-G+ψ_2Q+ψ_2RQ±A_{Ed}+EHF_{Dir2}	1.8	0.018	✔ Pass	Details...
St. 3 (3)	W6	3	3 (Operating) $SEIS_{1.1}$-G+ψ_2Q+ψ_2RQ±A_{Ed}+EHF_{Dir1}	1.8	0.017	5 (Operating) $SEIS_{1.1}$-G+ψ_2Q+ψ_2RQ±A_{Ed}+EHF_{Dir2}	1.8	0.018	✔ Pass	Details...
St. 4 (4)	W5	4	3 (Operating) $SEIS_{1.1}$-G+ψ_2Q+ψ_2RQ±A_{Ed}+EHF_{Dir1}	2.6	0.024	5 (Operating) $SEIS_{1.1}$-G+ψ_2Q+ψ_2RQ±A_{Ed}+EHF_{Dir2}	2.3	0.021	✔ Pass	Details...
St. 4 (4)	W6	4	3 (Operating) $SEIS_{1.1}$-G+ψ_2Q+ψ_2RQ±A_{Ed}+EHF_{Dir1}	2.2	0.020	5 (Operating) $SEIS_{1.1}$-G+ψ_2Q+ψ_2RQ±A_{Ed}+EHF_{Dir2}	2.3	0.022	✔ Pass	Details...
St. 5 (5)	W5	5	3 (Operating) $SEIS_{1.1}$-G+ψ_2Q+ψ_2RQ±A_{Ed}+EHF_{Dir1}	3.1	0.026	5 (Operating) $SEIS_{1.1}$-G+ψ_2Q+ψ_2RQ±A_{Ed}+EHF_{Dir2}	2.7	0.024	✔ Pass	Details...
St. 5 (5)	W6	5	3 (Operating) $SEIS_{1.1}$-G+ψ_2Q+ψ_2RQ±A_{Ed}+EHF_{Dir1}	2.5	0.022	5 (Operating) $SEIS_{1.1}$-G+ψ_2Q+ψ_2RQ±A_{Ed}+EHF_{Dir2}	2.8	0.025	✔ Pass	Details...
St. 6 (6)	W5	6	3 (Operating) $SEIS_{1.1}$-G+ψ_2Q+ψ_2RQ±A_{Ed}+EHF_{Dir1}	3.4	0.028	5 (Operating) $SEIS_{1.1}$-G+ψ_2Q+ψ_2RQ±A_{Ed}+EHF_{Dir2}	3.0	0.026	✔ Pass	Details...
St. 6 (6)	W6	6	3 (Operating) $SEIS_{1.1}$-G+ψ_2Q+ψ_2RQ±A_{Ed}+EHF_{Dir1}	3.1	0.025	5 (Operating) $SEIS_{1.1}$-G+ψ_2Q+ψ_2RQ±A_{Ed}+EHF_{Dir2}	3.1	0.027	✔ Pass	Details...
St. 7 (7)	W5	7	3 (Operating) $SEIS_{1.1}$-G+ψ_2Q+ψ_2RQ±A_{Ed}+EHF_{Dir1}	3.7	0.030	5 (Operating) $SEIS_{1.1}$-G+ψ_2Q+ψ_2RQ±A_{Ed}+EHF_{Dir2}	3.3	0.028	✔ Pass	Details...
St. 7 (7)	W6	7	3 (Operating) $SEIS_{1.1}$-G+ψ_2Q+ψ_2RQ±A_{Ed}+EHF_{Dir1}	3.3	0.026	5 (Operating) $SEIS_{1.1}$-G+ψ_2Q+ψ_2RQ±A_{Ed}+EHF_{Dir2}	3.4	0.028	✔ Pass	Details...
St. 8 (8)	C48	1	3 (Operating) $SEIS_{1.1}$-G+ψ_2Q+ψ_2RQ±A_{Ed}+EHF_{Dir1}	4.1	0.031	5 (Operating) $SEIS_{1.1}$-G+ψ_2Q+ψ_2RQ±A_{Ed}+EHF_{Dir2}	3.7	0.030	✔ Pass	Details...
St. 8 (8)	C26	1	3 (Operating) $SEIS_{1.1}$-G+ψ_2Q+ψ_2RQ±A_{Ed}+EHF_{Dir1}	3.5	0.026	5 (Operating) $SEIS_{1.1}$-G+ψ_2Q+ψ_2RQ±A_{Ed}+EHF_{Dir2}	3.7	0.030	✔ Pass	Details...
St. 9 (9)	W5	9	3 (Operating) $SEIS_{1.1}$-G+ψ_2Q+ψ_2RQ±A_{Ed}+EHF_{Dir1}	4.4	0.032	5 (Operating) $SEIS_{1.1}$-G+ψ_2Q+ψ_2RQ±A_{Ed}+EHF_{Dir2}	4.0	0.031	✔ Pass	Details...
St. 9 (9)	W6	9	3 (Operating) $SEIS_{1.1}$-G+ψ_2Q+ψ_2RQ±A_{Ed}+EHF_{Dir1}	3.9	0.029	5 (Operating) $SEIS_{1.1}$-G+ψ_2Q+ψ_2RQ±A_{Ed}+EHF_{Dir2}	4.1	0.031	✔ Pass	Details...
St. 10 (10)	W5	10	3 (Operating) $SEIS_{1.1}$-G+ψ_2Q+ψ_2RQ±A_{Ed}+EHF_{Dir1}	4.6	0.033	5 (Operating) $SEIS_{1.1}$-G+ψ_2Q+ψ_2RQ±A_{Ed}+EHF_{Dir2}	4.3	0.032	✔ Pass	Details...
St. 10 (10)	W6	10	3 (Operating) $SEIS_{1.1}$-G+ψ_2Q+ψ_2RQ±A_{Ed}+EHF_{Dir1}	3.9	0.028	5 (Operating) $SEIS_{1.1}$-G+ψ_2Q+ψ_2RQ±A_{Ed}+EHF_{Dir2}	4.3	0.032	✔ Pass	Details...
St. 11 (11)	W5	11	3 (Operating) $SEIS_{1.1}$-G+ψ_2Q+ψ_2RQ±A_{Ed}+EHF_{Dir1}	4.9	0.034	5 (Operating) $SEIS_{1.1}$-G+ψ_2Q+ψ_2RQ±A_{Ed}+EHF_{Dir2}	4.5	0.033	✔ Pass	Details...
St. 11 (11)	W6	11	3 (Operating) $SEIS_{1.1}$-G+ψ_2Q+ψ_2RQ±A_{Ed}+EHF_{Dir1}	4.7	0.032	5 (Operating) $SEIS_{1.1}$-G+ψ_2Q+ψ_2RQ±A_{Ed}+EHF_{Dir2}	4.6	0.033	✔ Pass	Details...
St. 12 (12)	W5	12	3 (Operating) $SEIS_{1.1}$-G+ψ_2Q+ψ_2RQ±A_{Ed}+EHF_{Dir1}	5.1	0.034	5 (Operating) $SEIS_{1.1}$-G+ψ_2Q+ψ_2RQ±A_{Ed}+EHF_{Dir2}	4.8	0.033	✔ Pass	Details...
St. 12 (12)	W6	12	3 (Operating) $SEIS_{1.1}$-G+ψ_2Q+ψ_2RQ±A_{Ed}+EHF_{Dir1}	4.4	0.029	5 (Operating) $SEIS_{1.1}$-G+ψ_2Q+ψ_2RQ±A_{Ed}+EHF_{Dir2}	4.8	0.034	✔ Pass	Details...
St. 13 (13)	W5	13	3 (Operating) $SEIS_{1.1}$-G+ψ_2Q+ψ_2RQ±A_{Ed}+EHF_{Dir1}	5.3	0.034	5 (Operating) $SEIS_{1.1}$-G+ψ_2Q+ψ_2RQ±A_{Ed}+EHF_{Dir2}	5.0	0.033	✔ Pass	Details...
St. 13 (13)	W6	13	3 (Operating) $SEIS_{1.1}$-G+ψ_2Q+ψ_2RQ±A_{Ed}+EHF_{Dir1}	5.1	0.033	5 (Operating) $SEIS_{1.1}$-G+ψ_2Q+ψ_2RQ±A_{Ed}+EHF_{Dir2}	5.0	0.034	✔ Pass	Details...
St. 14 (14)	C77	1	3 (Operating) $SEIS_{1.1}$-G+ψ_2Q+ψ_2RQ±A_{Ed}+EHF_{Dir1}	5.5	0.034	5 (Operating) $SEIS_{1.1}$-G+ψ_2Q+ψ_2RQ±A_{Ed}+EHF_{Dir2}	5.3	0.034	✔ Pass	Details...
St. 14 (14)	W6	14	3 (Operating) $SEIS_{1.1}$-G+ψ_2Q+ψ_2RQ±A_{Ed}+EHF_{Dir1}	4.8	0.030	5 (Operating) $SEIS_{1.1}$-G+ψ_2Q+ψ_2RQ±A_{Ed}+EHF_{Dir2}	5.3	0.034	✔ Pass	Details...
St. 15 (15)	W5	15	3 (Operating) $SEIS_{1.1}$-G+ψ_2Q+ψ_2RQ±A_{Ed}+EHF_{Dir1}	5.7	0.034	5 (Operating) $SEIS_{1.1}$-G+ψ_2Q+ψ_2RQ±A_{Ed}+EHF_{Dir2}	5.4	0.034	✔ Pass	Details...
St. 15 (15)	W6	15	3 (Operating) $SEIS_{1.1}$-G+ψ_2Q+ψ_2RQ±A_{Ed}+EHF_{Dir1}	5.5	0.033	5 (Operating) $SEIS_{1.1}$-G+ψ_2Q+ψ_2RQ±A_{Ed}+EHF_{Dir2}	5.5	0.035	✔ Pass	Details...
St. 16 (16)	W5	16	3 (Operating) $SEIS_{1.1}$-G+ψ_2Q+ψ_2RQ±A_{Ed}+EHF_{Dir1}	5.8	0.034	5 (Operating) $SEIS_{1.1}$-G+ψ_2Q+ψ_2RQ±A_{Ed}+EHF_{Dir2}	5.5	0.034	✔ Pass	Details...
St. 16 (16)	W6	16	3 (Operating) $SEIS_{1.1}$-G+ψ_2Q+ψ_2RQ±A_{Ed}+EHF_{Dir1}	5.2	0.031	5 (Operating) $SEIS_{1.1}$-G+ψ_2Q+ψ_2RQ±A_{Ed}+EHF_{Dir2}	5.6	0.034	✔ Pass	Details...
St. 17 (17)	W5	17	3 (Operating) $SEIS_{1.1}$-G+ψ_2Q+ψ_2RQ±A_{Ed}+EHF_{Dir1}	5.8	0.033	5 (Operating) $SEIS_{1.1}$-G+ψ_2Q+ψ_2RQ±A_{Ed}+EHF_{Dir2}	5.6	0.033	✔ Pass	Details...
St. 17 (17)	W6	17	3 (Operating) $SEIS_{1.1}$-G+ψ_2Q+ψ_2RQ±A_{Ed}+EHF_{Dir1}	5.3	0.030	5 (Operating) $SEIS_{1.1}$-G+ψ_2Q+ψ_2RQ±A_{Ed}+EHF_{Dir2}	5.7	0.034	✔ Pass	Details...
St. 18 (18)	W5	18	3 (Operating) $SEIS_{1.1}$-G+ψ_2Q+ψ_2RQ±A_{Ed}+EHF_{Dir1}	5.9	0.033	5 (Operating) $SEIS_{1.1}$-G+ψ_2Q+ψ_2RQ±A_{Ed}+EHF_{Dir2}	5.7	0.033	✔ Pass	Details...
St. 18 (18)	W6	18	3 (Operating) $SEIS_{1.1}$-G+ψ_2Q+ψ_2RQ±A_{Ed}+EHF_{Dir1}	5.4	0.030	5 (Operating) $SEIS_{1.1}$-G+ψ_2Q+ψ_2RQ±A_{Ed}+EHF_{Dir2}	5.8	0.033	✔ Pass	Details...
St. 19 (19)	W5	19	3 (Operating) $SEIS_{1.1}$-G+ψ_2Q+ψ_2RQ±A_{Ed}+EHF_{Dir1}	5.8	0.032	5 (Operating) $SEIS_{1.1}$-G+ψ_2Q+ψ_2RQ±A_{Ed}+EHF_{Dir2}	5.7	0.032	✔ Pass	Details...
St. 19 (19)	W6	19	3 (Operating) $SEIS_{1.1}$-G+ψ_2Q+ψ_2RQ±A_{Ed}+EHF_{Dir1}	5.2	0.028	5 (Operating) $SEIS_{1.1}$-G+ψ_2Q+ψ_2RQ±A_{Ed}+EHF_{Dir2}	5.8	0.033	✔ Pass	Details...

MODEL6

Level ▲	Ref.	Stack	Combination Dir 1	Drift Dir 1 [mm]	θ_{Dir1}	Combination Dir 2	Drift Dir 2 [mm]	θ_{Dir2}	Status	Details
St. 2 (2)	W5	2	3 (Operating) $SEIS_{1.1}$-G+ψ_2Q+ψ_2RQ±A_{Ed}+EHF_{Dir1+}	1.5	0.014	5 (Operating) $SEIS_{1.3}$-G+ψ_2Q+ψ_2RQ±A_{Ed}+EHF_{Dir2+}	1.2	0.013	✔ Pass	Details...
St. 2 (2)	W6	2	3 (Operating) $SEIS_{1.1}$-G+ψ_2Q+ψ_2RQ±A_{Ed}+EHF_{Dir1+}	1.2	0.011	5 (Operating) $SEIS_{1.3}$-G+ψ_2Q+ψ_2RQ±A_{Ed}+EHF_{Dir2+}	1.3	0.013	✔ Pass	Details...
St. 3 (3)	W5	3	3 (Operating) $SEIS_{1.1}$-G+ψ_2Q+ψ_2RQ±A_{Ed}+EHF_{Dir1+}	2.0	0.019	5 (Operating) $SEIS_{1.3}$-G+ψ_2Q+ψ_2RQ±A_{Ed}+EHF_{Dir2+}	1.8	0.018	✔ Pass	Details...
St. 3 (3)	W6	3	3 (Operating) $SEIS_{1.1}$-G+ψ_2Q+ψ_2RQ±A_{Ed}+EHF_{Dir1+}	1.7	0.015	5 (Operating) $SEIS_{1.3}$-G+ψ_2Q+ψ_2RQ±A_{Ed}+EHF_{Dir2+}	1.9	0.018	✔ Pass	Details...
St. 4 (4)	W5	4	3 (Operating) $SEIS_{1.1}$-G+ψ_2Q+ψ_2RQ±A_{Ed}+EHF_{Dir1+}	2.5	0.022	5 (Operating) $SEIS_{1.3}$-G+ψ_2Q+ψ_2RQ±A_{Ed}+EHF_{Dir2+}	2.3	0.021	✔ Pass	Details...
St. 4 (4)	W6	4	3 (Operating) $SEIS_{1.1}$-G+ψ_2Q+ψ_2RQ±A_{Ed}+EHF_{Dir1+}	2.1	0.019	5 (Operating) $SEIS_{1.3}$-G+ψ_2Q+ψ_2RQ±A_{Ed}+EHF_{Dir2+}	2.3	0.022	✔ Pass	Details...
St. 5 (5)	W5	5	3 (Operating) $SEIS_{1.1}$-G+ψ_2Q+ψ_2RQ±A_{Ed}+EHF_{Dir1+}	2.9	0.025	5 (Operating) $SEIS_{1.3}$-G+ψ_2Q+ψ_2RQ±A_{Ed}+EHF_{Dir2+}	2.7	0.024	✔ Pass	Details...
St. 5 (5)	W6	5	3 (Operating) $SEIS_{1.1}$-G+ψ_2Q+ψ_2RQ±A_{Ed}+EHF_{Dir1+}	2.4	0.020	5 (Operating) $SEIS_{1.3}$-G+ψ_2Q+ψ_2RQ±A_{Ed}+EHF_{Dir2+}	2.8	0.025	✔ Pass	Details...
St. 6 (6)	W5	6	3 (Operating) $SEIS_{1.1}$-G+ψ_2Q+ψ_2RQ±A_{Ed}+EHF_{Dir1+}	3.2	0.026	5 (Operating) $SEIS_{1.3}$-G+ψ_2Q+ψ_2RQ±A_{Ed}+EHF_{Dir2+}	3.1	0.026	✔ Pass	Details...
St. 6 (6)	W6	6	3 (Operating) $SEIS_{1.1}$-G+ψ_2Q+ψ_2RQ±A_{Ed}+EHF_{Dir1+}	2.9	0.024	5 (Operating) $SEIS_{1.3}$-G+ψ_2Q+ψ_2RQ±A_{Ed}+EHF_{Dir2+}	3.1	0.027	✔ Pass	Details...
St. 7 (7)	W5	7	3 (Operating) $SEIS_{1.1}$-G+ψ_2Q+ψ_2RQ±A_{Ed}+EHF_{Dir1+}	3.5	0.027	5 (Operating) $SEIS_{1.3}$-G+ψ_2Q+ψ_2RQ±A_{Ed}+EHF_{Dir2+}	3.4	0.027	✔ Pass	Details...
St. 7 (7)	W6	7	3 (Operating) $SEIS_{1.1}$-G+ψ_2Q+ψ_2RQ±A_{Ed}+EHF_{Dir1+}	3.1	0.024	5 (Operating) $SEIS_{1.3}$-G+ψ_2Q+ψ_2RQ±A_{Ed}+EHF_{Dir2+}	3.4	0.028	✔ Pass	Details...
St. 8 (8)	C48	1	3 (Operating) $SEIS_{1.1}$-G+ψ_2Q+ψ_2RQ±A_{Ed}+EHF_{Dir1+}	3.9	0.029	5 (Operating) $SEIS_{1.3}$-G+ψ_2Q+ψ_2RQ±A_{Ed}+EHF_{Dir2+}	3.8	0.030	✔ Pass	Details...
St. 8 (8)	C26	1	3 (Operating) $SEIS_{1.1}$-G+ψ_2Q+ψ_2RQ±A_{Ed}+EHF_{Dir1+}	3.3	0.024	5 (Operating) $SEIS_{1.3}$-G+ψ_2Q+ψ_2RQ±A_{Ed}+EHF_{Dir2+}	3.8	0.030	✔ Pass	Details...
St. 9 (9)	W5	9	3 (Operating) $SEIS_{1.1}$-G+ψ_2Q+ψ_2RQ±A_{Ed}+EHF_{Dir1+}	4.1	0.030	5 (Operating) $SEIS_{1.3}$-G+ψ_2Q+ψ_2RQ±A_{Ed}+EHF_{Dir2+}	4.0	0.030	✔ Pass	Details...
St. 9 (9)	W6	9	3 (Operating) $SEIS_{1.1}$-G+ψ_2Q+ψ_2RQ±A_{Ed}+EHF_{Dir1+}	3.7	0.026	5 (Operating) $SEIS_{1.3}$-G+ψ_2Q+ψ_2RQ±A_{Ed}+EHF_{Dir2+}	4.1	0.031	✔ Pass	Details...
St. 10 (10)	W5	10	3 (Operating) $SEIS_{1.1}$-G+ψ_2Q+ψ_2RQ±A_{Ed}+EHF_{Dir1+}	4.4	0.031	5 (Operating) $SEIS_{1.3}$-G+ψ_2Q+ψ_2RQ±A_{Ed}+EHF_{Dir2+}	4.3	0.031	✔ Pass	Details...
St. 10 (10)	W6	10	3 (Operating) $SEIS_{1.1}$-G+ψ_2Q+ψ_2RQ±A_{Ed}+EHF_{Dir1+}	3.7	0.026	5 (Operating) $SEIS_{1.3}$-G+ψ_2Q+ψ_2RQ±A_{Ed}+EHF_{Dir2+}	4.4	0.032	✔ Pass	Details...
St. 11 (11)	W5	11	3 (Operating) $SEIS_{1.1}$-G+ψ_2Q+ψ_2RQ±A_{Ed}+EHF_{Dir1+}	4.6	0.031	5 (Operating) $SEIS_{1.3}$-G+ψ_2Q+ψ_2RQ±A_{Ed}+EHF_{Dir2+}	4.6	0.032	✔ Pass	Details...
St. 11 (11)	W6	11	3 (Operating) $SEIS_{1.1}$-G+ψ_2Q+ψ_2RQ±A_{Ed}+EHF_{Dir1+}	4.4	0.030	5 (Operating) $SEIS_{1.3}$-G+ψ_2Q+ψ_2RQ±A_{Ed}+EHF_{Dir2+}	4.6	0.033	✔ Pass	Details...
St. 12 (12)	W5	12	3 (Operating) $SEIS_{1.1}$-G+ψ_2Q+ψ_2RQ±A_{Ed}+EHF_{Dir1+}	4.8	0.031	5 (Operating) $SEIS_{1.3}$-G+ψ_2Q+ψ_2RQ±A_{Ed}+EHF_{Dir2+}	4.8	0.033	✔ Pass	Details...
St. 12 (12)	W6	12	3 (Operating) $SEIS_{1.1}$-G+ψ_2Q+ψ_2RQ±A_{Ed}+EHF_{Dir1+}	4.2	0.027	5 (Operating) $SEIS_{1.3}$-G+ψ_2Q+ψ_2RQ±A_{Ed}+EHF_{Dir2+}	4.8	0.033	✔ Pass	Details...
St. 13 (13)	W5	13	3 (Operating) $SEIS_{1.1}$-G+ψ_2Q+ψ_2RQ±A_{Ed}+EHF_{Dir1+}	5.0	0.031	5 (Operating) $SEIS_{1.3}$-G+ψ_2Q+ψ_2RQ±A_{Ed}+EHF_{Dir2+}	5.0	0.033	✔ Pass	Details...
St. 13 (13)	W6	13	3 (Operating) $SEIS_{1.1}$-G+ψ_2Q+ψ_2RQ±A_{Ed}+EHF_{Dir1+}	4.8	0.030	5 (Operating) $SEIS_{1.3}$-G+ψ_2Q+ψ_2RQ±A_{Ed}+EHF_{Dir2+}	5.0	0.033	✔ Pass	Details...
St. 14 (14)	C77	1	3 (Operating) $SEIS_{1.1}$-G+ψ_2Q+ψ_2RQ±A_{Ed}+EHF_{Dir1+}	5.2	0.031	5 (Operating) $SEIS_{1.3}$-G+ψ_2Q+ψ_2RQ±A_{Ed}+EHF_{Dir2+}	5.3	0.034	✔ Pass	Details...
St. 14 (14)	C53	1	3 (Operating) $SEIS_{1.1}$-G+ψ_2Q+ψ_2RQ±A_{Ed}+EHF_{Dir1+}	4.5	0.027	5 (Operating) $SEIS_{1.3}$-G+ψ_2Q+ψ_2RQ±A_{Ed}+EHF_{Dir2+}	5.3	0.034	✔ Pass	Details...
St. 15 (15)	W5	15	3 (Operating) $SEIS_{1.1}$-G+ψ_2Q+ψ_2RQ±A_{Ed}+EHF_{Dir1+}	5.3	0.031	5 (Operating) $SEIS_{1.3}$-G+ψ_2Q+ψ_2RQ±A_{Ed}+EHF_{Dir2+}	5.3	0.033	✔ Pass	Details...
St. 15 (15)	W6	15	3 (Operating) $SEIS_{1.1}$-G+ψ_2Q+ψ_2RQ±A_{Ed}+EHF_{Dir1+}	5.2	0.031	5 (Operating) $SEIS_{1.3}$-G+ψ_2Q+ψ_2RQ±A_{Ed}+EHF_{Dir2+}	5.4	0.034	✔ Pass	Details...
St. 16 (16)	W5	16	3 (Operating) $SEIS_{1.1}$-G+ψ_2Q+ψ_2RQ±A_{Ed}+EHF_{Dir1+}	5.4	0.031	5 (Operating) $SEIS_{1.3}$-G+ψ_2Q+ψ_2RQ±A_{Ed}+EHF_{Dir2+}	5.5	0.033	✔ Pass	Details...
St. 16 (16)	W6	16	3 (Operating) $SEIS_{1.1}$-G+ψ_2Q+ψ_2RQ±A_{Ed}+EHF_{Dir1+}	4.9	0.028	5 (Operating) $SEIS_{1.3}$-G+ψ_2Q+ψ_2RQ±A_{Ed}+EHF_{Dir2+}	5.5	0.034	✔ Pass	Details...
St. 17 (17)	W5	17	3 (Operating) $SEIS_{1.1}$-G+ψ_2Q+ψ_2RQ±A_{Ed}+EHF_{Dir1+}	5.4	0.030	5 (Operating) $SEIS_{1.3}$-G+ψ_2Q+ψ_2RQ±A_{Ed}+EHF_{Dir2+}	5.5	0.033	✔ Pass	Details...
St. 17 (17)	W6	17	3 (Operating) $SEIS_{1.1}$-G+ψ_2Q+ψ_2RQ±A_{Ed}+EHF_{Dir1+}	4.9	0.028	5 (Operating) $SEIS_{1.3}$-G+ψ_2Q+ψ_2RQ±A_{Ed}+EHF_{Dir2+}	5.6	0.033	✔ Pass	Details...
St. 18 (18)	W5	18	3 (Operating) $SEIS_{1.1}$-G+ψ_2Q+ψ_2RQ±A_{Ed}+EHF_{Dir1+}	5.4	0.030	5 (Operating) $SEIS_{1.3}$-G+ψ_2Q+ψ_2RQ±A_{Ed}+EHF_{Dir2+}	5.6	0.032	✔ Pass	Details...
St. 18 (18)	W6	18	3 (Operating) $SEIS_{1.1}$-G+ψ_2Q+ψ_2RQ±A_{Ed}+EHF_{Dir1+}	5.0	0.027	5 (Operating) $SEIS_{1.3}$-G+ψ_2Q+ψ_2RQ±A_{Ed}+EHF_{Dir2+}	5.7	0.032	✔ Pass	Details...
St. 19 (19)	W5	19	3 (Operating) $SEIS_{1.1}$-G+ψ_2Q+ψ_2RQ±A_{Ed}+EHF_{Dir1+}	5.4	0.029	5 (Operating) $SEIS_{1.3}$-G+ψ_2Q+ψ_2RQ±A_{Ed}+EHF_{Dir2+}	5.6	0.031	✔ Pass	Details...
St. 19 (19)	W6	19	3 (Operating) $SEIS_{1.1}$-G+ψ_2Q+ψ_2RQ±A_{Ed}+EHF_{Dir1+}	4.9	0.026	5 (Operating) $SEIS_{1.3}$-G+ψ_2Q+ψ_2RQ±A_{Ed}+EHF_{Dir2+}	5.7	0.032	✔ Pass	Details...
St. 20 (roof)	W6	20	3 (Operating) $SEIS_{1.1}$-G+ψ_2Q+ψ_2RQ±A_{Ed}+EHF_{Dir1+}	5.4	0.028	5 (Operating) $SEIS_{1.3}$-G+ψ_2Q+ψ_2RQ±A_{Ed}+EHF_{Dir2+}	5.6	0.030	✔ Pass	Details...

MODEL7

Level ▲	Ref.	Stack	Combination Dir 1	Drift Dir 1 [mm]	$\theta_{Dir\,1}$	Combination Dir 2	Drift Dir 2 [mm]	$\theta_{Dir\,2}$	Status	Details
St. 1 (1)	W5	1	3 (Operating) $SEIS_{1.1}$-G+ψ_2Q+ψ_2RQ±A_{Ed}+EHF_{Dir1+}	0.8	0.008	5 (Operating) $SEIS_{1.1}$-G+ψ_2Q+ψ_2RQ±A_{Ed}+EHF_{Dir2+}	0.6	0.006	✔ Pass	Details...
St. 1 (1)	W6	1	3 (Operating) $SEIS_{1.1}$-G+ψ_2Q+ψ_2RQ±A_{Ed}+EHF_{Dir1+}	0.6	0.006	5 (Operating) $SEIS_{1.1}$-G+ψ_2Q+ψ_2RQ±A_{Ed}+EHF_{Dir2+}	0.6	0.007	✔ Pass	Details...
St. 2 (2)	W5	2	3 (Operating) $SEIS_{1.1}$-G+ψ_2Q+ψ_2RQ±A_{Ed}+EHF_{Dir1+}	1.5	0.014	5 (Operating) $SEIS_{1.1}$-G+ψ_2Q+ψ_2RQ±A_{Ed}+EHF_{Dir2+}	1.2	0.013	✔ Pass	Details...
St. 2 (2)	W6	2	3 (Operating) $SEIS_{1.1}$-G+ψ_2Q+ψ_2RQ±A_{Ed}+EHF_{Dir1+}	1.2	0.011	5 (Operating) $SEIS_{1.1}$-G+ψ_2Q+ψ_2RQ±A_{Ed}+EHF_{Dir2+}	1.3	0.013	✔ Pass	Details...
St. 3 (3)	W5	3	3 (Operating) $SEIS_{1.1}$-G+ψ_2Q+ψ_2RQ±A_{Ed}+EHF_{Dir1+}	2.0	0.019	5 (Operating) $SEIS_{1.1}$-G+ψ_2Q+ψ_2RQ±A_{Ed}+EHF_{Dir2+}	1.8	0.017	✔ Pass	Details...
St. 3 (3)	W6	3	3 (Operating) $SEIS_{1.1}$-G+ψ_2Q+ψ_2RQ±A_{Ed}+EHF_{Dir1+}	1.7	0.015	5 (Operating) $SEIS_{1.1}$-G+ψ_2Q+ψ_2RQ±A_{Ed}+EHF_{Dir2+}	1.9	0.018	✔ Pass	Details...
St. 4 (4)	W5	4	3 (Operating) $SEIS_{1.1}$-G+ψ_2Q+ψ_2RQ±A_{Ed}+EHF_{Dir1+}	2.5	0.022	5 (Operating) $SEIS_{1.1}$-G+ψ_2Q+ψ_2RQ±A_{Ed}+EHF_{Dir2+}	2.3	0.021	✔ Pass	Details...
St. 4 (4)	W6	4	3 (Operating) $SEIS_{1.1}$-G+ψ_2Q+ψ_2RQ±A_{Ed}+EHF_{Dir1+}	2.1	0.019	5 (Operating) $SEIS_{1.1}$-G+ψ_2Q+ψ_2RQ±A_{Ed}+EHF_{Dir2+}	2.3	0.022	✔ Pass	Details...
St. 5 (5)	W5	5	3 (Operating) $SEIS_{1.1}$-G+ψ_2Q+ψ_2RQ±A_{Ed}+EHF_{Dir1+}	2.9	0.025	5 (Operating) $SEIS_{1.1}$-G+ψ_2Q+ψ_2RQ±A_{Ed}+EHF_{Dir2+}	2.7	0.024	✔ Pass	Details...
St. 5 (5)	W6	5	3 (Operating) $SEIS_{1.1}$-G+ψ_2Q+ψ_2RQ±A_{Ed}+EHF_{Dir1+}	2.5	0.021	5 (Operating) $SEIS_{1.1}$-G+ψ_2Q+ψ_2RQ±A_{Ed}+EHF_{Dir2+}	2.8	0.024	✔ Pass	Details...
St. 6 (6)	W5	6	3 (Operating) $SEIS_{1.1}$-G+ψ_2Q+ψ_2RQ±A_{Ed}+EHF_{Dir1+}	3.3	0.026	5 (Operating) $SEIS_{1.1}$-G+ψ_2Q+ψ_2RQ±A_{Ed}+EHF_{Dir2+}	3.1	0.026	✔ Pass	Details...
St. 6 (6)	W6	6	3 (Operating) $SEIS_{1.1}$-G+ψ_2Q+ψ_2RQ±A_{Ed}+EHF_{Dir1+}	2.7	0.022	5 (Operating) $SEIS_{1.1}$-G+ψ_2Q+ψ_2RQ±A_{Ed}+EHF_{Dir2+}	3.1	0.027	✔ Pass	Details...
St. 7 (7)	W5	7	3 (Operating) $SEIS_{1.1}$-G+ψ_2Q+ψ_2RQ±A_{Ed}+EHF_{Dir1+}	3.6	0.028	5 (Operating) $SEIS_{1.1}$-G+ψ_2Q+ψ_2RQ±A_{Ed}+EHF_{Dir2+}	3.4	0.027	✔ Pass	Details...
St. 7 (7)	W6	7	3 (Operating) $SEIS_{1.1}$-G+ψ_2Q+ψ_2RQ±A_{Ed}+EHF_{Dir1+}	3.2	0.025	5 (Operating) $SEIS_{1.1}$-G+ψ_2Q+ψ_2RQ±A_{Ed}+EHF_{Dir2+}	3.4	0.028	✔ Pass	Details...
St. 8 (8)	C48	1	3 (Operating) $SEIS_{1.1}$-G+ψ_2Q+ψ_2RQ±A_{Ed}+EHF_{Dir1+}	3.9	0.029	5 (Operating) $SEIS_{1.1}$-G+ψ_2Q+ψ_2RQ±A_{Ed}+EHF_{Dir2+}	3.8	0.030	✔ Pass	Details...
St. 8 (8)	C26	1	3 (Operating) $SEIS_{1.1}$-G+ψ_2Q+ψ_2RQ±A_{Ed}+EHF_{Dir1+}	3.3	0.025	5 (Operating) $SEIS_{1.1}$-G+ψ_2Q+ψ_2RQ±A_{Ed}+EHF_{Dir2+}	3.8	0.030	✔ Pass	Details...
St. 9 (9)	W5	9	3 (Operating) $SEIS_{1.1}$-G+ψ_2Q+ψ_2RQ±A_{Ed}+EHF_{Dir1+}	4.2	0.030	5 (Operating) $SEIS_{1.1}$-G+ψ_2Q+ψ_2RQ±A_{Ed}+EHF_{Dir2+}	4.0	0.030	✔ Pass	Details...
St. 9 (9)	W6	9	3 (Operating) $SEIS_{1.1}$-G+ψ_2Q+ψ_2RQ±A_{Ed}+EHF_{Dir1+}	3.7	0.027	5 (Operating) $SEIS_{1.1}$-G+ψ_2Q+ψ_2RQ±A_{Ed}+EHF_{Dir2+}	4.1	0.031	✔ Pass	Details...
St. 10 (10)	W5	10	3 (Operating) $SEIS_{1.1}$-G+ψ_2Q+ψ_2RQ±A_{Ed}+EHF_{Dir1+}	4.4	0.031	5 (Operating) $SEIS_{1.1}$-G+ψ_2Q+ψ_2RQ±A_{Ed}+EHF_{Dir2+}	4.3	0.031	✔ Pass	Details...
St. 10 (10)	W6	10	3 (Operating) $SEIS_{1.1}$-G+ψ_2Q+ψ_2RQ±A_{Ed}+EHF_{Dir1+}	3.9	0.027	5 (Operating) $SEIS_{1.1}$-G+ψ_2Q+ψ_2RQ±A_{Ed}+EHF_{Dir2+}	4.4	0.032	✔ Pass	Details...
St. 11 (11)	W5	11	3 (Operating) $SEIS_{1.1}$-G+ψ_2Q+ψ_2RQ±A_{Ed}+EHF_{Dir1+}	4.6	0.031	5 (Operating) $SEIS_{1.1}$-G+ψ_2Q+ψ_2RQ±A_{Ed}+EHF_{Dir2+}	4.5	0.032	✔ Pass	Details...
St. 11 (11)	W6	11	3 (Operating) $SEIS_{1.1}$-G+ψ_2Q+ψ_2RQ±A_{Ed}+EHF_{Dir1+}	4.0	0.027	5 (Operating) $SEIS_{1.1}$-G+ψ_2Q+ψ_2RQ±A_{Ed}+EHF_{Dir2+}	4.6	0.033	✔ Pass	Details...
St. 12 (12)	W5	12	3 (Operating) $SEIS_{1.1}$-G+ψ_2Q+ψ_2RQ±A_{Ed}+EHF_{Dir1+}	4.8	0.031	5 (Operating) $SEIS_{1.1}$-G+ψ_2Q+ψ_2RQ±A_{Ed}+EHF_{Dir2+}	4.8	0.033	✔ Pass	Details...
St. 12 (12)	W6	12	3 (Operating) $SEIS_{1.1}$-G+ψ_2Q+ψ_2RQ±A_{Ed}+EHF_{Dir1+}	4.6	0.030	5 (Operating) $SEIS_{1.1}$-G+ψ_2Q+ψ_2RQ±A_{Ed}+EHF_{Dir2+}	4.8	0.033	✔ Pass	Details...
St. 13 (13)	W5	13	3 (Operating) $SEIS_{1.1}$-G+ψ_2Q+ψ_2RQ±A_{Ed}+EHF_{Dir1+}	5.0	0.031	5 (Operating) $SEIS_{1.1}$-G+ψ_2Q+ψ_2RQ±A_{Ed}+EHF_{Dir2+}	5.0	0.033	✔ Pass	Details...
St. 13 (13)	W6	13	3 (Operating) $SEIS_{1.1}$-G+ψ_2Q+ψ_2RQ±A_{Ed}+EHF_{Dir1+}	4.5	0.028	5 (Operating) $SEIS_{1.1}$-G+ψ_2Q+ψ_2RQ±A_{Ed}+EHF_{Dir2+}	5.0	0.033	✔ Pass	Details...
St. 14 (14)	C77	1	3 (Operating) $SEIS_{1.1}$-G+ψ_2Q+ψ_2RQ±A_{Ed}+EHF_{Dir1+}	5.2	0.032	5 (Operating) $SEIS_{1.1}$-G+ψ_2Q+ψ_2RQ±A_{Ed}+EHF_{Dir2+}	5.2	0.034	✔ Pass	Details...
St. 14 (14)	C53	1	3 (Operating) $SEIS_{1.1}$-G+ψ_2Q+ψ_2RQ±A_{Ed}+EHF_{Dir1+}	4.5	0.028	5 (Operating) $SEIS_{1.1}$-G+ψ_2Q+ψ_2RQ±A_{Ed}+EHF_{Dir2+}	5.2	0.034	✔ Pass	Details...
St. 15 (15)	W5	15	3 (Operating) $SEIS_{1.1}$-G+ψ_2Q+ψ_2RQ±A_{Ed}+EHF_{Dir1+}	5.3	0.031	5 (Operating) $SEIS_{1.1}$-G+ψ_2Q+ψ_2RQ±A_{Ed}+EHF_{Dir2+}	5.3	0.033	✔ Pass	Details...
St. 15 (15)	W6	15	3 (Operating) $SEIS_{1.1}$-G+ψ_2Q+ψ_2RQ±A_{Ed}+EHF_{Dir1+}	4.8	0.028	5 (Operating) $SEIS_{1.1}$-G+ψ_2Q+ψ_2RQ±A_{Ed}+EHF_{Dir2+}	5.4	0.034	✔ Pass	Details...
St. 16 (16)	W5	16	3 (Operating) $SEIS_{1.1}$-G+ψ_2Q+ψ_2RQ±A_{Ed}+EHF_{Dir1+}	5.4	0.031	5 (Operating) $SEIS_{1.1}$-G+ψ_2Q+ψ_2RQ±A_{Ed}+EHF_{Dir2+}	5.4	0.033	✔ Pass	Details...
St. 16 (16)	W6	16	3 (Operating) $SEIS_{1.1}$-G+ψ_2Q+ψ_2RQ±A_{Ed}+EHF_{Dir1+}	5.3	0.031	5 (Operating) $SEIS_{1.1}$-G+ψ_2Q+ψ_2RQ±A_{Ed}+EHF_{Dir2+}	5.5	0.033	✔ Pass	Details...
St. 17 (17)	W5	17	3 (Operating) $SEIS_{1.1}$-G+ψ_2Q+ψ_2RQ±A_{Ed}+EHF_{Dir1+}	5.4	0.030	5 (Operating) $SEIS_{1.1}$-G+ψ_2Q+ψ_2RQ±A_{Ed}+EHF_{Dir2+}	5.5	0.032	✔ Pass	Details...
St. 17 (17)	W6	17	3 (Operating) $SEIS_{1.1}$-G+ψ_2Q+ψ_2RQ±A_{Ed}+EHF_{Dir1+}	4.9	0.028	5 (Operating) $SEIS_{1.1}$-G+ψ_2Q+ψ_2RQ±A_{Ed}+EHF_{Dir2+}	5.6	0.033	✔ Pass	Details...
St. 18 (18)	W5	18	3 (Operating) $SEIS_{1.1}$-G+ψ_2Q+ψ_2RQ±A_{Ed}+EHF_{Dir1+}	5.5	0.030	5 (Operating) $SEIS_{1.1}$-G+ψ_2Q+ψ_2RQ±A_{Ed}+EHF_{Dir2+}	5.6	0.032	✔ Pass	Details...
St. 18 (18)	W6	18	3 (Operating) $SEIS_{1.1}$-G+ψ_2Q+ψ_2RQ±A_{Ed}+EHF_{Dir1+}	5.0	0.027	5 (Operating) $SEIS_{1.1}$-G+ψ_2Q+ψ_2RQ±A_{Ed}+EHF_{Dir2+}	5.7	0.032	✔ Pass	Details...
St. 19 (19)	W5	19	3 (Operating) $SEIS_{1.1}$-G+ψ_2Q+ψ_2RQ±A_{Ed}+EHF_{Dir1+}	5.4	0.029	5 (Operating) $SEIS_{1.1}$-G+ψ_2Q+ψ_2RQ±A_{Ed}+EHF_{Dir2+}	5.6	0.031	✔ Pass	Details...
St. 19 (19)	W6	19	3 (Operating) $SEIS_{1.1}$-G+ψ_2Q+ψ_2RQ±A_{Ed}+EHF_{Dir1+}	5.0	0.026	5 (Operating) $SEIS_{1.1}$-G+ψ_2Q+ψ_2RQ±A_{Ed}+EHF_{Dir2+}	5.6	0.031	✔ Pass	Details...

MODEL 8

Seismic Drift

Level ▲	Ref.	Stack	Combination Dir 1	Drift Dir 1 [mm]	$\theta_{Dir\,1}$	Combination Dir 2	Drift Dir 2 [mm]	$\theta_{Dir\,2}$	Status	Details
St. 1 (1)	W5	1	3 (Operating) $SEIS_{1.1}$-G+ψ_2Q+ψ_2RQ±A_{Ed}+EHF_{Dir1+}	0.7	0.008	5 (Operating) $SEIS_{1.3}$-G+ψ_2Q+ψ_2RQ±A_{Ed}+EHF_{Dir2+}	0.6	0.006	✔ Pass	Details...
St. 1 (1)	C5	1	3 (Operating) $SEIS_{1.1}$-G+ψ_2Q+ψ_2RQ±A_{Ed}+EHF_{Dir1+}	0.5	0.005	5 (Operating) $SEIS_{1.3}$-G+ψ_2Q+ψ_2RQ±A_{Ed}+EHF_{Dir2+}	0.6	0.006	✔ Pass	Details...
St. 2 (2)	W5	2	3 (Operating) $SEIS_{1.1}$-G+ψ_2Q+ψ_2RQ±A_{Ed}+EHF_{Dir1+}	1.5	0.014	5 (Operating) $SEIS_{1.3}$-G+ψ_2Q+ψ_2RQ±A_{Ed}+EHF_{Dir2+}	1.2	0.012	✔ Pass	Details...
St. 2 (2)	W6	2	3 (Operating) $SEIS_{1.1}$-G+ψ_2Q+ψ_2RQ±A_{Ed}+EHF_{Dir1+}	1.2	0.011	5 (Operating) $SEIS_{1.3}$-G+ψ_2Q+ψ_2RQ±A_{Ed}+EHF_{Dir2+}	1.3	0.013	✔ Pass	Details...
St. 3 (3)	W5	3	3 (Operating) $SEIS_{1.1}$-G+ψ_2Q+ψ_2RQ±A_{Ed}+EHF_{Dir1+}	2.0	0.019	5 (Operating) $SEIS_{1.3}$-G+ψ_2Q+ψ_2RQ±A_{Ed}+EHF_{Dir2+}	1.8	0.017	✔ Pass	Details...
St. 3 (3)	W6	3	3 (Operating) $SEIS_{1.1}$-G+ψ_2Q+ψ_2RQ±A_{Ed}+EHF_{Dir1+}	1.7	0.016	5 (Operating) $SEIS_{1.3}$-G+ψ_2Q+ψ_2RQ±A_{Ed}+EHF_{Dir2+}	1.8	0.018	✔ Pass	Details...
St. 4 (4)	W5	4	3 (Operating) $SEIS_{1.1}$-G+ψ_2Q+ψ_2RQ±A_{Ed}+EHF_{Dir1+}	2.5	0.022	5 (Operating) $SEIS_{1.3}$-G+ψ_2Q+ψ_2RQ±A_{Ed}+EHF_{Dir2+}	2.3	0.021	✔ Pass	Details...
St. 4 (4)	W6	4	3 (Operating) $SEIS_{1.1}$-G+ψ_2Q+ψ_2RQ±A_{Ed}+EHF_{Dir1+}	2.0	0.018	5 (Operating) $SEIS_{1.3}$-G+ψ_2Q+ψ_2RQ±A_{Ed}+EHF_{Dir2+}	2.3	0.022	✔ Pass	Details...
St. 5 (5)	W5	5	3 (Operating) $SEIS_{1.1}$-G+ψ_2Q+ψ_2RQ±A_{Ed}+EHF_{Dir1+}	2.9	0.025	5 (Operating) $SEIS_{1.3}$-G+ψ_2Q+ψ_2RQ±A_{Ed}+EHF_{Dir2+}	2.7	0.024	✔ Pass	Details...
St. 5 (5)	W6	5	3 (Operating) $SEIS_{1.1}$-G+ψ_2Q+ψ_2RQ±A_{Ed}+EHF_{Dir1+}	2.6	0.022	5 (Operating) $SEIS_{1.3}$-G+ψ_2Q+ψ_2RQ±A_{Ed}+EHF_{Dir2+}	2.8	0.024	✔ Pass	Details...
St. 6 (6)	W5	6	3 (Operating) $SEIS_{1.1}$-G+ψ_2Q+ψ_2RQ±A_{Ed}+EHF_{Dir1+}	3.3	0.027	5 (Operating) $SEIS_{1.3}$-G+ψ_2Q+ψ_2RQ±A_{Ed}+EHF_{Dir2+}	3.0	0.026	✔ Pass	Details...
St. 6 (6)	W6	6	3 (Operating) $SEIS_{1.1}$-G+ψ_2Q+ψ_2RQ±A_{Ed}+EHF_{Dir1+}	2.8	0.023	5 (Operating) $SEIS_{1.3}$-G+ψ_2Q+ψ_2RQ±A_{Ed}+EHF_{Dir2+}	3.1	0.026	✔ Pass	Details...
St. 7 (7)	W5	7	3 (Operating) $SEIS_{1.1}$-G+ψ_2Q+ψ_2RQ±A_{Ed}+EHF_{Dir1+}	3.6	0.028	5 (Operating) $SEIS_{1.3}$-G+ψ_2Q+ψ_2RQ±A_{Ed}+EHF_{Dir2+}	3.4	0.027	✔ Pass	Details...
St. 7 (7)	W6	7	3 (Operating) $SEIS_{1.1}$-G+ψ_2Q+ψ_2RQ±A_{Ed}+EHF_{Dir1+}	3.1	0.024	5 (Operating) $SEIS_{1.3}$-G+ψ_2Q+ψ_2RQ±A_{Ed}+EHF_{Dir2+}	3.4	0.028	✔ Pass	Details...
St. 8 (8)	C48	1	3 (Operating) $SEIS_{1.1}$-G+ψ_2Q+ψ_2RQ±A_{Ed}+EHF_{Dir1+}	3.9	0.029	5 (Operating) $SEIS_{1.3}$-G+ψ_2Q+ψ_2RQ±A_{Ed}+EHF_{Dir2+}	3.8	0.030	✔ Pass	Details...
St. 8 (8)	C26	1	3 (Operating) $SEIS_{1.1}$-G+ψ_2Q+ψ_2RQ±A_{Ed}+EHF_{Dir1+}	3.3	0.025	5 (Operating) $SEIS_{1.3}$-G+ψ_2Q+ψ_2RQ±A_{Ed}+EHF_{Dir2+}	3.8	0.030	✔ Pass	Details...
St. 9 (9)	W5	9	3 (Operating) $SEIS_{1.1}$-G+ψ_2Q+ψ_2RQ±A_{Ed}+EHF_{Dir1+}	4.2	0.030	5 (Operating) $SEIS_{1.3}$-G+ψ_2Q+ψ_2RQ±A_{Ed}+EHF_{Dir2+}	4.0	0.030	✔ Pass	Details...
St. 9 (9)	W6	9	3 (Operating) $SEIS_{1.1}$-G+ψ_2Q+ψ_2RQ±A_{Ed}+EHF_{Dir1+}	3.5	0.025	5 (Operating) $SEIS_{1.3}$-G+ψ_2Q+ψ_2RQ±A_{Ed}+EHF_{Dir2+}	4.1	0.031	✔ Pass	Details...
St. 10 (10)	W5	10	3 (Operating) $SEIS_{1.1}$-G+ψ_2Q+ψ_2RQ±A_{Ed}+EHF_{Dir1+}	4.4	0.031	5 (Operating) $SEIS_{1.3}$-G+ψ_2Q+ψ_2RQ±A_{Ed}+EHF_{Dir2+}	4.3	0.031	✔ Pass	Details...
St. 10 (10)	W6	10	3 (Operating) $SEIS_{1.1}$-G+ψ_2Q+ψ_2RQ±A_{Ed}+EHF_{Dir1+}	4.2	0.029	5 (Operating) $SEIS_{1.3}$-G+ψ_2Q+ψ_2RQ±A_{Ed}+EHF_{Dir2+}	4.4	0.032	✔ Pass	Details...
St. 11 (11)	W5	11	3 (Operating) $SEIS_{1.1}$-G+ψ_2Q+ψ_2RQ±A_{Ed}+EHF_{Dir1+}	4.7	0.031	5 (Operating) $SEIS_{1.3}$-G+ψ_2Q+ψ_2RQ±A_{Ed}+EHF_{Dir2+}	4.5	0.032	✔ Pass	Details...
St. 11 (11)	W6	11	3 (Operating) $SEIS_{1.1}$-G+ψ_2Q+ψ_2RQ±A_{Ed}+EHF_{Dir1+}	4.0	0.027	5 (Operating) $SEIS_{1.3}$-G+ψ_2Q+ψ_2RQ±A_{Ed}+EHF_{Dir2+}	4.6	0.033	✔ Pass	Details...
St. 12 (12)	W5	12	3 (Operating) $SEIS_{1.1}$-G+ψ_2Q+ψ_2RQ±A_{Ed}+EHF_{Dir1+}	4.8	0.032	5 (Operating) $SEIS_{1.3}$-G+ψ_2Q+ψ_2RQ±A_{Ed}+EHF_{Dir2+}	4.8	0.033	✔ Pass	Details...
St. 12 (12)	W6	12	3 (Operating) $SEIS_{1.1}$-G+ψ_2Q+ψ_2RQ±A_{Ed}+EHF_{Dir1+}	4.3	0.028	5 (Operating) $SEIS_{1.3}$-G+ψ_2Q+ψ_2RQ±A_{Ed}+EHF_{Dir2+}	4.8	0.033	✔ Pass	Details...
St. 13 (13)	W5	13	3 (Operating) $SEIS_{1.1}$-G+ψ_2Q+ψ_2RQ±A_{Ed}+EHF_{Dir1+}	5.0	0.032	5 (Operating) $SEIS_{1.3}$-G+ψ_2Q+ψ_2RQ±A_{Ed}+EHF_{Dir2+}	5.0	0.033	✔ Pass	Details...
St. 13 (13)	W6	13	3 (Operating) $SEIS_{1.1}$-G+ψ_2Q+ψ_2RQ±A_{Ed}+EHF_{Dir1+}	4.8	0.031	5 (Operating) $SEIS_{1.3}$-G+ψ_2Q+ψ_2RQ±A_{Ed}+EHF_{Dir2+}	5.0	0.033	✔ Pass	Details...
St. 14 (14)	C77	1	3 (Operating) $SEIS_{1.1}$-G+ψ_2Q+ψ_2RQ±A_{Ed}+EHF_{Dir1+}	5.2	0.032	5 (Operating) $SEIS_{1.3}$-G+ψ_2Q+ψ_2RQ±A_{Ed}+EHF_{Dir2+}	5.2	0.034	✔ Pass	Details...
St. 14 (14)	C53	1	3 (Operating) $SEIS_{1.1}$-G+ψ_2Q+ψ_2RQ±A_{Ed}+EHF_{Dir1+}	4.5	0.028	5 (Operating) $SEIS_{1.3}$-G+ψ_2Q+ψ_2RQ±A_{Ed}+EHF_{Dir2+}	5.2	0.034	✔ Pass	Details...
St. 15 (15)	W5	15	3 (Operating) $SEIS_{1.1}$-G+ψ_2Q+ψ_2RQ±A_{Ed}+EHF_{Dir1+}	5.3	0.032	5 (Operating) $SEIS_{1.3}$-G+ψ_2Q+ψ_2RQ±A_{Ed}+EHF_{Dir2+}	5.3	0.033	✔ Pass	Details...
St. 15 (15)	W6	15	3 (Operating) $SEIS_{1.1}$-G+ψ_2Q+ψ_2RQ±A_{Ed}+EHF_{Dir1+}	4.8	0.029	5 (Operating) $SEIS_{1.3}$-G+ψ_2Q+ψ_2RQ±A_{Ed}+EHF_{Dir2+}	5.4	0.034	✔ Pass	Details...
St. 16 (16)	W5	16	3 (Operating) $SEIS_{1.1}$-G+ψ_2Q+ψ_2RQ±A_{Ed}+EHF_{Dir1+}	5.4	0.031	5 (Operating) $SEIS_{1.3}$-G+ψ_2Q+ψ_2RQ±A_{Ed}+EHF_{Dir2+}	5.4	0.033	✔ Pass	Details...
St. 16 (16)	W6	16	3 (Operating) $SEIS_{1.1}$-G+ψ_2Q+ψ_2RQ±A_{Ed}+EHF_{Dir1+}	4.9	0.028	5 (Operating) $SEIS_{1.3}$-G+ψ_2Q+ψ_2RQ±A_{Ed}+EHF_{Dir2+}	5.5	0.033	✔ Pass	Details...
St. 17 (17)	W5	17	3 (Operating) $SEIS_{1.1}$-G+ψ_2Q+ψ_2RQ±A_{Ed}+EHF_{Dir1+}	5.4	0.031	5 (Operating) $SEIS_{1.3}$-G+ψ_2Q+ψ_2RQ±A_{Ed}+EHF_{Dir2+}	5.5	0.032	✔ Pass	Details...
St. 17 (17)	W6	17	3 (Operating) $SEIS_{1.1}$-G+ψ_2Q+ψ_2RQ±A_{Ed}+EHF_{Dir1+}	5.0	0.028	5 (Operating) $SEIS_{1.3}$-G+ψ_2Q+ψ_2RQ±A_{Ed}+EHF_{Dir2+}	5.6	0.033	✔ Pass	Details...
St. 18 (18)	W5	18	3 (Operating) $SEIS_{1.1}$-G+ψ_2Q+ψ_2RQ±A_{Ed}+EHF_{Dir1+}	5.5	0.030	5 (Operating) $SEIS_{1.3}$-G+ψ_2Q+ψ_2RQ±A_{Ed}+EHF_{Dir2+}	5.6	0.032	✔ Pass	Details...
St. 18 (18)	W6	18	3 (Operating) $SEIS_{1.1}$-G+ψ_2Q+ψ_2RQ±A_{Ed}+EHF_{Dir1+}	4.9	0.027	5 (Operating) $SEIS_{1.3}$-G+ψ_2Q+ψ_2RQ±A_{Ed}+EHF_{Dir2+}	5.6	0.032	✔ Pass	Details...
St. 19 (19)	W6	19	3 (Operating) $SEIS_{1.1}$-G+ψ_2Q+ψ_2RQ±A_{Ed}+EHF_{Dir1+}	5.5	0.029	5 (Operating) $SEIS_{1.3}$-G+ψ_2Q+ψ_2RQ±A_{Ed}+EHF_{Dir2+}	5.6	0.031	✔ Pass	Details...
St. 20 (roof)	W5	20	3 (Operating) $SEIS_{1.1}$-G+ψ_2Q+ψ_2RQ±A_{Ed}+EHF_{Dir1+}	5.4	0.028	5 (Operating) $SEIS_{1.3}$-G+ψ_2Q+ψ_2RQ±A_{Ed}+EHF_{Dir2+}	5.5	0.030	✔ Pass	Details...

MODEL9

Level ▲	Ref.	Stack	Combination Dir 1	Drift Dir 1 [mm]	$\theta_{Dir\,1}$	Combination Dir 2	Drift Dir 2 [mm]	$\theta_{Dir\,2}$	Status	Details
St. 1 (1)	C23	1	5 (Operating) $SEIS_{1.3}$-G+ψ_2Q+ψ_2RQ±A_{Ec}+EHF_{Dir2+}	2.8	0.033	5 (Operating) $SEIS_{1.3}$-G+ψ_2Q+ψ_2RQ±A_{Ec}+EHF_{Dir2+}	1.9	0.022	✔ Pass	Details...
St. 1 (1)	C1	1	5 (Operating) $SEIS_{1.3}$-G+ψ_2Q+ψ_2RQ±A_{Ec}+EHF_{Dir2+}	2.0	0.024	5 (Operating) $SEIS_{1.3}$-G+ψ_2Q+ψ_2RQ±A_{Ec}+EHF_{Dir2+}	1.9	0.022	✔ Pass	Details...
St. 2 (2)	C23	2	5 (Operating) $SEIS_{1.3}$-G+ψ_2Q+ψ_2RQ±A_{Ec}+EHF_{Dir2+}	3.0	0.033	5 (Operating) $SEIS_{1.3}$-G+ψ_2Q+ψ_2RQ±A_{Ec}+EHF_{Dir2+}	2.2	0.023	✔ Pass	Details...
St. 2 (2)	C1	2	5 (Operating) $SEIS_{1.3}$-G+ψ_2Q+ψ_2RQ±A_{Ec}+EHF_{Dir2+}	2.3	0.026	5 (Operating) $SEIS_{1.3}$-G+ψ_2Q+ψ_2RQ±A_{Ec}+EHF_{Dir2+}	2.2	0.023	✔ Pass	Details...
St. 3 (3)	C23	3	5 (Operating) $SEIS_{1.3}$-G+ψ_2Q+ψ_2RQ±A_{Ec}+EHF_{Dir2+}	3.2	0.033	5 (Operating) $SEIS_{1.3}$-G+ψ_2Q+ψ_2RQ±A_{Ec}+EHF_{Dir2+}	2.4	0.025	✔ Pass	Details...
St. 3 (3)	C1	3	5 (Operating) $SEIS_{1.3}$-G+ψ_2Q+ψ_2RQ±A_{Ec}+EHF_{Dir2+}	2.6	0.027	5 (Operating) $SEIS_{1.3}$-G+ψ_2Q+ψ_2RQ±A_{Ec}+EHF_{Dir2+}	2.4	0.025	✔ Pass	Details...
St. 4 (4)	C23	4	5 (Operating) $SEIS_{1.3}$-G+ψ_2Q+ψ_2RQ±A_{Ec}+EHF_{Dir2+}	3.2	0.033	5 (Operating) $SEIS_{1.3}$-G+ψ_2Q+ψ_2RQ±A_{Ec}+EHF_{Dir2+}	2.5	0.025	✔ Pass	Details...
St. 4 (4)	C11	4	3 (Operating) $SEIS_{1.1}$-G+ψ_2Q+ψ_2RQ±A_{Ec}+EHF_{Dir1+}	1.7	0.017	5 (Operating) $SEIS_{1.3}$-G+ψ_2Q+ψ_2RQ±A_{Ec}+EHF_{Dir2+}	2.5	0.025	✔ Pass	Details...
St. 5 (5)	C23	5	3 (Operating) $SEIS_{1.1}$-G+ψ_2Q+ψ_2RQ±A_{Ec}+EHF_{Dir1+}	3.3	0.032	5 (Operating) $SEIS_{1.3}$-G+ψ_2Q+ψ_2RQ±A_{Ec}+EHF_{Dir2+}	2.7	0.025	✔ Pass	Details...
St. 5 (5)	C1	5	5 (Operating) $SEIS_{1.3}$-G+ψ_2Q+ψ_2RQ±A_{Ec}+EHF_{Dir2+}	2.9	0.028	5 (Operating) $SEIS_{1.3}$-G+ψ_2Q+ψ_2RQ±A_{Ec}+EHF_{Dir2+}	2.7	0.025	✔ Pass	Details...
St. 6 (6)	C23	6	3 (Operating) $SEIS_{1.1}$-G+ψ_2Q+ψ_2RQ±A_{Ec}+EHF_{Dir1+}	3.5	0.032	5 (Operating) $SEIS_{1.3}$-G+ψ_2Q+ψ_2RQ±A_{Ec}+EHF_{Dir2+}	2.8	0.025	✔ Pass	Details...
St. 6 (6)	C20	6	3 (Operating) $SEIS_{1.1}$-G+ψ_2Q+ψ_2RQ±A_{Ec}+EHF_{Dir1+}	3.0	0.028	5 (Operating) $SEIS_{1.3}$-G+ψ_2Q+ψ_2RQ±A_{Ec}+EHF_{Dir2+}	2.8	0.025	✔ Pass	Details...
St. 7 (7)	C23	7	3 (Operating) $SEIS_{1.1}$-G+ψ_2Q+ψ_2RQ±A_{Ec}+EHF_{Dir1+}	3.7	0.032	5 (Operating) $SEIS_{1.3}$-G+ψ_2Q+ψ_2RQ±A_{Ec}+EHF_{Dir2+}	2.9	0.025	✔ Pass	Details...
St. 7 (7)	C11	7	3 (Operating) $SEIS_{1.1}$-G+ψ_2Q+ψ_2RQ±A_{Ec}+EHF_{Dir1+}	2.5	0.022	5 (Operating) $SEIS_{1.3}$-G+ψ_2Q+ψ_2RQ±A_{Ec}+EHF_{Dir2+}	2.9	0.025	✔ Pass	Details...
St. 8 (8)	C48	1	3 (Operating) $SEIS_{1.1}$-G+ψ_2Q+ψ_2RQ±A_{Ec}+EHF_{Dir1+}	4.1	0.035	5 (Operating) $SEIS_{1.3}$-G+ψ_2Q+ψ_2RQ±A_{Ec}+EHF_{Dir2+}	3.2	0.027	✔ Pass	Details...
St. 8 (8)	C45	1	3 (Operating) $SEIS_{1.1}$-G+ψ_2Q+ψ_2RQ±A_{Ec}+EHF_{Dir1+}	3.5	0.030	5 (Operating) $SEIS_{1.3}$-G+ψ_2Q+ψ_2RQ±A_{Ec}+EHF_{Dir2+}	3.2	0.027	✔ Pass	Details...
St. 9 (9)	C48	2	3 (Operating) $SEIS_{1.1}$-G+ψ_2Q+ψ_2RQ±A_{Ec}+EHF_{Dir1+}	4.2	0.035	5 (Operating) $SEIS_{1.3}$-G+ψ_2Q+ψ_2RQ±A_{Ec}+EHF_{Dir2+}	3.3	0.027	✔ Pass	Details...
St. 9 (9)	C26	2	5 (Operating) $SEIS_{1.3}$-G+ψ_2Q+ψ_2RQ±A_{Ec}+EHF_{Dir2+}	3.7	0.030	5 (Operating) $SEIS_{1.3}$-G+ψ_2Q+ψ_2RQ±A_{Ec}+EHF_{Dir2+}	3.3	0.027	✔ Pass	Details...
St. 10 (10)	C48	3	3 (Operating) $SEIS_{1.1}$-G+ψ_2Q+ψ_2RQ±A_{Ec}+EHF_{Dir1+}	4.3	0.034	5 (Operating) $SEIS_{1.3}$-G+ψ_2Q+ψ_2RQ±A_{Ec}+EHF_{Dir2+}	3.3	0.026	✔ Pass	Details...
St. 10 (10)	C26	3	3 (Operating) $SEIS_{1.1}$-G+ψ_2Q+ψ_2RQ±A_{Ec}+EHF_{Dir1+}	3.8	0.030	5 (Operating) $SEIS_{1.3}$-G+ψ_2Q+ψ_2RQ±A_{Ec}+EHF_{Dir2+}	3.3	0.026	✔ Pass	Details...
St. 11 (11)	C48	4	3 (Operating) $SEIS_{1.1}$-G+ψ_2Q+ψ_2RQ±A_{Ec}+EHF_{Dir1+}	4.4	0.034	5 (Operating) $SEIS_{1.3}$-G+ψ_2Q+ψ_2RQ±A_{Ec}+EHF_{Dir2+}	3.3	0.025	✔ Pass	Details...
St. 11 (11)	C45	4	3 (Operating) $SEIS_{1.1}$-G+ψ_2Q+ψ_2RQ±A_{Ec}+EHF_{Dir1+}	4.0	0.031	5 (Operating) $SEIS_{1.3}$-G+ψ_2Q+ψ_2RQ±A_{Ec}+EHF_{Dir2+}	3.3	0.025	✔ Pass	Details...
St. 12 (12)	C48	5	3 (Operating) $SEIS_{1.1}$-G+ψ_2Q+ψ_2RQ±A_{Ec}+EHF_{Dir1+}	4.5	0.033	3 (Operating) $SEIS_{1.1}$-G+ψ_2Q+ψ_2RQ±A_{Ec}+EHF_{Dir1+}	3.3	0.025	✔ Pass	Details...
St. 12 (12)	C36	5	3 (Operating) $SEIS_{1.1}$-G+ψ_2Q+ψ_2RQ±A_{Ec}+EHF_{Dir1+}	3.6	0.027	3 (Operating) $SEIS_{1.1}$-G+ψ_2Q+ψ_2RQ±A_{Ec}+EHF_{Dir1+}	3.3	0.025	✔ Pass	Details...
St. 13 (13)	C48	6	3 (Operating) $SEIS_{1.1}$-G+ψ_2Q+ψ_2RQ±A_{Ec}+EHF_{Dir1+}	4.5	0.032	3 (Operating) $SEIS_{1.1}$-G+ψ_2Q+ψ_2RQ±A_{Ec}+EHF_{Dir1+}	3.4	0.024	✔ Pass	Details...
St. 13 (13)	C45	6	3 (Operating) $SEIS_{1.1}$-G+ψ_2Q+ψ_2RQ±A_{Ec}+EHF_{Dir1+}	4.2	0.030	3 (Operating) $SEIS_{1.1}$-G+ψ_2Q+ψ_2RQ±A_{Ec}+EHF_{Dir1+}	3.4	0.024	✔ Pass	Details...
St. 14 (14)	C77	1	3 (Operating) $SEIS_{1.1}$-G+ψ_2Q+ψ_2RQ±A_{Ec}+EHF_{Dir1+}	4.7	0.033	5 (Operating) $SEIS_{1.3}$-G+ψ_2Q+ψ_2RQ±A_{Ec}+EHF_{Dir2+}	3.6	0.024	✔ Pass	Details...
St. 14 (14)	C53	1	3 (Operating) $SEIS_{1.1}$-G+ψ_2Q+ψ_2RQ±A_{Ec}+EHF_{Dir1+}	4.4	0.031	5 (Operating) $SEIS_{1.3}$-G+ψ_2Q+ψ_2RQ±A_{Ec}+EHF_{Dir2+}	3.6	0.024	✔ Pass	Details...
St. 15 (15)	W6	15	3 (Operating) $SEIS_{1.1}$-G+ψ_2Q+ψ_2RQ±A_{Ec}+EHF_{Dir1+}	5.2	0.035	3 (Operating) $SEIS_{1.1}$-G+ψ_2Q+ψ_2RQ±A_{Ec}+EHF_{Dir1+}	2.8	0.019	✔ Pass	Details...
St. 15 (15)	W8	15	3 (Operating) $SEIS_{1.1}$-G+ψ_2Q+ψ_2RQ±A_{Ec}+EHF_{Dir1+}	4.0	0.027	3 (Operating) $SEIS_{1.1}$-G+ψ_2Q+ψ_2RQ±A_{Ec}+EHF_{Dir1+}	3.8	0.025	✔ Pass	Details...
St. 16 (16)	C77	3	3 (Operating) $SEIS_{1.1}$-G+ψ_2Q+ψ_2RQ±A_{Ec}+EHF_{Dir1+}	4.7	0.031	5 (Operating) $SEIS_{1.3}$-G+ψ_2Q+ψ_2RQ±A_{Ec}+EHF_{Dir2+}	3.5	0.023	✔ Pass	Details...
St. 16 (16)	C58	3	3 (Operating) $SEIS_{1.1}$-G+ψ_2Q+ψ_2RQ±A_{Ec}+EHF_{Dir1+}	4.2	0.028	5 (Operating) $SEIS_{1.3}$-G+ψ_2Q+ψ_2RQ±A_{Ec}+EHF_{Dir2+}	3.5	0.023	✔ Pass	Details...
St. 17 (17)	C77	4	3 (Operating) $SEIS_{1.1}$-G+ψ_2Q+ψ_2RQ±A_{Ec}+EHF_{Dir1+}	4.6	0.029	5 (Operating) $SEIS_{1.3}$-G+ψ_2Q+ψ_2RQ±A_{Ec}+EHF_{Dir2+}	3.4	0.021	✔ Pass	Details...
St. 17 (17)	C58	4	3 (Operating) $SEIS_{1.1}$-G+ψ_2Q+ψ_2RQ±A_{Ec}+EHF_{Dir1+}	4.3	0.027	5 (Operating) $SEIS_{1.3}$-G+ψ_2Q+ψ_2RQ±A_{Ec}+EHF_{Dir2+}	3.4	0.021	✔ Pass	Details...
St. 18 (18)	C77	5	3 (Operating) $SEIS_{1.1}$-G+ψ_2Q+ψ_2RQ±A_{Ec}+EHF_{Dir1+}	4.6	0.029	5 (Operating) $SEIS_{1.3}$-G+ψ_2Q+ψ_2RQ±A_{Ec}+EHF_{Dir2+}	3.4	0.021	✔ Pass	Details...
St. 18 (18)	C53	5	3 (Operating) $SEIS_{1.1}$-G+ψ_2Q+ψ_2RQ±A_{Ec}+EHF_{Dir1+}	4.5	0.028	5 (Operating) $SEIS_{1.3}$-G+ψ_2Q+ψ_2RQ±A_{Ec}+EHF_{Dir2+}	3.4	0.021	✔ Pass	Details...
St. 19 (19)	C77	6	3 (Operating) $SEIS_{1.1}$-G+ψ_2Q+ψ_2RQ±A_{Ec}+EHF_{Dir1+}	4.4	0.027	5 (Operating) $SEIS_{1.3}$-G+ψ_2Q+ψ_2RQ±A_{Ec}+EHF_{Dir2+}	3.2	0.019	✔ Pass	Details...
St. 19 (19)	C58	6	3 (Operating) $SEIS_{1.1}$-G+ψ_2Q+ψ_2RQ±A_{Ec}+EHF_{Dir1+}	4.2	0.026	5 (Operating) $SEIS_{1.3}$-G+ψ_2Q+ψ_2RQ±A_{Ec}+EHF_{Dir2+}	3.2	0.019	✔ Pass	Details...

MODEL10

Level ▲	Ref.	Stack	Combination Dir 1	Drift Dir 1 [mm]	θ_{Dir1}	Combination Dir 2	Drift Dir 2 [mm]	θ_{Dir2}	Status	Details
St. 2 (2)	C1	2	5 (Operating) $SEIS_{1.3}$·G+ψ_2Q+ψ_2RQ±A_{Ed}+EHF_{Dir2+}	2.4	0.027	5 (Operating) $SEIS_{1.3}$·G+ψ_2Q+ψ_2RQ±A_{Ed}+EHF_{Dir2+}	2.2	0.023	✔ Pass	Details...
St. 3 (3)	C23	3	5 (Operating) $SEIS_{1.3}$·G+ψ_2Q+ψ_2RQ±A_{Ed}+EHF_{Dir2+}	3.4	0.036	5 (Operating) $SEIS_{1.3}$·G+ψ_2Q+ψ_2RQ±A_{Ed}+EHF_{Dir2+}	2.4	0.024	✔ Pass	Details...
St. 3 (3)	C11	3	3 (Operating) $SEIS_{1.1}$·G+ψ_2Q+ψ_2RQ±A_{Ed}+EHF_{Dir1+}	1.4	0.014	5 (Operating) $SEIS_{1.3}$·G+ψ_2Q+ψ_2RQ±A_{Ed}+EHF_{Dir2+}	2.4	0.024	✔ Pass	Details...
St. 4 (4)	C23	4	5 (Operating) $SEIS_{1.3}$·G+ψ_2Q+ψ_2RQ±A_{Ed}+EHF_{Dir2+}	3.5	0.035	5 (Operating) $SEIS_{1.3}$·G+ψ_2Q+ψ_2RQ±A_{Ed}+EHF_{Dir2+}	2.5	0.024	✔ Pass	Details...
St. 4 (4)	C1	4	5 (Operating) $SEIS_{1.3}$·G+ψ_2Q+ψ_2RQ±A_{Ed}+EHF_{Dir2+}	2.8	0.028	5 (Operating) $SEIS_{1.3}$·G+ψ_2Q+ψ_2RQ±A_{Ed}+EHF_{Dir2+}	2.5	0.024	✔ Pass	Details...
St. 5 (5)	C23	5	5 (Operating) $SEIS_{1.3}$·G+ψ_2Q+ψ_2RQ±A_{Ed}+EHF_{Dir2+}	3.6	0.034	5 (Operating) $SEIS_{1.3}$·G+ψ_2Q+ψ_2RQ±A_{Ed}+EHF_{Dir2+}	2.6	0.024	✔ Pass	Details...
St. 5 (5)	C1	5	5 (Operating) $SEIS_{1.3}$·G+ψ_2Q+ψ_2RQ±A_{Ed}+EHF_{Dir2+}	3.0	0.029	5 (Operating) $SEIS_{1.3}$·G+ψ_2Q+ψ_2RQ±A_{Ed}+EHF_{Dir2+}	2.6	0.024	✔ Pass	Details...
St. 6 (6)	C23	6	3 (Operating) $SEIS_{1.1}$·G+ψ_2Q+ψ_2RQ±A_{Ed}+EHF_{Dir1+}	3.7	0.034	5 (Operating) $SEIS_{1.3}$·G+ψ_2Q+ψ_2RQ±A_{Ed}+EHF_{Dir2+}	2.7	0.024	✔ Pass	Details...
St. 6 (6)	C11	6	3 (Operating) $SEIS_{1.1}$·G+ψ_2Q+ψ_2RQ±A_{Ed}+EHF_{Dir1+}	2.3	0.021	5 (Operating) $SEIS_{1.3}$·G+ψ_2Q+ψ_2RQ±A_{Ed}+EHF_{Dir2+}	2.7	0.024	✔ Pass	Details...
St. 7 (7)	C23	7	3 (Operating) $SEIS_{1.1}$·G+ψ_2Q+ψ_2RQ±A_{Ed}+EHF_{Dir1+}	3.8	0.034	5 (Operating) $SEIS_{1.3}$·G+ψ_2Q+ψ_2RQ±A_{Ed}+EHF_{Dir2+}	2.8	0.024	✔ Pass	Details...
St. 7 (7)	C1	7	5 (Operating) $SEIS_{1.3}$·G+ψ_2Q+ψ_2RQ±A_{Ed}+EHF_{Dir2+}	3.3	0.029	5 (Operating) $SEIS_{1.3}$·G+ψ_2Q+ψ_2RQ±A_{Ed}+EHF_{Dir2+}	2.8	0.024	✔ Pass	Details...
St. 8 (8)	C48	1	3 (Operating) $SEIS_{1.1}$·G+ψ_2Q+ψ_2RQ±A_{Ed}+EHF_{Dir1+}	4.3	0.036	5 (Operating) $SEIS_{1.3}$·G+ψ_2Q+ψ_2RQ±A_{Ed}+EHF_{Dir2+}	3.1	0.025	✔ Pass	Details...
St. 8 (8)	C26	1	5 (Operating) $SEIS_{1.3}$·G+ψ_2Q+ψ_2RQ±A_{Ed}+EHF_{Dir2+}	3.6	0.031	5 (Operating) $SEIS_{1.3}$·G+ψ_2Q+ψ_2RQ±A_{Ed}+EHF_{Dir2+}	3.1	0.025	✔ Pass	Details...
St. 9 (9)	C48	2	3 (Operating) $SEIS_{1.1}$·G+ψ_2Q+ψ_2RQ±A_{Ed}+EHF_{Dir1+}	4.4	0.036	5 (Operating) $SEIS_{1.3}$·G+ψ_2Q+ψ_2RQ±A_{Ed}+EHF_{Dir2+}	3.1	0.025	✔ Pass	Details...
St. 9 (9)	C45	2	3 (Operating) $SEIS_{1.1}$·G+ψ_2Q+ψ_2RQ±A_{Ed}+EHF_{Dir1+}	3.8	0.031	5 (Operating) $SEIS_{1.3}$·G+ψ_2Q+ψ_2RQ±A_{Ed}+EHF_{Dir2+}	3.1	0.025	✔ Pass	Details...
St. 10 (10)	C48	3	3 (Operating) $SEIS_{1.1}$·G+ψ_2Q+ψ_2RQ±A_{Ed}+EHF_{Dir1+}	4.5	0.035	3 (Operating) $SEIS_{1.1}$·G+ψ_2Q+ψ_2RQ±A_{Ed}+EHF_{Dir1+}	3.1	0.024	✔ Pass	Details...
St. 10 (10)	C36	3	3 (Operating) $SEIS_{1.1}$·G+ψ_2Q+ψ_2RQ±A_{Ed}+EHF_{Dir1+}	3.2	0.025	3 (Operating) $SEIS_{1.1}$·G+ψ_2Q+ψ_2RQ±A_{Ed}+EHF_{Dir1+}	3.1	0.024	✔ Pass	Details...
St. 11 (11)	C48	4	3 (Operating) $SEIS_{1.1}$·G+ψ_2Q+ψ_2RQ±A_{Ed}+EHF_{Dir1+}	4.5	0.035	3 (Operating) $SEIS_{1.1}$·G+ψ_2Q+ψ_2RQ±A_{Ed}+EHF_{Dir1+}	3.2	0.024	✔ Pass	Details...
St. 11 (11)	C26	4	3 (Operating) $SEIS_{1.1}$·G+ψ_2Q+ψ_2RQ±A_{Ed}+EHF_{Dir1+}	3.9	0.030	3 (Operating) $SEIS_{1.1}$·G+ψ_2Q+ψ_2RQ±A_{Ed}+EHF_{Dir1+}	3.2	0.024	✔ Pass	Details...
St. 12 (12)	C48	5	3 (Operating) $SEIS_{1.1}$·G+ψ_2Q+ψ_2RQ±A_{Ed}+EHF_{Dir1+}	4.6	0.034	3 (Operating) $SEIS_{1.1}$·G+ψ_2Q+ψ_2RQ±A_{Ed}+EHF_{Dir1+}	3.2	0.023	✔ Pass	Details...
St. 12 (12)	C45	5	3 (Operating) $SEIS_{1.1}$·G+ψ_2Q+ψ_2RQ±A_{Ed}+EHF_{Dir1+}	4.1	0.030	3 (Operating) $SEIS_{1.1}$·G+ψ_2Q+ψ_2RQ±A_{Ed}+EHF_{Dir1+}	3.2	0.023	✔ Pass	Details...
St. 13 (13)	W6	13	3 (Operating) $SEIS_{1.1}$·G+ψ_2Q+ψ_2RQ±A_{Ed}+EHF_{Dir1+}	5.1	0.036	3 (Operating) $SEIS_{1.1}$·G+ψ_2Q+ψ_2RQ±A_{Ed}+EHF_{Dir1+}	2.5	0.017	✔ Pass	Details...
St. 13 (13)	W8	13	3 (Operating) $SEIS_{1.1}$·G+ψ_2Q+ψ_2RQ±A_{Ed}+EHF_{Dir1+}	3.7	0.026	3 (Operating) $SEIS_{1.1}$·G+ψ_2Q+ψ_2RQ±A_{Ed}+EHF_{Dir1+}	3.3	0.023	✔ Pass	Details...
St. 14 (14)	C77	1	3 (Operating) $SEIS_{1.1}$·G+ψ_2Q+ψ_2RQ±A_{Ed}+EHF_{Dir1+}	4.8	0.033	3 (Operating) $SEIS_{1.1}$·G+ψ_2Q+ψ_2RQ±A_{Ed}+EHF_{Dir1+}	3.4	0.023	✔ Pass	Details...
St. 14 (14)	C71	1	3 (Operating) $SEIS_{1.1}$·G+ψ_2Q+ψ_2RQ±A_{Ed}+EHF_{Dir1+}	4.1	0.028	3 (Operating) $SEIS_{1.1}$·G+ψ_2Q+ψ_2RQ±A_{Ed}+EHF_{Dir1+}	3.4	0.023	✔ Pass	Details...
St. 15 (15)	C77	2	3 (Operating) $SEIS_{1.1}$·G+ψ_2Q+ψ_2RQ±A_{Ed}+EHF_{Dir1+}	4.7	0.032	3 (Operating) $SEIS_{1.1}$·G+ψ_2Q+ψ_2RQ±A_{Ed}+EHF_{Dir1+}	3.3	0.022	✔ Pass	Details...
St. 15 (15)	C53	2	3 (Operating) $SEIS_{1.1}$·G+ψ_2Q+ψ_2RQ±A_{Ed}+EHF_{Dir1+}	4.4	0.029	3 (Operating) $SEIS_{1.1}$·G+ψ_2Q+ψ_2RQ±A_{Ed}+EHF_{Dir1+}	3.3	0.022	✔ Pass	Details...
St. 16 (16)	C77	3	3 (Operating) $SEIS_{1.1}$·G+ψ_2Q+ψ_2RQ±A_{Ed}+EHF_{Dir1+}	4.6	0.030	3 (Operating) $SEIS_{1.1}$·G+ψ_2Q+ψ_2RQ±A_{Ed}+EHF_{Dir1+}	3.3	0.021	✔ Pass	Details...
St. 16 (16)	C71	3	3 (Operating) $SEIS_{1.1}$·G+ψ_2Q+ψ_2RQ±A_{Ed}+EHF_{Dir1+}	4.2	0.027	3 (Operating) $SEIS_{1.1}$·G+ψ_2Q+ψ_2RQ±A_{Ed}+EHF_{Dir1+}	3.3	0.021	✔ Pass	Details...
St. 17 (17)	C77	4	3 (Operating) $SEIS_{1.1}$·G+ψ_2Q+ψ_2RQ±A_{Ed}+EHF_{Dir1+}	4.6	0.029	5 (Operating) $SEIS_{1.3}$·G+ψ_2Q+ψ_2RQ±A_{Ed}+EHF_{Dir2+}	3.2	0.020	✔ Pass	Details...
St. 17 (17)	W8	17	3 (Operating) $SEIS_{1.1}$·G+ψ_2Q+ψ_2RQ±A_{Ed}+EHF_{Dir1+}	4.1	0.026	5 (Operating) $SEIS_{1.3}$·G+ψ_2Q+ψ_2RQ±A_{Ed}+EHF_{Dir2+}	3.3	0.020	✔ Pass	Details...
St. 18 (18)	W6	18	3 (Operating) $SEIS_{1.1}$·G+ψ_2Q+ψ_2RQ±A_{Ed}+EHF_{Dir1+}	5.4	0.034	3 (Operating) $SEIS_{1.1}$·G+ψ_2Q+ψ_2RQ±A_{Ed}+EHF_{Dir1+}	2.7	0.016	✔ Pass	Details...
St. 18 (18)	W8	18	3 (Operating) $SEIS_{1.1}$·G+ψ_2Q+ψ_2RQ±A_{Ed}+EHF_{Dir1+}	4.1	0.025	3 (Operating) $SEIS_{1.1}$·G+ψ_2Q+ψ_2RQ±A_{Ed}+EHF_{Dir1+}	3.9	0.023	✔ Pass	Details...
St. 19 (19)	C77	6	3 (Operating) $SEIS_{1.1}$·G+ψ_2Q+ψ_2RQ±A_{Ed}+EHF_{Dir1+}	4.4	0.026	5 (Operating) $SEIS_{1.3}$·G+ψ_2Q+ψ_2RQ±A_{Ed}+EHF_{Dir2+}	3.1	0.018	✔ Pass	Details...
St. 19 (19)	C71	6	3 (Operating) $SEIS_{1.1}$·G+ψ_2Q+ψ_2RQ±A_{Ed}+EHF_{Dir1+}	4.2	0.025	5 (Operating) $SEIS_{1.3}$·G+ψ_2Q+ψ_2RQ±A_{Ed}+EHF_{Dir2+}	3.1	0.018	✔ Pass	Details...
St. 20 (roof)	C77	7	3 (Operating) $SEIS_{1.1}$·G+ψ_2Q+ψ_2RQ±A_{Ed}+EHF_{Dir1+}	4.2	0.025	3 (Operating) $SEIS_{1.1}$·G+ψ_2Q+ψ_2RQ±A_{Ed}+EHF_{Dir1+}	2.9	0.016	✔ Pass	Details...
St. 20 (roof)	C53	7	3 (Operating) $SEIS_{1.1}$·G+ψ_2Q+ψ_2RQ±A_{Ed}+EHF_{Dir1+}	4.1	0.024	3 (Operating) $SEIS_{1.1}$·G+ψ_2Q+ψ_2RQ±A_{Ed}+EHF_{Dir1+}	2.9	0.016	✔ Pass	Details...

MODEL11

Level ▲	Ref.	Stack	Combination Dir 1	Drift Dir 1 [mm]	θ_{Dir1}	Combination Dir 2	Drift Dir 2 [mm]	θ_{Dir2}	Status	Details
St. 1 (1)	C23	1	5 (Operating) $SEIS_{1.3}$-G+ψ_2Q+ψ_2RQ±A_{Ed}+EHF_{Dir2+}	3.1	0.036	5 (Operating) $SEIS_{1.3}$-G+ψ_2Q+ψ_2RQ±A_{Ed}+EHF_{Dir2+}	1.9	0.021	Pass	Details...
St. 1 (1)	C1	1	5 (Operating) $SEIS_{1.3}$-G+ψ_2Q+ψ_2RQ±A_{Ed}+EHF_{Dir2+}	2.2	0.026	5 (Operating) $SEIS_{1.3}$-G+ψ_2Q+ψ_2RQ±A_{Ed}+EHF_{Dir2+}	1.9	0.021	Pass	Details...
St. 2 (2)	C23	2	5 (Operating) $SEIS_{1.3}$-G+ψ_2Q+ψ_2RQ±A_{Ed}+EHF_{Dir2+}	3.4	0.037	5 (Operating) $SEIS_{1.3}$-G+ψ_2Q+ψ_2RQ±A_{Ed}+EHF_{Dir2+}	2.1	0.022	Pass	Details...
St. 2 (2)	C1	2	5 (Operating) $SEIS_{1.3}$-G+ψ_2Q+ψ_2RQ±A_{Ed}+EHF_{Dir2+}	2.5	0.027	5 (Operating) $SEIS_{1.3}$-G+ψ_2Q+ψ_2RQ±A_{Ed}+EHF_{Dir2+}	2.1	0.022	Pass	Details...
St. 3 (3)	C23	3	5 (Operating) $SEIS_{1.3}$-G+ψ_2Q+ψ_2RQ±A_{Ed}+EHF_{Dir2+}	3.6	0.037	5 (Operating) $SEIS_{1.3}$-G+ψ_2Q+ψ_2RQ±A_{Ed}+EHF_{Dir2+}	2.3	0.022	Pass	Details...
St. 3 (3)	C11	3	3 (Operating) $SEIS_{1.1}$-G+ψ_2Q+ψ_2RQ±A_{Ed}+EHF_{Dir1+}	1.4	0.014	5 (Operating) $SEIS_{1.3}$-G+ψ_2Q+ψ_2RQ±A_{Ed}+EHF_{Dir2+}	2.3	0.022	Pass	Details...
St. 4 (4)	C23	4	5 (Operating) $SEIS_{1.3}$-G+ψ_2Q+ψ_2RQ±A_{Ed}+EHF_{Dir2+}	3.7	0.036	5 (Operating) $SEIS_{1.3}$-G+ψ_2Q+ψ_2RQ±A_{Ed}+EHF_{Dir2+}	2.4	0.022	Pass	Details...
St. 4 (4)	C1	4	5 (Operating) $SEIS_{1.3}$-G+ψ_2Q+ψ_2RQ±A_{Ed}+EHF_{Dir2+}	2.8	0.028	5 (Operating) $SEIS_{1.3}$-G+ψ_2Q+ψ_2RQ±A_{Ed}+EHF_{Dir2+}	2.4	0.022	Pass	Details...
St. 5 (5)	C23	5	5 (Operating) $SEIS_{1.3}$-G+ψ_2Q+ψ_2RQ±A_{Ed}+EHF_{Dir2+}	3.7	0.036	5 (Operating) $SEIS_{1.3}$-G+ψ_2Q+ψ_2RQ±A_{Ed}+EHF_{Dir2+}	2.4	0.022	Pass	Details...
St. 5 (5)	C1	5	5 (Operating) $SEIS_{1.3}$-G+ψ_2Q+ψ_2RQ±A_{Ed}+EHF_{Dir2+}	3.0	0.028	5 (Operating) $SEIS_{1.3}$-G+ψ_2Q+ψ_2RQ±A_{Ed}+EHF_{Dir2+}	2.4	0.022	Pass	Details...
St. 6 (6)	C23	6	3 (Operating) $SEIS_{1.1}$-G+ψ_2Q+ψ_2RQ±A_{Ed}+EHF_{Dir1+}	3.8	0.035	5 (Operating) $SEIS_{1.3}$-G+ψ_2Q+ψ_2RQ±A_{Ed}+EHF_{Dir2+}	2.5	0.022	Pass	Details...
St. 6 (6)	C11	6	3 (Operating) $SEIS_{1.1}$-G+ψ_2Q+ψ_2RQ±A_{Ed}+EHF_{Dir1+}	2.2	0.020	5 (Operating) $SEIS_{1.3}$-G+ψ_2Q+ψ_2RQ±A_{Ed}+EHF_{Dir2+}	2.5	0.022	Pass	Details...
St. 7 (7)	C23	7	3 (Operating) $SEIS_{1.1}$-G+ψ_2Q+ψ_2RQ±A_{Ed}+EHF_{Dir1+}	4.0	0.035	5 (Operating) $SEIS_{1.3}$-G+ψ_2Q+ψ_2RQ±A_{Ed}+EHF_{Dir2+}	2.6	0.021	Pass	Details...
St. 7 (7)	C1	7	5 (Operating) $SEIS_{1.3}$-G+ψ_2Q+ψ_2RQ±A_{Ed}+EHF_{Dir2+}	3.2	0.028	5 (Operating) $SEIS_{1.3}$-G+ψ_2Q+ψ_2RQ±A_{Ed}+EHF_{Dir2+}	2.6	0.021	Pass	Details...
St. 8 (8)	C48	1	3 (Operating) $SEIS_{1.1}$-G+ψ_2Q+ψ_2RQ±A_{Ed}+EHF_{Dir1+}	4.4	0.037	5 (Operating) $SEIS_{1.3}$-G+ψ_2Q+ψ_2RQ±A_{Ed}+EHF_{Dir2+}	2.9	0.023	Pass	Details...
St. 8 (8)	C45	1	3 (Operating) $SEIS_{1.1}$-G+ψ_2Q+ψ_2RQ±A_{Ed}+EHF_{Dir1+}	3.8	0.032	5 (Operating) $SEIS_{1.3}$-G+ψ_2Q+ψ_2RQ±A_{Ed}+EHF_{Dir2+}	2.9	0.023	Pass	Details...
St. 9 (9)	C48	2	3 (Operating) $SEIS_{1.1}$-G+ψ_2Q+ψ_2RQ±A_{Ed}+EHF_{Dir1+}	4.5	0.037	3 (Operating) $SEIS_{1.1}$-G+ψ_2Q+ψ_2RQ±A_{Ed}+EHF_{Dir1+}	3.0	0.023	Pass	Details...
St. 9 (9)	C45	2	3 (Operating) $SEIS_{1.1}$-G+ψ_2Q+ψ_2RQ±A_{Ed}+EHF_{Dir1+}	3.9	0.032	3 (Operating) $SEIS_{1.1}$-G+ψ_2Q+ψ_2RQ±A_{Ed}+EHF_{Dir1+}	3.0	0.023	Pass	Details...
St. 10 (10)	C48	3	3 (Operating) $SEIS_{1.1}$-G+ψ_2Q+ψ_2RQ±A_{Ed}+EHF_{Dir1+}	4.6	0.036	3 (Operating) $SEIS_{1.1}$-G+ψ_2Q+ψ_2RQ±A_{Ed}+EHF_{Dir1+}	3.0	0.023	Pass	Details...
St. 10 (10)	C26	3	3 (Operating) $SEIS_{1.1}$-G+ψ_2Q+ψ_2RQ±A_{Ed}+EHF_{Dir1+}	3.8	0.030	3 (Operating) $SEIS_{1.1}$-G+ψ_2Q+ψ_2RQ±A_{Ed}+EHF_{Dir1+}	3.0	0.023	Pass	Details...
St. 11 (11)	C48	4	3 (Operating) $SEIS_{1.1}$-G+ψ_2Q+ψ_2RQ±A_{Ed}+EHF_{Dir1+}	4.7	0.035	3 (Operating) $SEIS_{1.1}$-G+ψ_2Q+ψ_2RQ±A_{Ed}+EHF_{Dir1+}	3.1	0.022	Pass	Details...
St. 11 (11)	C36	4	3 (Operating) $SEIS_{1.1}$-G+ψ_2Q+ψ_2RQ±A_{Ed}+EHF_{Dir1+}	3.3	0.025	3 (Operating) $SEIS_{1.1}$-G+ψ_2Q+ψ_2RQ±A_{Ed}+EHF_{Dir1+}	3.1	0.022	Pass	Details...
St. 12 (12)	C48	5	3 (Operating) $SEIS_{1.1}$-G+ψ_2Q+ψ_2RQ±A_{Ed}+EHF_{Dir1+}	4.7	0.034	3 (Operating) $SEIS_{1.1}$-G+ψ_2Q+ψ_2RQ±A_{Ed}+EHF_{Dir1+}	3.1	0.022	Pass	Details...
St. 12 (12)	C26	5	3 (Operating) $SEIS_{1.1}$-G+ψ_2Q+ψ_2RQ±A_{Ed}+EHF_{Dir1+}	4.0	0.029	3 (Operating) $SEIS_{1.1}$-G+ψ_2Q+ψ_2RQ±A_{Ed}+EHF_{Dir1+}	3.1	0.022	Pass	Details...
St. 13 (13)	C48	6	3 (Operating) $SEIS_{1.1}$-G+ψ_2Q+ψ_2RQ±A_{Ed}+EHF_{Dir1+}	4.6	0.033	3 (Operating) $SEIS_{1.1}$-G+ψ_2Q+ψ_2RQ±A_{Ed}+EHF_{Dir1+}	3.1	0.021	Pass	Details...
St. 13 (13)	C36	6	3 (Operating) $SEIS_{1.1}$-G+ψ_2Q+ψ_2RQ±A_{Ed}+EHF_{Dir1+}	3.6	0.026	3 (Operating) $SEIS_{1.1}$-G+ψ_2Q+ψ_2RQ±A_{Ed}+EHF_{Dir1+}	3.1	0.021	Pass	Details...
St. 14 (14)	C77	1	3 (Operating) $SEIS_{1.1}$-G+ψ_2Q+ψ_2RQ±A_{Ed}+EHF_{Dir1+}	4.8	0.033	3 (Operating) $SEIS_{1.1}$-G+ψ_2Q+ψ_2RQ±A_{Ed}+EHF_{Dir1+}	3.3	0.021	Pass	Details...
St. 14 (14)	W8	14	3 (Operating) $SEIS_{1.1}$-G+ψ_2Q+ψ_2RQ±A_{Ed}+EHF_{Dir1+}	3.8	0.026	5 (Operating) $SEIS_{1.3}$-G+ψ_2Q+ψ_2RQ±A_{Ed}+EHF_{Dir2+}	3.3	0.022	Pass	Details...
St. 15 (15)	W6	15	3 (Operating) $SEIS_{1.1}$-G+ψ_2Q+ψ_2RQ±A_{Ed}+EHF_{Dir1+}	5.5	0.037	3 (Operating) $SEIS_{1.1}$-G+ψ_2Q+ψ_2RQ±A_{Ed}+EHF_{Dir1+}	2.6	0.016	Pass	Details...
St. 15 (15)	W8	15	3 (Operating) $SEIS_{1.1}$-G+ψ_2Q+ψ_2RQ±A_{Ed}+EHF_{Dir1+}	3.9	0.026	3 (Operating) $SEIS_{1.1}$-G+ψ_2Q+ψ_2RQ±A_{Ed}+EHF_{Dir1+}	3.5	0.022	Pass	Details...
St. 16 (16)	C77	3	3 (Operating) $SEIS_{1.1}$-G+ψ_2Q+ψ_2RQ±A_{Ed}+EHF_{Dir1+}	4.7	0.030	3 (Operating) $SEIS_{1.1}$-G+ψ_2Q+ψ_2RQ±A_{Ed}+EHF_{Dir1+}	3.2	0.020	Pass	Details...
St. 16 (16)	C53	3	3 (Operating) $SEIS_{1.1}$-G+ψ_2Q+ψ_2RQ±A_{Ed}+EHF_{Dir1+}	4.3	0.028	3 (Operating) $SEIS_{1.1}$-G+ψ_2Q+ψ_2RQ±A_{Ed}+EHF_{Dir1+}	3.2	0.020	Pass	Details...
St. 17 (17)	C77	4	3 (Operating) $SEIS_{1.1}$-G+ψ_2Q+ψ_2RQ±A_{Ed}+EHF_{Dir1+}	4.6	0.029	3 (Operating) $SEIS_{1.1}$-G+ψ_2Q+ψ_2RQ±A_{Ed}+EHF_{Dir1+}	3.1	0.019	Pass	Details...
St. 17 (17)	C71	4	3 (Operating) $SEIS_{1.1}$-G+ψ_2Q+ψ_2RQ±A_{Ed}+EHF_{Dir1+}	4.1	0.026	3 (Operating) $SEIS_{1.1}$-G+ψ_2Q+ψ_2RQ±A_{Ed}+EHF_{Dir1+}	3.1	0.019	Pass	Details...
St. 18 (18)	C77	5	3 (Operating) $SEIS_{1.1}$-G+ψ_2Q+ψ_2RQ±A_{Ed}+EHF_{Dir1+}	4.6	0.028	5 (Operating) $SEIS_{1.3}$-G+ψ_2Q+ψ_2RQ±A_{Ed}+EHF_{Dir2+}	3.1	0.018	Pass	Details...
St. 18 (18)	C58	5	3 (Operating) $SEIS_{1.1}$-G+ψ_2Q+ψ_2RQ±A_{Ed}+EHF_{Dir1+}	4.1	0.026	5 (Operating) $SEIS_{1.3}$-G+ψ_2Q+ψ_2RQ±A_{Ed}+EHF_{Dir2+}	3.1	0.018	Pass	Details...
St. 19 (19)	C77	6	3 (Operating) $SEIS_{1.1}$-G+ψ_2Q+ψ_2RQ±A_{Ed}+EHF_{Dir1+}	4.4	0.026	5 (Operating) $SEIS_{1.3}$-G+ψ_2Q+ψ_2RQ±A_{Ed}+EHF_{Dir2+}	3.0	0.017	Pass	Details...
St. 19 (19)	C71	6	3 (Operating) $SEIS_{1.1}$-G+ψ_2Q+ψ_2RQ±A_{Ed}+EHF_{Dir1+}	4.1	0.025	5 (Operating) $SEIS_{1.3}$-G+ψ_2Q+ψ_2RQ±A_{Ed}+EHF_{Dir2+}	3.0	0.017	Pass	Details...

MODEL 12

Level ▲	Ref.	Stack	Combination Dir 1	Drift Dir 1 [mm]	θ_{Dir1}	Combination Dir 2	Drift Dir 2 [mm]	θ_{Dir2}	Status	Details
St. 1 (1)	C23	1	5 (Operating) $SEIS_{1.1}$·G+ψ_2Q+ψ_2RQ±A_{Ed}+EHF_{Dir2+}	2.3	0.027	5 (Operating) $SEIS_{1.1}$·G+ψ_2Q+ψ_2RQ±A_{Ed}+EHF_{Dir2+}	1.7	0.019	✔ Pass	Details...
St. 1 (1)	C1	1	5 (Operating) $SEIS_{1.1}$·G+ψ_2Q+ψ_2RQ±A_{Ed}+EHF_{Dir2+}	1.7	0.019	5 (Operating) $SEIS_{1.1}$·G+ψ_2Q+ψ_2RQ±A_{Ed}+EHF_{Dir2+}	1.7	0.019	✔ Pass	Details...
St. 2 (2)	C23	2	5 (Operating) $SEIS_{1.1}$·G+ψ_2Q+ψ_2RQ±A_{Ed}+EHF_{Dir2+}	2.5	0.028	5 (Operating) $SEIS_{1.1}$·G+ψ_2Q+ψ_2RQ±A_{Ed}+EHF_{Dir2+}	2.0	0.021	✔ Pass	Details...
St. 2 (2)	C1	2	5 (Operating) $SEIS_{1.1}$·G+ψ_2Q+ψ_2RQ±A_{Ed}+EHF_{Dir2+}	2.0	0.021	5 (Operating) $SEIS_{1.1}$·G+ψ_2Q+ψ_2RQ±A_{Ed}+EHF_{Dir2+}	2.0	0.021	✔ Pass	Details...
St. 3 (3)	C23	3	5 (Operating) $SEIS_{1.1}$·G+ψ_2Q+ψ_2RQ±A_{Ed}+EHF_{Dir2+}	2.7	0.028	5 (Operating) $SEIS_{1.1}$·G+ψ_2Q+ψ_2RQ±A_{Ed}+EHF_{Dir2+}	2.2	0.022	✔ Pass	Details...
St. 3 (3)	C1	3	5 (Operating) $SEIS_{1.1}$·G+ψ_2Q+ψ_2RQ±A_{Ed}+EHF_{Dir2+}	2.2	0.023	5 (Operating) $SEIS_{1.1}$·G+ψ_2Q+ψ_2RQ±A_{Ed}+EHF_{Dir2+}	2.2	0.022	✔ Pass	Details...
St. 4 (4)	C23	4	3 (Operating) $SEIS_{1.1}$·G+ψ_2Q+ψ_2RQ±A_{Ed}+EHF_{Dir1+}	2.8	0.028	5 (Operating) $SEIS_{1.1}$·G+ψ_2Q+ψ_2RQ±A_{Ed}+EHF_{Dir2+}	2.4	0.023	✔ Pass	Details...
St. 4 (4)	C11	4	3 (Operating) $SEIS_{1.1}$·G+ψ_2Q+ψ_2RQ±A_{Ed}+EHF_{Dir1+}	1.7	0.016	5 (Operating) $SEIS_{1.1}$·G+ψ_2Q+ψ_2RQ±A_{Ed}+EHF_{Dir2+}	2.4	0.023	✔ Pass	Details...
St. 5 (5)	C23	5	3 (Operating) $SEIS_{1.1}$·G+ψ_2Q+ψ_2RQ±A_{Ed}+EHF_{Dir1+}	3.0	0.028	5 (Operating) $SEIS_{1.1}$·G+ψ_2Q+ψ_2RQ±A_{Ed}+EHF_{Dir2+}	2.6	0.024	✔ Pass	Details...
St. 5 (5)	C1	5	5 (Operating) $SEIS_{1.1}$·G+ψ_2Q+ψ_2RQ±A_{Ed}+EHF_{Dir2+}	2.6	0.025	5 (Operating) $SEIS_{1.1}$·G+ψ_2Q+ψ_2RQ±A_{Ed}+EHF_{Dir2+}	2.6	0.024	✔ Pass	Details...
St. 6 (6)	C23	6	3 (Operating) $SEIS_{1.1}$·G+ψ_2Q+ψ_2RQ±A_{Ed}+EHF_{Dir1+}	3.1	0.029	5 (Operating) $SEIS_{1.1}$·G+ψ_2Q+ψ_2RQ±A_{Ed}+EHF_{Dir2+}	2.7	0.024	✔ Pass	Details...
St. 6 (6)	C1	6	5 (Operating) $SEIS_{1.1}$·G+ψ_2Q+ψ_2RQ±A_{Ed}+EHF_{Dir2+}	2.8	0.025	5 (Operating) $SEIS_{1.1}$·G+ψ_2Q+ψ_2RQ±A_{Ed}+EHF_{Dir2+}	2.7	0.024	✔ Pass	Details...
St. 7 (7)	C23	7	3 (Operating) $SEIS_{1.1}$·G+ψ_2Q+ψ_2RQ±A_{Ed}+EHF_{Dir1+}	3.3	0.029	5 (Operating) $SEIS_{1.1}$·G+ψ_2Q+ψ_2RQ±A_{Ed}+EHF_{Dir2+}	2.8	0.024	✔ Pass	Details...
St. 7 (7)	C20	7	3 (Operating) $SEIS_{1.1}$·G+ψ_2Q+ψ_2RQ±A_{Ed}+EHF_{Dir1+}	3.0	0.026	5 (Operating) $SEIS_{1.1}$·G+ψ_2Q+ψ_2RQ±A_{Ed}+EHF_{Dir2+}	2.8	0.024	✔ Pass	Details...
St. 8 (8)	C48	1	3 (Operating) $SEIS_{1.1}$·G+ψ_2Q+ψ_2RQ±A_{Ed}+EHF_{Dir1+}	3.7	0.031	5 (Operating) $SEIS_{1.1}$·G+ψ_2Q+ψ_2RQ±A_{Ed}+EHF_{Dir2+}	3.2	0.026	✔ Pass	Details...
St. 8 (8)	C36	1	3 (Operating) $SEIS_{1.1}$·G+ψ_2Q+ψ_2RQ±A_{Ed}+EHF_{Dir1+}	2.7	0.023	5 (Operating) $SEIS_{1.1}$·G+ψ_2Q+ψ_2RQ±A_{Ed}+EHF_{Dir2+}	3.2	0.026	✔ Pass	Details...
St. 9 (9)	C48	2	3 (Operating) $SEIS_{1.1}$·G+ψ_2Q+ψ_2RQ±A_{Ed}+EHF_{Dir1+}	3.8	0.031	5 (Operating) $SEIS_{1.1}$·G+ψ_2Q+ψ_2RQ±A_{Ed}+EHF_{Dir2+}	3.2	0.025	✔ Pass	Details...
St. 9 (9)	C26	2	3 (Operating) $SEIS_{1.1}$·G+ψ_2Q+ψ_2RQ±A_{Ed}+EHF_{Dir1+}	3.4	0.028	5 (Operating) $SEIS_{1.1}$·G+ψ_2Q+ψ_2RQ±A_{Ed}+EHF_{Dir2+}	3.2	0.025	✔ Pass	Details...
St. 10 (10)	C48	3	3 (Operating) $SEIS_{1.1}$·G+ψ_2Q+ψ_2RQ±A_{Ed}+EHF_{Dir1+}	4.0	0.031	5 (Operating) $SEIS_{1.1}$·G+ψ_2Q+ψ_2RQ±A_{Ed}+EHF_{Dir2+}	3.3	0.025	✔ Pass	Details...
St. 10 (10)	C45	3	3 (Operating) $SEIS_{1.1}$·G+ψ_2Q+ψ_2RQ±A_{Ed}+EHF_{Dir1+}	3.7	0.029	5 (Operating) $SEIS_{1.1}$·G+ψ_2Q+ψ_2RQ±A_{Ed}+EHF_{Dir2+}	3.3	0.025	✔ Pass	Details...
St. 11 (11)	C48	4	3 (Operating) $SEIS_{1.1}$·G+ψ_2Q+ψ_2RQ±A_{Ed}+EHF_{Dir1+}	4.1	0.031	5 (Operating) $SEIS_{1.1}$·G+ψ_2Q+ψ_2RQ±A_{Ed}+EHF_{Dir2+}	3.3	0.025	✔ Pass	Details...
St. 11 (11)	C26	4	3 (Operating) $SEIS_{1.1}$·G+ψ_2Q+ψ_2RQ±A_{Ed}+EHF_{Dir1+}	3.7	0.028	5 (Operating) $SEIS_{1.1}$·G+ψ_2Q+ψ_2RQ±A_{Ed}+EHF_{Dir2+}	3.3	0.025	✔ Pass	Details...
St. 12 (12)	C48	5	3 (Operating) $SEIS_{1.1}$·G+ψ_2Q+ψ_2RQ±A_{Ed}+EHF_{Dir1+}	4.2	0.031	5 (Operating) $SEIS_{1.1}$·G+ψ_2Q+ψ_2RQ±A_{Ed}+EHF_{Dir2+}	3.4	0.024	✔ Pass	Details...
St. 12 (12)	C26	5	3 (Operating) $SEIS_{1.1}$·G+ψ_2Q+ψ_2RQ±A_{Ed}+EHF_{Dir1+}	3.9	0.028	5 (Operating) $SEIS_{1.1}$·G+ψ_2Q+ψ_2RQ±A_{Ed}+EHF_{Dir2+}	3.4	0.024	✔ Pass	Details...
St. 13 (13)	W6	13	3 (Operating) $SEIS_{1.1}$·G+ψ_2Q+ψ_2RQ±A_{Ed}+EHF_{Dir1+}	4.5	0.032	3 (Operating) $SEIS_{1.1}$·G+ψ_2Q+ψ_2RQ±A_{Ed}+EHF_{Dir1+}	2.6	0.018	✔ Pass	Details...
St. 13 (13)	W8	13	3 (Operating) $SEIS_{1.1}$·G+ψ_2Q+ψ_2RQ±A_{Ed}+EHF_{Dir1+}	3.6	0.026	5 (Operating) $SEIS_{1.1}$·G+ψ_2Q+ψ_2RQ±A_{Ed}+EHF_{Dir2+}	3.5	0.024	✔ Pass	Details...
St. 14 (14)	C77	1	3 (Operating) $SEIS_{1.1}$·G+ψ_2Q+ψ_2RQ±A_{Ed}+EHF_{Dir1+}	4.5	0.031	5 (Operating) $SEIS_{1.1}$·G+ψ_2Q+ψ_2RQ±A_{Ed}+EHF_{Dir2+}	3.5	0.024	✔ Pass	Details...
St. 14 (14)	C74	1	3 (Operating) $SEIS_{1.1}$·G+ψ_2Q+ψ_2RQ±A_{Ed}+EHF_{Dir1+}	4.2	0.029	5 (Operating) $SEIS_{1.1}$·G+ψ_2Q+ψ_2RQ±A_{Ed}+EHF_{Dir2+}	3.5	0.024	✔ Pass	Details...
St. 15 (15)	C77	2	3 (Operating) $SEIS_{1.1}$·G+ψ_2Q+ψ_2RQ±A_{Ed}+EHF_{Dir1+}	4.5	0.030	5 (Operating) $SEIS_{1.1}$·G+ψ_2Q+ψ_2RQ±A_{Ed}+EHF_{Dir2+}	3.5	0.023	✔ Pass	Details...
St. 15 (15)	C71	2	3 (Operating) $SEIS_{1.1}$·G+ψ_2Q+ψ_2RQ±A_{Ed}+EHF_{Dir1+}	4.0	0.027	5 (Operating) $SEIS_{1.1}$·G+ψ_2Q+ψ_2RQ±A_{Ed}+EHF_{Dir2+}	3.5	0.023	✔ Pass	Details...
St. 16 (16)	C77	3	3 (Operating) $SEIS_{1.1}$·G+ψ_2Q+ψ_2RQ±A_{Ed}+EHF_{Dir1+}	4.4	0.029	5 (Operating) $SEIS_{1.1}$·G+ψ_2Q+ψ_2RQ±A_{Ed}+EHF_{Dir2+}	3.5	0.022	✔ Pass	Details...
St. 16 (16)	C53	3	3 (Operating) $SEIS_{1.1}$·G+ψ_2Q+ψ_2RQ±A_{Ed}+EHF_{Dir1+}	4.2	0.027	5 (Operating) $SEIS_{1.1}$·G+ψ_2Q+ψ_2RQ±A_{Ed}+EHF_{Dir2+}	3.5	0.022	✔ Pass	Details...
St. 17 (17)	C77	4	3 (Operating) $SEIS_{1.1}$·G+ψ_2Q+ψ_2RQ±A_{Ed}+EHF_{Dir1+}	4.4	0.027	5 (Operating) $SEIS_{1.1}$·G+ψ_2Q+ψ_2RQ±A_{Ed}+EHF_{Dir2+}	3.4	0.021	✔ Pass	Details...
St. 17 (17)	C58	4	3 (Operating) $SEIS_{1.1}$·G+ψ_2Q+ψ_2RQ±A_{Ed}+EHF_{Dir1+}	4.0	0.025	5 (Operating) $SEIS_{1.1}$·G+ψ_2Q+ψ_2RQ±A_{Ed}+EHF_{Dir2+}	3.4	0.021	✔ Pass	Details...
St. 18 (18)	W6	18	3 (Operating) $SEIS_{1.1}$·G+ψ_2Q+ψ_2RQ±A_{Ed}+EHF_{Dir1+}	4.9	0.030	3 (Operating) $SEIS_{1.1}$·G+ψ_2Q+ψ_2RQ±A_{Ed}+EHF_{Dir1+}	2.9	0.017	✔ Pass	Details...
St. 18 (18)	W8	18	3 (Operating) $SEIS_{1.1}$·G+ψ_2Q+ψ_2RQ±A_{Ed}+EHF_{Dir1+}	4.0	0.024	5 (Operating) $SEIS_{1.1}$·G+ψ_2Q+ψ_2RQ±A_{Ed}+EHF_{Dir2+}	4.1	0.024	✔ Pass	Details...
St. 19 (19)	C77	6	3 (Operating) $SEIS_{1.1}$·G+ψ_2Q+ψ_2RQ±A_{Ed}+EHF_{Dir1+}	4.2	0.025	5 (Operating) $SEIS_{1.1}$·G+ψ_2Q+ψ_2RQ±A_{Ed}+EHF_{Dir2+}	3.2	0.019	✔ Pass	Details...
St. 19 (19)	C58	6	3 (Operating) $SEIS_{1.1}$·G+ψ_2Q+ψ_2RQ±A_{Ed}+EHF_{Dir1+}	4.0	0.024	5 (Operating) $SEIS_{1.1}$·G+ψ_2Q+ψ_2RQ±A_{Ed}+EHF_{Dir2+}	3.2	0.019	✔ Pass	Details...

MODEL13

Level ▲	Ref.	Stack	Combination Dir 1	Drift Dir 1 [mm]	$\theta_{Dir\,1}$	Combination Dir 2	Drift Dir 2 [mm]	$\theta_{Dir\,2}$	Status	Details
St. 1 (1)	C23	1	5 (Operating) $SEIS_{1,1}$-G+ψ_2Q+ψ_2RQ±A_{Ed}+EHF_{Dir2+}	2.5	0.029	5 (Operating) $SEIS_{1,1}$-G+ψ_2Q+ψ_2RQ±A_{Ed}+EHF_{Dir2+}	1.7	0.019	Pass	Details...
St. 1 (1)	C1	1	5 (Operating) $SEIS_{1,1}$-G+ψ_2Q+ψ_2RQ±A_{Ed}+EHF_{Dir2+}	1.9	0.021	5 (Operating) $SEIS_{1,1}$-G+ψ_2Q+ψ_2RQ±A_{Ed}+EHF_{Dir2+}	1.7	0.019	Pass	Details...
St. 2 (2)	C23	2	5 (Operating) $SEIS_{1,1}$-G+ψ_2Q+ψ_2RQ±A_{Ed}+EHF_{Dir2+}	2.7	0.030	5 (Operating) $SEIS_{1,1}$-G+ψ_2Q+ψ_2RQ±A_{Ed}+EHF_{Dir2+}	2.0	0.021	Pass	Details...
St. 2 (2)	C1	2	5 (Operating) $SEIS_{1,1}$-G+ψ_2Q+ψ_2RQ±A_{Ed}+EHF_{Dir2+}	2.1	0.023	5 (Operating) $SEIS_{1,1}$-G+ψ_2Q+ψ_2RQ±A_{Ed}+EHF_{Dir2+}	2.0	0.021	Pass	Details...
St. 3 (3)	C23	3	5 (Operating) $SEIS_{1,1}$-G+ψ_2Q+ψ_2RQ±A_{Ed}+EHF_{Dir2+}	2.9	0.030	5 (Operating) $SEIS_{1,1}$-G+ψ_2Q+ψ_2RQ±A_{Ed}+EHF_{Dir2+}	2.3	0.023	Pass	Details...
St. 3 (3)	C1	3	5 (Operating) $SEIS_{1,1}$-G+ψ_2Q+ψ_2RQ±A_{Ed}+EHF_{Dir2+}	2.4	0.025	5 (Operating) $SEIS_{1,1}$-G+ψ_2Q+ψ_2RQ±A_{Ed}+EHF_{Dir2+}	2.3	0.023	Pass	Details...
St. 4 (4)	C23	4	5 (Operating) $SEIS_{1,1}$-G+ψ_2Q+ψ_2RQ±A_{Ed}+EHF_{Dir2+}	2.9	0.029	5 (Operating) $SEIS_{1,1}$-G+ψ_2Q+ψ_2RQ±A_{Ed}+EHF_{Dir2+}	2.4	0.023	Pass	Details...
St. 4 (4)	C11	4	3 (Operating) $SEIS_{1,1}$-G+ψ_2Q+ψ_2RQ±A_{Ed}+EHF_{Dir1+}	1.6	0.016	5 (Operating) $SEIS_{1,1}$-G+ψ_2Q+ψ_2RQ±A_{Ed}+EHF_{Dir2+}	2.4	0.023	Pass	Details...
St. 5 (5)	C23	5	3 (Operating) $SEIS_{1,1}$-G+ψ_2Q+ψ_2RQ±A_{Ed}+EHF_{Dir1+}	3.1	0.030	5 (Operating) $SEIS_{1,1}$-G+ψ_2Q+ψ_2RQ±A_{Ed}+EHF_{Dir2+}	2.6	0.024	Pass	Details...
St. 5 (5)	C1	5	5 (Operating) $SEIS_{1,1}$-G+ψ_2Q+ψ_2RQ±A_{Ed}+EHF_{Dir2+}	2.7	0.026	5 (Operating) $SEIS_{1,1}$-G+ψ_2Q+ψ_2RQ±A_{Ed}+EHF_{Dir2+}	2.6	0.024	Pass	Details...
St. 6 (6)	C23	6	3 (Operating) $SEIS_{1,1}$-G+ψ_2Q+ψ_2RQ±A_{Ed}+EHF_{Dir1+}	3.3	0.030	5 (Operating) $SEIS_{1,1}$-G+ψ_2Q+ψ_2RQ±A_{Ed}+EHF_{Dir2+}	2.7	0.024	Pass	Details...
St. 6 (6)	C1	6	5 (Operating) $SEIS_{1,1}$-G+ψ_2Q+ψ_2RQ±A_{Ed}+EHF_{Dir2+}	2.9	0.026	5 (Operating) $SEIS_{1,1}$-G+ψ_2Q+ψ_2RQ±A_{Ed}+EHF_{Dir2+}	2.7	0.024	Pass	Details...
St. 7 (7)	C23	7	3 (Operating) $SEIS_{1,1}$-G+ψ_2Q+ψ_2RQ±A_{Ed}+EHF_{Dir1+}	3.4	0.030	5 (Operating) $SEIS_{1,1}$-G+ψ_2Q+ψ_2RQ±A_{Ed}+EHF_{Dir2+}	2.8	0.024	Pass	Details...
St. 7 (7)	C11	7	3 (Operating) $SEIS_{1,1}$-G+ψ_2Q+ψ_2RQ±A_{Ed}+EHF_{Dir1+}	2.4	0.021	5 (Operating) $SEIS_{1,1}$-G+ψ_2Q+ψ_2RQ±A_{Ed}+EHF_{Dir2+}	2.8	0.024	Pass	Details...
St. 8 (8)	C48	1	3 (Operating) $SEIS_{1,1}$-G+ψ_2Q+ψ_2RQ±A_{Ed}+EHF_{Dir1+}	3.8	0.032	5 (Operating) $SEIS_{1,1}$-G+ψ_2Q+ψ_2RQ±A_{Ed}+EHF_{Dir2+}	3.1	0.025	Pass	Details...
St. 8 (8)	C26	1	5 (Operating) $SEIS_{1,1}$-G+ψ_2Q+ψ_2RQ±A_{Ed}+EHF_{Dir2+}	3.4	0.028	5 (Operating) $SEIS_{1,1}$-G+ψ_2Q+ψ_2RQ±A_{Ed}+EHF_{Dir2+}	3.1	0.025	Pass	Details...
St. 9 (9)	C48	2	3 (Operating) $SEIS_{1,1}$-G+ψ_2Q+ψ_2RQ±A_{Ed}+EHF_{Dir1+}	3.9	0.032	5 (Operating) $SEIS_{1,1}$-G+ψ_2Q+ψ_2RQ±A_{Ed}+EHF_{Dir2+}	3.2	0.025	Pass	Details...
St. 9 (9)	C26	2	5 (Operating) $SEIS_{1,1}$-G+ψ_2Q+ψ_2RQ±A_{Ed}+EHF_{Dir2+}	3.5	0.028	5 (Operating) $SEIS_{1,1}$-G+ψ_2Q+ψ_2RQ±A_{Ed}+EHF_{Dir2+}	3.2	0.025	Pass	Details...
St. 10 (10)	C48	3	3 (Operating) $SEIS_{1,1}$-G+ψ_2Q+ψ_2RQ±A_{Ed}+EHF_{Dir1+}	4.1	0.032	5 (Operating) $SEIS_{1,1}$-G+ψ_2Q+ψ_2RQ±A_{Ed}+EHF_{Dir2+}	3.2	0.024	Pass	Details...
St. 10 (10)	C36	3	3 (Operating) $SEIS_{1,1}$-G+ψ_2Q+ψ_2RQ±A_{Ed}+EHF_{Dir1+}	3.1	0.024	5 (Operating) $SEIS_{1,1}$-G+ψ_2Q+ψ_2RQ±A_{Ed}+EHF_{Dir2+}	3.2	0.024	Pass	Details...
St. 11 (11)	W6	11	3 (Operating) $SEIS_{1,1}$-G+ψ_2Q+ψ_2RQ±A_{Ed}+EHF_{Dir1+}	4.3	0.033	3 (Operating) $SEIS_{1,1}$-G+ψ_2Q+ψ_2RQ±A_{Ed}+EHF_{Dir1+}	2.4	0.017	Pass	Details...
St. 11 (11)	C26	4	3 (Operating) $SEIS_{1,1}$-G+ψ_2Q+ψ_2RQ±A_{Ed}+EHF_{Dir1+}	3.7	0.028	5 (Operating) $SEIS_{1,1}$-G+ψ_2Q+ψ_2RQ±A_{Ed}+EHF_{Dir2+}	3.2	0.023	Pass	Details...
St. 12 (12)	C48	5	3 (Operating) $SEIS_{1,1}$-G+ψ_2Q+ψ_2RQ±A_{Ed}+EHF_{Dir1+}	4.2	0.031	5 (Operating) $SEIS_{1,1}$-G+ψ_2Q+ψ_2RQ±A_{Ed}+EHF_{Dir2+}	3.2	0.023	Pass	Details...
St. 12 (12)	C36	5	3 (Operating) $SEIS_{1,1}$-G+ψ_2Q+ψ_2RQ±A_{Ed}+EHF_{Dir1+}	3.4	0.025	5 (Operating) $SEIS_{1,1}$-G+ψ_2Q+ψ_2RQ±A_{Ed}+EHF_{Dir2+}	3.2	0.023	Pass	Details...
St. 13 (13)	C48	6	3 (Operating) $SEIS_{1,1}$-G+ψ_2Q+ψ_2RQ±A_{Ed}+EHF_{Dir1+}	4.3	0.030	5 (Operating) $SEIS_{1,1}$-G+ψ_2Q+ψ_2RQ±A_{Ed}+EHF_{Dir2+}	3.2	0.022	Pass	Details...
St. 13 (13)	C36	6	3 (Operating) $SEIS_{1,1}$-G+ψ_2Q+ψ_2RQ±A_{Ed}+EHF_{Dir1+}	3.6	0.025	5 (Operating) $SEIS_{1,1}$-G+ψ_2Q+ψ_2RQ±A_{Ed}+EHF_{Dir2+}	3.2	0.022	Pass	Details...
St. 14 (14)	C77	1	3 (Operating) $SEIS_{1,1}$-G+ψ_2Q+ψ_2RQ±A_{Ed}+EHF_{Dir1+}	4.4	0.030	5 (Operating) $SEIS_{1,1}$-G+ψ_2Q+ψ_2RQ±A_{Ed}+EHF_{Dir2+}	3.4	0.022	Pass	Details...
St. 14 (14)	C53	1	3 (Operating) $SEIS_{1,1}$-G+ψ_2Q+ψ_2RQ±A_{Ed}+EHF_{Dir1+}	4.1	0.028	5 (Operating) $SEIS_{1,1}$-G+ψ_2Q+ψ_2RQ±A_{Ed}+EHF_{Dir2+}	3.4	0.022	Pass	Details...
St. 15 (15)	C77	2	3 (Operating) $SEIS_{1,1}$-G+ψ_2Q+ψ_2RQ±A_{Ed}+EHF_{Dir1+}	4.4	0.030	5 (Operating) $SEIS_{1,1}$-G+ψ_2Q+ψ_2RQ±A_{Ed}+EHF_{Dir2+}	3.3	0.021	Pass	Details...
St. 15 (15)	C58	2	3 (Operating) $SEIS_{1,1}$-G+ψ_2Q+ψ_2RQ±A_{Ed}+EHF_{Dir1+}	4.0	0.026	5 (Operating) $SEIS_{1,1}$-G+ψ_2Q+ψ_2RQ±A_{Ed}+EHF_{Dir2+}	3.3	0.021	Pass	Details...
St. 16 (16)	C77	3	3 (Operating) $SEIS_{1,1}$-G+ψ_2Q+ψ_2RQ±A_{Ed}+EHF_{Dir1+}	4.4	0.028	5 (Operating) $SEIS_{1,1}$-G+ψ_2Q+ψ_2RQ±A_{Ed}+EHF_{Dir2+}	3.3	0.020	Pass	Details...
St. 16 (16)	C58	3	3 (Operating) $SEIS_{1,1}$-G+ψ_2Q+ψ_2RQ±A_{Ed}+EHF_{Dir1+}	4.0	0.026	5 (Operating) $SEIS_{1,1}$-G+ψ_2Q+ψ_2RQ±A_{Ed}+EHF_{Dir2+}	3.3	0.020	Pass	Details...
St. 17 (17)	W6	17	3 (Operating) $SEIS_{1,1}$-G+ψ_2Q+ψ_2RQ±A_{Ed}+EHF_{Dir1+}	4.9	0.031	3 (Operating) $SEIS_{1,1}$-G+ψ_2Q+ψ_2RQ±A_{Ed}+EHF_{Dir1+}	2.7	0.016	Pass	Details...
St. 17 (17)	W8	17	3 (Operating) $SEIS_{1,1}$-G+ψ_2Q+ψ_2RQ±A_{Ed}+EHF_{Dir1+}	3.9	0.024	5 (Operating) $SEIS_{1,1}$-G+ψ_2Q+ψ_2RQ±A_{Ed}+EHF_{Dir2+}	3.9	0.023	Pass	Details...
St. 18 (18)	C77	5	3 (Operating) $SEIS_{1,1}$-G+ψ_2Q+ψ_2RQ±A_{Ed}+EHF_{Dir1+}	4.3	0.026	5 (Operating) $SEIS_{1,1}$-G+ψ_2Q+ψ_2RQ±A_{Ed}+EHF_{Dir2+}	3.2	0.019	Pass	Details...
St. 18 (18)	C71	5	3 (Operating) $SEIS_{1,1}$-G+ψ_2Q+ψ_2RQ±A_{Ed}+EHF_{Dir1+}	4.0	0.025	5 (Operating) $SEIS_{1,1}$-G+ψ_2Q+ψ_2RQ±A_{Ed}+EHF_{Dir2+}	3.2	0.019	Pass	Details...
St. 19 (19)	C77	6	3 (Operating) $SEIS_{1,1}$-G+ψ_2Q+ψ_2RQ±A_{Ed}+EHF_{Dir1+}	4.2	0.025	5 (Operating) $SEIS_{1,1}$-G+ψ_2Q+ψ_2RQ±A_{Ed}+EHF_{Dir2+}	3.0	0.017	Pass	Details...
St. 19 (19)	C53	6	3 (Operating) $SEIS_{1,1}$-G+ψ_2Q+ψ_2RQ±A_{Ed}+EHF_{Dir1+}	4.1	0.024	5 (Operating) $SEIS_{1,1}$-G+ψ_2Q+ψ_2RQ±A_{Ed}+EHF_{Dir2+}	3.0	0.017	Pass	Details...

MODEL14

Level ▲	Ref.	Stack	Combination Dir 1	Drift Dir 1 [mm]	θ_{Dir1}	Combination Dir 2	Drift Dir 2 [mm]	θ_{Dir2}	Status	Details
St. 2 (2)	C20	2	5 (Operating) $SEIS_{1.3}$·G+ψ_2Q+ψ_2RQ±A_{Ed}+EHF_{Dir2+}	2.2	0.024	5 (Operating) $SEIS_{1.3}$·G+ψ_2Q+ψ_2RQ±A_{Ed}+EHF_{Dir2+}	2.1	0.021	✔ Pass	Details...
St. 3 (3)	C23	3	5 (Operating) $SEIS_{1.3}$·G+ψ_2Q+ψ_2RQ±A_{Ed}+EHF_{Dir2+}	3.1	0.032	5 (Operating) $SEIS_{1.3}$·G+ψ_2Q+ψ_2RQ±A_{Ed}+EHF_{Dir2+}	2.3	0.022	✔ Pass	Details...
St. 3 (3)	C1	3	5 (Operating) $SEIS_{1.3}$·G+ψ_2Q+ψ_2RQ±A_{Ed}+EHF_{Dir2+}	2.5	0.026	5 (Operating) $SEIS_{1.3}$·G+ψ_2Q+ψ_2RQ±A_{Ed}+EHF_{Dir2+}	2.3	0.022	✔ Pass	Details...
St. 4 (4)	C23	4	5 (Operating) $SEIS_{1.3}$·G+ψ_2Q+ψ_2RQ±A_{Ed}+EHF_{Dir2+}	3.2	0.032	5 (Operating) $SEIS_{1.3}$·G+ψ_2Q+ψ_2RQ±A_{Ed}+EHF_{Dir2+}	2.4	0.023	✔ Pass	Details...
St. 4 (4)	C1	4	5 (Operating) $SEIS_{1.3}$·G+ψ_2Q+ψ_2RQ±A_{Ed}+EHF_{Dir2+}	2.7	0.027	5 (Operating) $SEIS_{1.3}$·G+ψ_2Q+ψ_2RQ±A_{Ed}+EHF_{Dir2+}	2.4	0.023	✔ Pass	Details...
St. 5 (5)	C23	5	3 (Operating) $SEIS_{1.1}$·G+ψ_2Q+ψ_2RQ±A_{Ed}+EHF_{Dir1+}	3.3	0.031	5 (Operating) $SEIS_{1.3}$·G+ψ_2Q+ψ_2RQ±A_{Ed}+EHF_{Dir2+}	2.6	0.023	✔ Pass	Details...
St. 5 (5)	C20	5	3 (Operating) $SEIS_{1.1}$·G+ψ_2Q+ψ_2RQ±A_{Ed}+EHF_{Dir1+}	2.7	0.026	5 (Operating) $SEIS_{1.3}$·G+ψ_2Q+ψ_2RQ±A_{Ed}+EHF_{Dir2+}	2.6	0.023	✔ Pass	Details...
St. 6 (6)	C23	6	3 (Operating) $SEIS_{1.1}$·G+ψ_2Q+ψ_2RQ±A_{Ed}+EHF_{Dir1+}	3.4	0.031	5 (Operating) $SEIS_{1.3}$·G+ψ_2Q+ψ_2RQ±A_{Ed}+EHF_{Dir2+}	2.7	0.023	✔ Pass	Details...
St. 6 (6)	C1	6	5 (Operating) $SEIS_{1.3}$·G+ψ_2Q+ψ_2RQ±A_{Ed}+EHF_{Dir2+}	3.0	0.027	5 (Operating) $SEIS_{1.3}$·G+ψ_2Q+ψ_2RQ±A_{Ed}+EHF_{Dir2+}	2.7	0.023	✔ Pass	Details...
St. 7 (7)	C23	7	3 (Operating) $SEIS_{1.1}$·G+ψ_2Q+ψ_2RQ±A_{Ed}+EHF_{Dir1+}	3.6	0.031	5 (Operating) $SEIS_{1.3}$·G+ψ_2Q+ψ_2RQ±A_{Ed}+EHF_{Dir2+}	2.7	0.023	✔ Pass	Details...
St. 7 (7)	C20	7	3 (Operating) $SEIS_{1.1}$·G+ψ_2Q+ψ_2RQ±A_{Ed}+EHF_{Dir1+}	3.1	0.027	5 (Operating) $SEIS_{1.3}$·G+ψ_2Q+ψ_2RQ±A_{Ed}+EHF_{Dir2+}	2.7	0.023	✔ Pass	Details...
St. 8 (8)	C48	1	3 (Operating) $SEIS_{1.1}$·G+ψ_2Q+ψ_2RQ±A_{Ed}+EHF_{Dir1+}	3.9	0.033	5 (Operating) $SEIS_{1.3}$·G+ψ_2Q+ψ_2RQ±A_{Ed}+EHF_{Dir2+}	3.0	0.024	✔ Pass	Details...
St. 8 (8)	C26	1	5 (Operating) $SEIS_{1.3}$·G+ψ_2Q+ψ_2RQ±A_{Ed}+EHF_{Dir2+}	3.4	0.029	5 (Operating) $SEIS_{1.3}$·G+ψ_2Q+ψ_2RQ±A_{Ed}+EHF_{Dir2+}	3.0	0.024	✔ Pass	Details...
St. 9 (9)	C48	2	3 (Operating) $SEIS_{1.1}$·G+ψ_2Q+ψ_2RQ±A_{Ed}+EHF_{Dir1+}	4.1	0.033	5 (Operating) $SEIS_{1.3}$·G+ψ_2Q+ψ_2RQ±A_{Ed}+EHF_{Dir2+}	3.0	0.023	✔ Pass	Details...
St. 9 (9)	C26	2	5 (Operating) $SEIS_{1.3}$·G+ψ_2Q+ψ_2RQ±A_{Ed}+EHF_{Dir2+}	3.5	0.028	5 (Operating) $SEIS_{1.3}$·G+ψ_2Q+ψ_2RQ±A_{Ed}+EHF_{Dir2+}	3.0	0.023	✔ Pass	Details...
St. 10 (10)	W6	10	3 (Operating) $SEIS_{1.1}$·G+ψ_2Q+ψ_2RQ±A_{Ed}+EHF_{Dir1+}	4.3	0.033	3 (Operating) $SEIS_{1.1}$·G+ψ_2Q+ψ_2RQ±A_{Ed}+EHF_{Dir1+}	2.1	0.016	✔ Pass	Details...
St. 10 (10)	C26	3	3 (Operating) $SEIS_{1.1}$·G+ψ_2Q+ψ_2RQ±A_{Ed}+EHF_{Dir1+}	3.6	0.028	5 (Operating) $SEIS_{1.3}$·G+ψ_2Q+ψ_2RQ±A_{Ed}+EHF_{Dir2+}	3.1	0.023	✔ Pass	Details...
St. 11 (11)	C48	4	3 (Operating) $SEIS_{1.1}$·G+ψ_2Q+ψ_2RQ±A_{Ed}+EHF_{Dir1+}	4.2	0.032	3 (Operating) $SEIS_{1.1}$·G+ψ_2Q+ψ_2RQ±A_{Ed}+EHF_{Dir1+}	3.1	0.022	✔ Pass	Details...
St. 11 (11)	C45	4	3 (Operating) $SEIS_{1.1}$·G+ψ_2Q+ψ_2RQ±A_{Ed}+EHF_{Dir1+}	3.8	0.029	3 (Operating) $SEIS_{1.1}$·G+ψ_2Q+ψ_2RQ±A_{Ed}+EHF_{Dir1+}	3.1	0.022	✔ Pass	Details...
St. 12 (12)	W6	12	3 (Operating) $SEIS_{1.1}$·G+ψ_2Q+ψ_2RQ±A_{Ed}+EHF_{Dir1+}	4.6	0.033	3 (Operating) $SEIS_{1.1}$·G+ψ_2Q+ψ_2RQ±A_{Ed}+EHF_{Dir1+}	2.3	0.016	✔ Pass	Details...
St. 12 (12)	C36	5	3 (Operating) $SEIS_{1.1}$·G+ψ_2Q+ψ_2RQ±A_{Ed}+EHF_{Dir1+}	3.4	0.025	3 (Operating) $SEIS_{1.1}$·G+ψ_2Q+ψ_2RQ±A_{Ed}+EHF_{Dir1+}	3.1	0.021	✔ Pass	Details...
St. 13 (13)	C48	6	3 (Operating) $SEIS_{1.1}$·G+ψ_2Q+ψ_2RQ±A_{Ed}+EHF_{Dir1+}	4.3	0.030	3 (Operating) $SEIS_{1.1}$·G+ψ_2Q+ψ_2RQ±A_{Ed}+EHF_{Dir1+}	3.1	0.021	✔ Pass	Details...
St. 13 (13)	C36	6	3 (Operating) $SEIS_{1.1}$·G+ψ_2Q+ψ_2RQ±A_{Ed}+EHF_{Dir1+}	3.5	0.025	3 (Operating) $SEIS_{1.1}$·G+ψ_2Q+ψ_2RQ±A_{Ed}+EHF_{Dir1+}	3.1	0.021	✔ Pass	Details...
St. 14 (14)	C77	1	3 (Operating) $SEIS_{1.1}$·G+ψ_2Q+ψ_2RQ±A_{Ed}+EHF_{Dir1+}	4.4	0.030	3 (Operating) $SEIS_{1.1}$·G+ψ_2Q+ψ_2RQ±A_{Ed}+EHF_{Dir1+}	3.3	0.021	✔ Pass	Details...
St. 14 (14)	C53	1	3 (Operating) $SEIS_{1.1}$·G+ψ_2Q+ψ_2RQ±A_{Ed}+EHF_{Dir1+}	4.1	0.028	3 (Operating) $SEIS_{1.1}$·G+ψ_2Q+ψ_2RQ±A_{Ed}+EHF_{Dir1+}	3.3	0.021	✔ Pass	Details...
St. 15 (15)	C77	2	3 (Operating) $SEIS_{1.1}$·G+ψ_2Q+ψ_2RQ±A_{Ed}+EHF_{Dir1+}	4.4	0.029	3 (Operating) $SEIS_{1.1}$·G+ψ_2Q+ψ_2RQ±A_{Ed}+EHF_{Dir1+}	3.2	0.020	✔ Pass	Details...
St. 15 (15)	C58	2	3 (Operating) $SEIS_{1.1}$·G+ψ_2Q+ψ_2RQ±A_{Ed}+EHF_{Dir1+}	3.9	0.026	3 (Operating) $SEIS_{1.1}$·G+ψ_2Q+ψ_2RQ±A_{Ed}+EHF_{Dir1+}	3.2	0.020	✔ Pass	Details...
St. 16 (16)	C77	3	3 (Operating) $SEIS_{1.1}$·G+ψ_2Q+ψ_2RQ±A_{Ed}+EHF_{Dir1+}	4.4	0.028	5 (Operating) $SEIS_{1.3}$·G+ψ_2Q+ψ_2RQ±A_{Ed}+EHF_{Dir2+}	3.1	0.019	✔ Pass	Details...
St. 16 (16)	C58	3	3 (Operating) $SEIS_{1.1}$·G+ψ_2Q+ψ_2RQ±A_{Ed}+EHF_{Dir1+}	3.9	0.025	5 (Operating) $SEIS_{1.3}$·G+ψ_2Q+ψ_2RQ±A_{Ed}+EHF_{Dir2+}	3.1	0.019	✔ Pass	Details...
St. 17 (17)	C77	4	3 (Operating) $SEIS_{1.1}$·G+ψ_2Q+ψ_2RQ±A_{Ed}+EHF_{Dir1+}	4.3	0.027	5 (Operating) $SEIS_{1.3}$·G+ψ_2Q+ψ_2RQ±A_{Ed}+EHF_{Dir2+}	3.1	0.018	✔ Pass	Details...
St. 17 (17)	C71	4	3 (Operating) $SEIS_{1.1}$·G+ψ_2Q+ψ_2RQ±A_{Ed}+EHF_{Dir1+}	4.0	0.025	5 (Operating) $SEIS_{1.3}$·G+ψ_2Q+ψ_2RQ±A_{Ed}+EHF_{Dir2+}	3.1	0.018	✔ Pass	Details...
St. 18 (18)	W7	18	3 (Operating) $SEIS_{1.1}$·G+ψ_2Q+ψ_2RQ±A_{Ed}+EHF_{Dir1+}	4.4	0.027	3 (Operating) $SEIS_{1.1}$·G+ψ_2Q+ψ_2RQ±A_{Ed}+EHF_{Dir1+}	2.6	0.015	✔ Pass	Details...
St. 18 (18)	C53	5	3 (Operating) $SEIS_{1.1}$·G+ψ_2Q+ψ_2RQ±A_{Ed}+EHF_{Dir1+}	4.1	0.025	5 (Operating) $SEIS_{1.3}$·G+ψ_2Q+ψ_2RQ±A_{Ed}+EHF_{Dir2+}	3.1	0.018	✔ Pass	Details...
St. 19 (19)	W6	19	3 (Operating) $SEIS_{1.1}$·G+ψ_2Q+ψ_2RQ±A_{Ed}+EHF_{Dir1+}	4.9	0.029	3 (Operating) $SEIS_{1.1}$·G+ψ_2Q+ψ_2RQ±A_{Ed}+EHF_{Dir1+}	2.6	0.015	✔ Pass	Details...
St. 19 (19)	W8	19	3 (Operating) $SEIS_{1.1}$·G+ψ_2Q+ψ_2RQ±A_{Ed}+EHF_{Dir1+}	3.8	0.023	5 (Operating) $SEIS_{1.3}$·G+ψ_2Q+ψ_2RQ±A_{Ed}+EHF_{Dir2+}	3.9	0.022	✔ Pass	Details...
St. 20 (roof)	C77	7	3 (Operating) $SEIS_{1.1}$·G+ψ_2Q+ψ_2RQ±A_{Ed}+EHF_{Dir1+}	4.0	0.023	3 (Operating) $SEIS_{1.1}$·G+ψ_2Q+ψ_2RQ±A_{Ed}+EHF_{Dir1+}	2.8	0.015	✔ Pass	Details...
St. 20 (roof)	C53	7	3 (Operating) $SEIS_{1.1}$·G+ψ_2Q+ψ_2RQ±A_{Ed}+EHF_{Dir1+}	3.9	0.023	3 (Operating) $SEIS_{1.1}$·G+ψ_2Q+ψ_2RQ±A_{Ed}+EHF_{Dir1+}	2.8	0.015	✔ Pass	Details...